

This report not to be quoted without reference to the Council*

International Council for the
Exploration of the Sea

C.M. 1991/Assess:7

PART 2

*REPORT OF THE MULTISPECIES ASSESSMENT
WORKING GROUP*

Woods Hole, 4-13 December, 1990

This document is a report of a Working Group of the International Council for the Exploration of the Sea and does not necessarily represent the views of the Council. Therefore, it should not be quoted without consultation with the General Secretary.

* General Secretary
ICES
Palægade 2-4
DK-1261 Copenhagen K
DENMARK

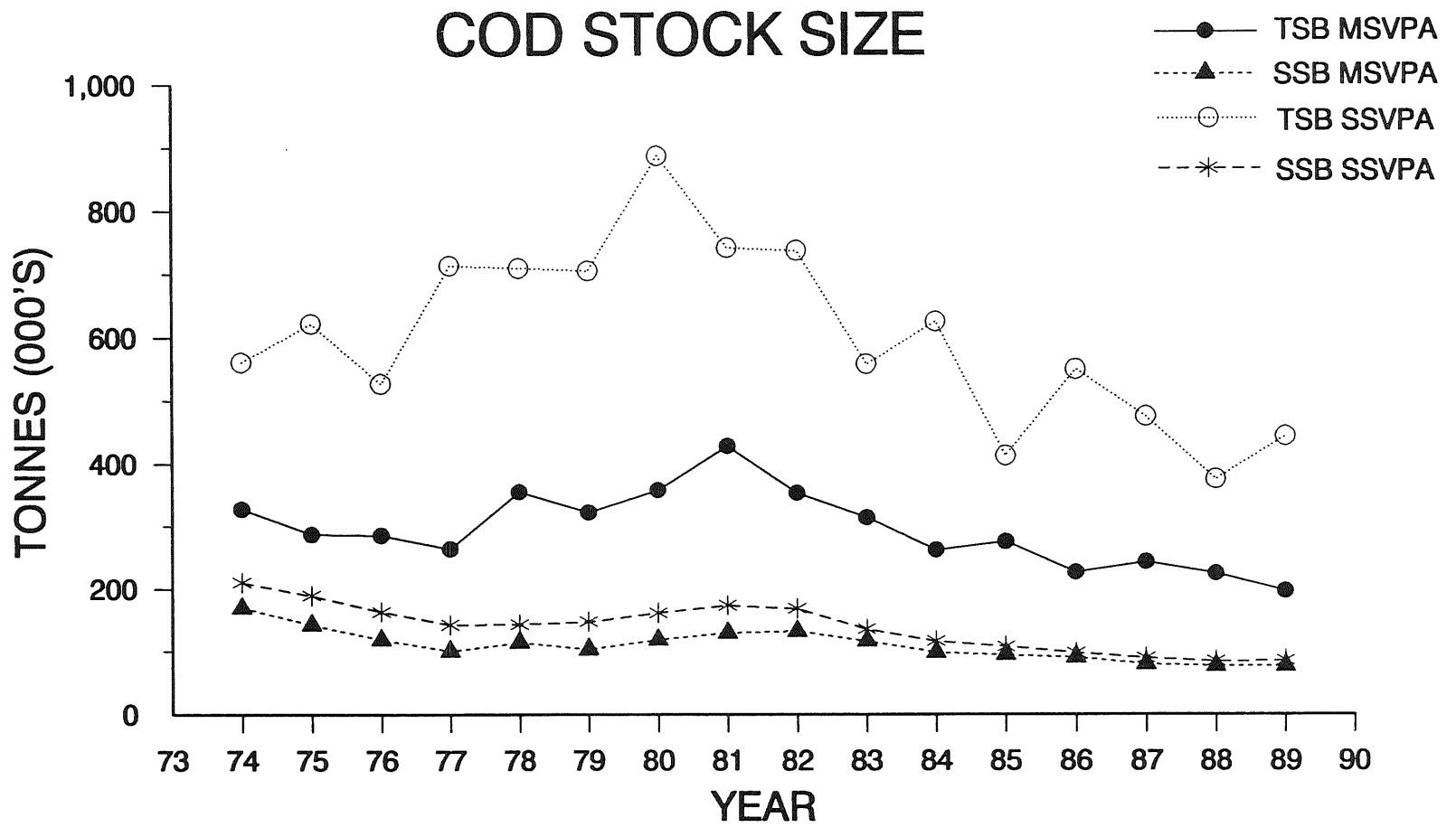


Figure 2.7.1a. The total stock biomass (TSB) and spawning stock biomass (SSB) of cod from the MSVPA and the SSVPA.

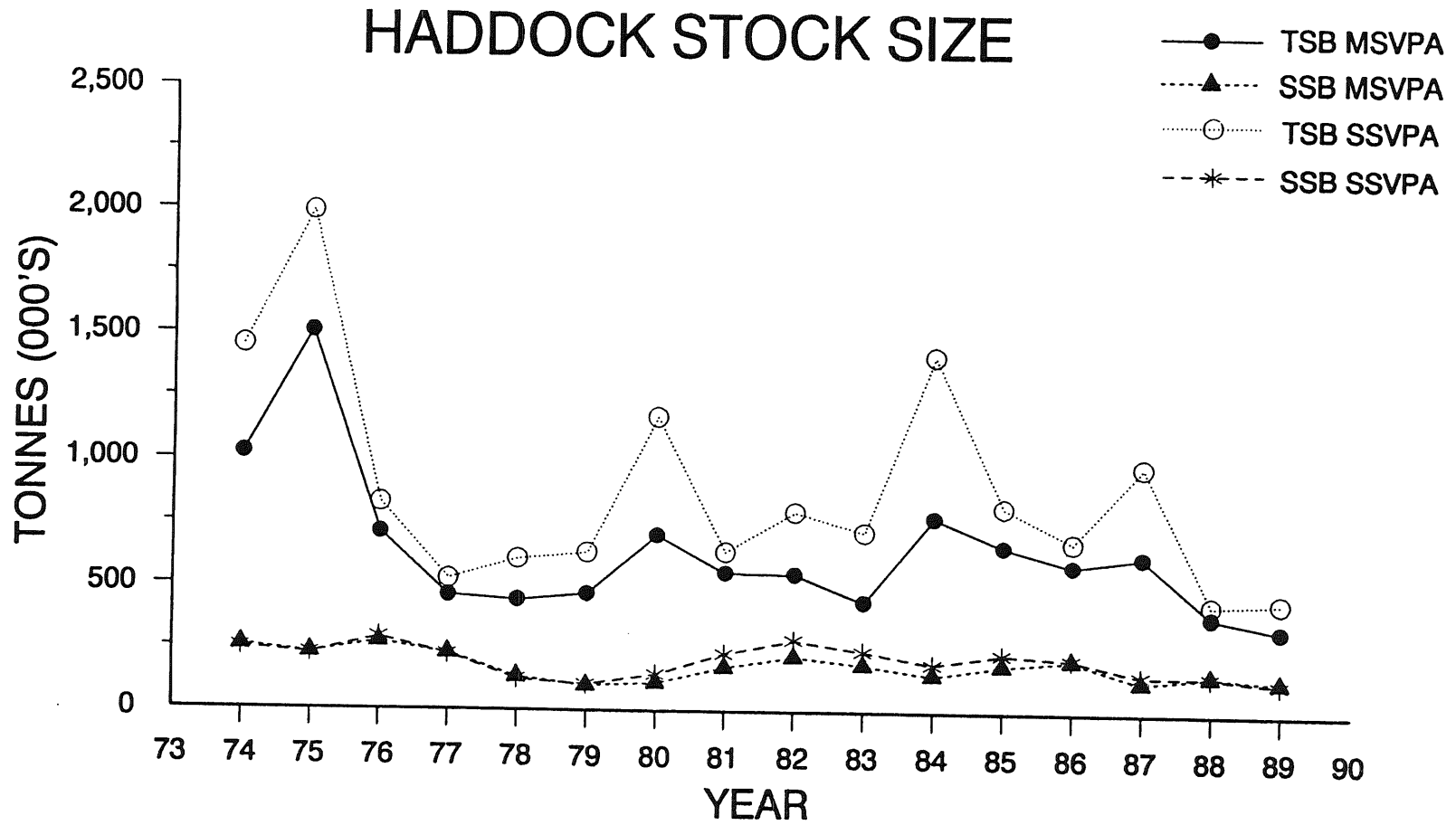


Figure 2.7.1b. The total stock biomass (TSB) and spawning stock biomass (SSB) of haddock from the MSVPA and the SSVPA.

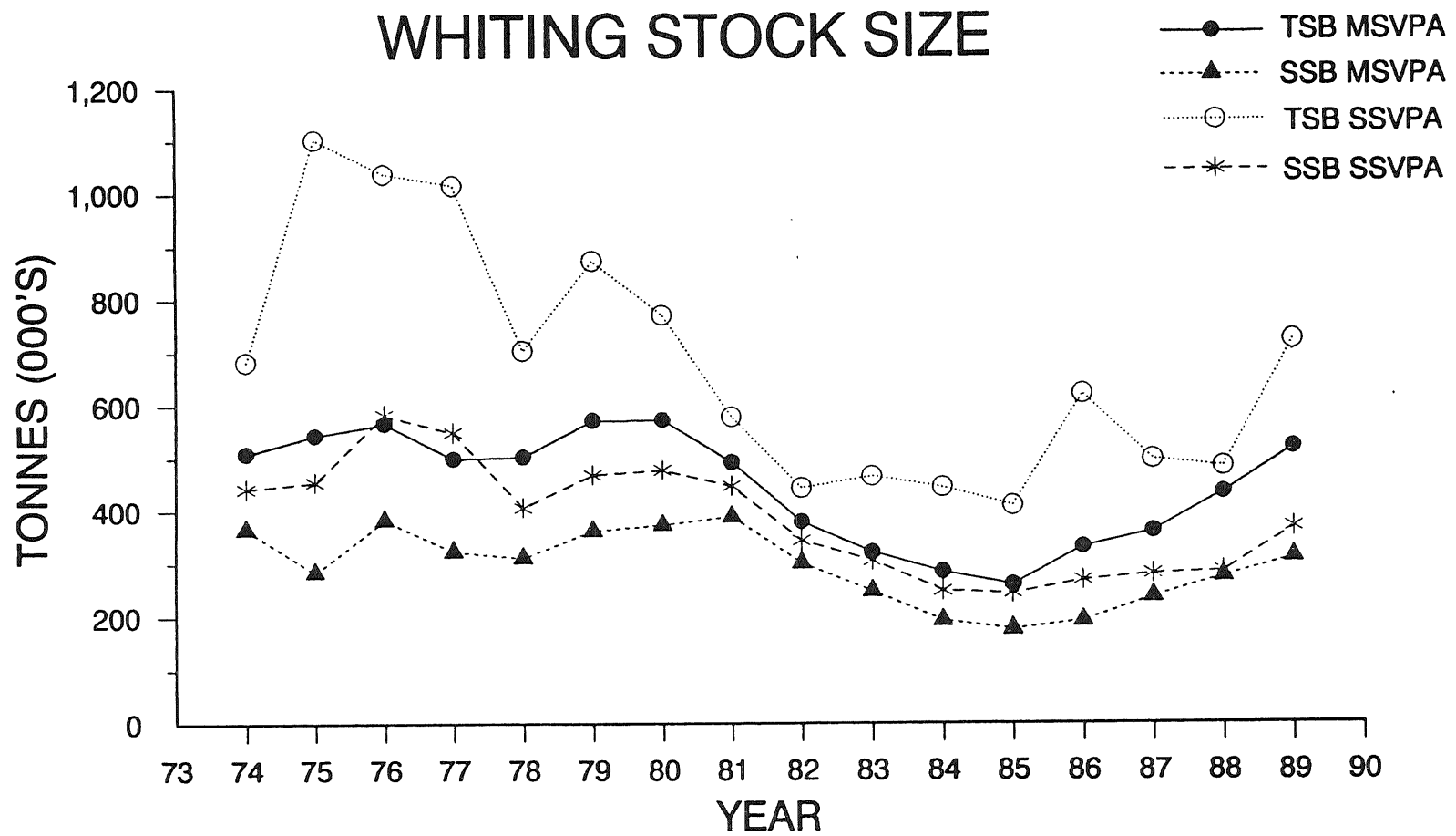


Figure 2.7.1c. The total stock biomass (TSB) and spawning stock biomass (SSB) of whiting from the MSVPA and the SSVPA.

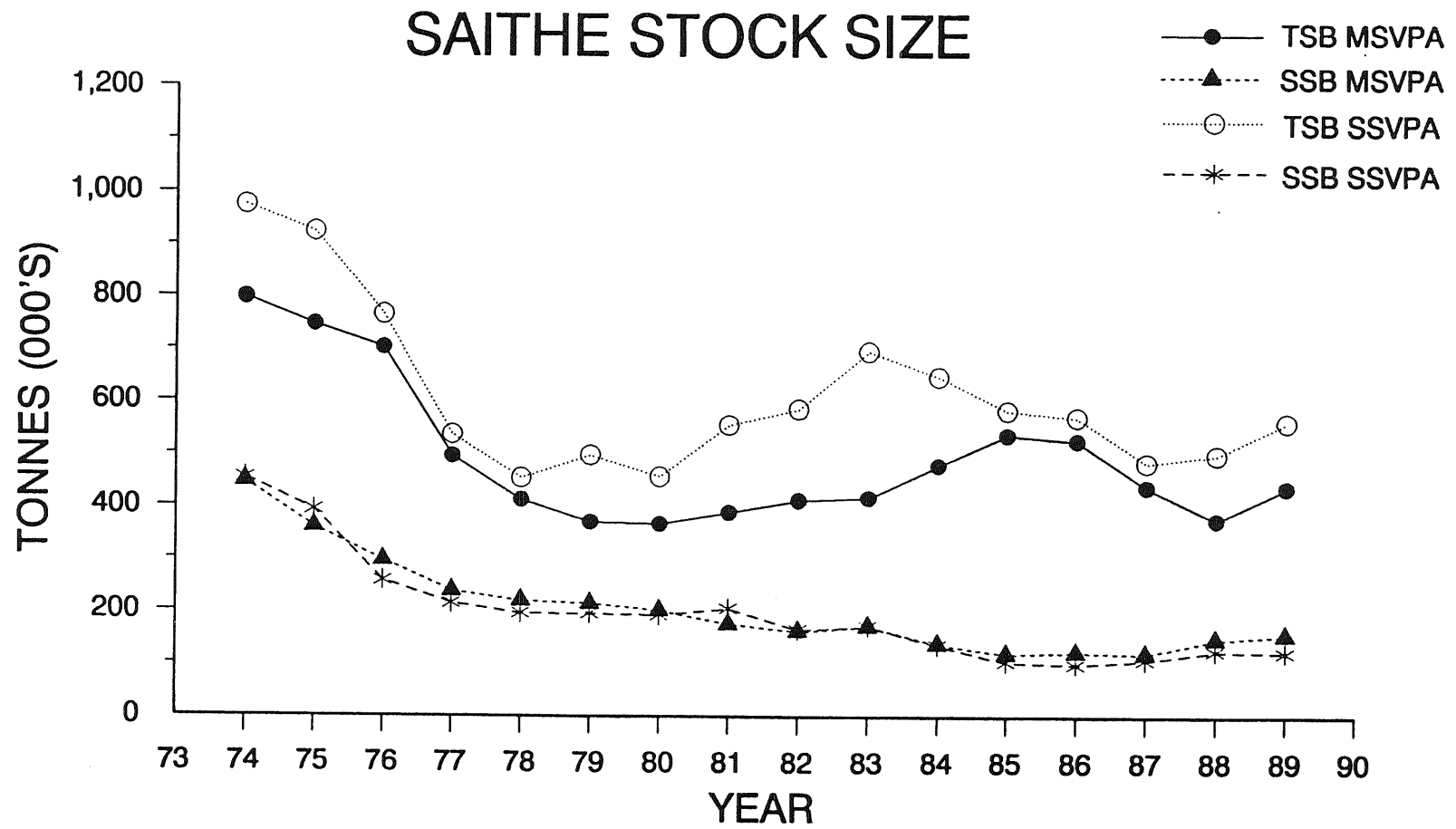


Figure 2.7.1d. The total stock biomass (TSB) and spawning stock biomass (SSB) of saithe from the MSVPA and the SSVPA.

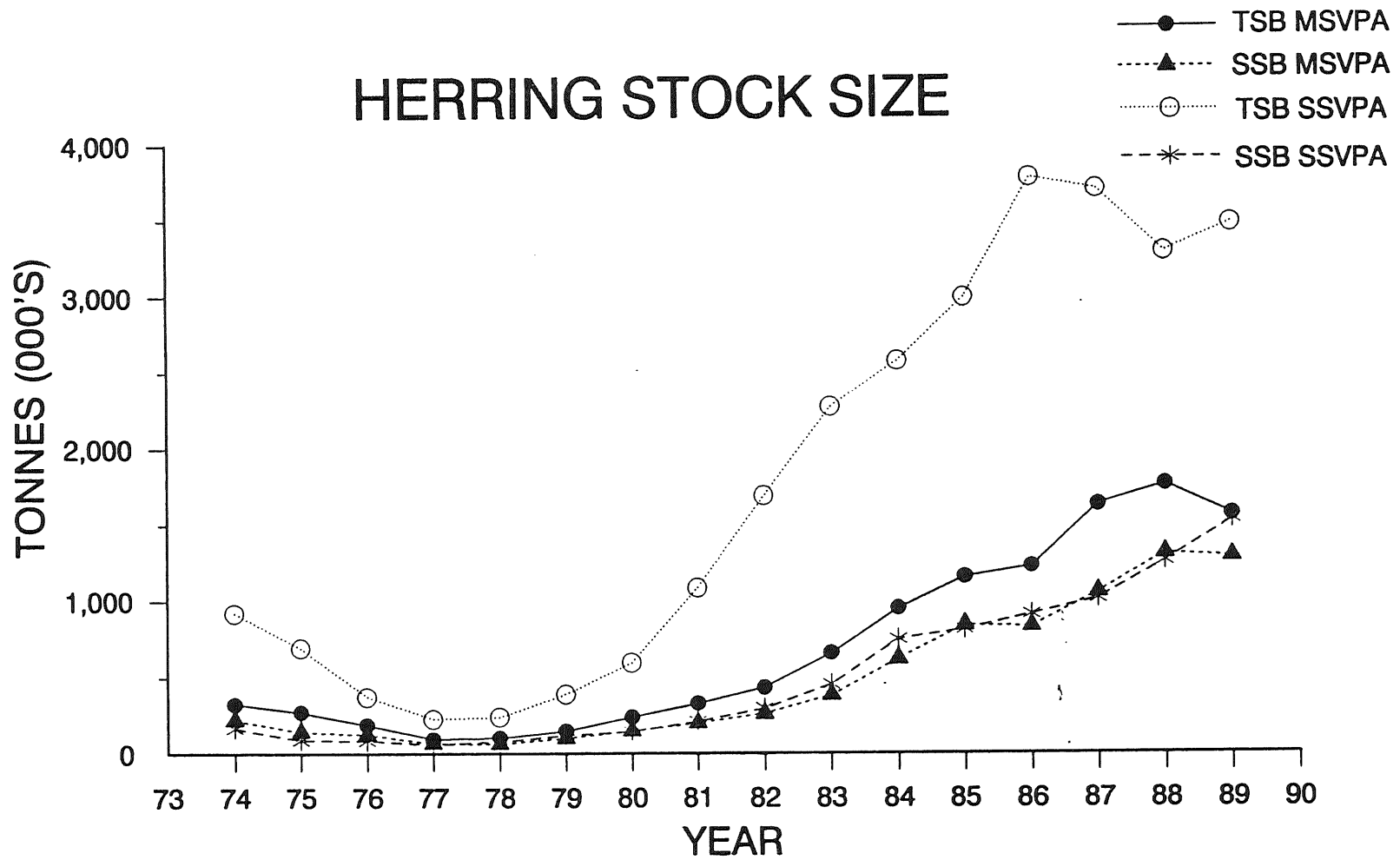


Figure 2.7.1e. The total stock biomass (TSB) and spawning stock biomass (SSB) of herring from the MSVPA and the SSVPA.

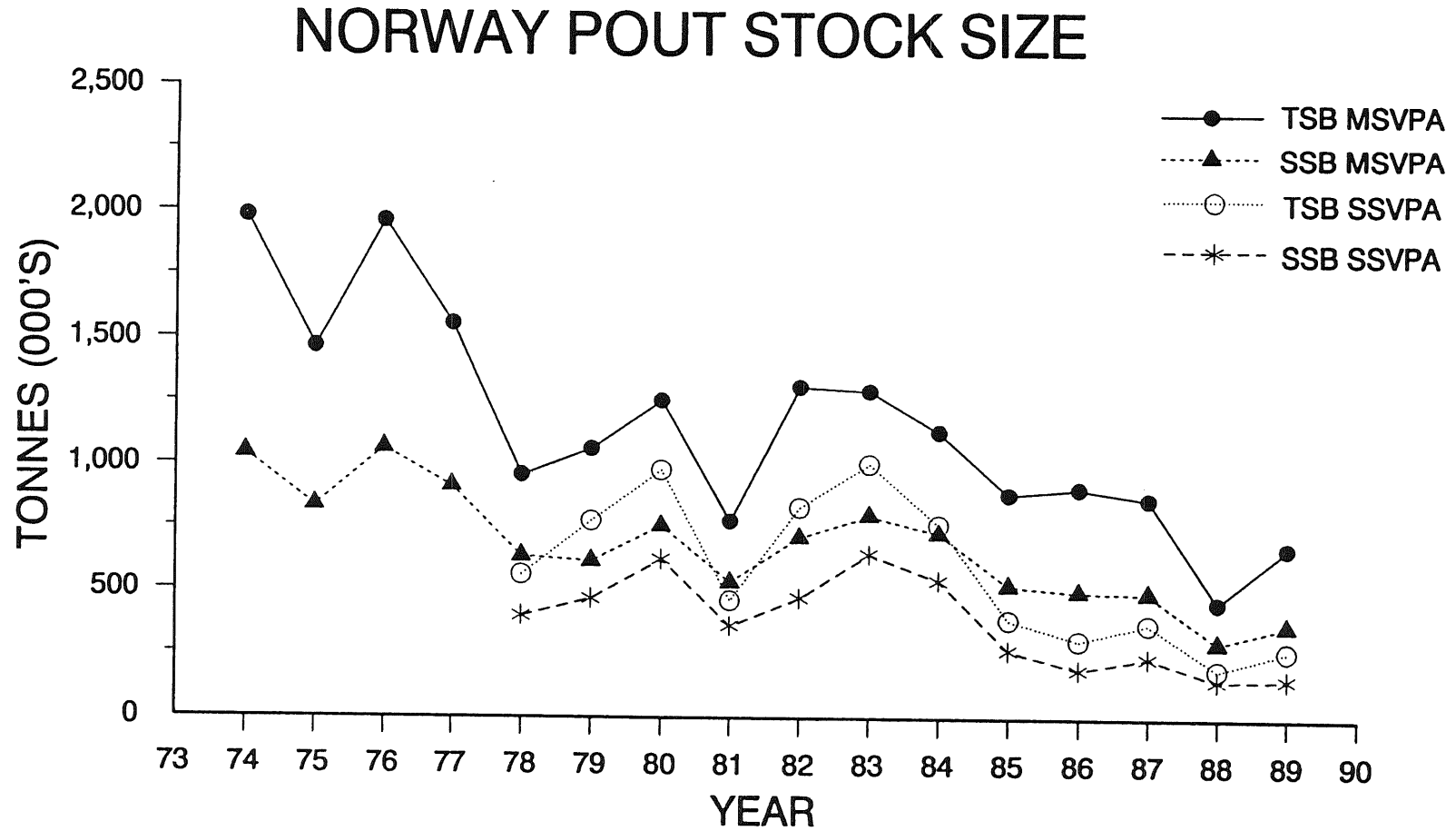


Figure 2.7.1f. The total stock biomass (TSB) and spawning stock biomass (SSB) of Norway pout from the MSVPA and the SSVPA.

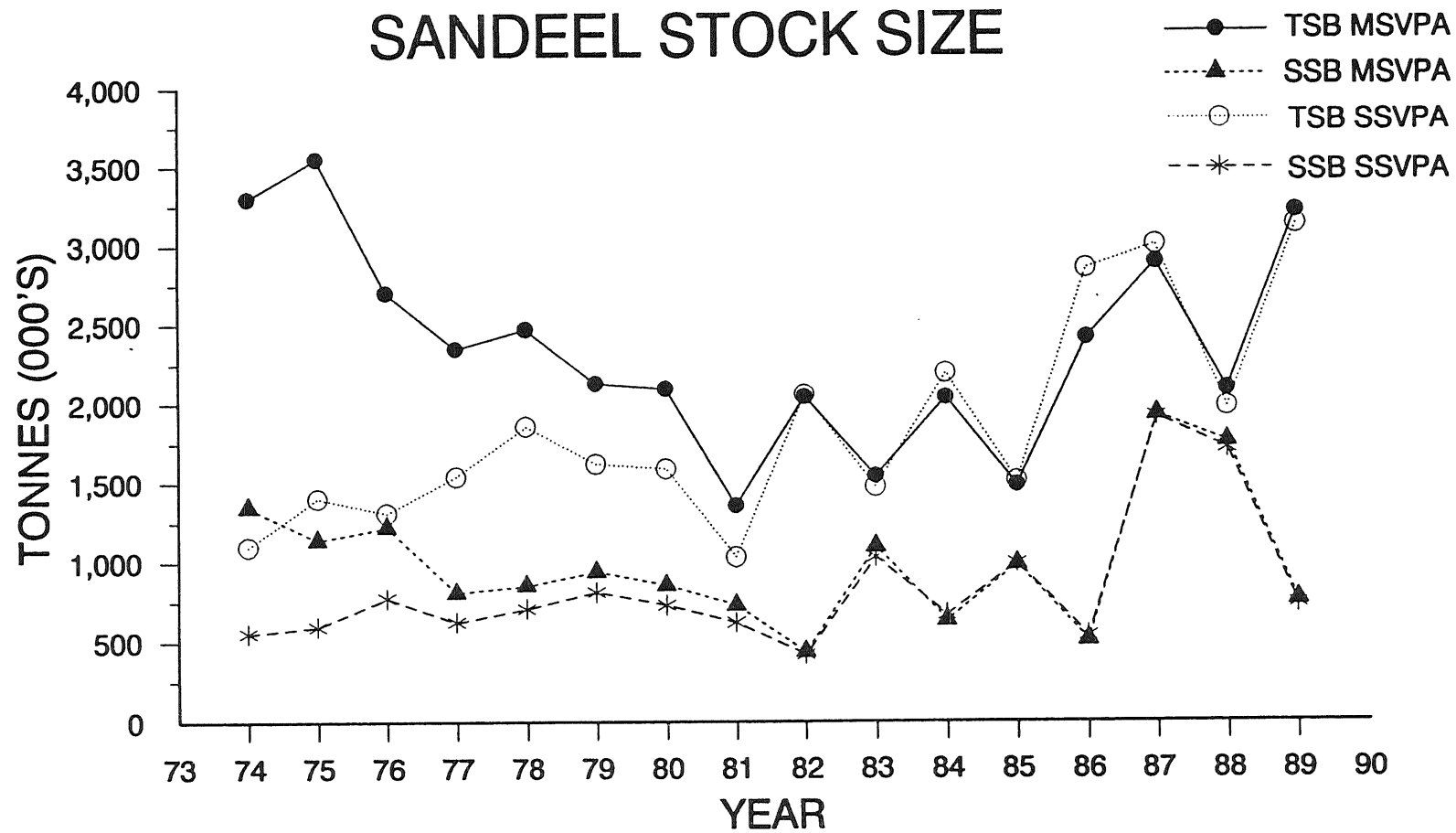


Figure 2.7.1g. The total stock biomass (TSB) and spawning stock biomass (SSB) of sandeel from the MSVPA and the SSVPA.

Relative Sensitivities MSVPA Responses to MSVPA Parameters

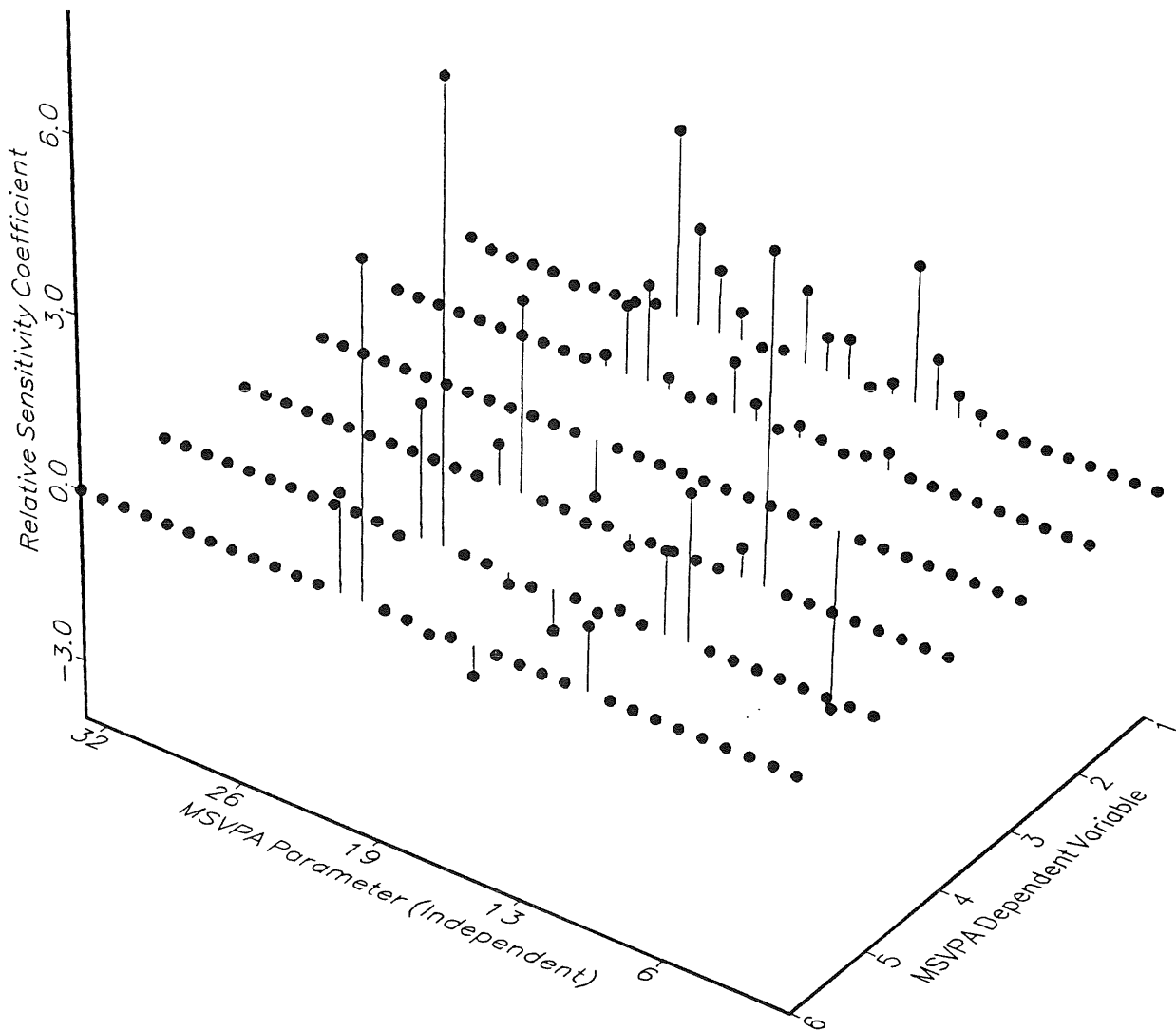


Figure 2.8.3.1. Relative sensitivities of MSVPA responses to MSVPA parameters. Sensitivities are expressed as the percent change in the response variable (% of mean) caused by a 10% change in the parameter. MSVPA parameters are listed in Table 2.8.1.1 (#1-#33). Response variables are: (1) TOTAL BIOMASS of all MSVPA species in 1974, (2) TOTAL BIOMASS of all MSVPA species in 1989, (3) average F for age 1 cod, (4) average population numbers (N) for age 1 cod, (5) average predation deaths (D) for age 1 cod, and (6) average M2 for age 1 cod.

MEAN BIOMASS, YIELD AND PREDATION ALL MSVPA SPECIES

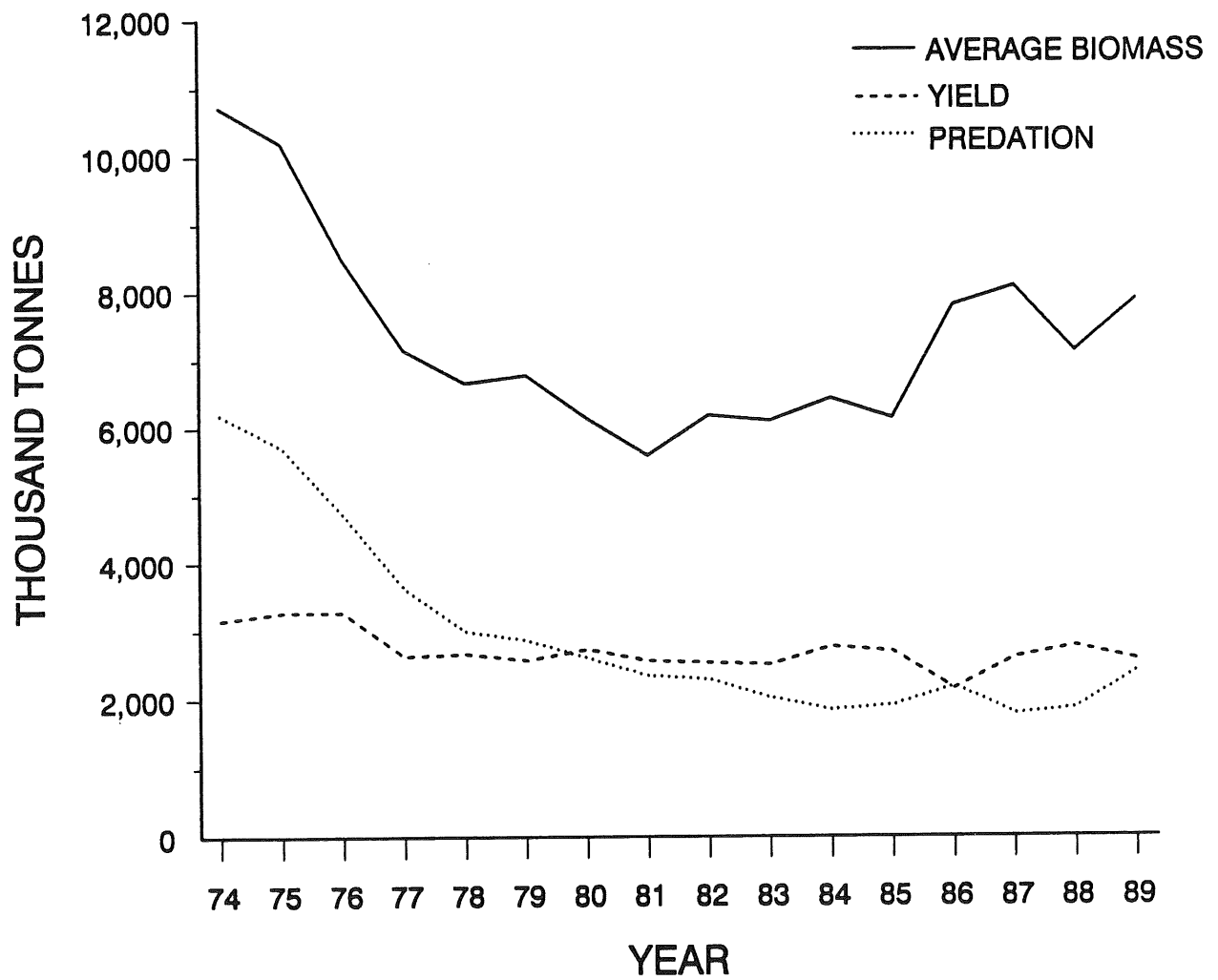


Figure 3.1.1 Trends in mean total biomass, yield and predation (in thousands of tonnes) for all MSVPA species considered, 1974-1989.

MEAN BIOMASS OF MSVPA PREDATORS

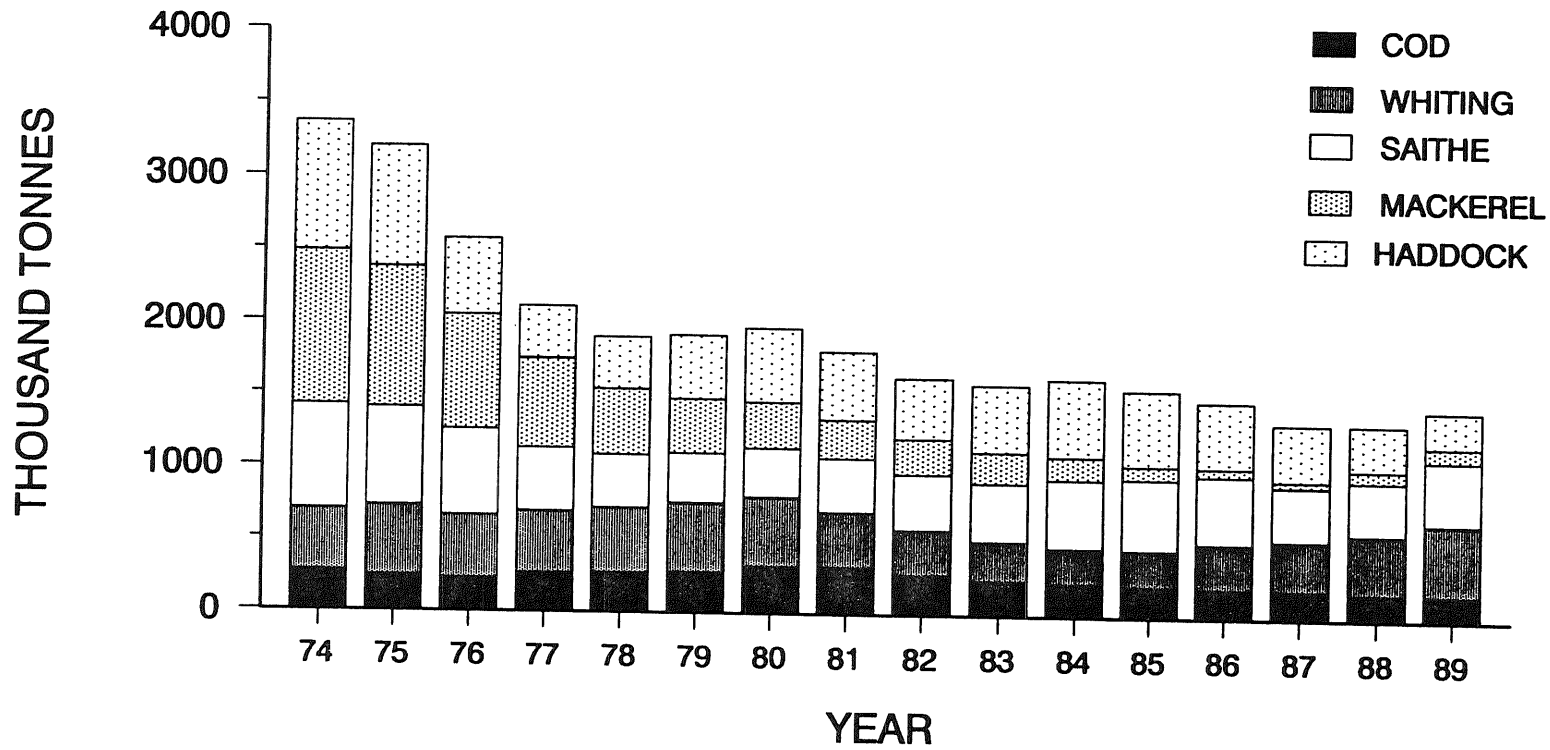


Figure 3.1.2 Trends in mean total biomass (thousands of tonnes) of MSVPA predator species, 1974-1989.

MEAN BIOMASS OF MSVPA PREY

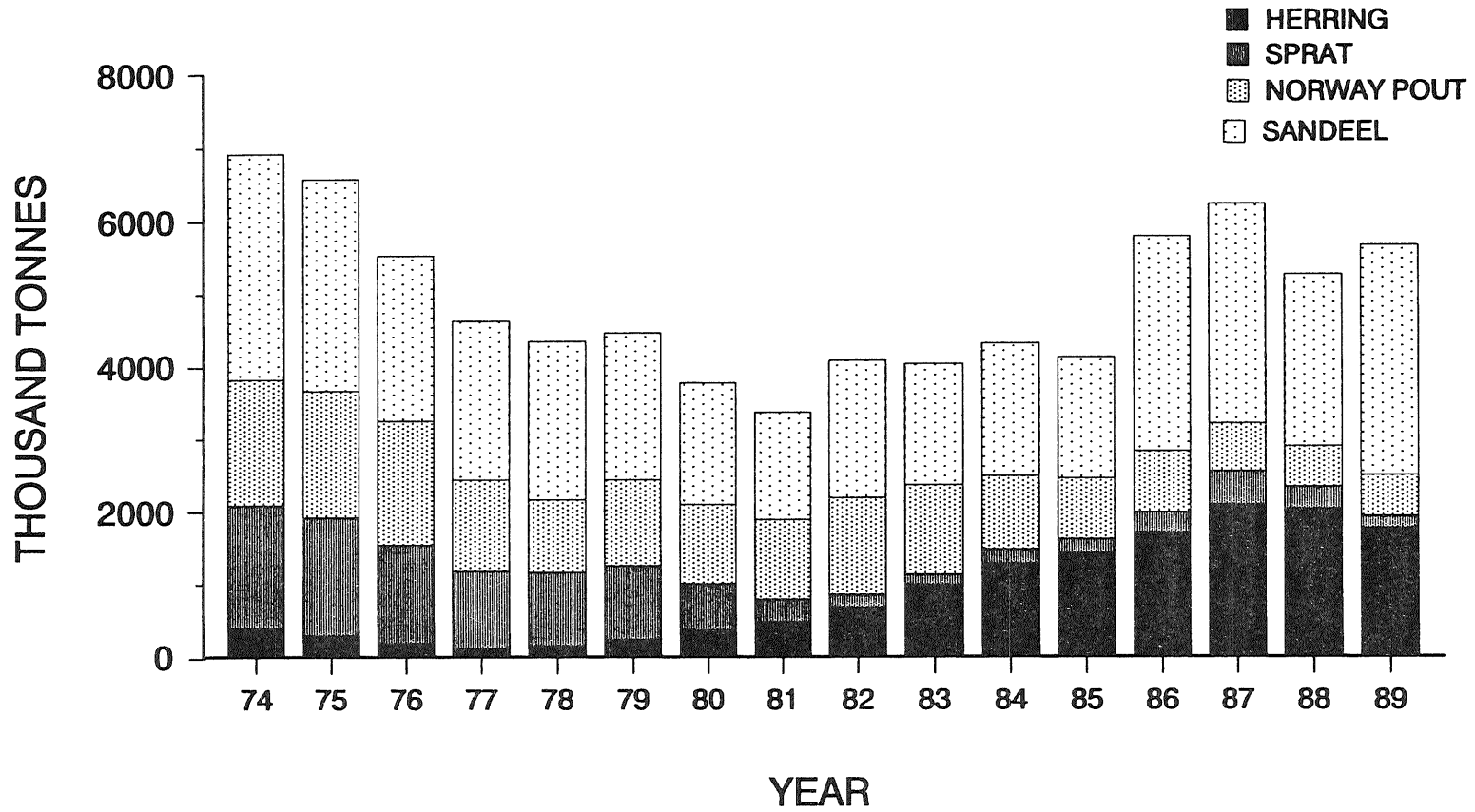
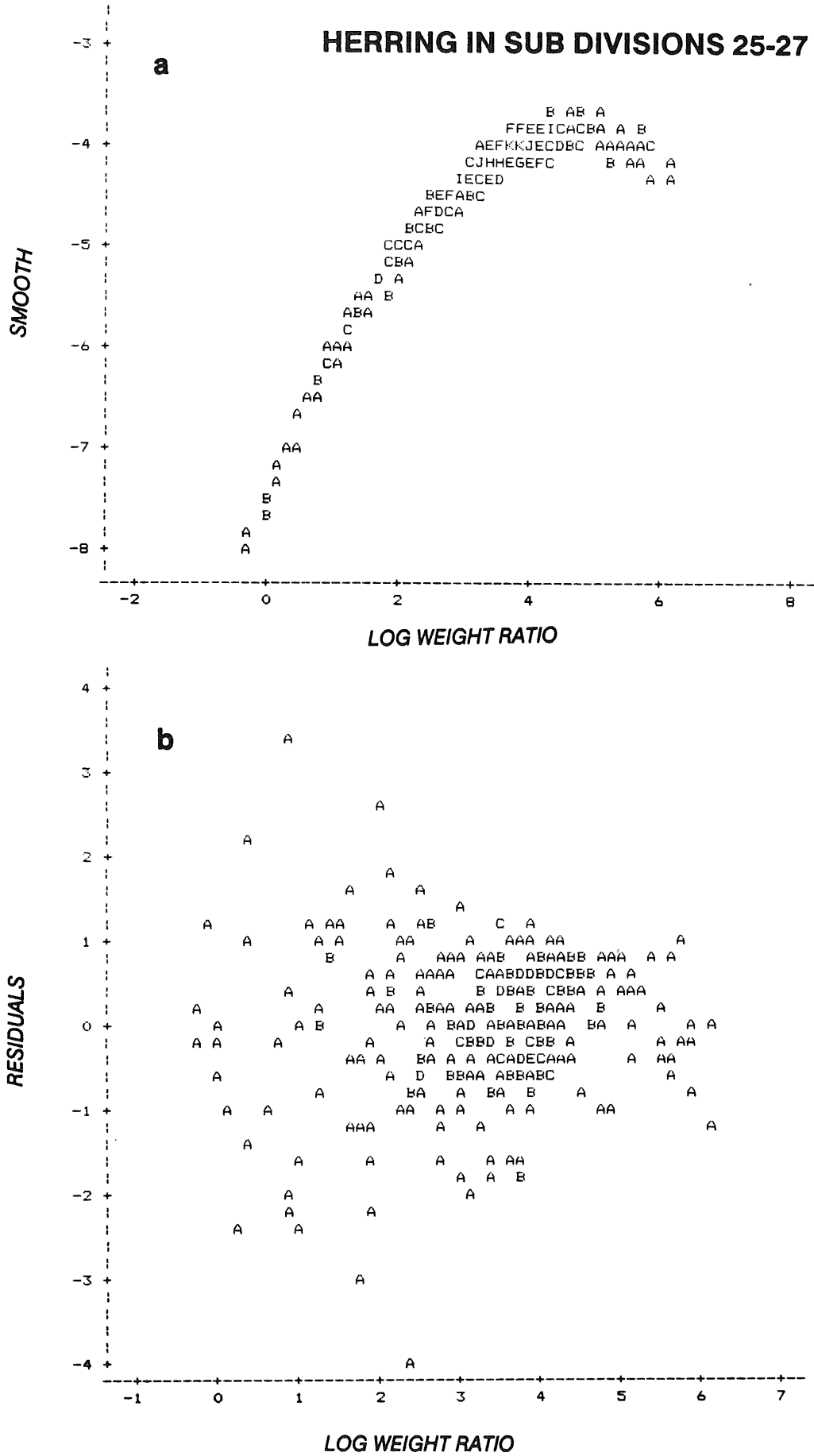
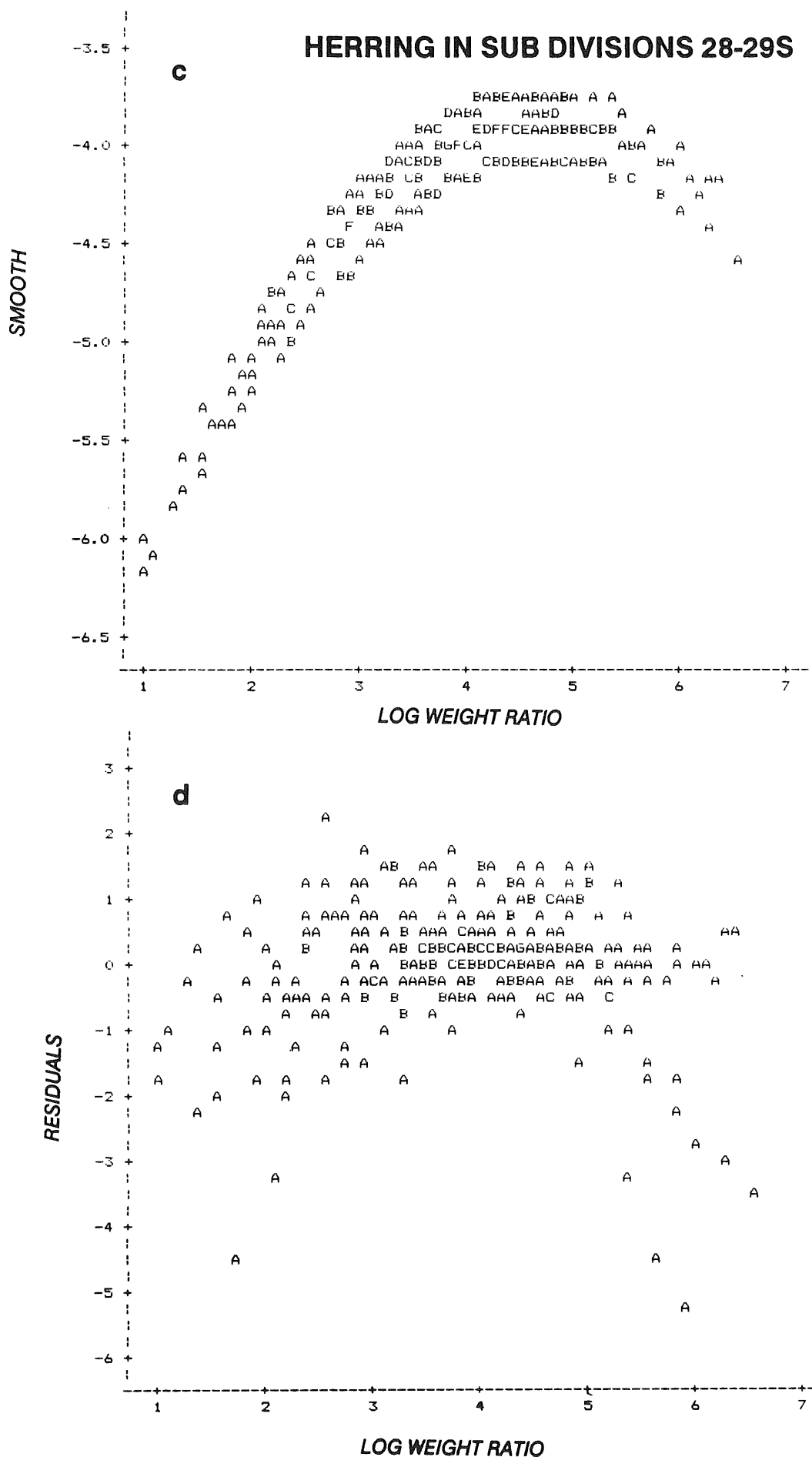


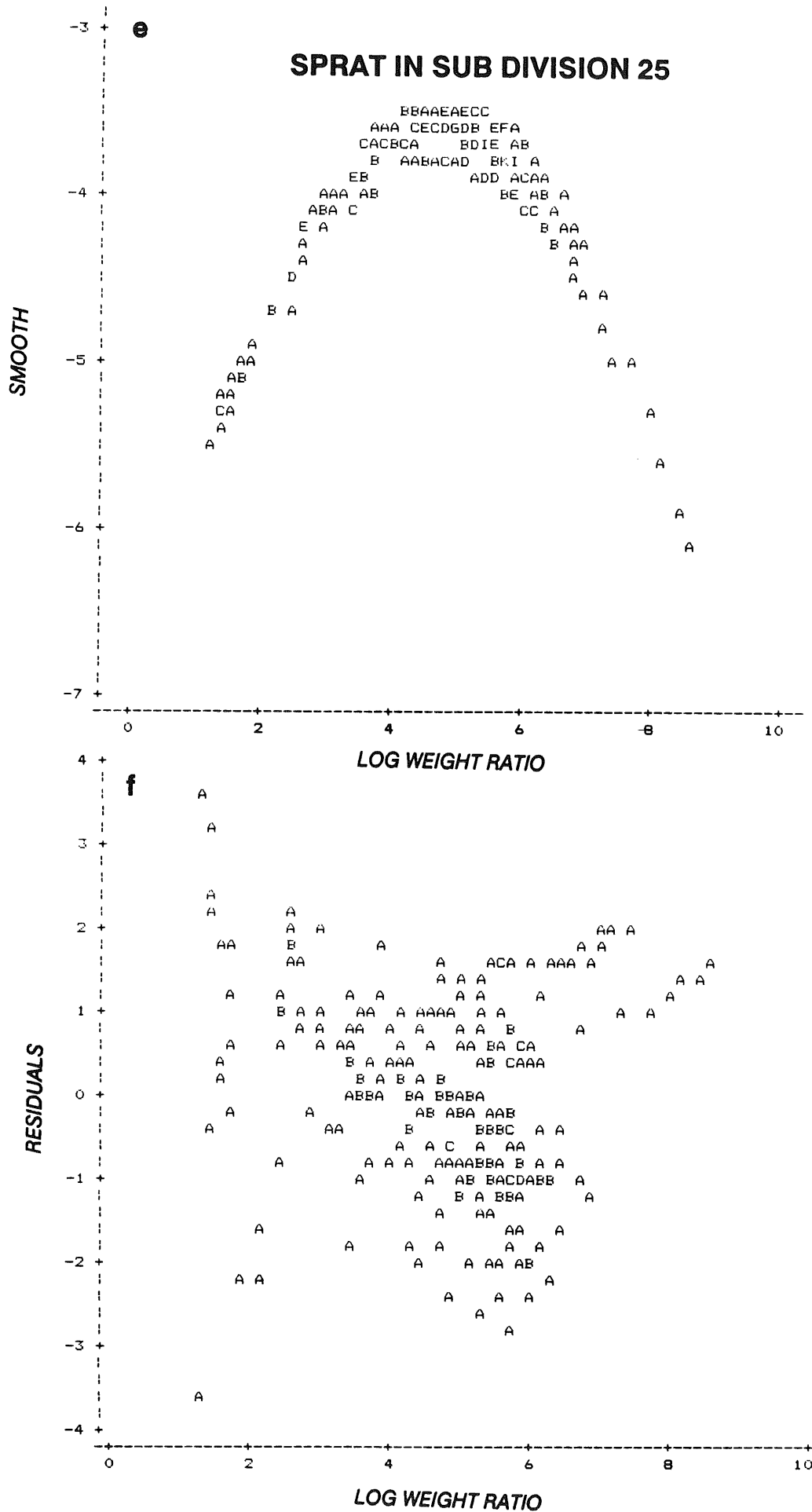
Figure 3.1.3 Trends in mean total biomass (thousands of tonnes) of MSVPA prey species, 1974-1989.



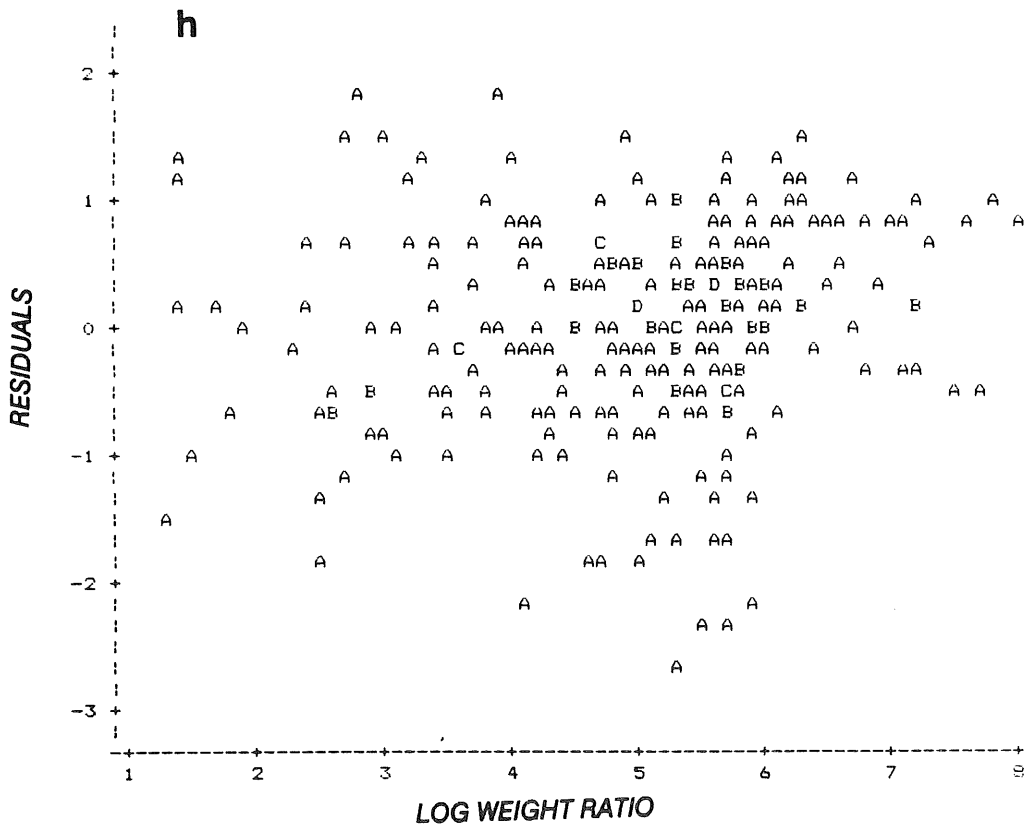
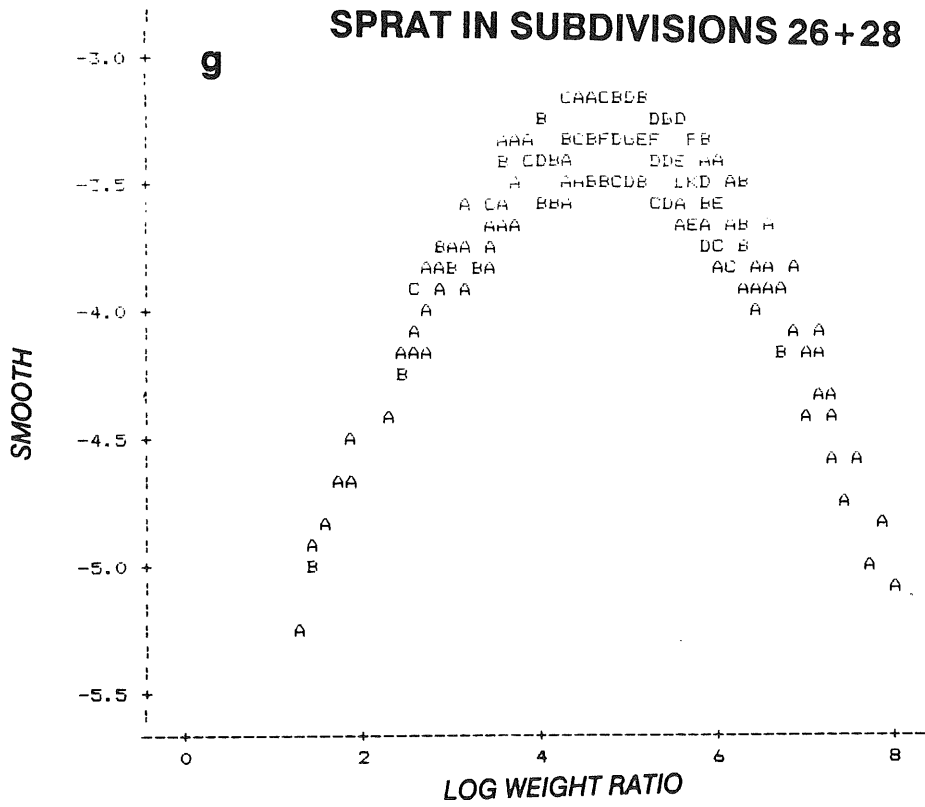
Figures 3.2.1.a,b. Plot of predicted suitabilities (SMOOTH) vs. log weight ratio (W_{pred}/W_{prey} ; a) and residuals (b) for Baltic herring in Sub Divisions 25-27 as prey for cod.



Figures 3.2.1.c,d. Plot of predicted suitabilities (SMOOTH) vs. log weight ratio (W_{pred}/W_{prey} ; c) and residuals (d) for Baltic herring in Sub Divisions 28-29s as prey for cod.



Figures 3.2.1.e,f. Plot of predicted suitabilities (SMOOTH) vs. log weight ratio (W_{pred}/W_{prey} ; e) and residuals (f) for Baltic sprat in Sub Division 25 as prey for cod.



Figures 3.2.1.g,h. Plot of predicted suitabilities (SMOOTH) vs. log weight ratio (W_{pred}/W_{prey} ; g) and residuals (h) for Baltic sprat in Sub Divisions 26+28 as prey for cod.

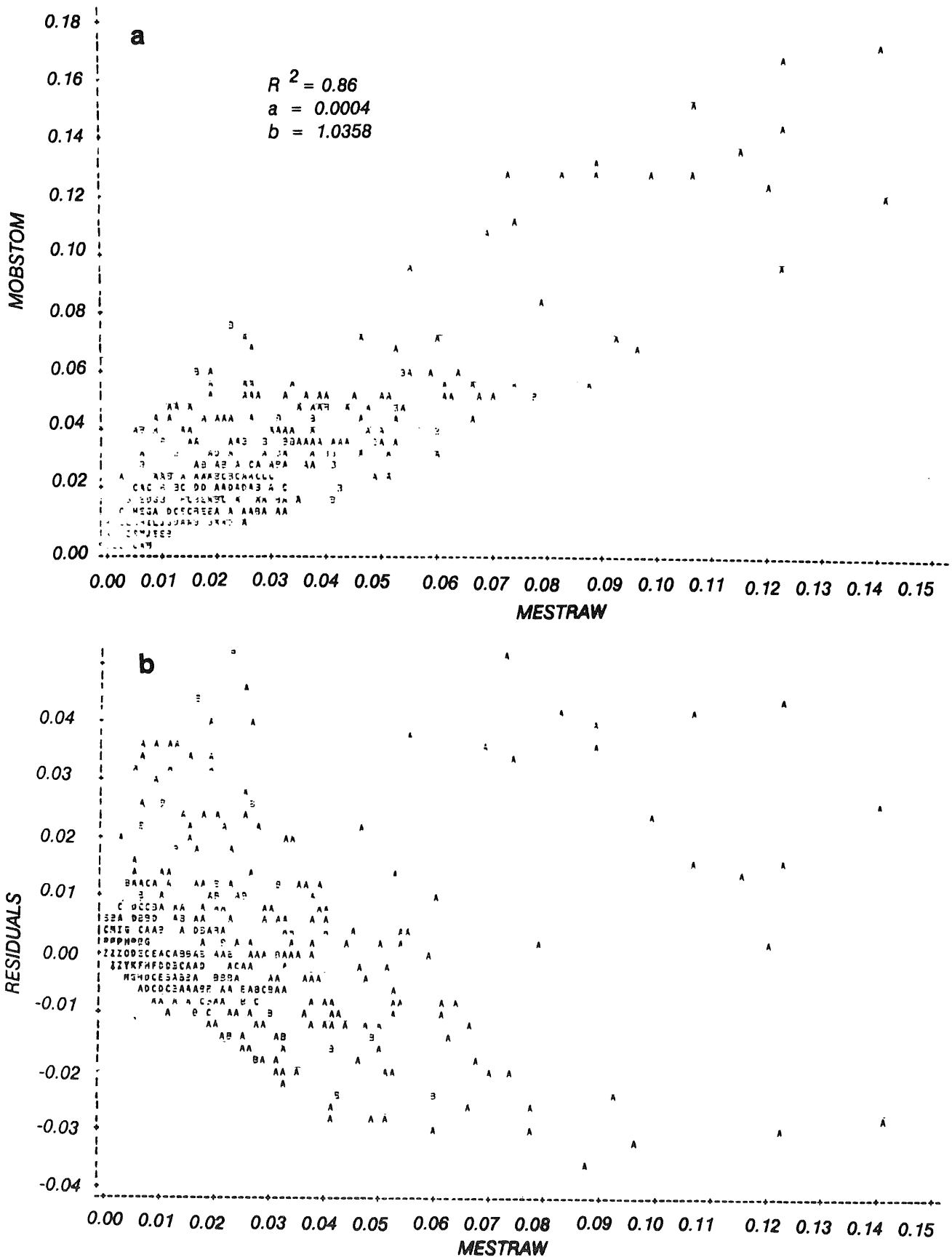
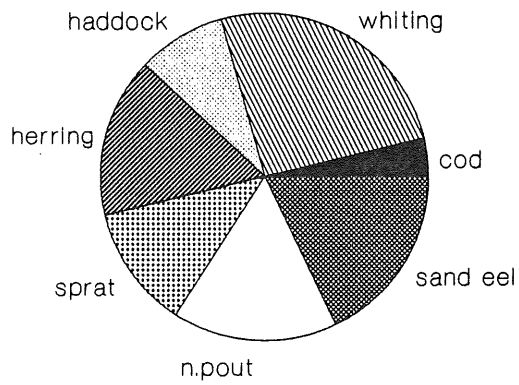


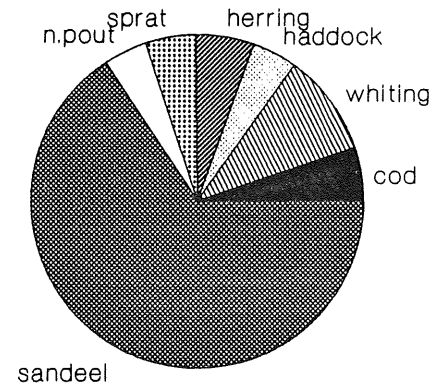
Figure 3.2.2. Observed stomach contents in odd years vs. predicted stomach contents in even years for cod as predator in MSVPA results for the Baltic Sea. Regression results are given in plot a (above), residuals from the regression are given in plot b (below). Analyses are based on use of 'raw' rather than smoothed suitability values.

PREDATOR = COD

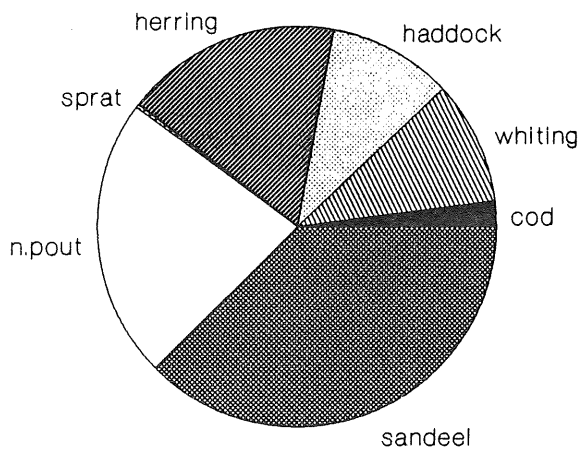
Qrt 1



Qrt 2



Qrt 3



Qrt 4

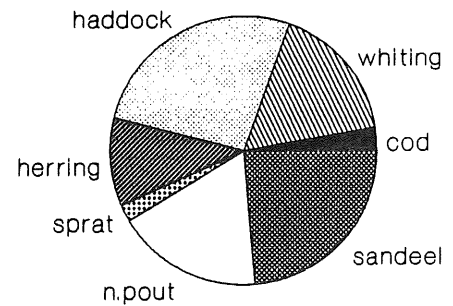
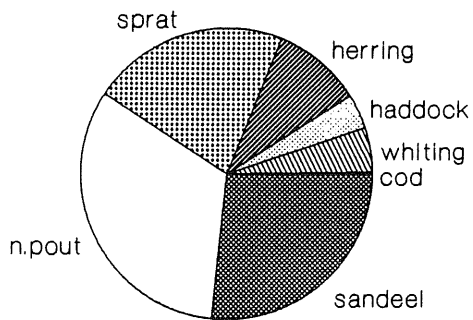


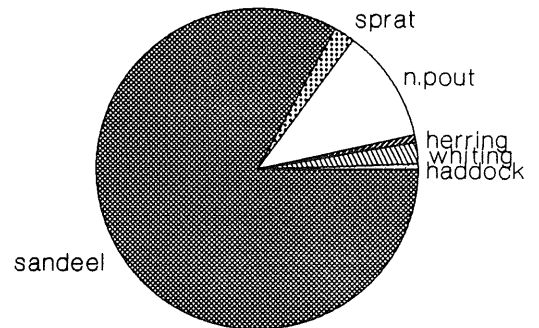
Figure 3.3.1a. Predicted 1991 consumption of MSVPA prey fish species (in percent wet weight) by North Sea cod. Data are presented by quarter, the area of the pies is proportional to total fish consumption among the quarters.

PREDATOR = WHITING

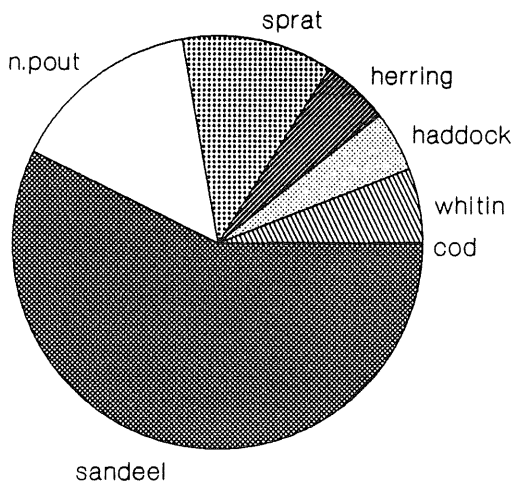
Qrt 1



Qrt 2



Qrt 3



Qrt 4

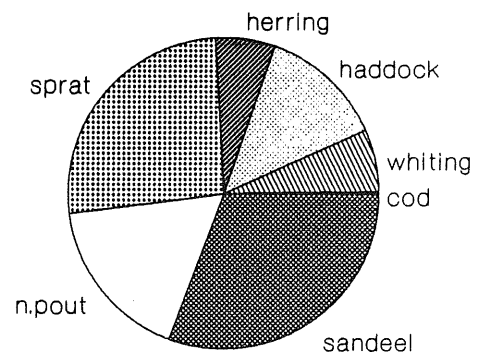
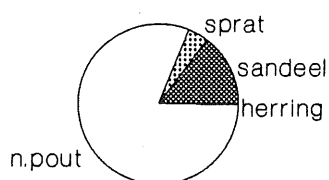


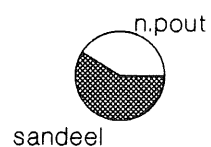
Figure 3.3.1b. Predicted 1991 consumption of MSVPA prey fish species (in percent wet weight) by North Sea whiting. Data are presented by quarter, the area of the pies is proportional to total fish consumption among the quarters.

PREDATOR = HADDOCK

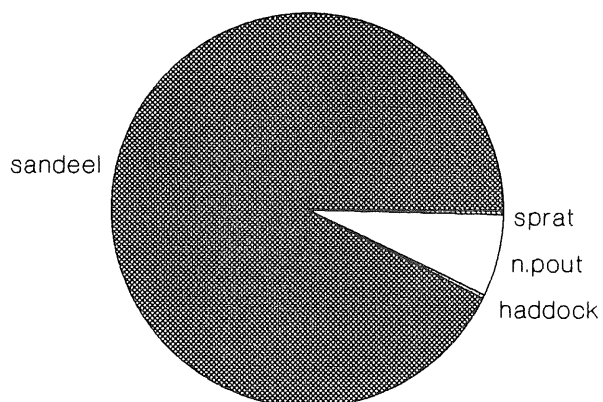
Qrt 1



Qrt 2



Qrt 3



Qrt 4

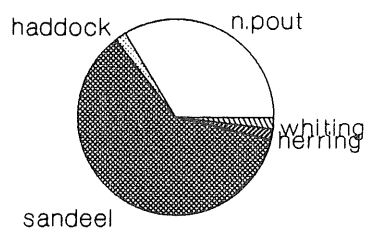


Figure 3.3.1c. Predicted 1991 consumption of MSVPA prey fish species (in percent wet weight) by North Sea haddock. Data are presented by quarter, the area of the pies is proportional to total fish consumption among the quarters.

PREDATOR = MACKEREL

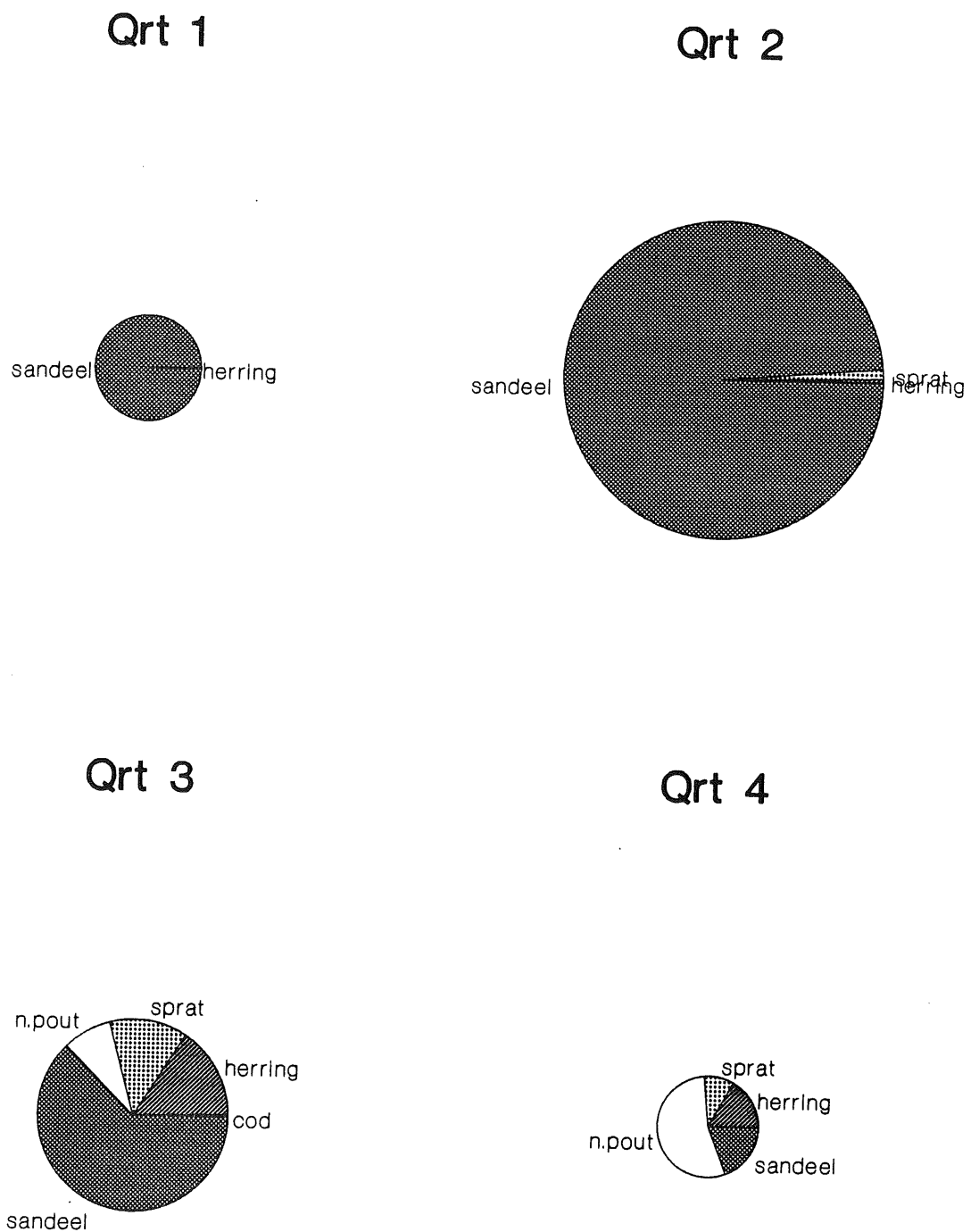


Figure 3.3.1d. Predicted 1991 consumption of MSVPA prey fish species (in percent wet weight) by mackerel. Data are presented by quarter, the area of the pies is proportional to total fish consumption among the quarters.

PREDATOR = SAITHE

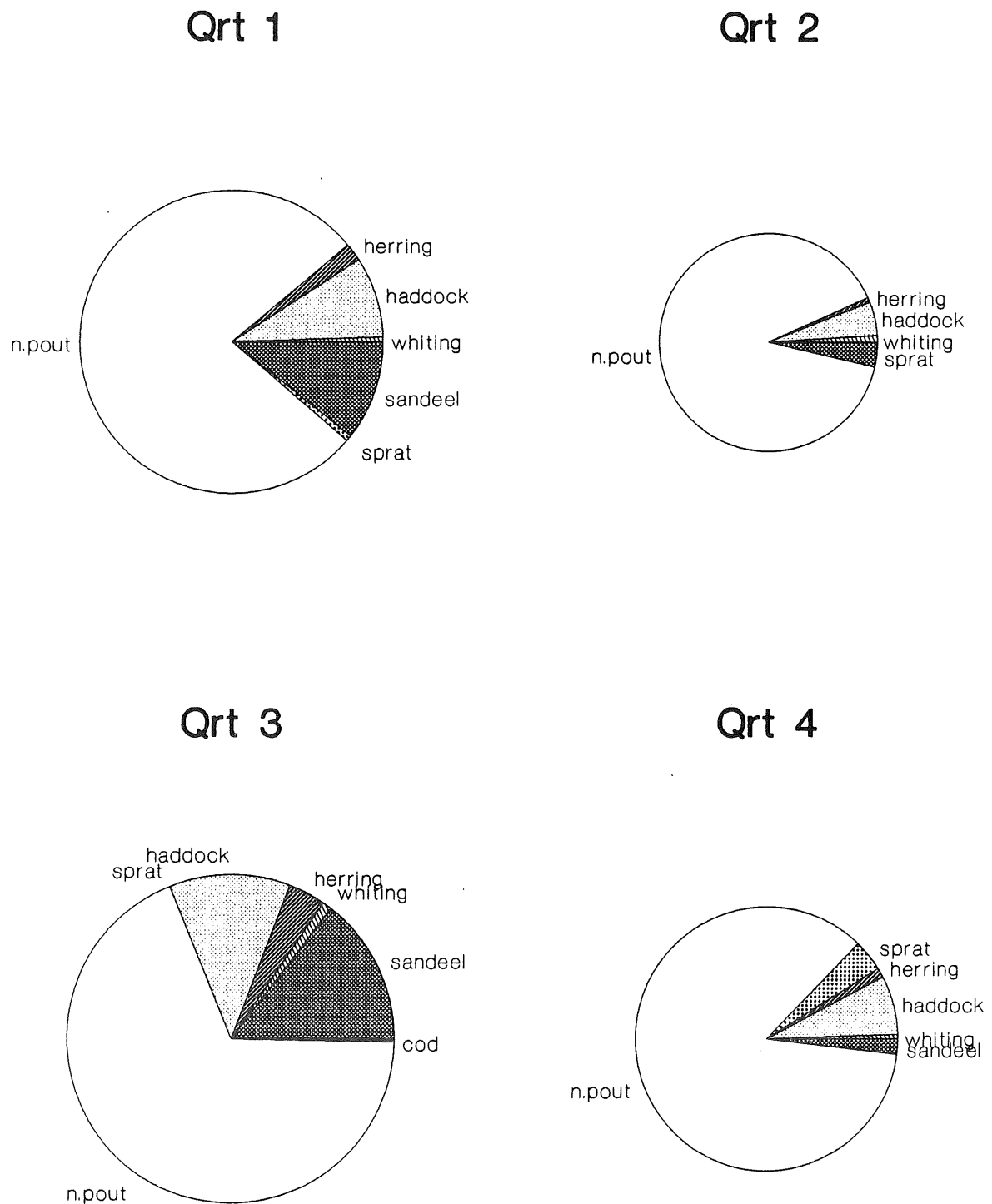


Figure 3.3.1e. Predicted 1991 consumption of MSVPA prey fish species (in percent wet weight) by saithe. Data are presented by quarter, the area of the pies is proportional to total fish consumption among the quarters.

Sensitivity Analysis Response of Fish Yield

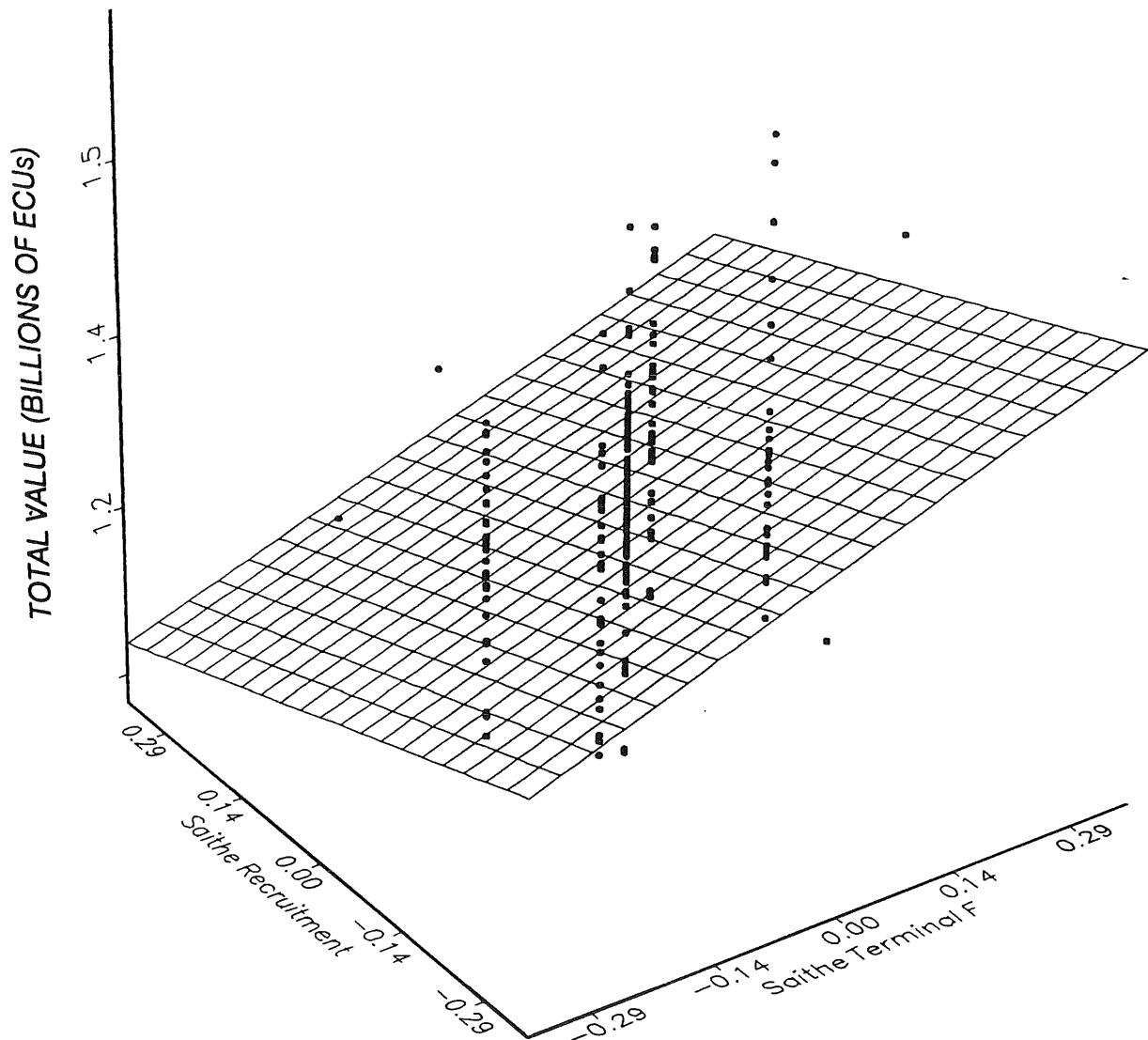


Figure 4.3.3.1. Sensitivity of long-term total system yield in value (billions of ECUs) to changes in average saithe recruitment and terminal fishing mortality rate on saithe. Results are from fractional factorial simulation experiments using the MSFOR model (Table 4.3.3.2). Dots represent total system value calculated for each of the 128 simulation experiments in two-dimensional state space (e.g., parameters = saithe recruitment and saithe terminal F). Slopes of the linear plane in these two dimensions are given by the sensitivity coefficients (Table 4.3.2.2). Values are extrapolated to $\pm 30\%$ of the nominal parameter values.

Sensitivity Analysis Response of Fish Yield

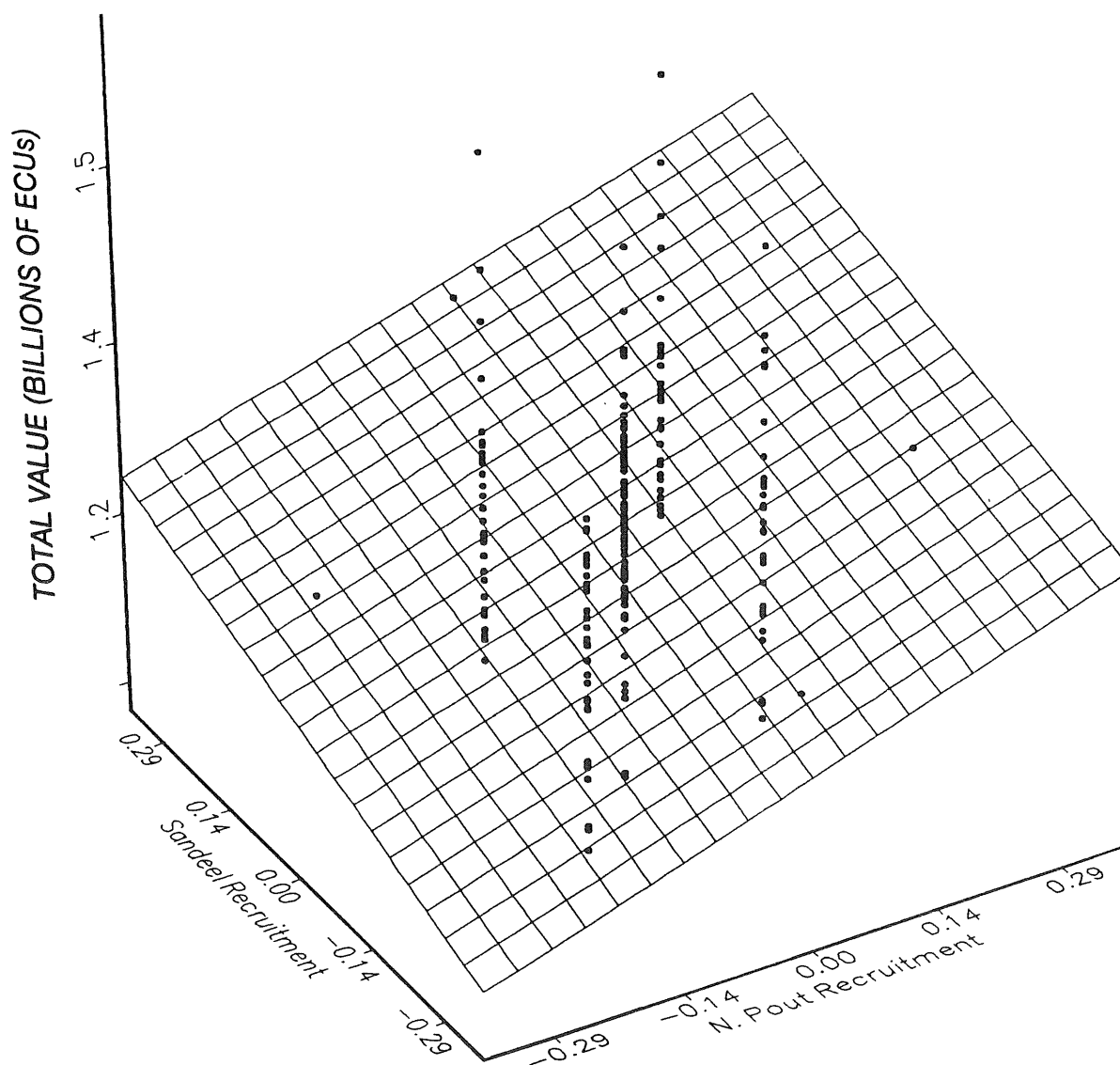


Figure 4.3.3.2. Sensitivity of long-term total system yield in value (billions of ECUs) to changes in average sandeel and Norway pout recruitment. Results are from fractional factorial simulation experiments using the MSFOR model (Table 4.3.3.2). Dots represent total system value calculated for each of the 128 simulation experiments in two-dimensional state space (e.g., parameters = sandeel recruitment and Norway pout recruitment). Slopes of the linear plane in these two dimensions are given by the sensitivity coefficients (Table 4.3.2.2). Values are extrapolated to $\pm 30\%$ of the nominal parameter values.

Sensitivity Analysis Response of Fish Yield

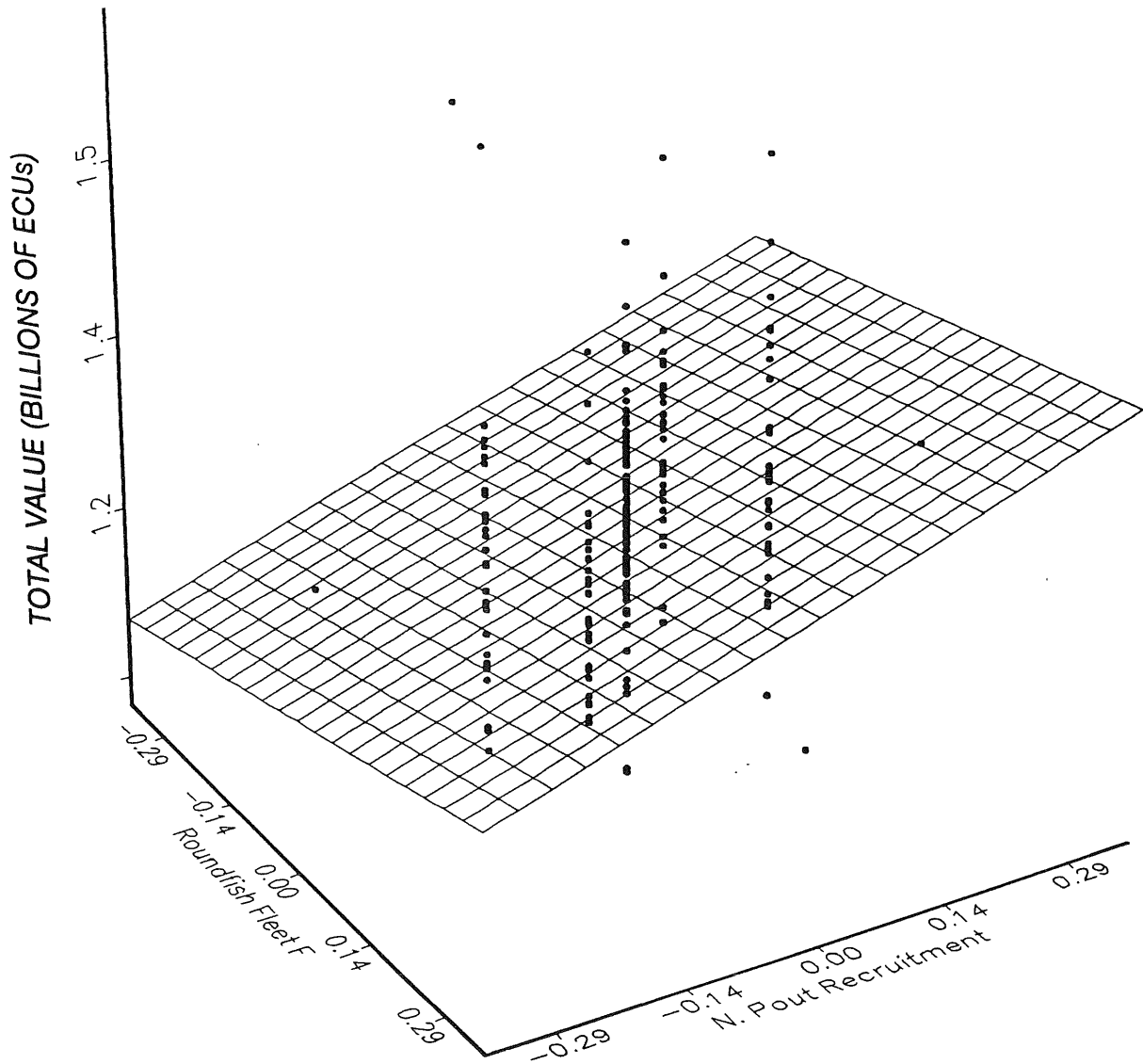


Figure 4.3.3.3. Sensitivity of long-term total system yield in value (billions of ECUs) to changes in roundfish fleet fishing effort and Norway pout recruitment. Results are from fractional factorial simulation experiments using the MSFOR model (Table 4.3.3.2). Dots represent total system value calculated for each of the 128 simulation experiments in two-dimensional state space (e.g., parameters = roundfish fleet fishing effort and Norway pout recruitment). Slopes of the linear plane in these two dimensions are given by the sensitivity coefficients (Table 4.3.2.2). Values are extrapolated to $\pm 30\%$ of the nominal parameter values.

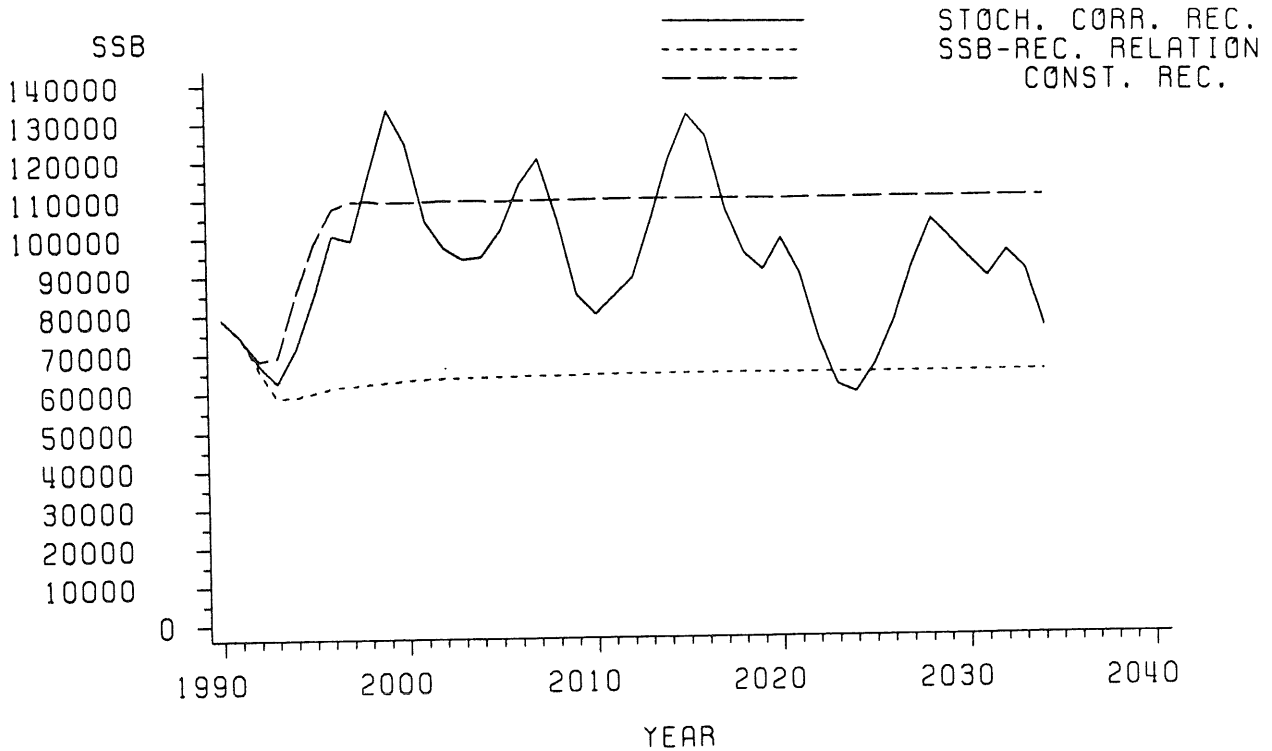


Figure 4.4a. Results of long-term stochastic simulations with MSFOR for spawning stock biomass of cod in the North Sea. Simulations compare three methods for incorporating recruitment into forecasts: (1) constant recruitment based on the mean estimated from MSVPA, (2) from parametric SSB-recruitment, and (3) stochastic simulations with recruitment strength correlated among some species.

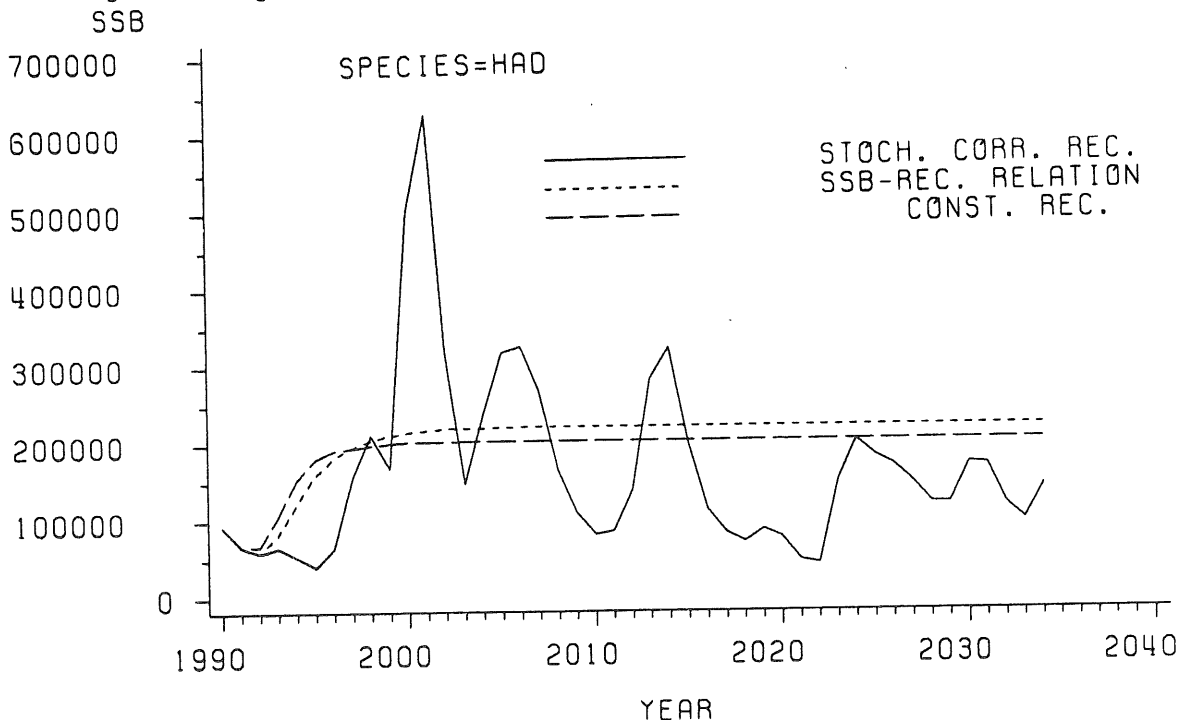


Figure 4.4b. Results of long-term stochastic simulations with MSFOR for spawning stock biomass of haddock in the North Sea. Simulations compare three methods for incorporating recruitment into forecasts: (1) constant recruitment based on the mean estimated from MSVPA, (2) from parametric SSB-recruitment, and (3) stochastic simulations with recruitment strength correlated among some species.

SPECIES=WHI

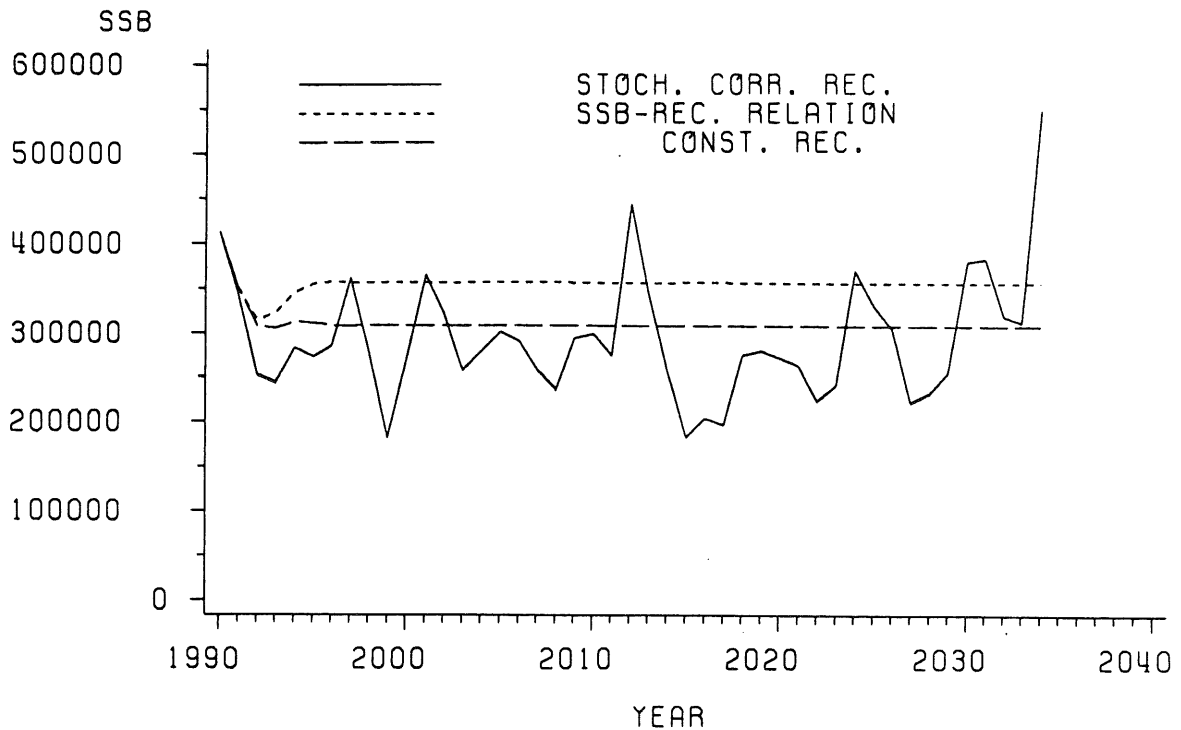


Figure 4.4c. Results of long-term stochastic simulations with MSFOR for spawning stock biomass of whiting in the North Sea. Simulations compare three methods for incorporating recruitment into forecasts: (1) constant recruitment based on the mean estimated from MSVPA, (2) from parametric SSB-recruitment, and (3) stochastic simulations with recruitment strength correlated among some species.

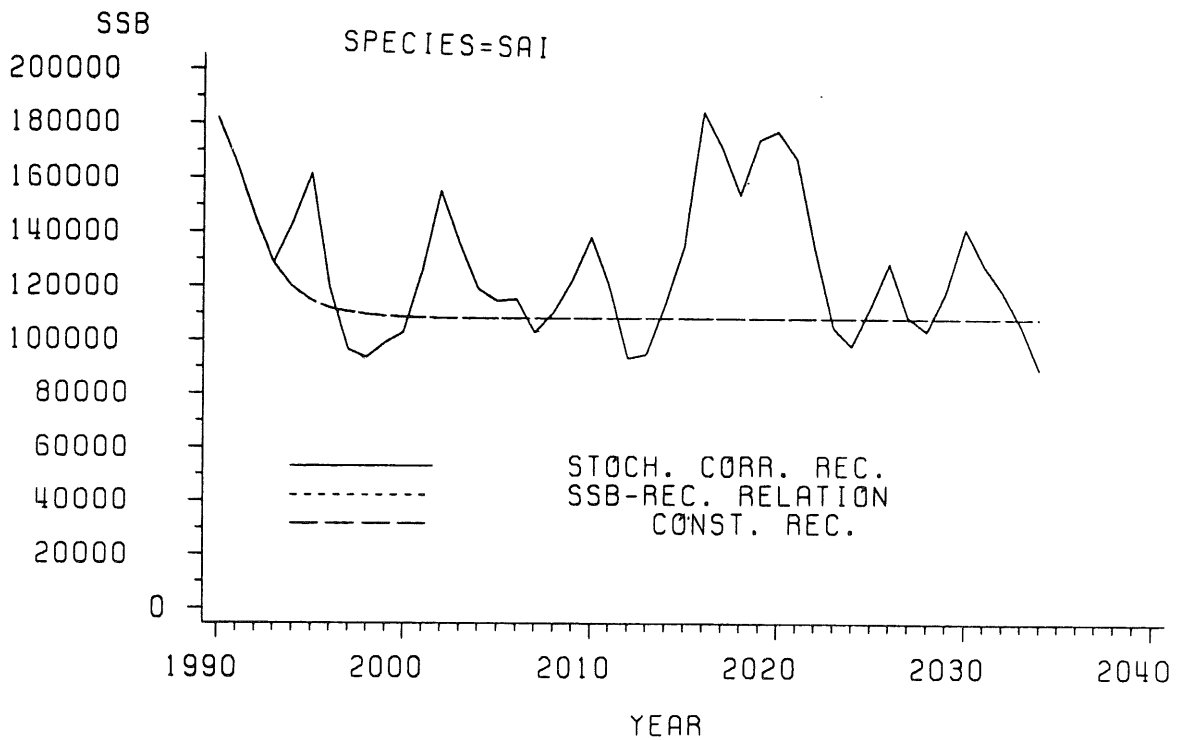


Figure 4.4d. Results of long-term stochastic simulations with MSFOR for spawning stock biomass of saithe in the North Sea. Simulations compare three methods for incorporating recruitment into forecasts: (1) constant recruitment based on the mean estimated from MSVPA, (2) from parametric SSB-recruitment, and (3) stochastic simulations with recruitment strength correlated among some species.

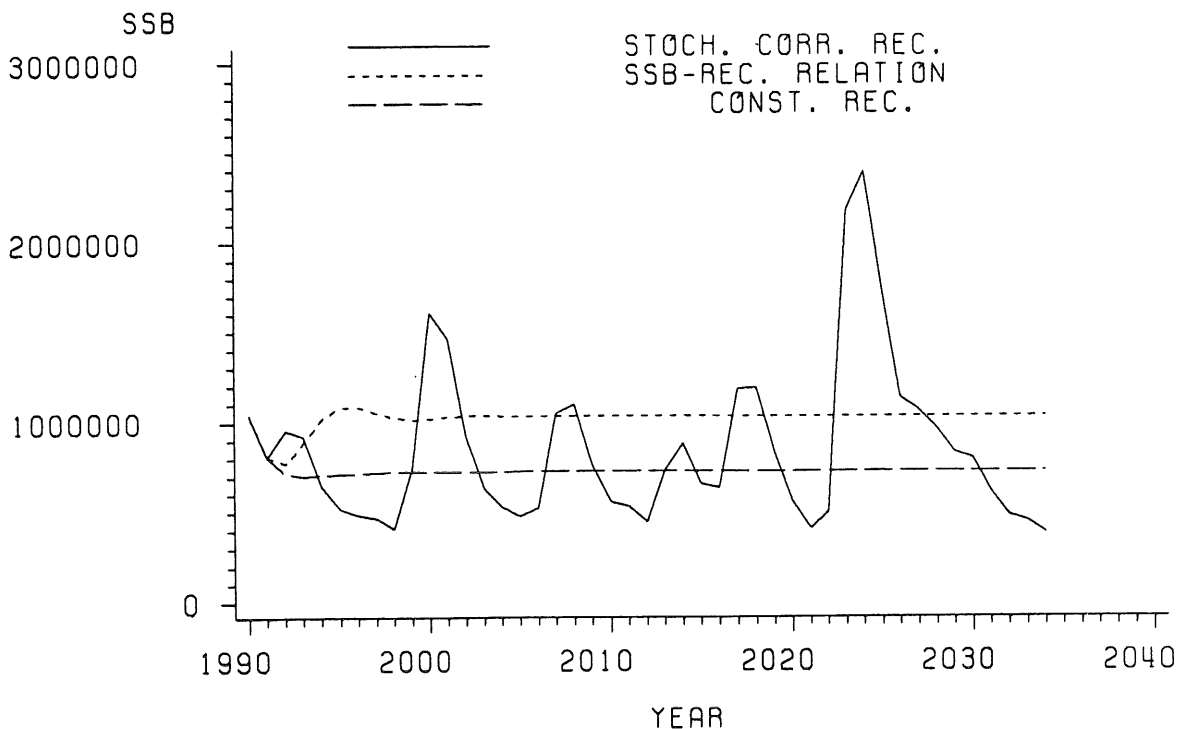


Figure 4.4e. Results of long-term stochastic simulations with MSFOR for spawning stock biomass of herring in the North Sea. Simulations compare three methods for incorporating recruitment into forecasts: (1) constant recruitment based on the mean estimated from MSVPA, (2) from parametric SSB-recruitment, and (3) stochastic simulations with recruitment strength correlated among some species.

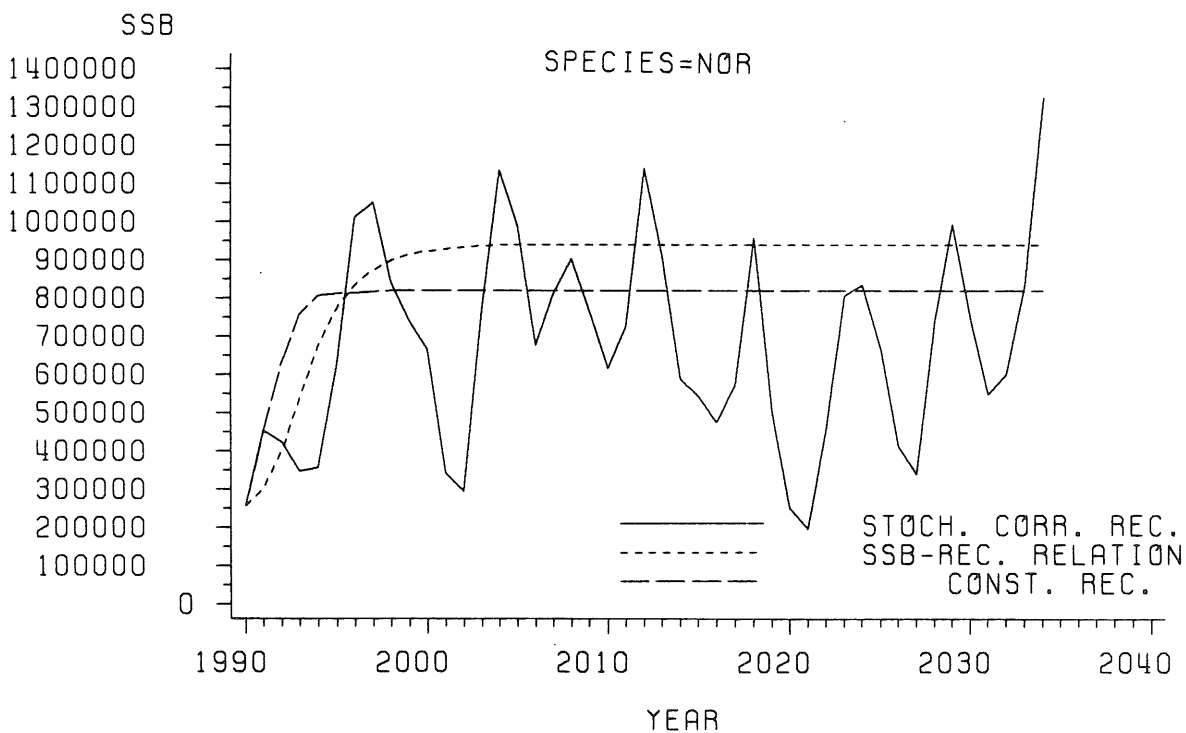


Figure 4.4f. Results of long-term stochastic simulations with MSFOR for spawning stock biomass of Norway pout in the North Sea. Simulations compare three methods for incorporating recruitment into forecasts: (1) constant recruitment based on the mean estimated from MSVPA, (2) from parametric SSB-recruitment, and (3) stochastic simulations with recruitment strength correlated among some species.

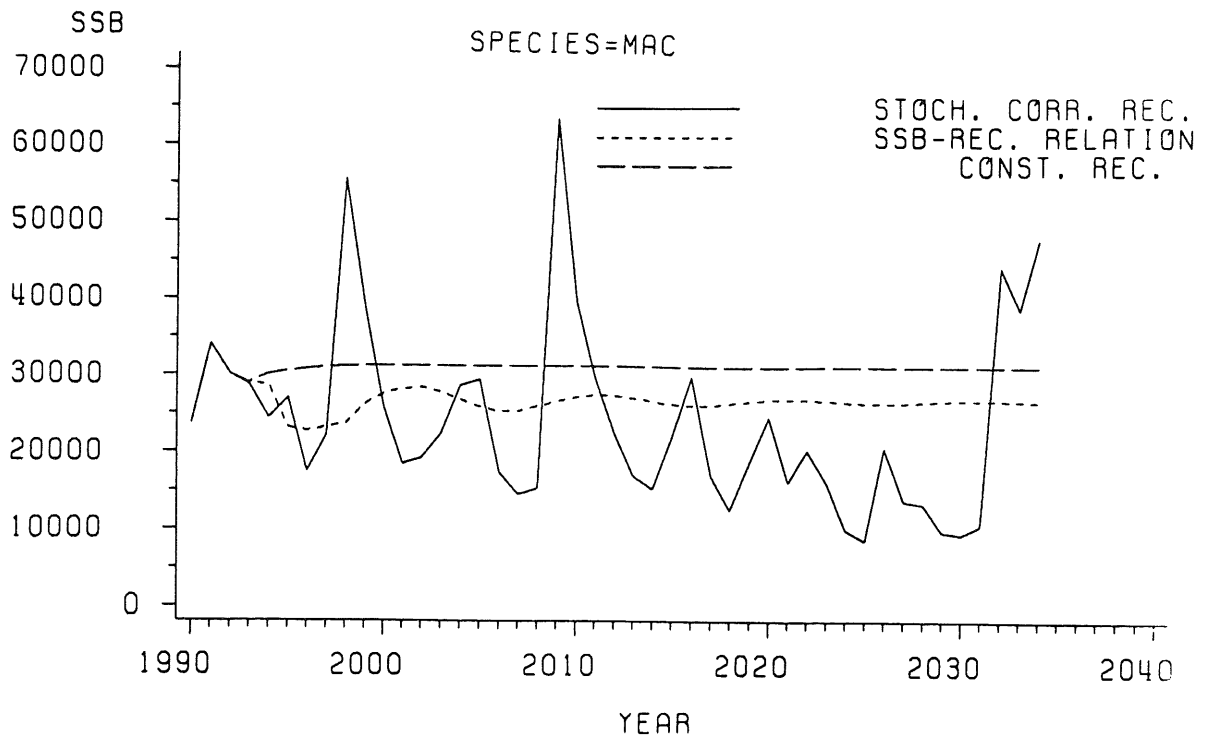


Figure 4.4g. Results of long-term stochastic simulations with MSFOR for spawning stock biomass of mackerel in the North Sea. Simulations compare three methods for incorporating recruitment into forecasts: (1) constant recruitment based on the mean estimated from MSVPA, (2) from parametric SSB-recruitment, and (3) stochastic simulations with recruitment strength correlated among some species.

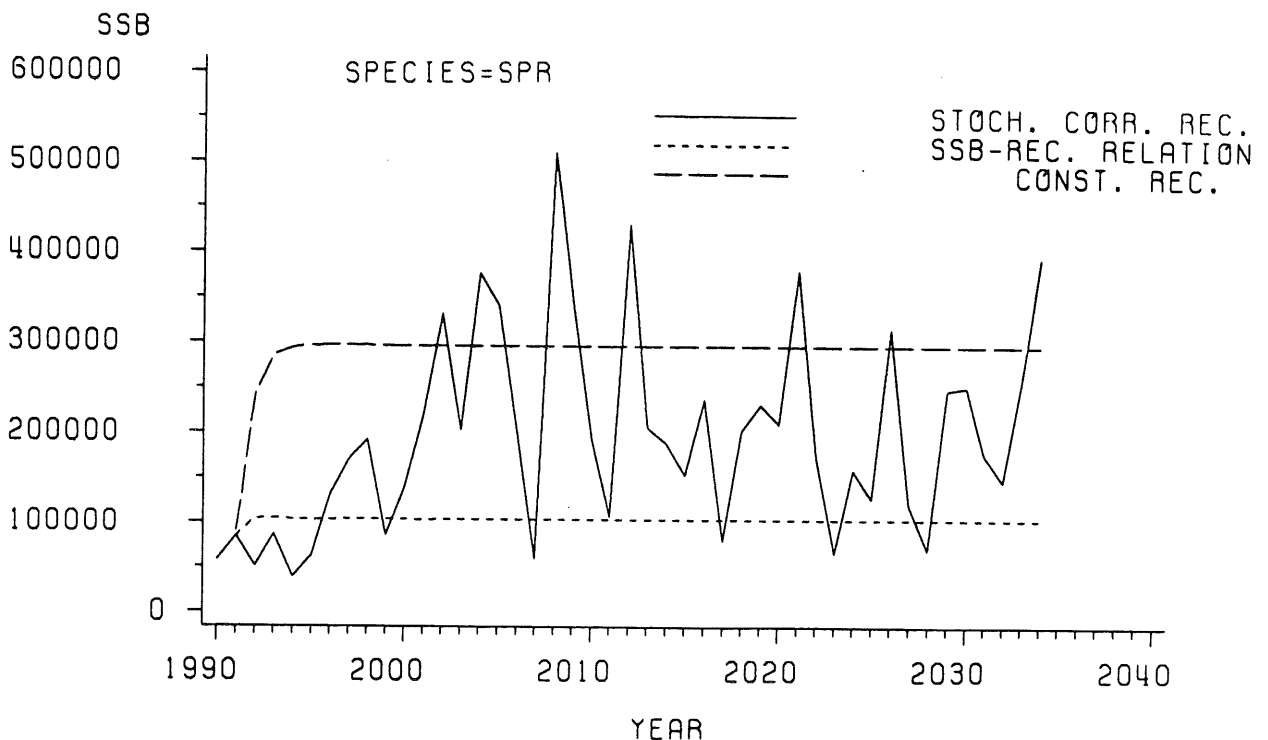


Figure 4.4h. Results of long-term stochastic simulations with MSFOR for spawning stock biomass of sprat in the North Sea. Simulations compare three methods for incorporating recruitment into forecasts: (1) constant recruitment based on the mean estimated from MSVPA, (2) from parametric SSB-recruitment, and (3) stochastic simulations with recruitment strength correlated among some species.

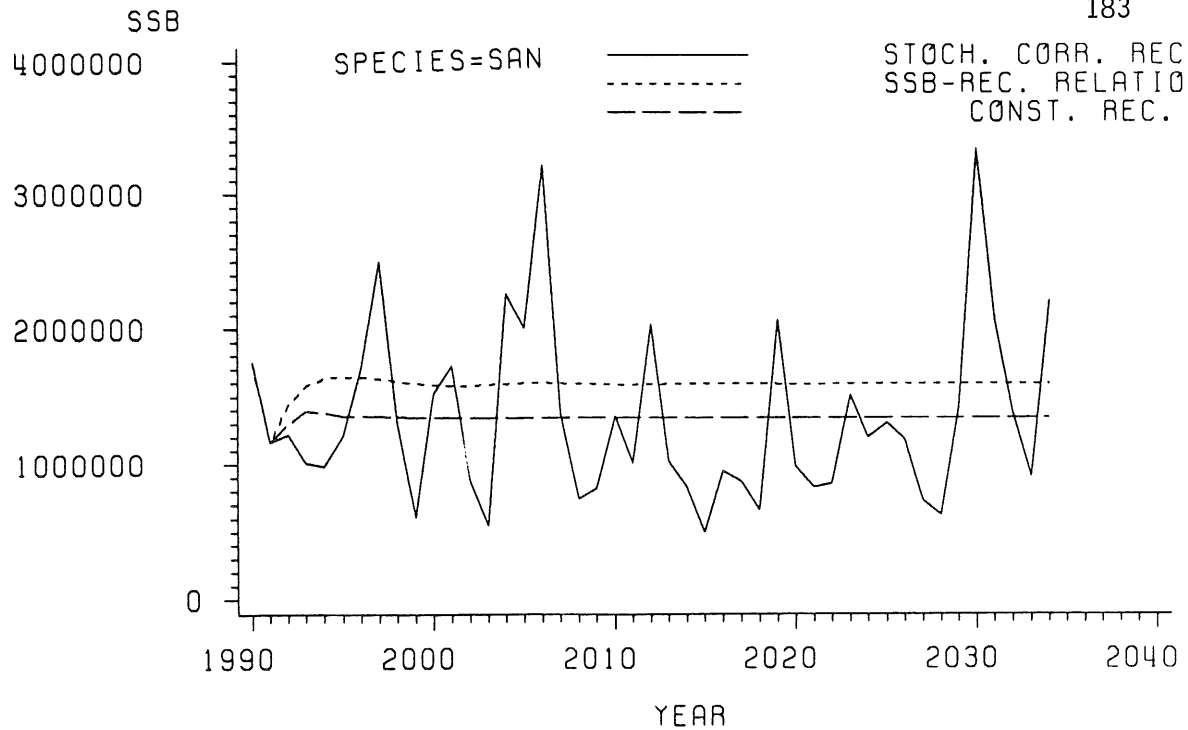


Figure 4.4i. Results of long-term stochastic simulations with MSFOR for spawning stock biomass of sand eel in the North Sea. Simulations compare three methods for incorporating recruitment into forecasts: (1) constant recruitment based on the mean estimated from MSVPA, (2) from parametric SSB-recruitment, and (3) stochastic simulations with recruitment strength correlated among some species.

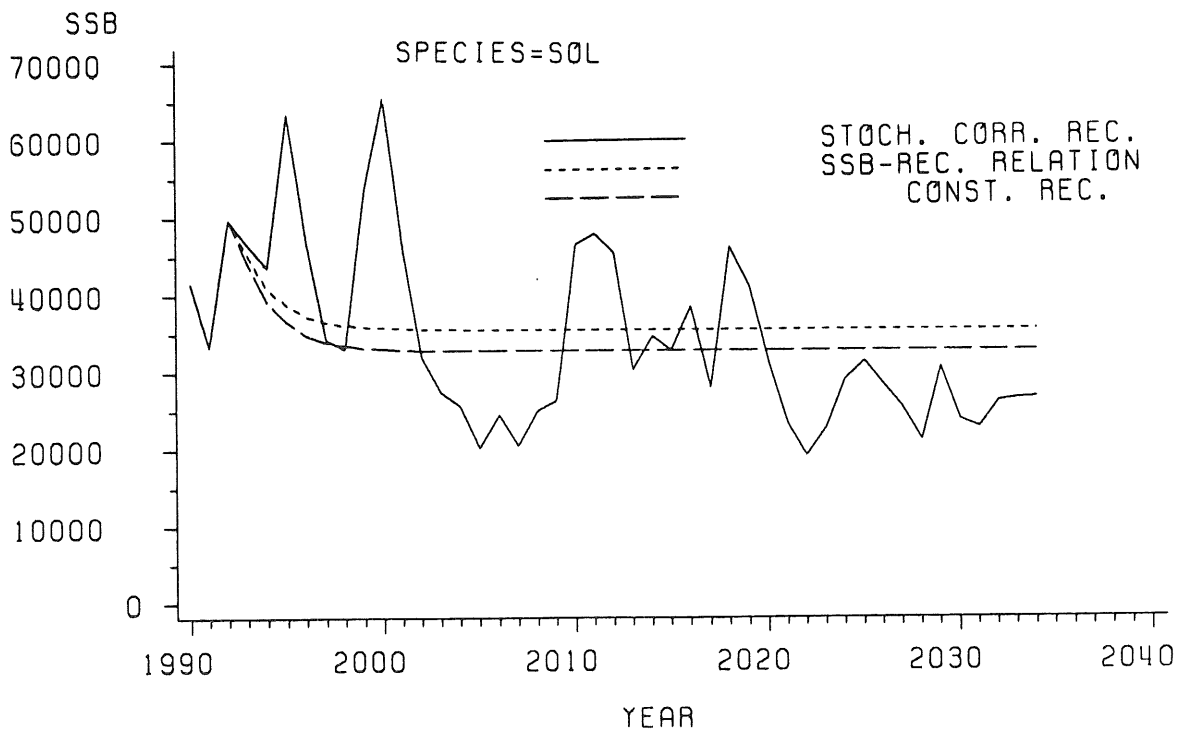


Figure 4.4j. Results of long-term stochastic simulations with MSFOR for spawning stock biomass of sole in the North Sea. Simulations compare three methods for incorporating recruitment into forecasts: (1) constant recruitment based on the mean estimated from MSVPA, (2) from parametric SSB-recruitment, and (3) stochastic simulations with recruitment strength correlated among some species.

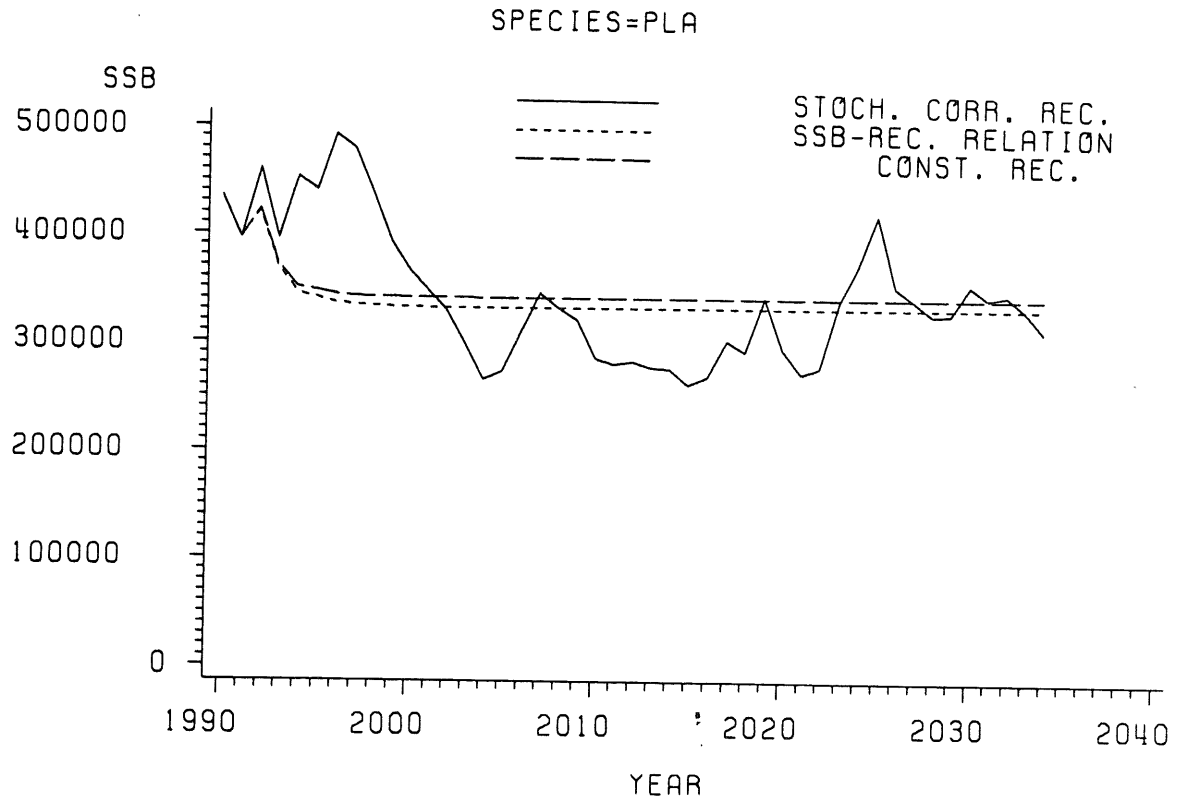


Figure 4.4k. Results of long-term stochastic simulations with MSFOR for spawning stock biomass of plaice in the North Sea. Simulations compare three methods for incorporating recruitment into forecasts: (1) constant recruitment based on the mean estimated from MSVPA, (2) from parametric SSB-recruitment, and (3) stochastic simulations with recruitment strength correlated among some species.

BARENTS SEA

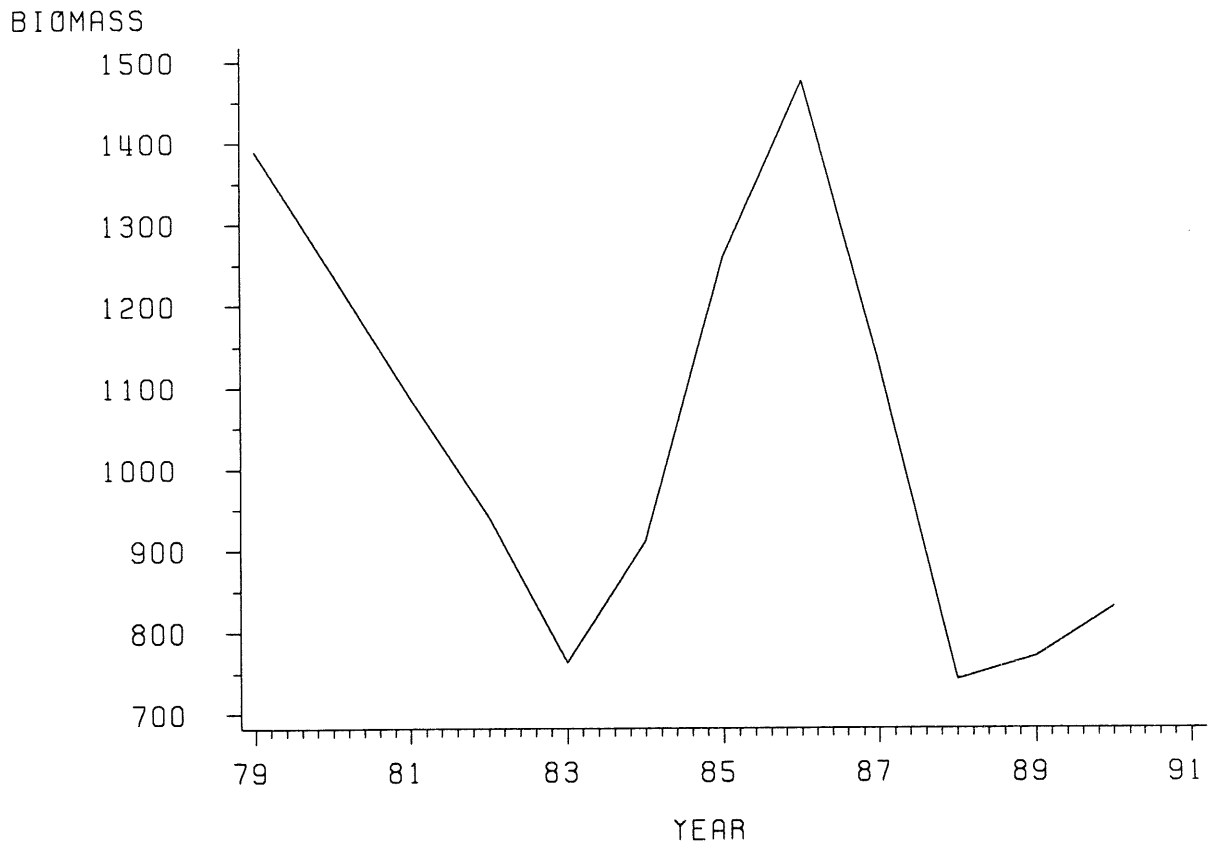


Figure 5.1.1.1. Cod biomass ('000tons) in the Barent Sea for the years 1979-90.

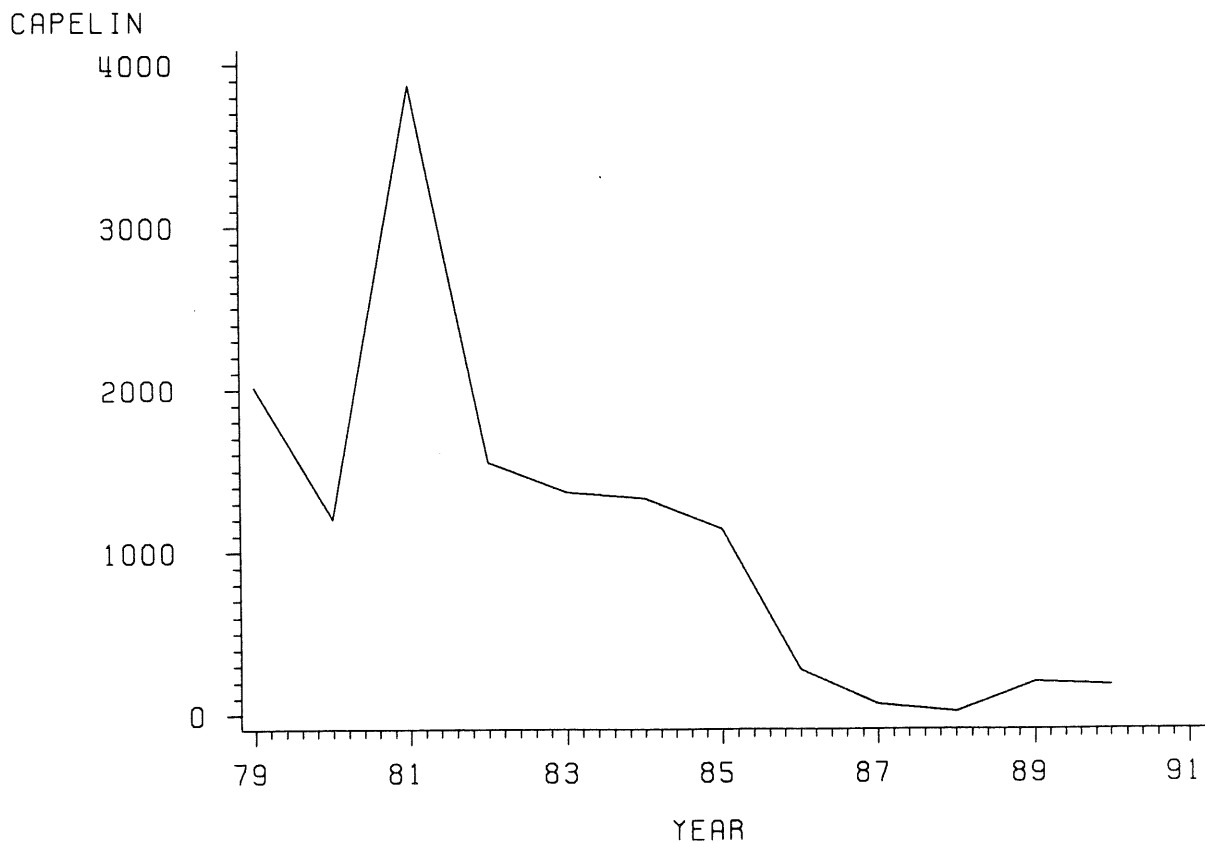


Figure 5.1.1.2. Capelin biomass ('000tons) in the Barents Sea for the years 1979-90.

BARENTS SEA

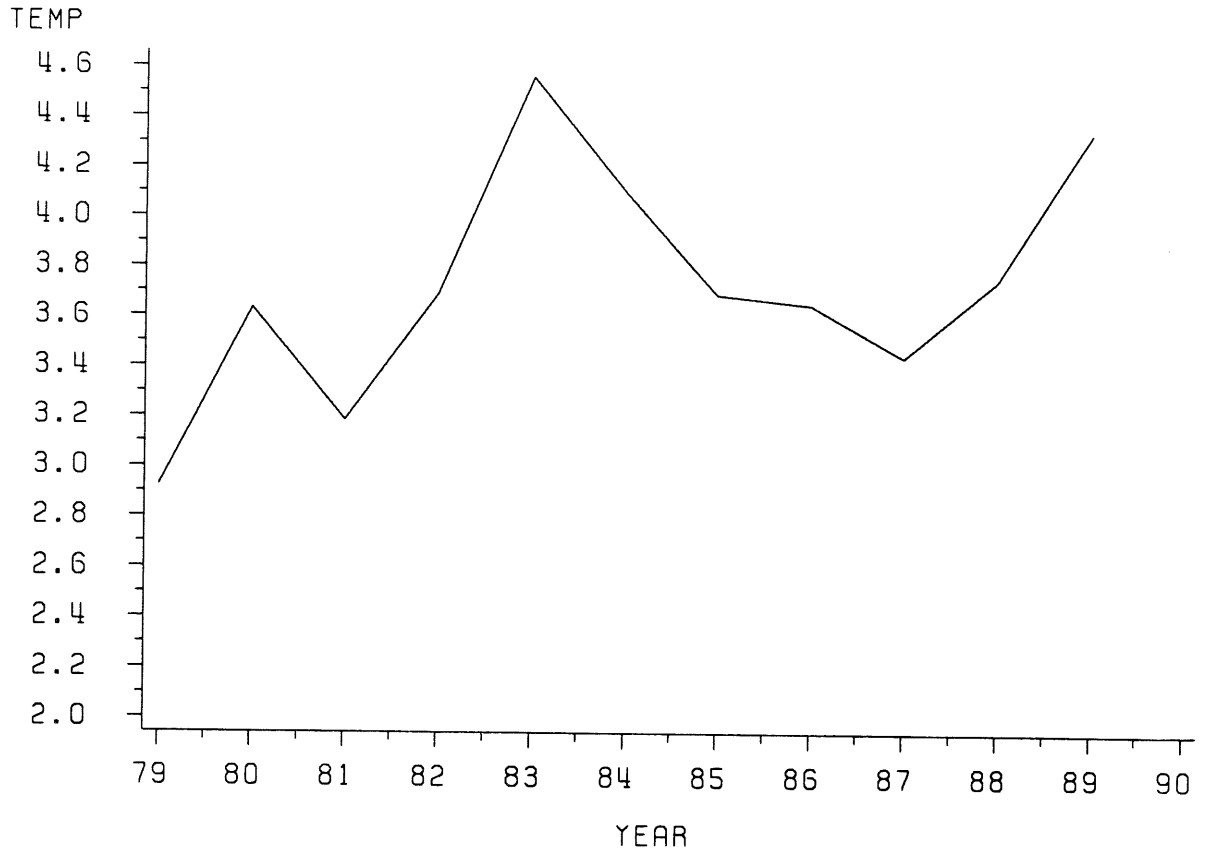


Figure 5.1.1.3. Temperature (°C) in the Barents Sea for the period 1979-89.

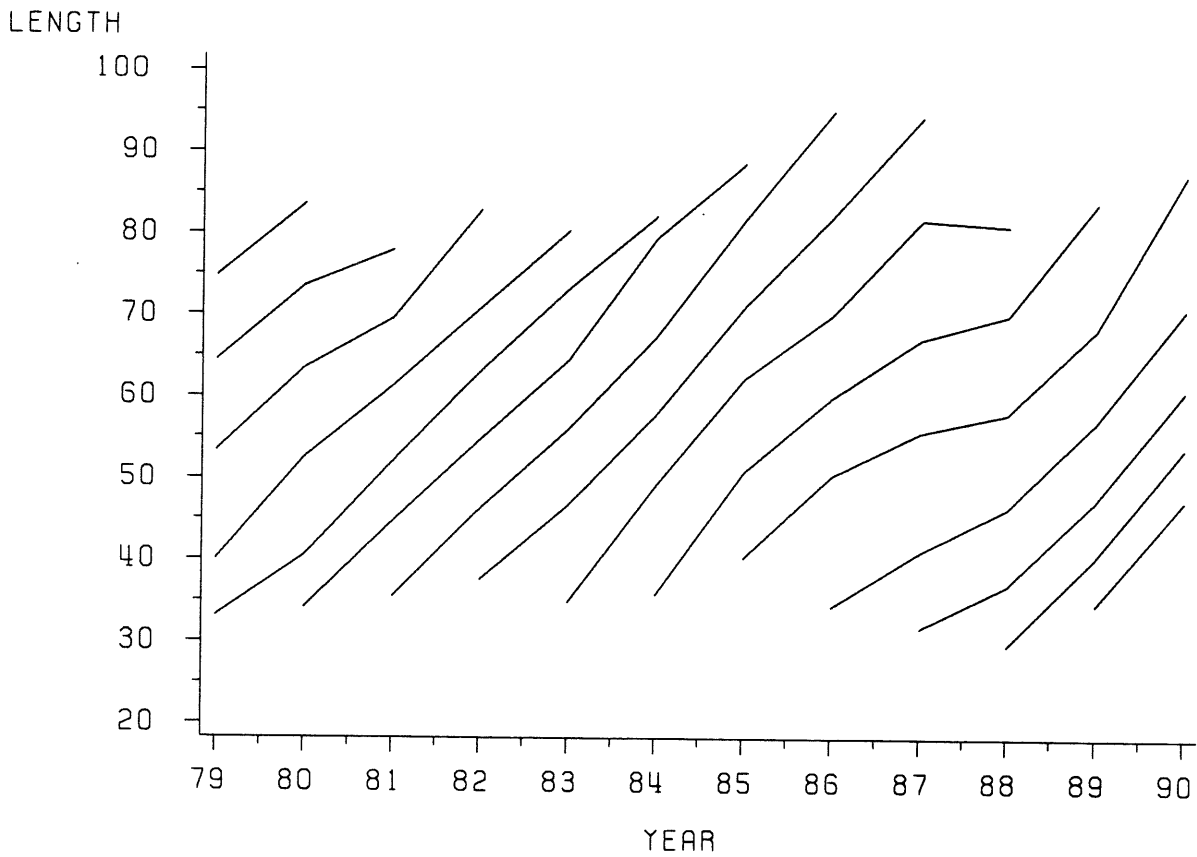


Figure 5.1.1.4. Cohort growth in the Barents Sea in terms of length at year.

BARENTS SEA

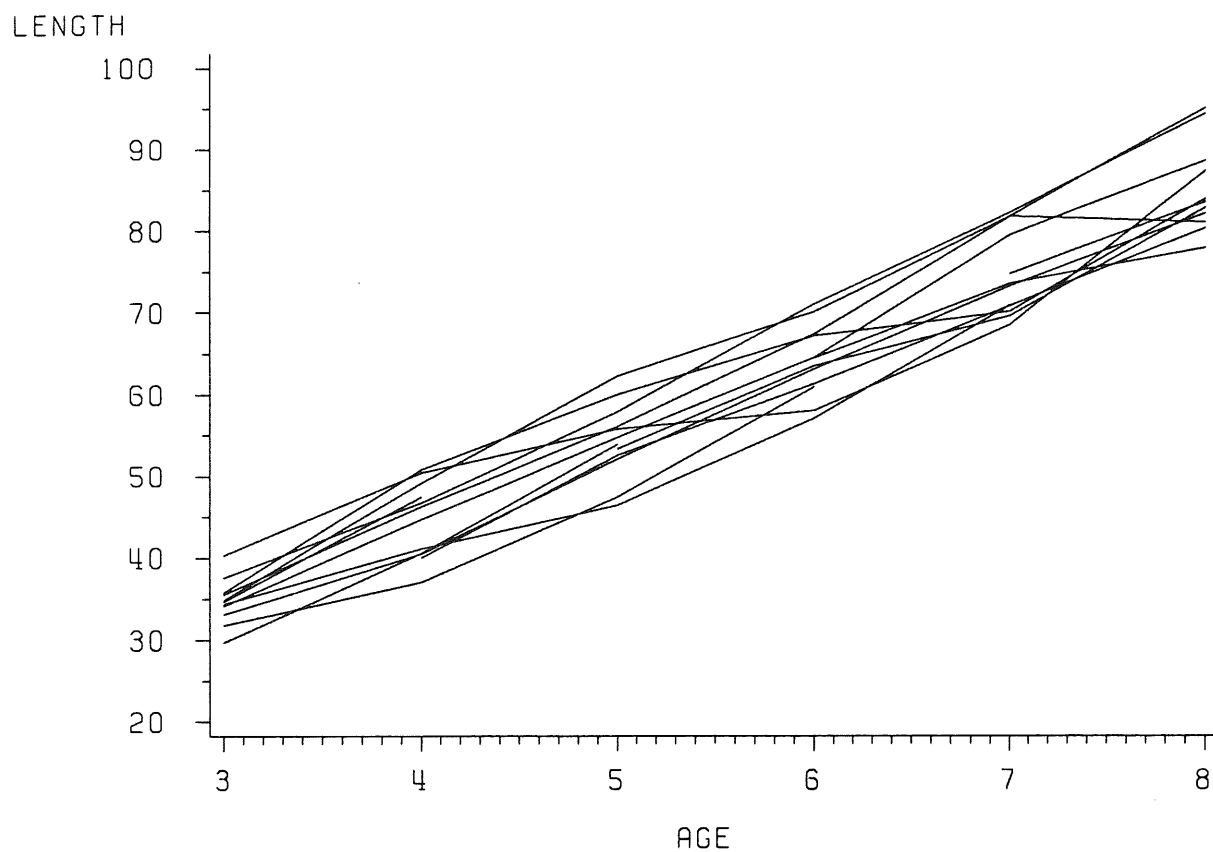


Figure 5.1.1.5. Cohort growth in the Barents Sea in terms of length at age.

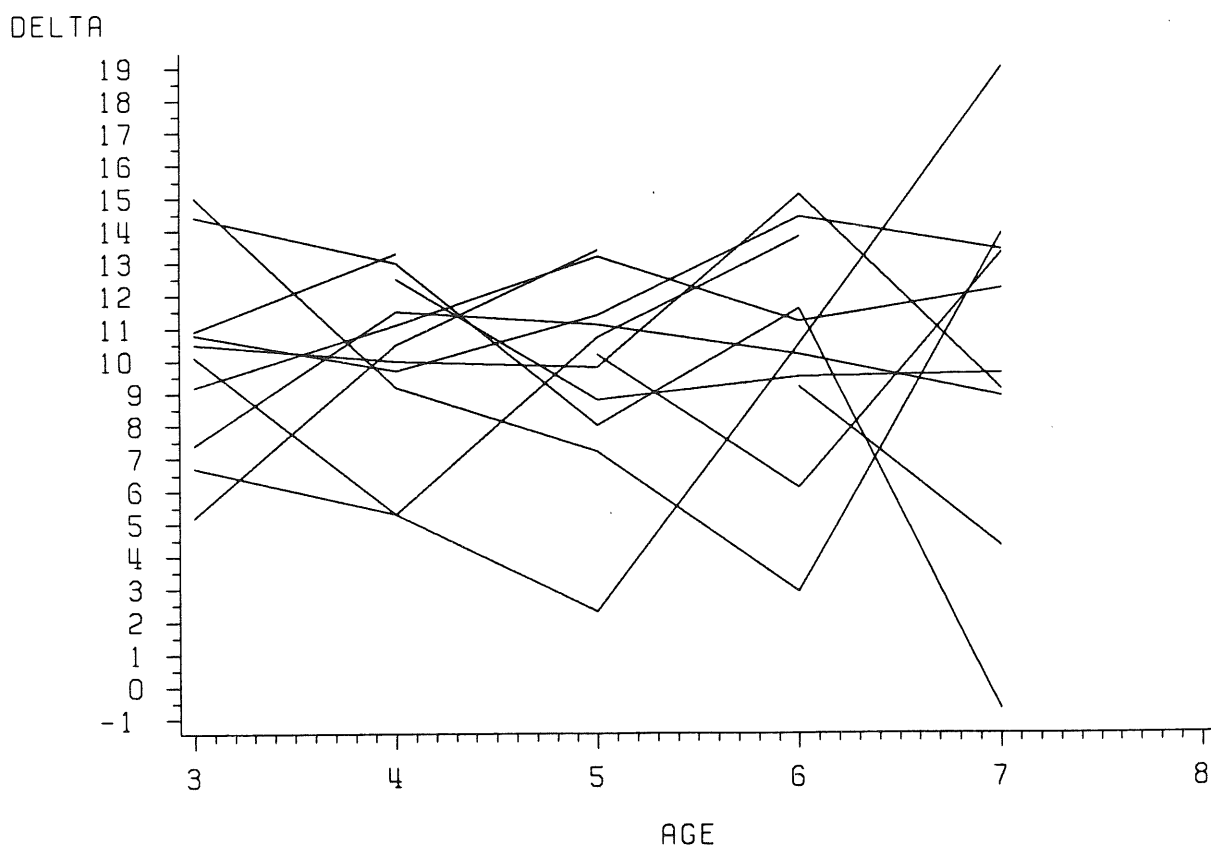


Figure 5.1.1.6. Length increment (delta) by cohort at each age for the Barents Sea.

BARENTS SEA

DELTA

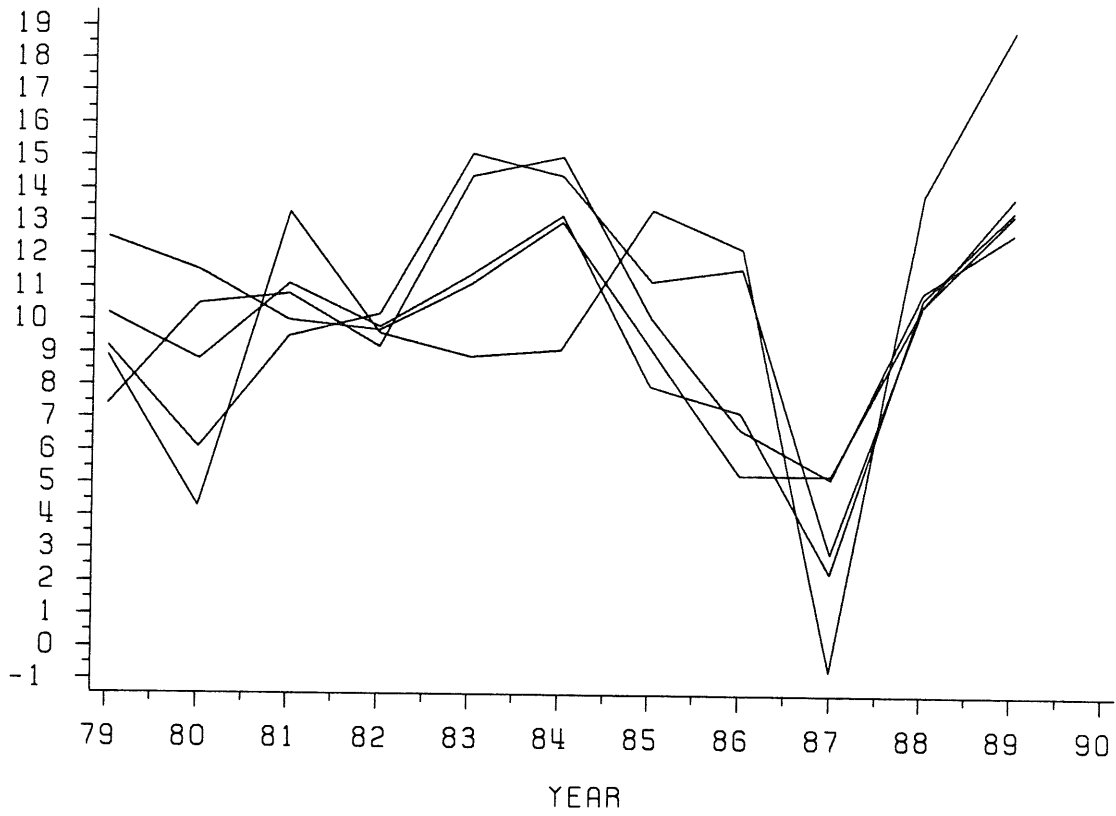


Figure 5.1.1.7. Length increment (delta) by cohort at each year for the Barents Sea.

LENGTH

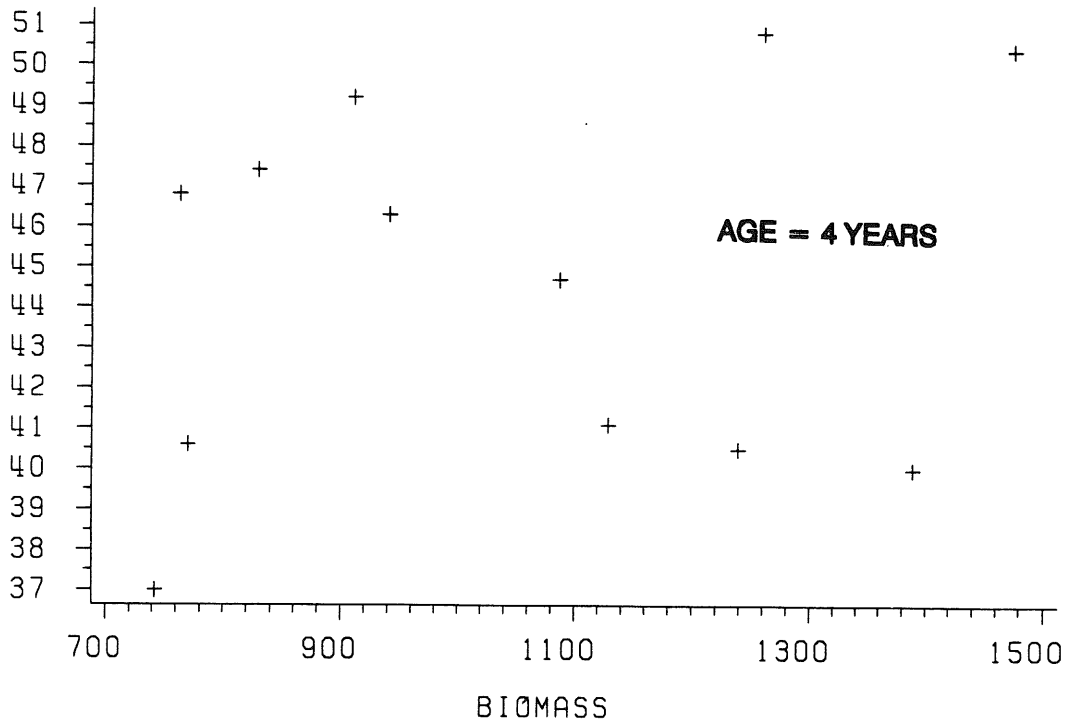


Figure 5.1.1.8. Length at age 4 against cod biomass for the Barents Sea.

BARENTS SEA

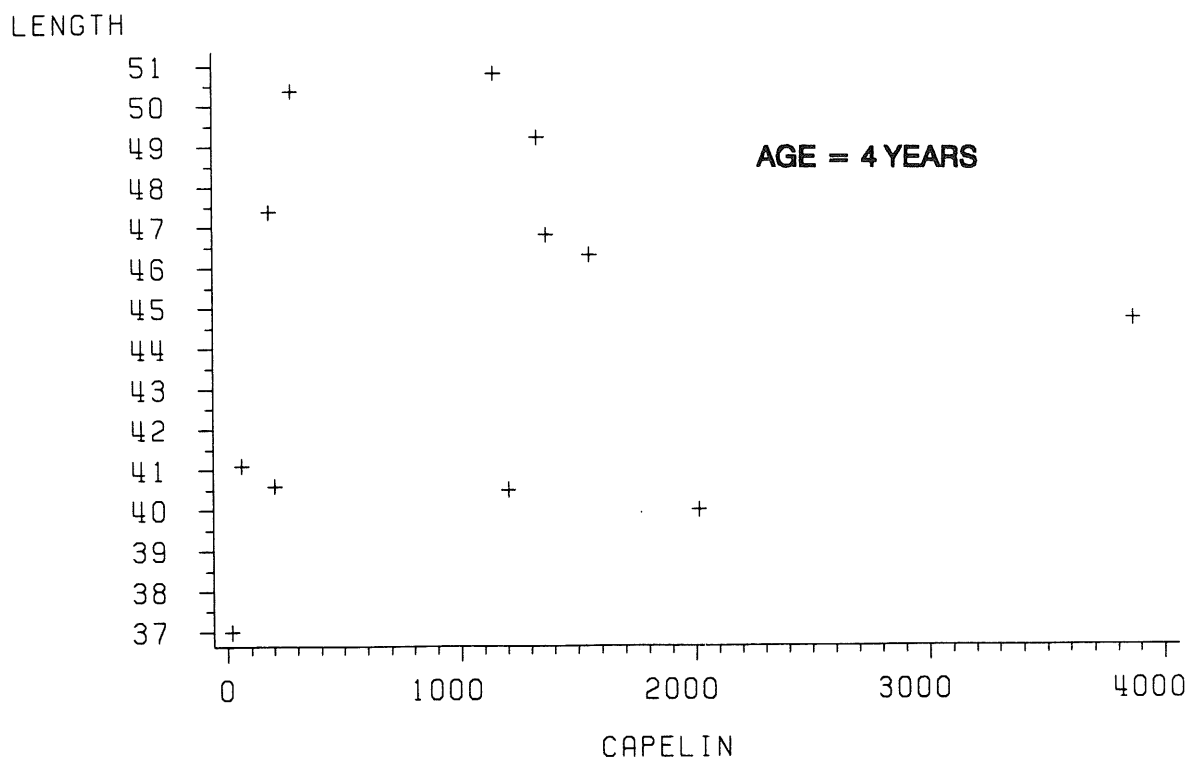


Figure 5.1.1.9. Length at age 4 against capelin biomass for the Barents Sea.

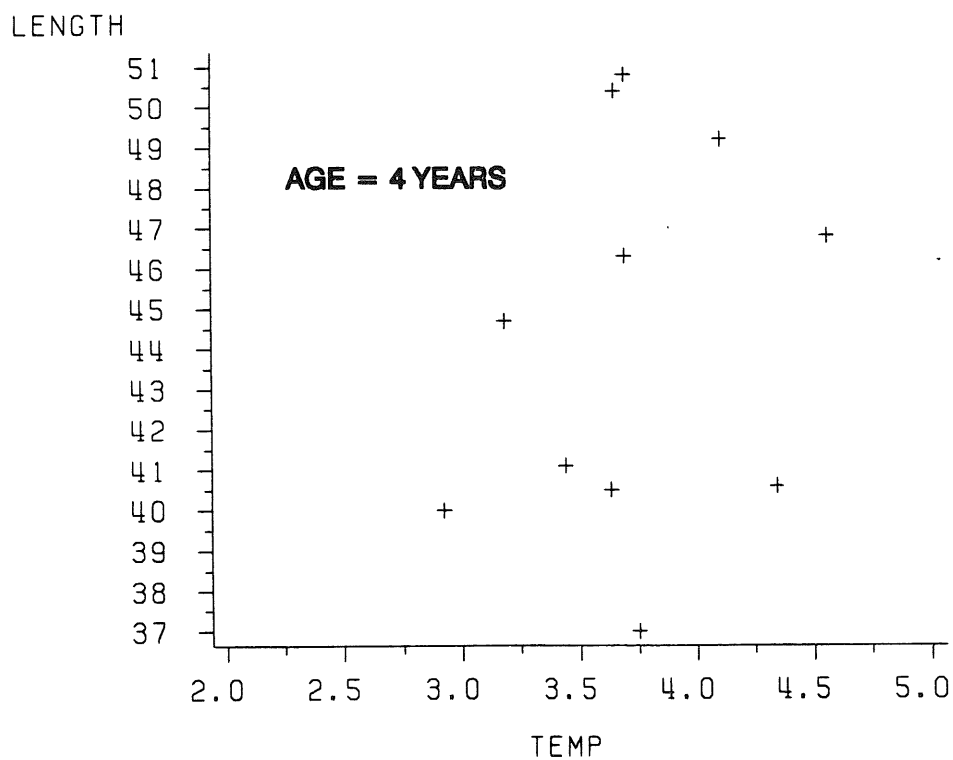


Figure 5.1.1.10. Length at age 4 against temperature for the Barents Sea.

BARENTS SEA

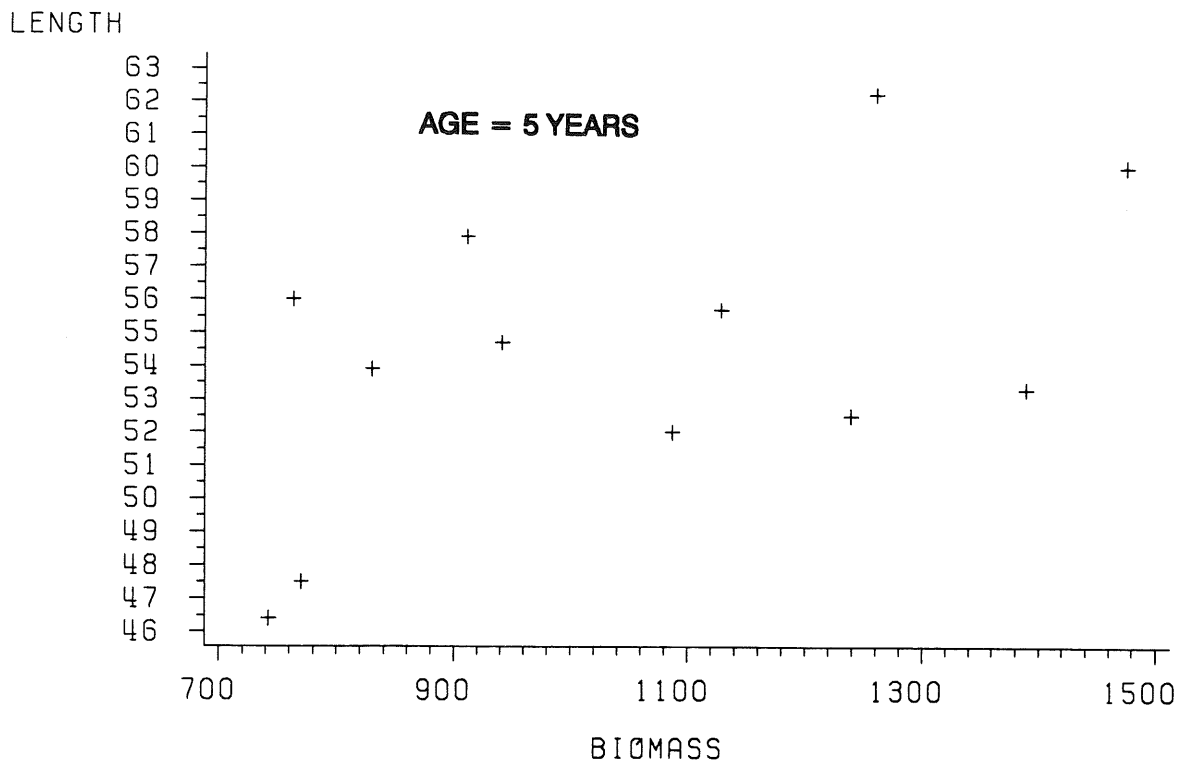


Figure 5.1.1.11. Length at age 5 against cod biomass for the Barents Sea.

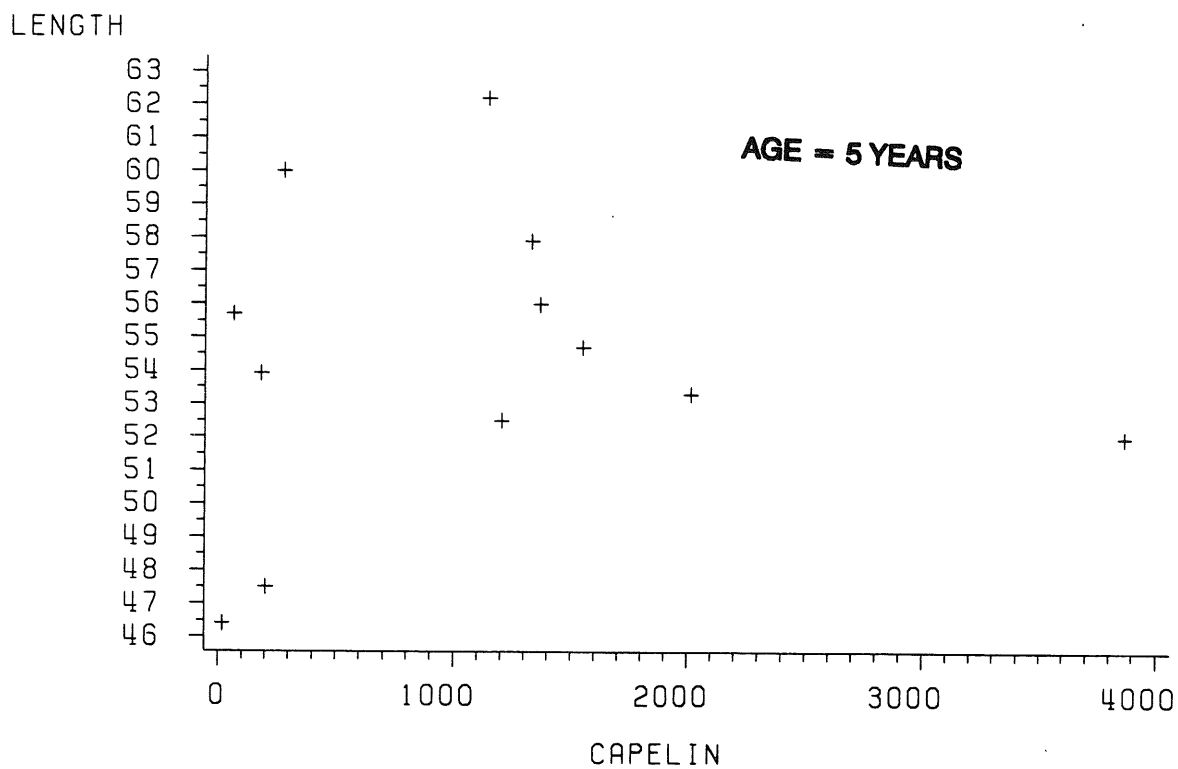


Figure 5.1.1.12. Length at age 5 against capelin biomass for the Barents Sea.

BARENTS SEA

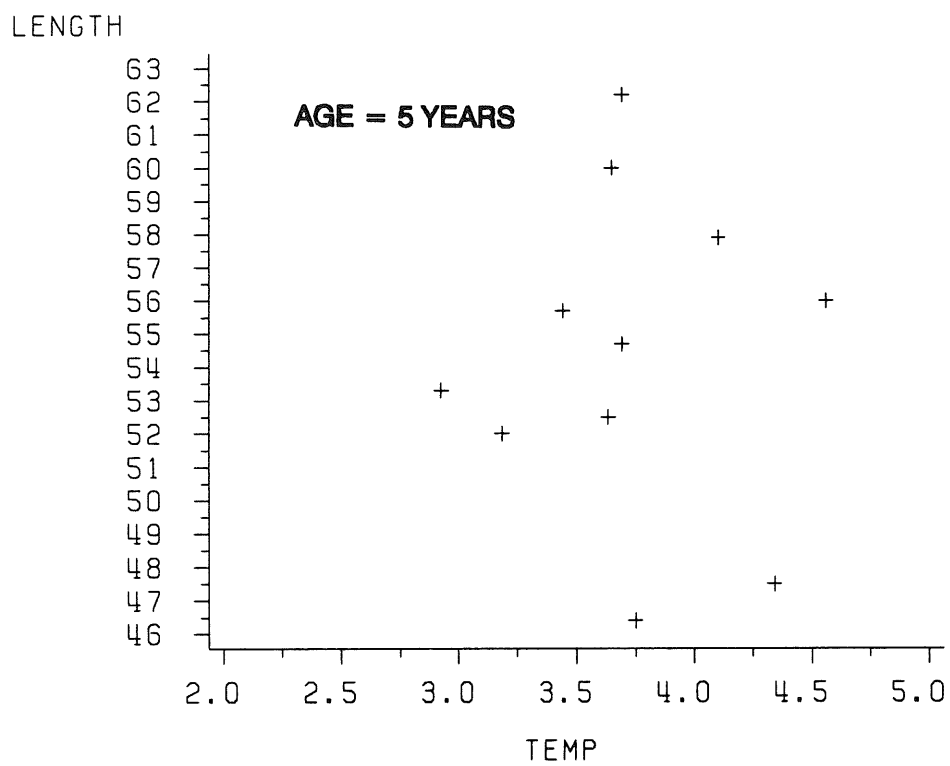


Figure 5.1.1.13. Length at age 5 against temperature for the Barents Sea.

WEST GREENLAND

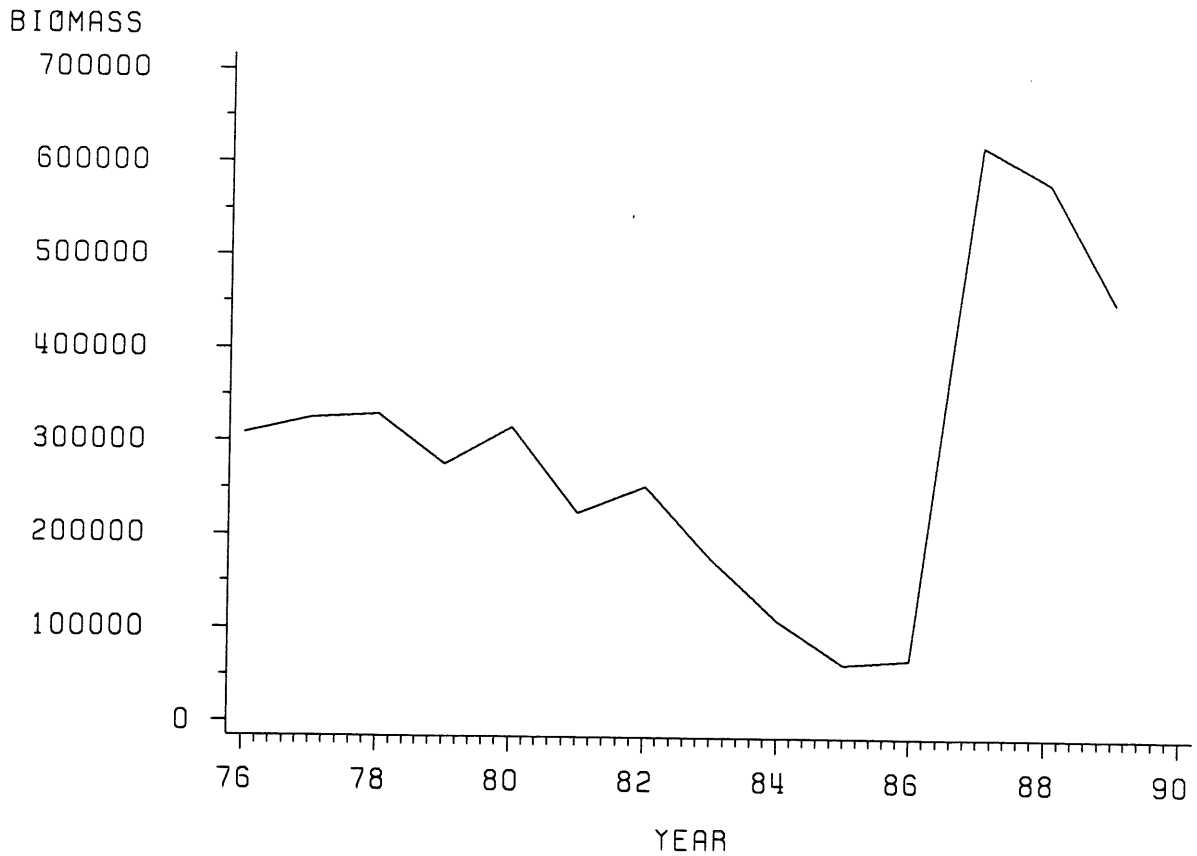


Figure 5.1.2.1. Cod biomass timeseries (tons) 1976-89 from VPA estimates in Subarea 1.

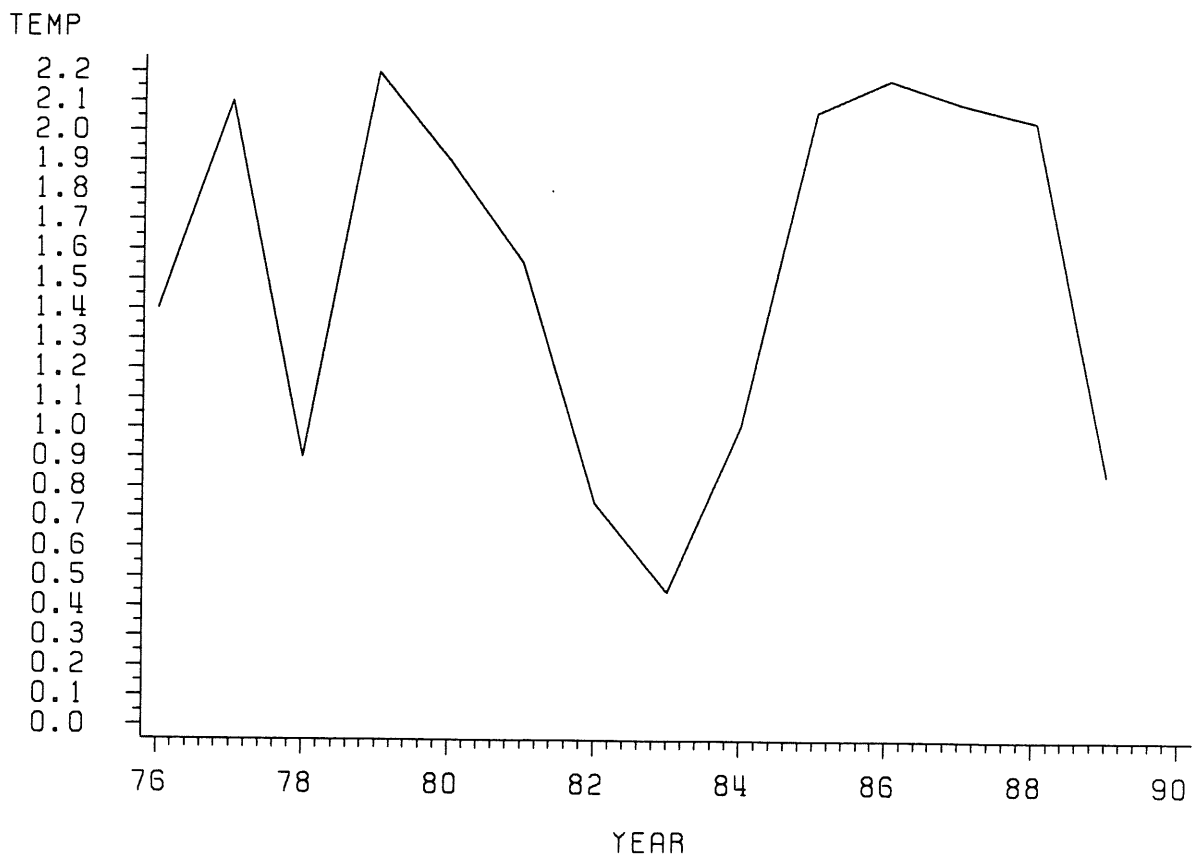


Figure 5.1.2.2. Annual mean surface temperature on Fylla Bank (64°N) for the period 1976-89.

WEST GREENLAND

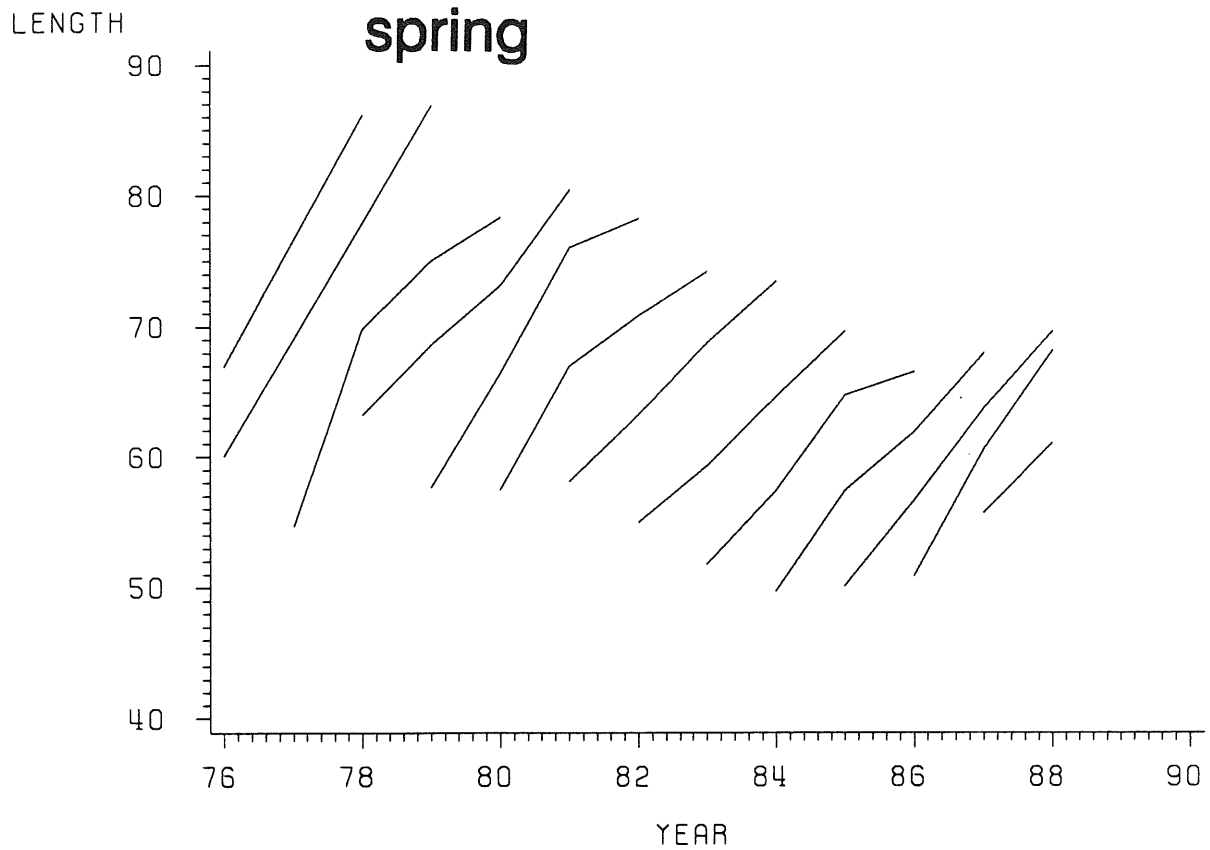


Figure 5.1.2.3. Cohort growth in terms of length at year in spring.

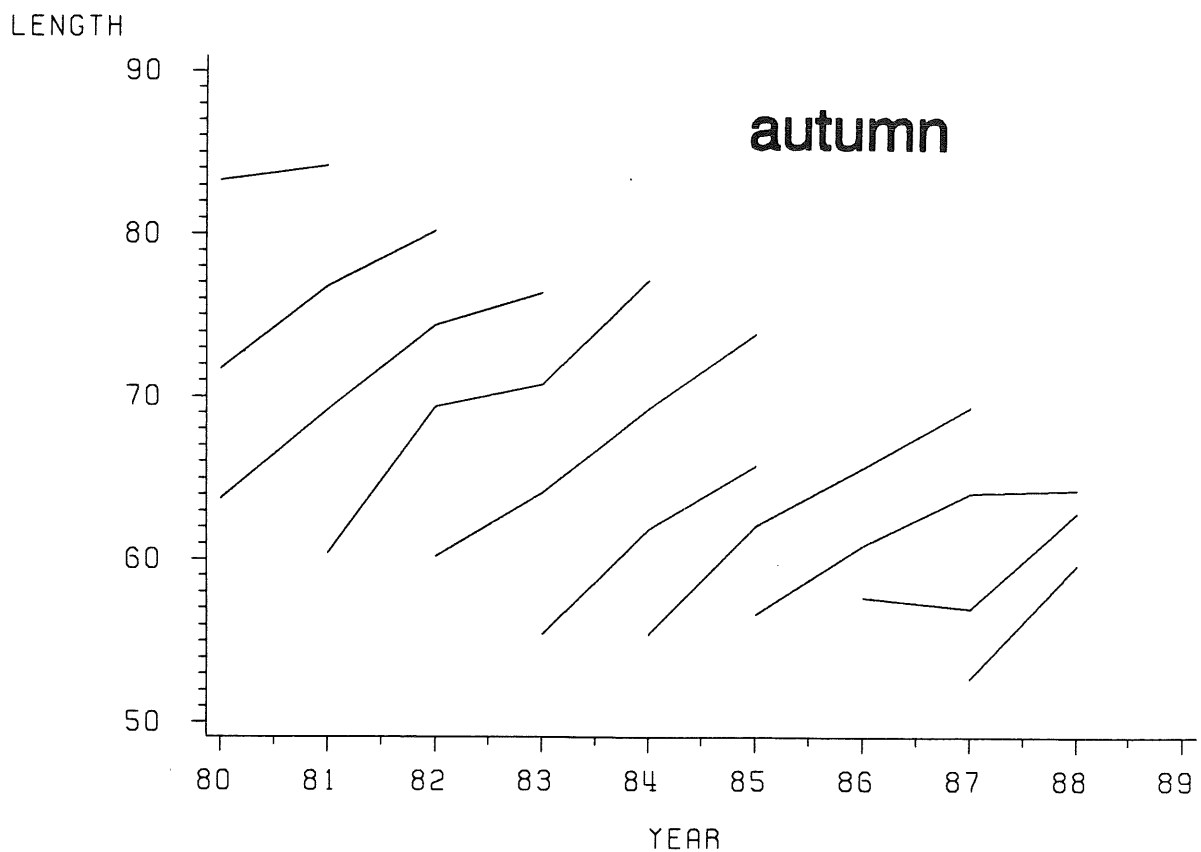


Figure 5.1.2.4. Cohort growth in terms of length at year in autumn.

WEST GREENLAND

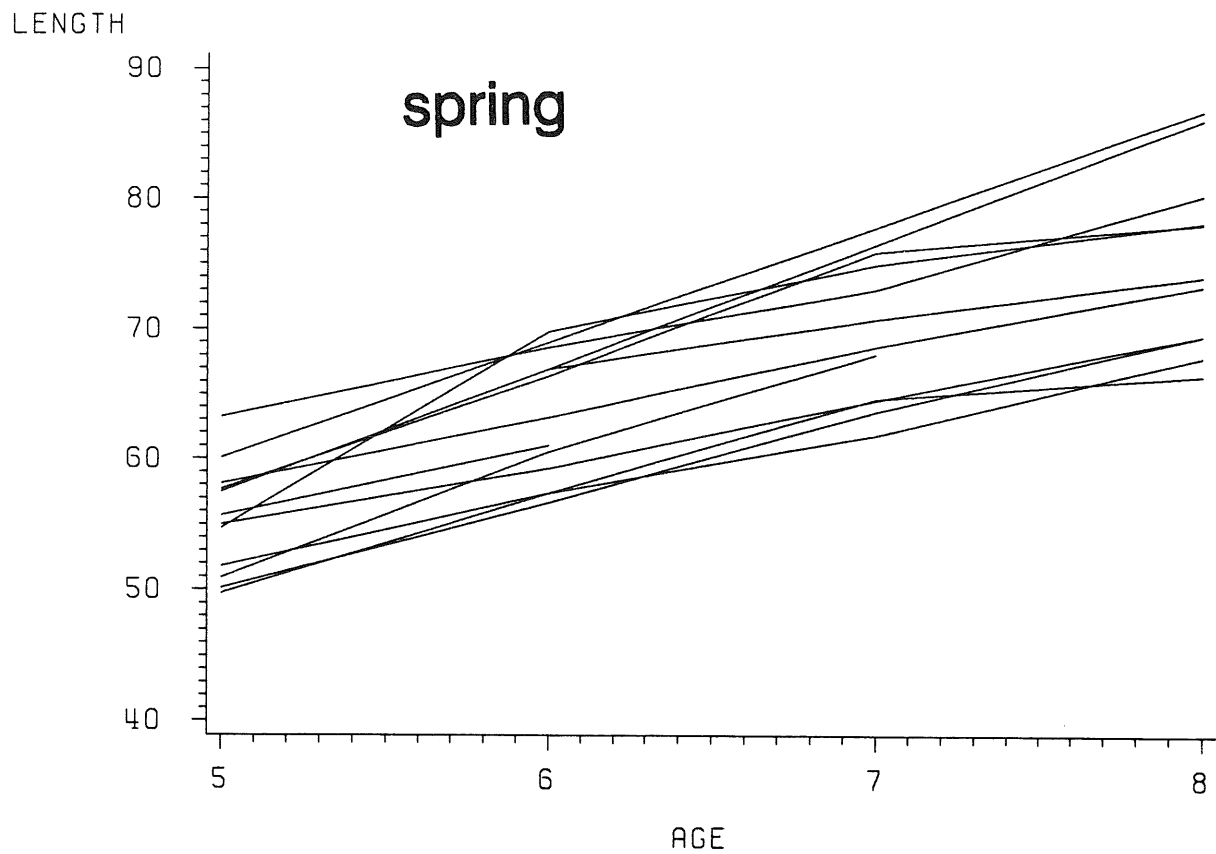


Figure 5.1.2.5. Cohort growth in terms of length at age in spring.

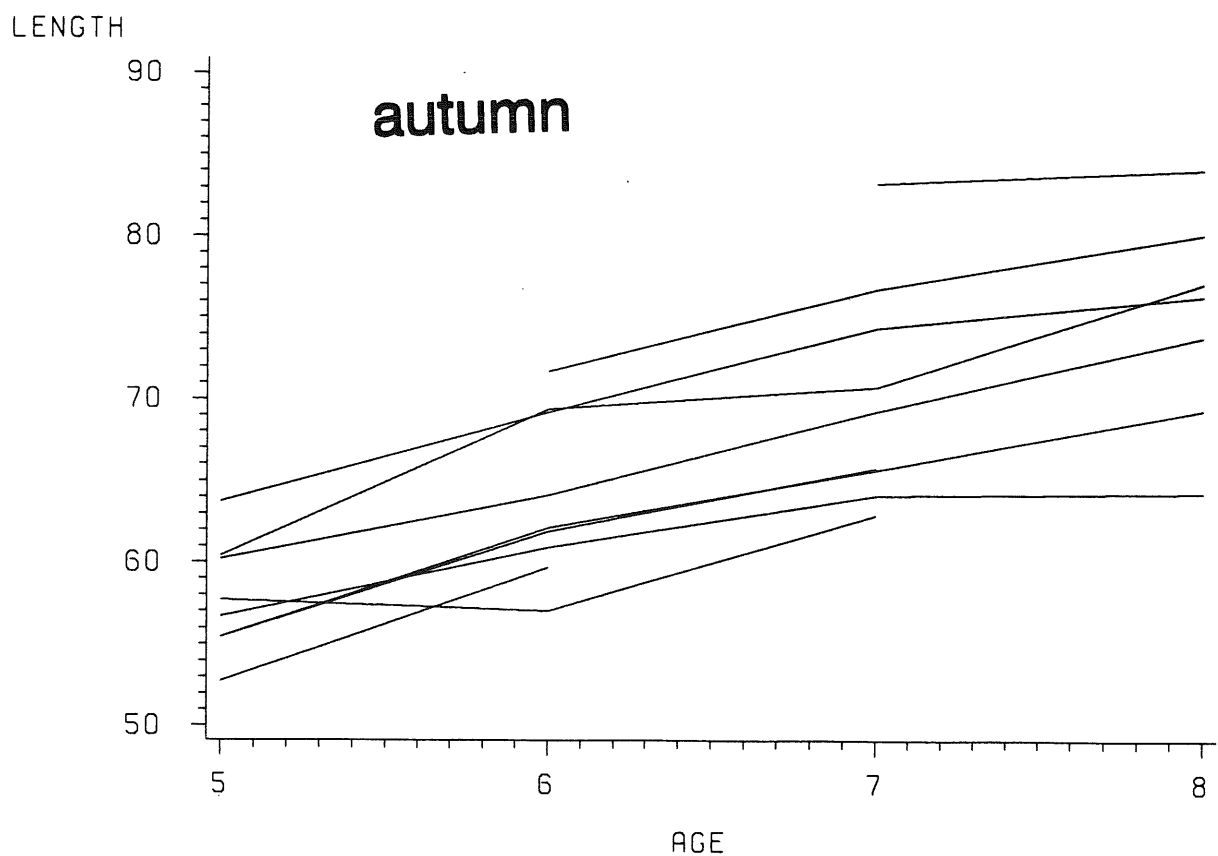


Figure 5.1.2.6. Cohort growth in terms of length at age in autumn.

WEST GREENLAND

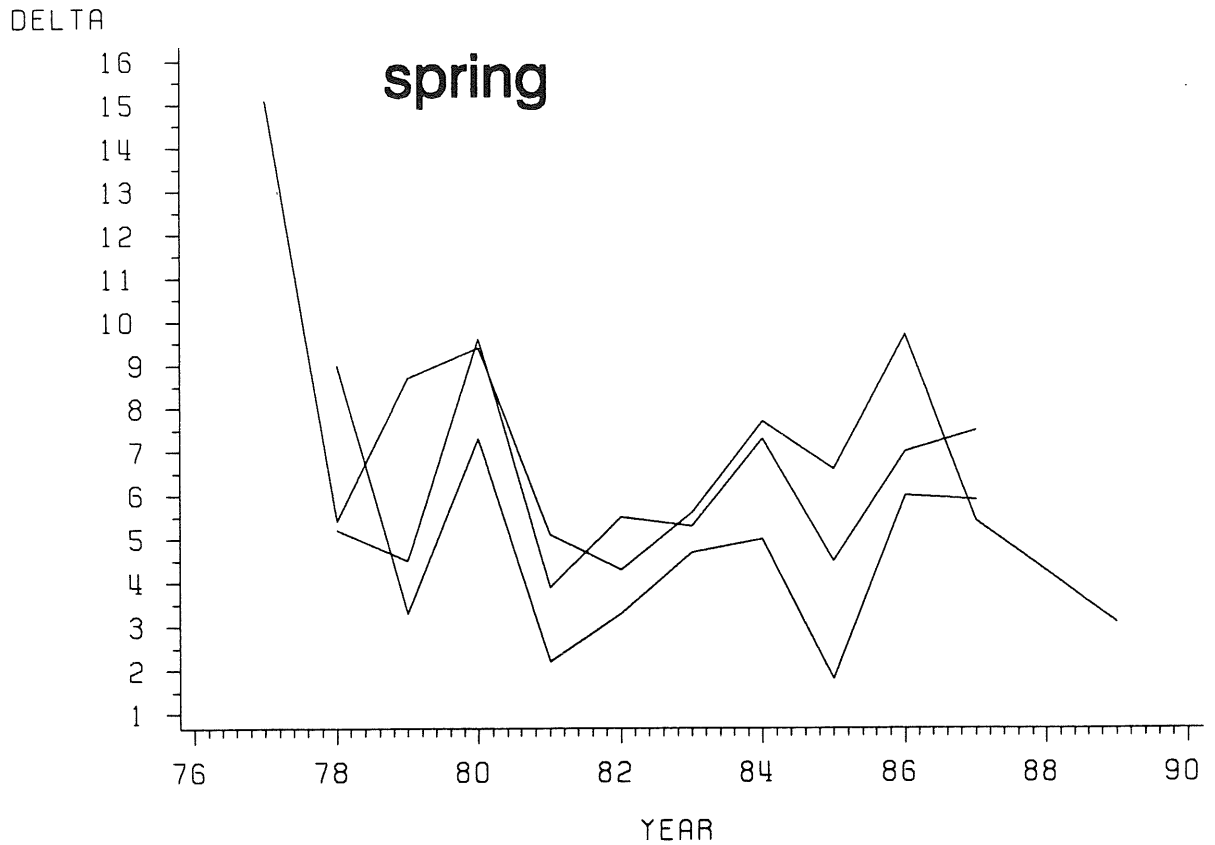


Figure 5.1.2.7. Length increment (delta) by cohort at each year in spring.

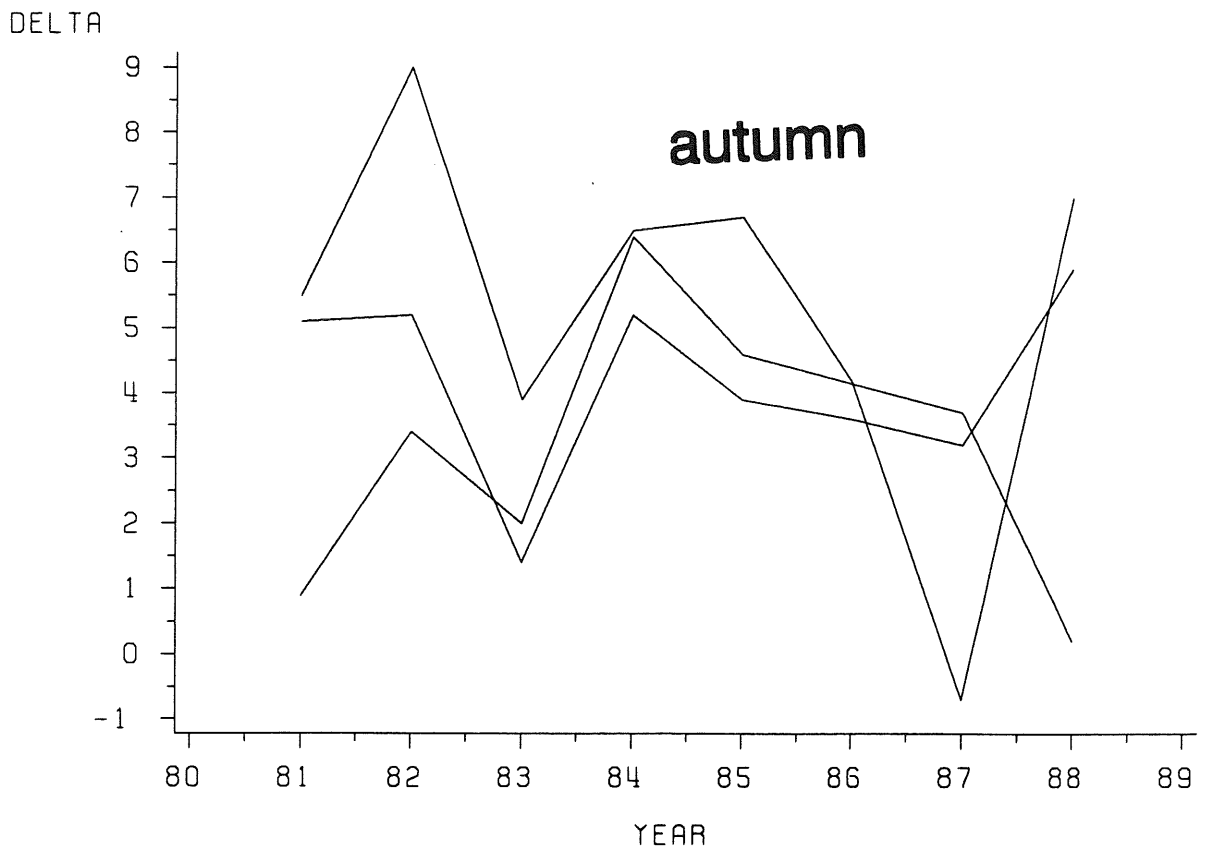


Figure 5.1.2.8. Length increment (delta) by cohort at each year in autumn.

WEST GREENLAND, spring

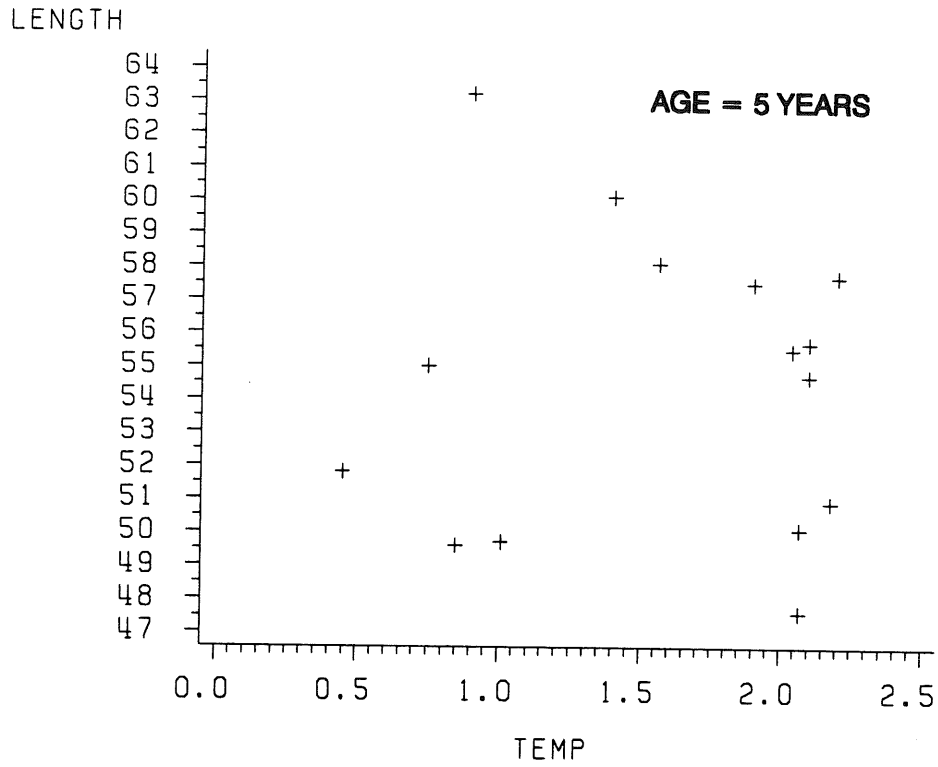


Figure 5.1.2.9. Length at age 5 in spring against temperature.

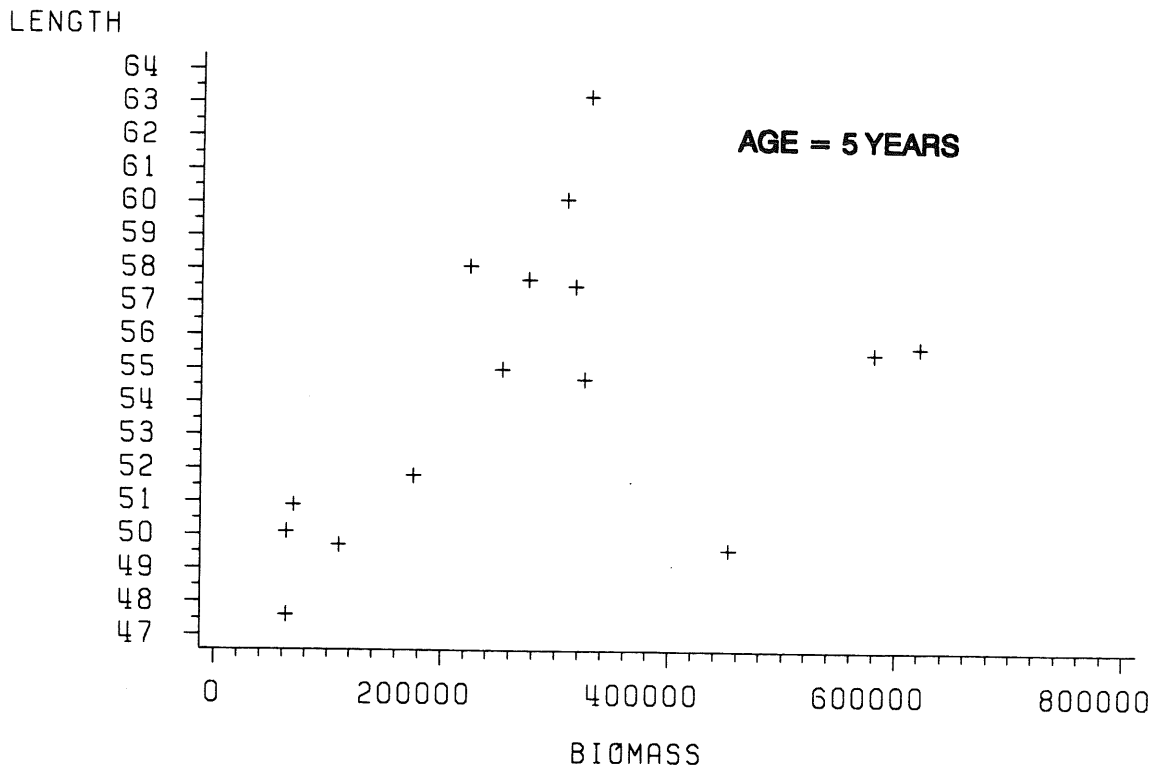


Fig. 5.1.2.10 Length at age 5 in spring against biomass.

WEST GREENLAND, autumn 197

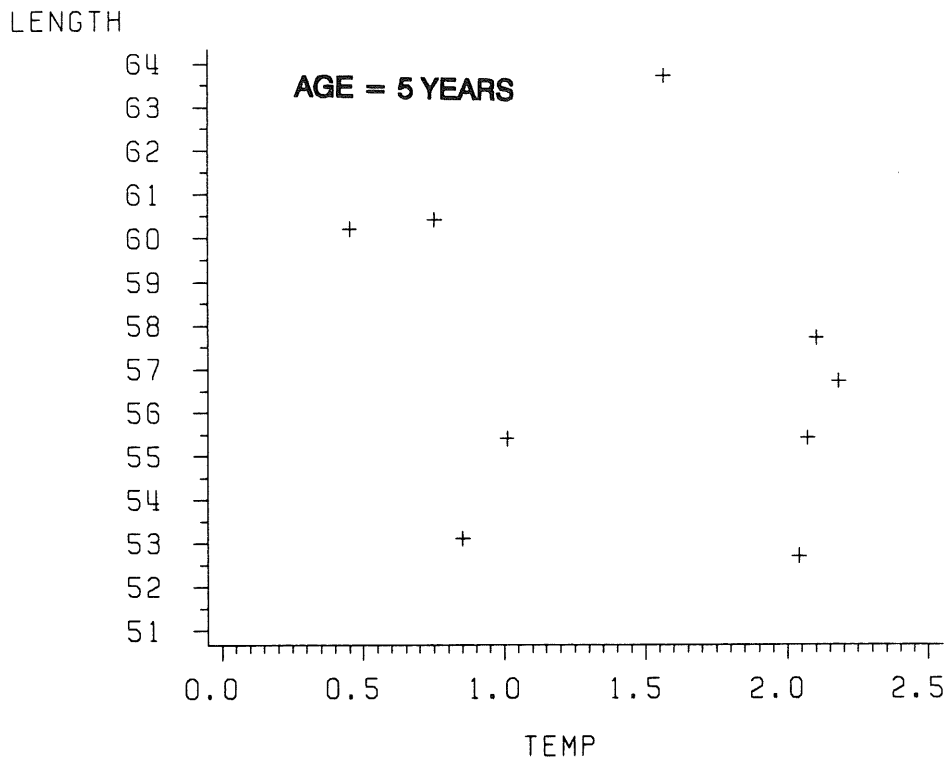


Figure 5.1.2.11. Length at age 5 in autumn against temperature.

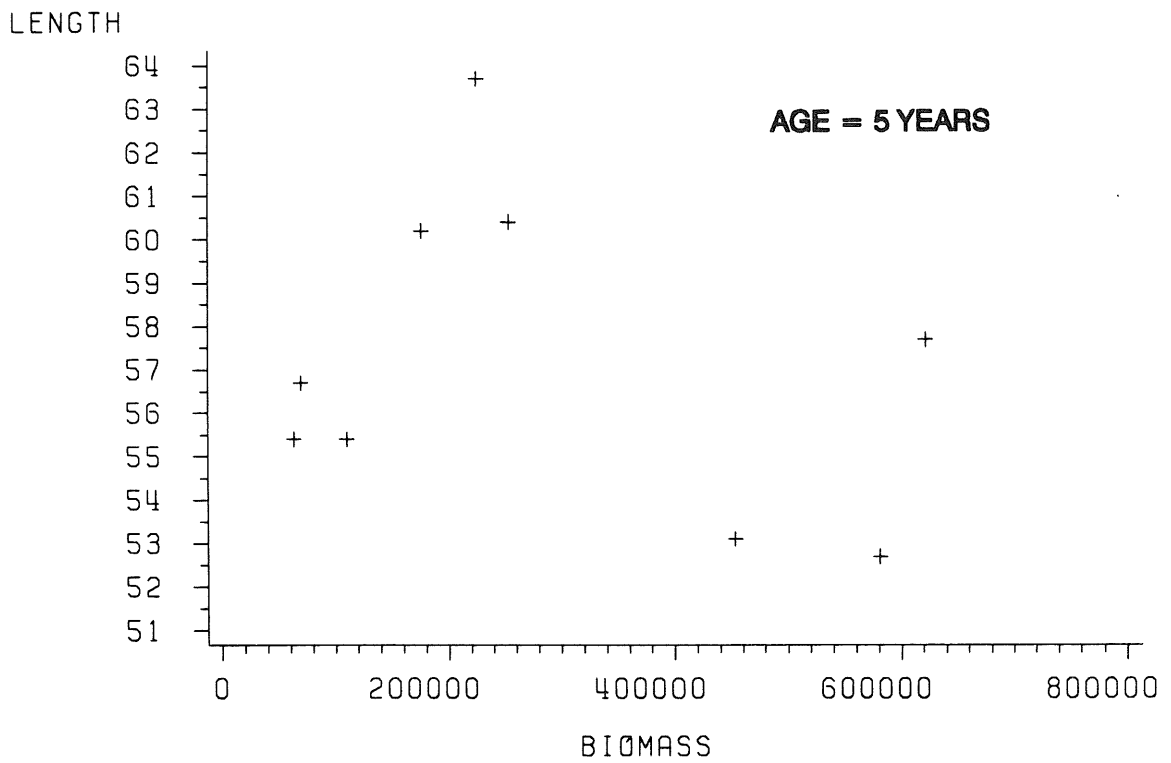


Figure 5.1.2.12. Length at age 5 in autumn against biomass.

Iceland NE area

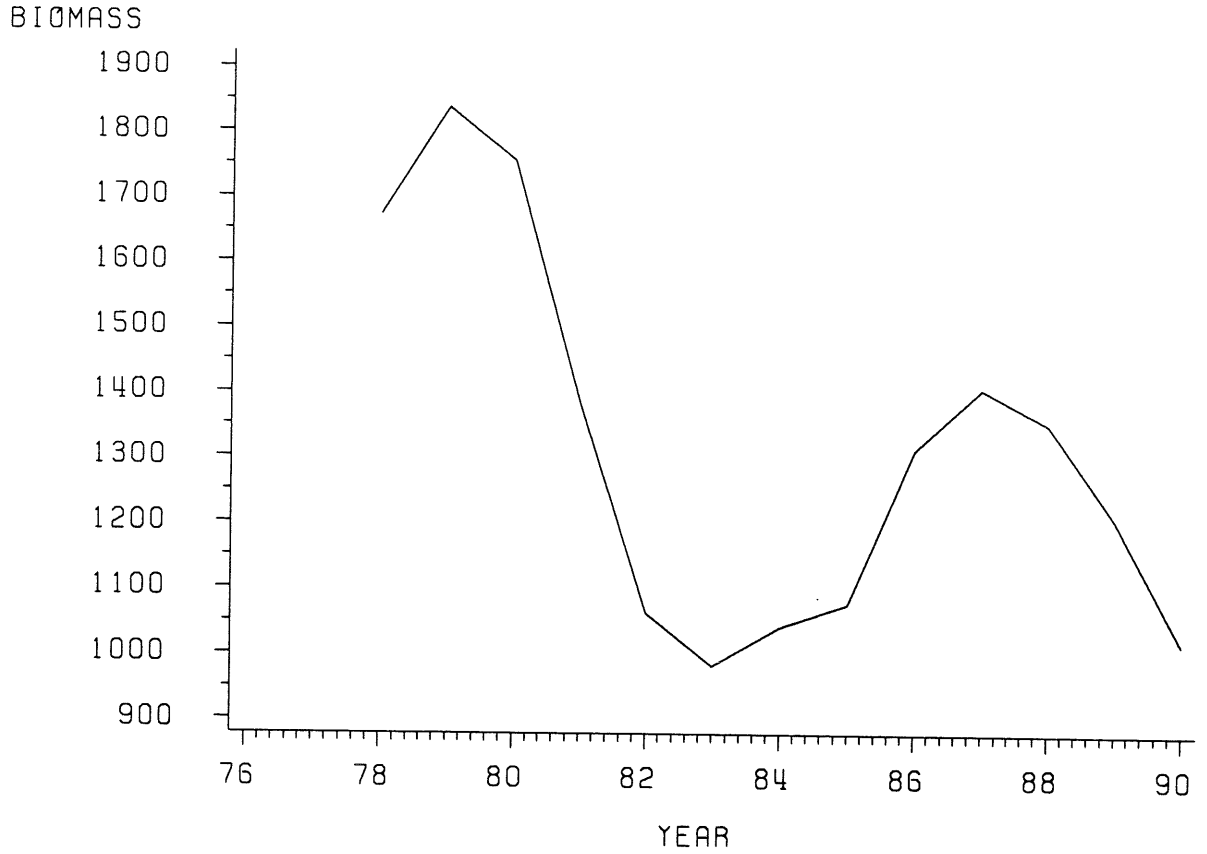


Figure 5.1.3.1. Cod biomass ('000tons) off NE Iceland for the years 1977-90.

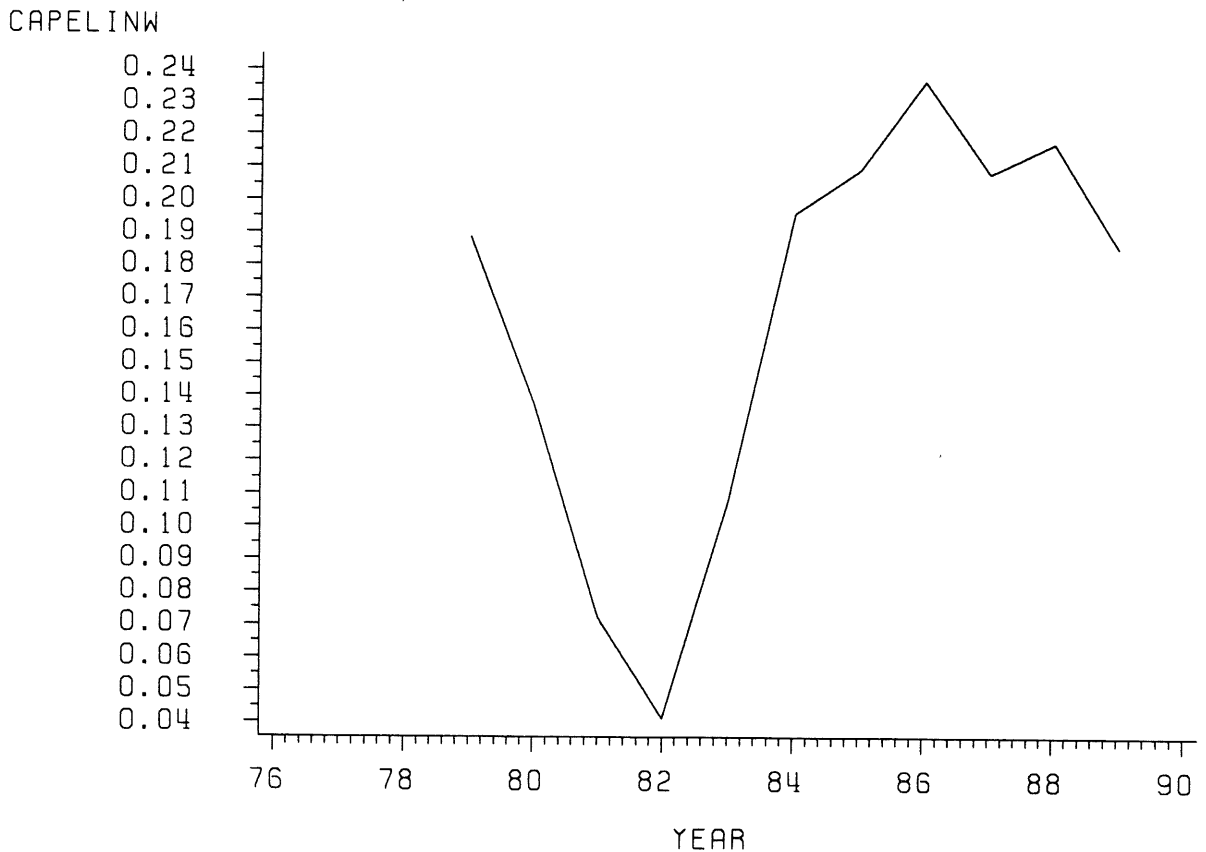


Figure 5.1.3.2. Capelin biomass index off NE Iceland for the years 1979-89.

Iceland NE area

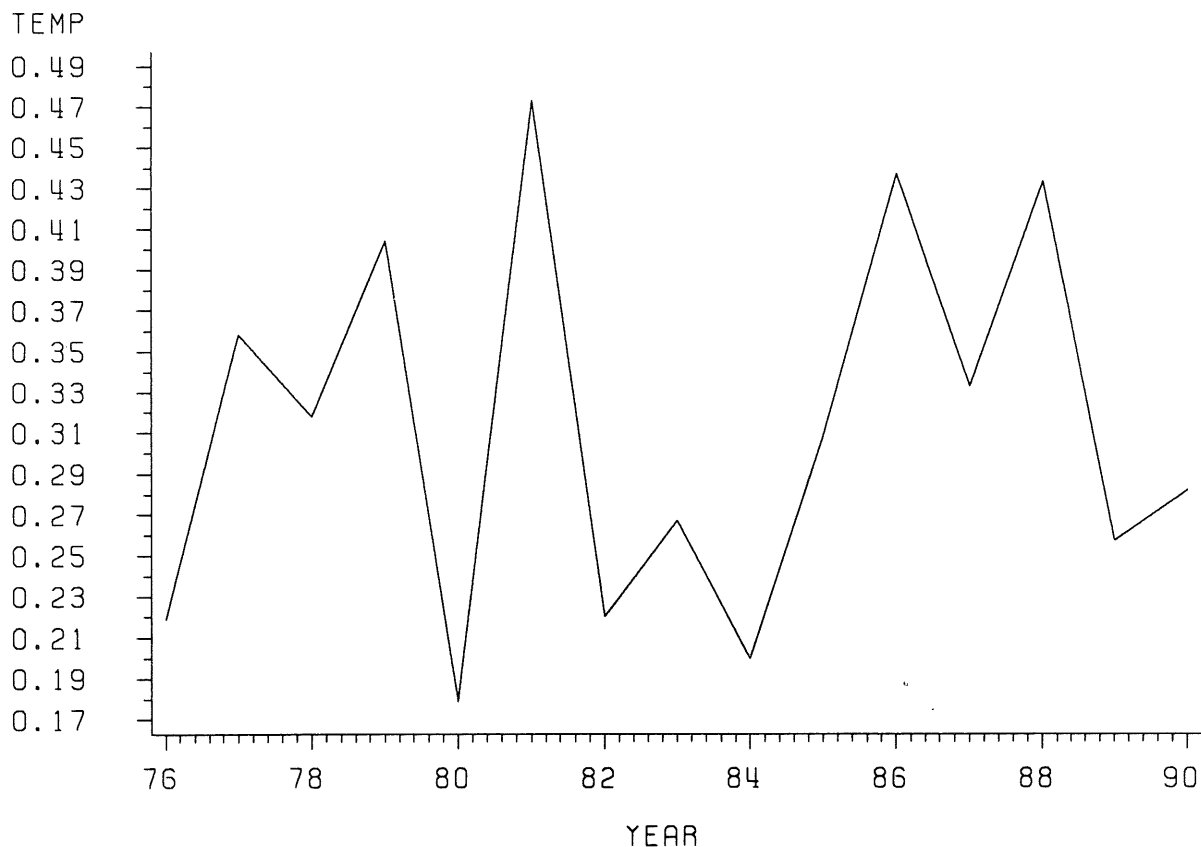


Figure 5.1.3.3. Temperature deviations off NE Iceland for the period 1976-90.

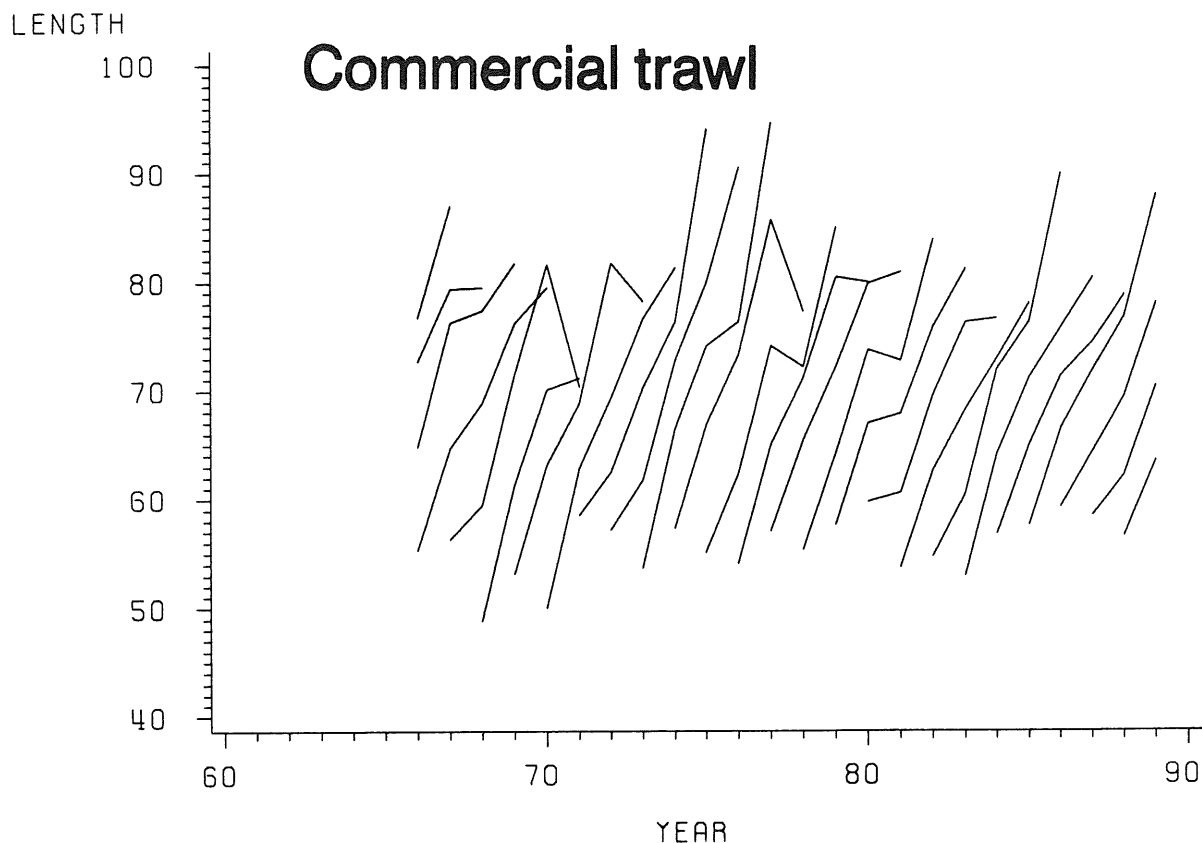


Figure 5.1.3.4. Cohort growth off NE Iceland in terms of length at year.

Iceland NE area, Commercial trawl

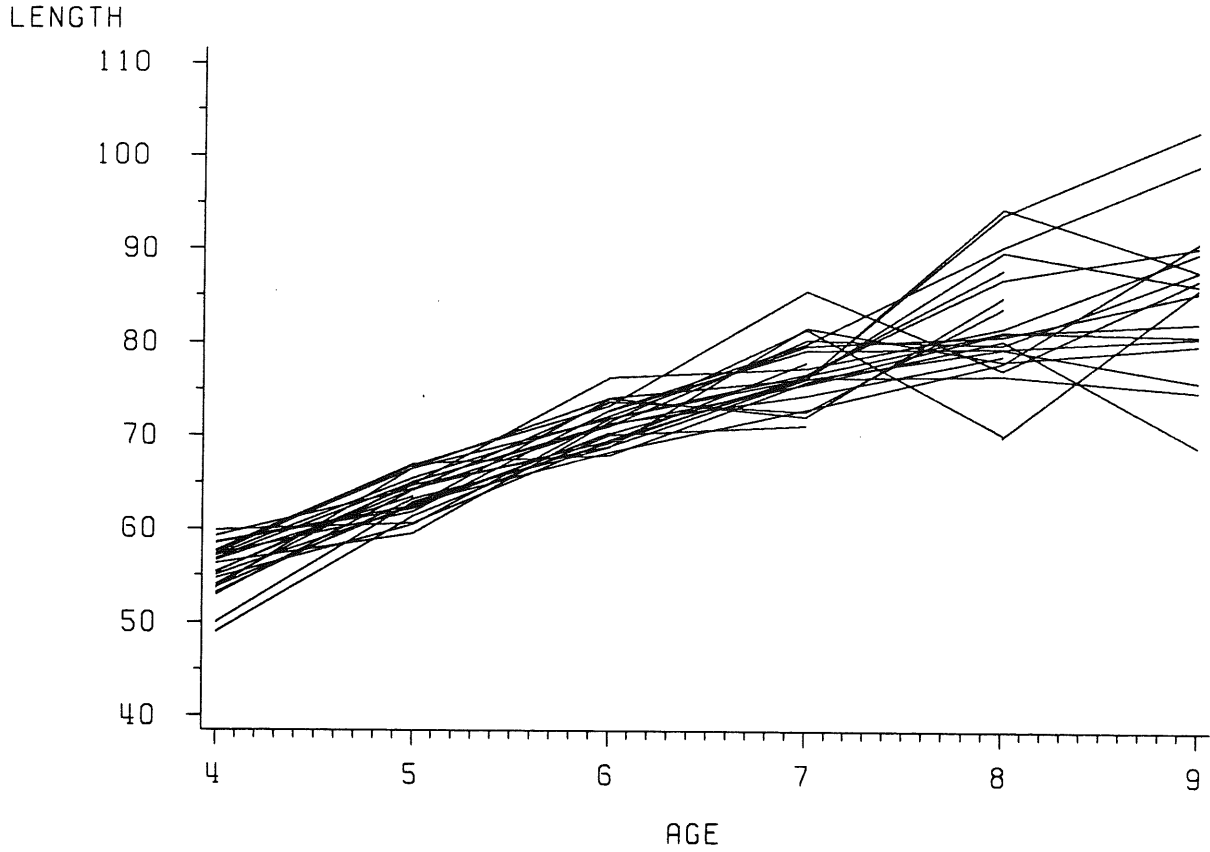


Figure 5.1.3.5. Cohort growth off NE Iceland in terms of length at age.

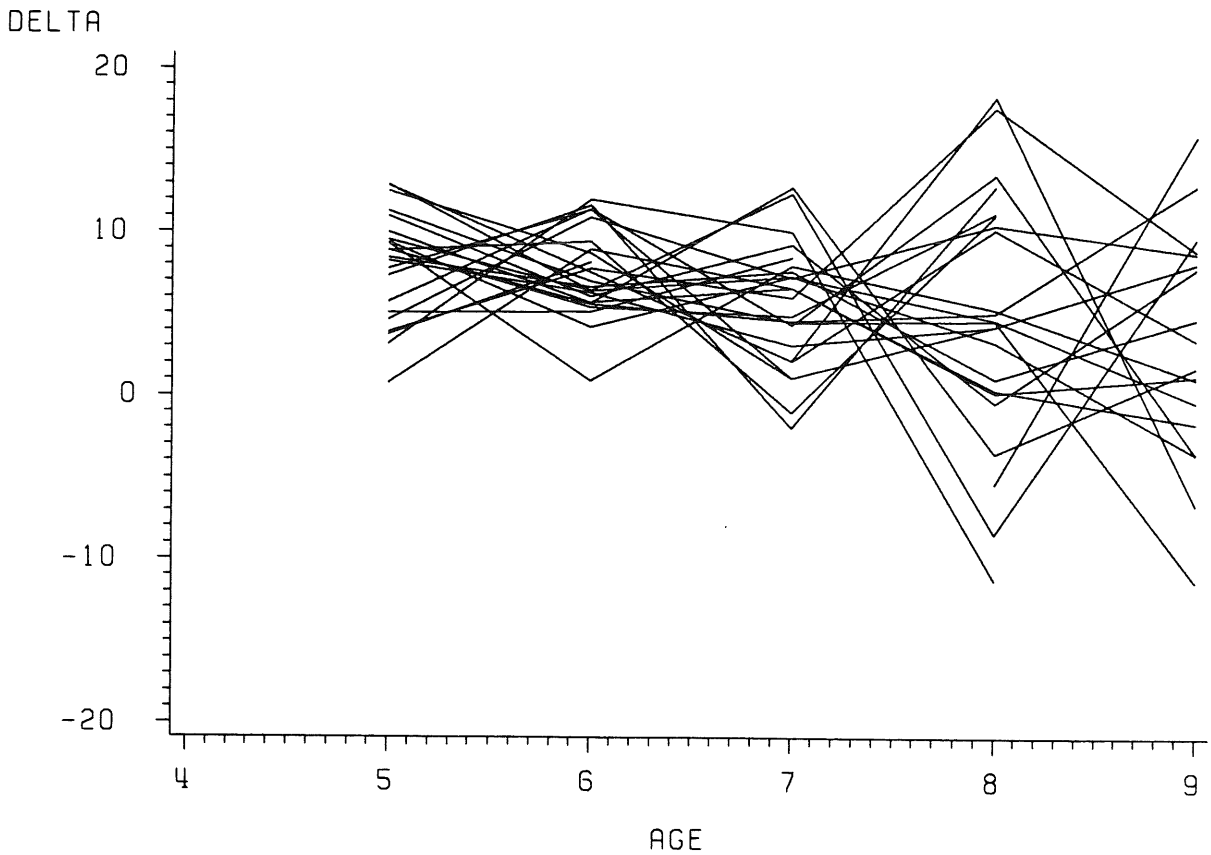


Figure 5.1.3.6. Length increment (delta) by cohort at each age for NE Iceland.

Iceland NE area, Commercial trawl

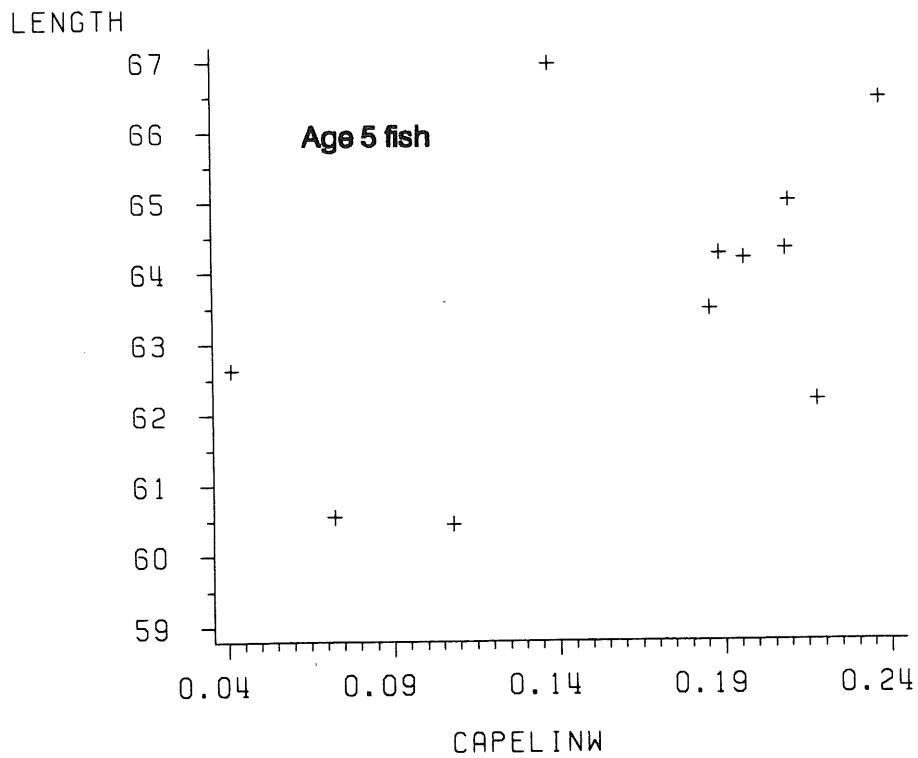


Figure 5.1.3.7. Length at age 5 against capelin biomass for NE Iceland.

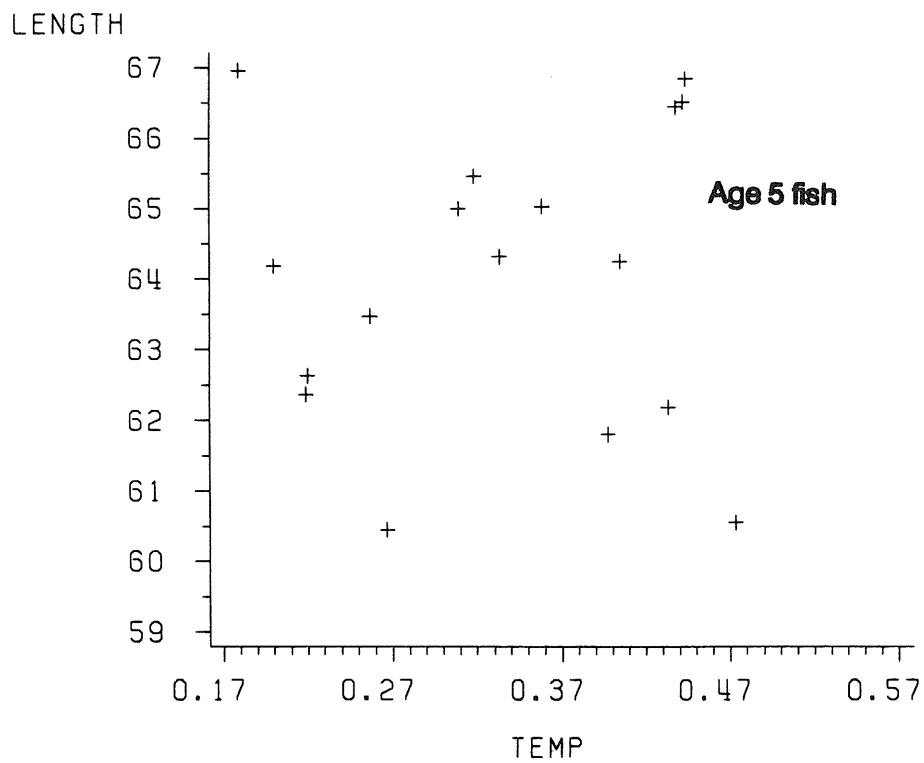


Figure 5.1.3.8. Length at age 5 against temperature for NE Iceland.

Newfoundland Div 2J3KL

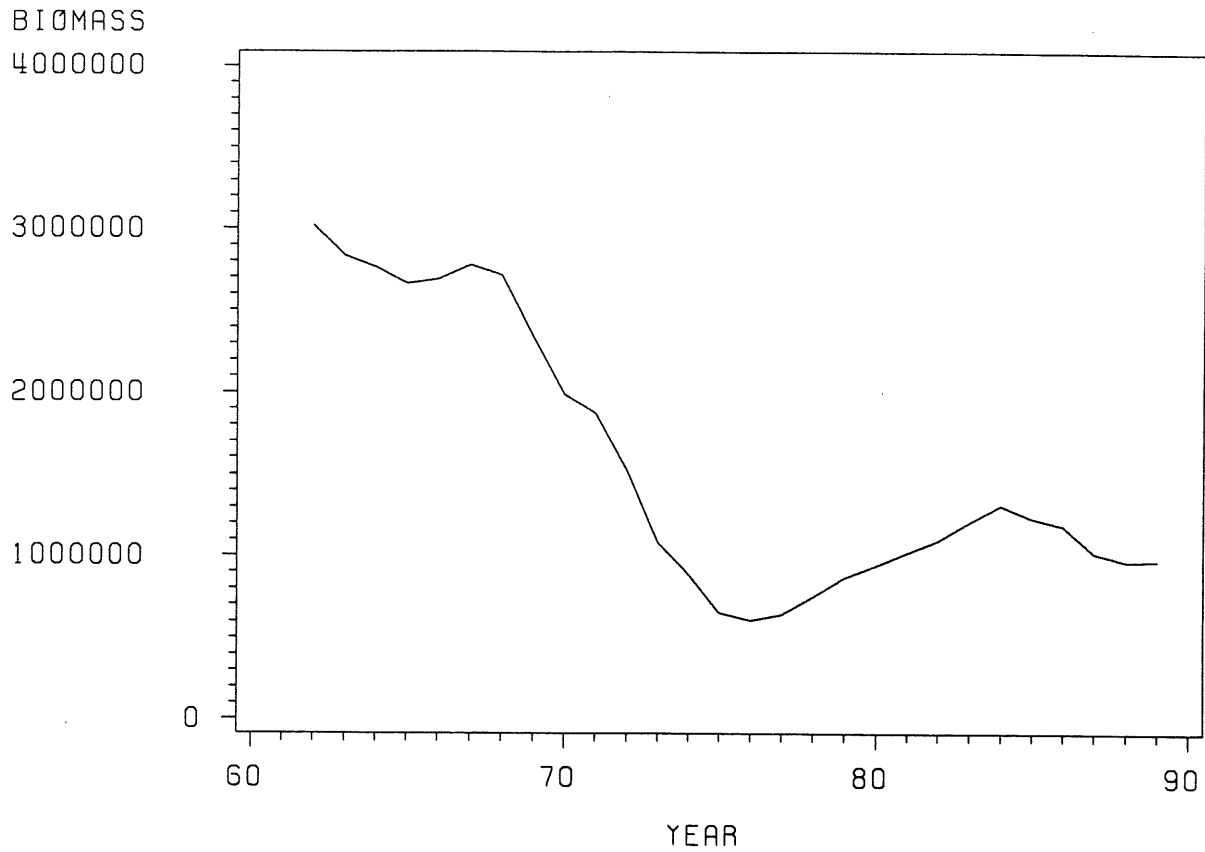


Figure 5.1.4.1. Cod biomass timeseries (tons) 1962-89 from ADAPT estimates of numbers at age and commercial catch weights at age for NAFO Divs. 2J3KL.

CAPELIN

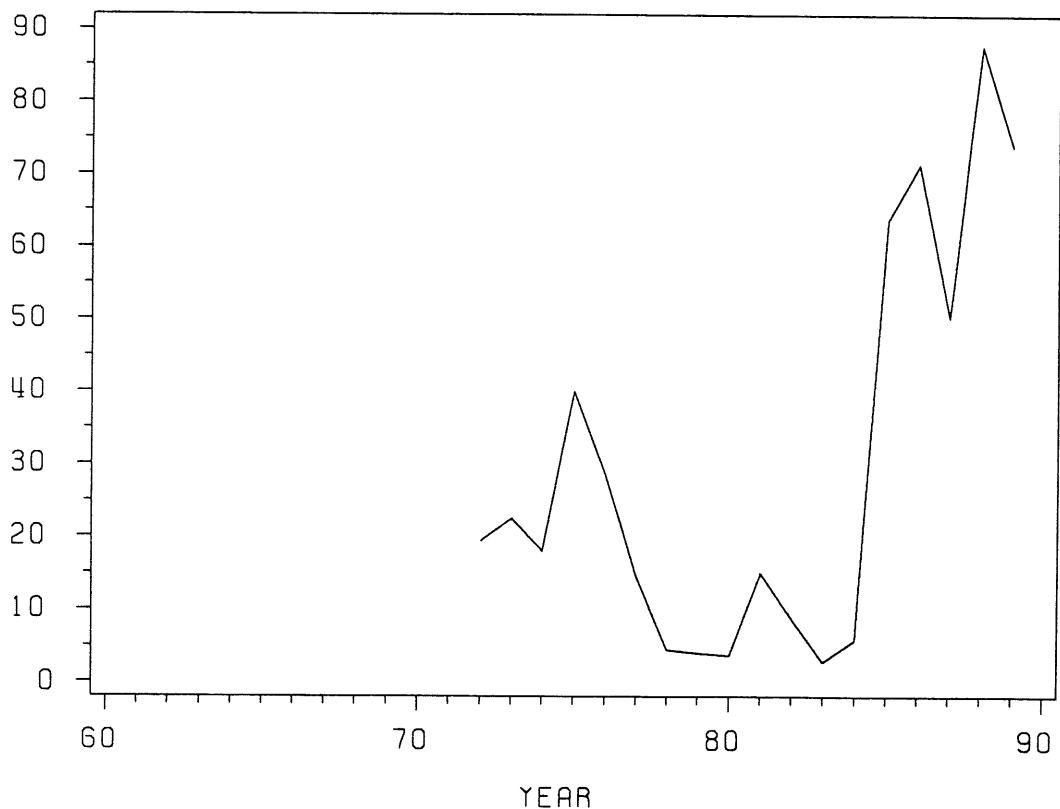


Figure 5.1.4.2. Capelin abundance index for the period 1972-89 assembled from several sources (see text).

Newfoundland Div 2J3KL

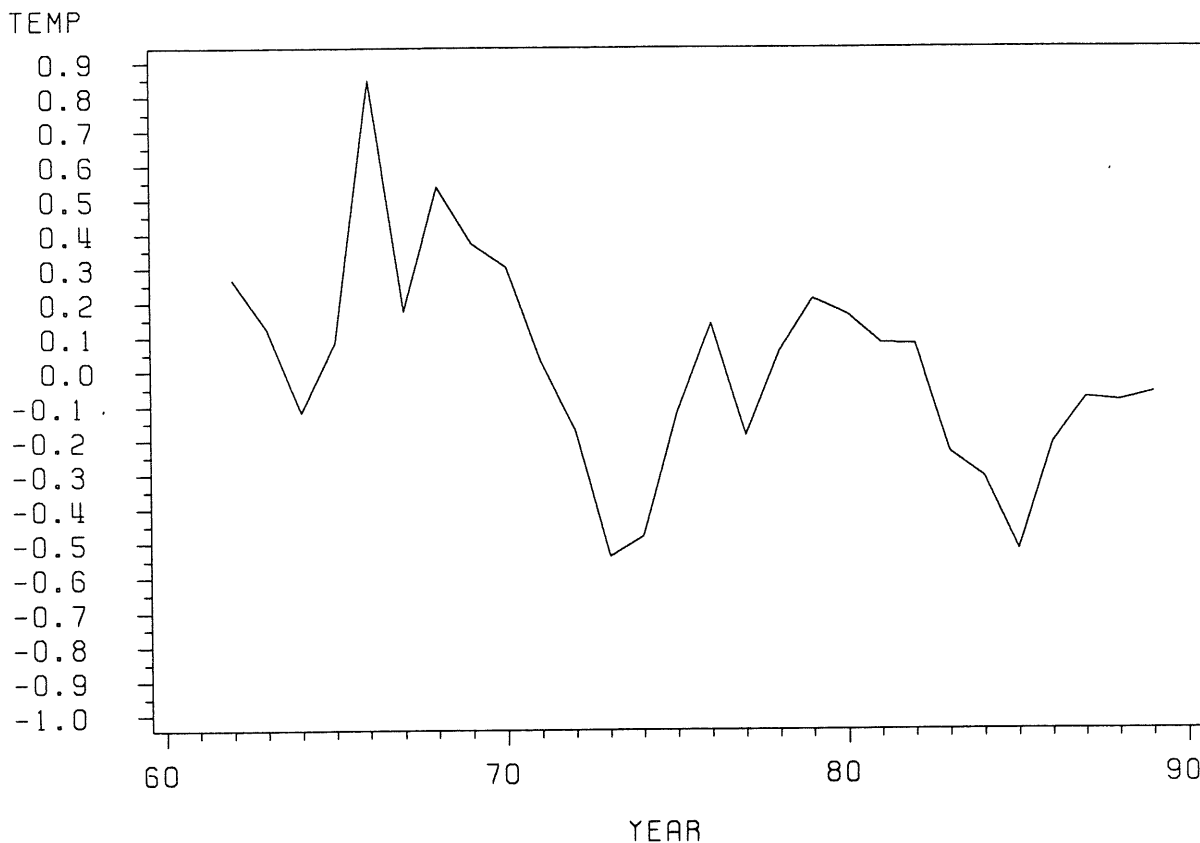


Figure 5.1.4.3. Annual mean bottom temperature anomaly from Station 27 for the period 1962-89.

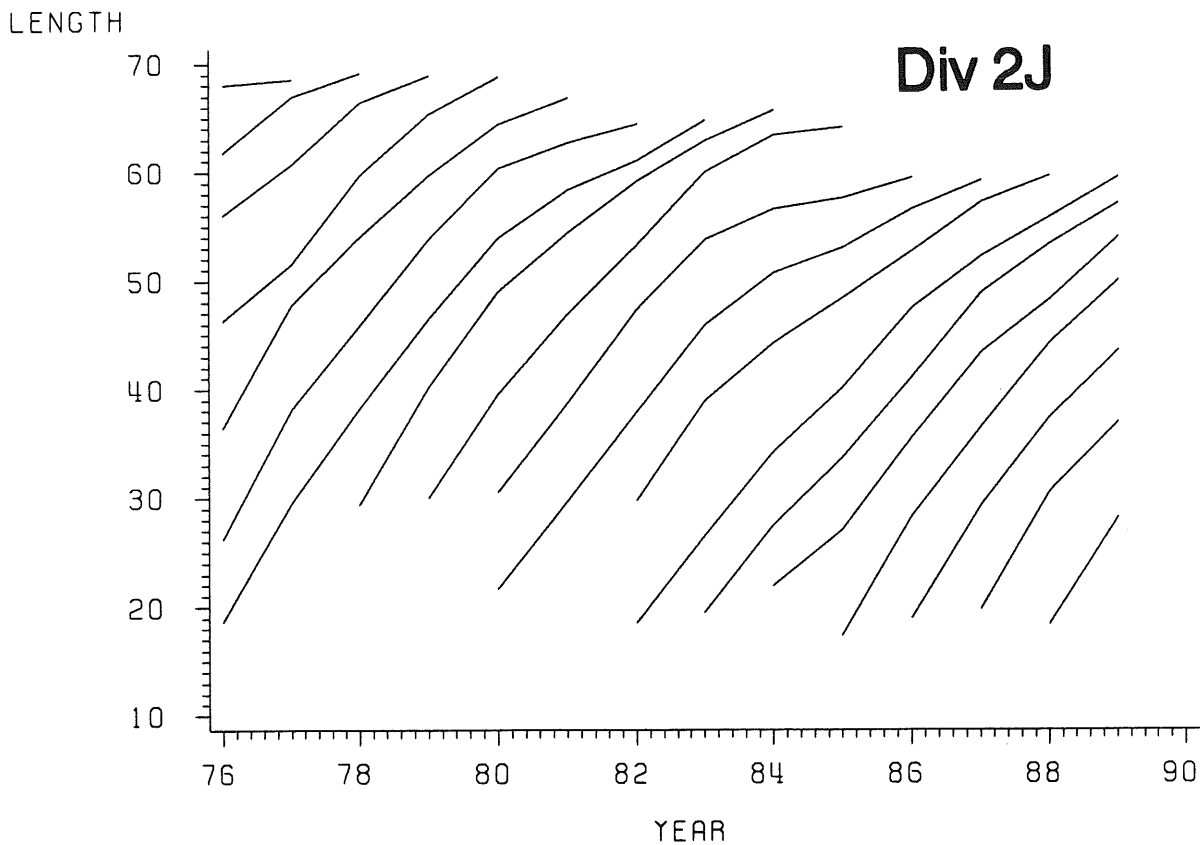


Figure 5.1.4.4. Cohort growth in terms of length at year in Div. 2J.

LENGTH

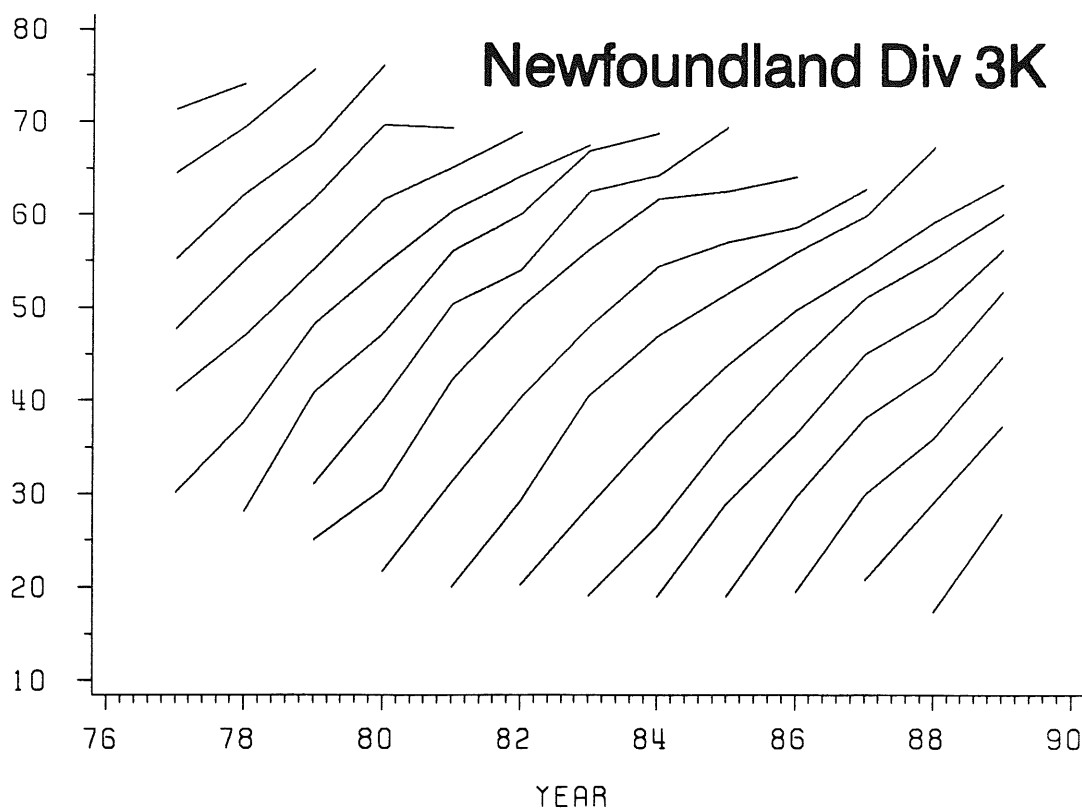


Figure 5.1.4.5. Cohort growth in terms of length at year in Div. 3K.

Newfoundland Div 3L

LENGTH

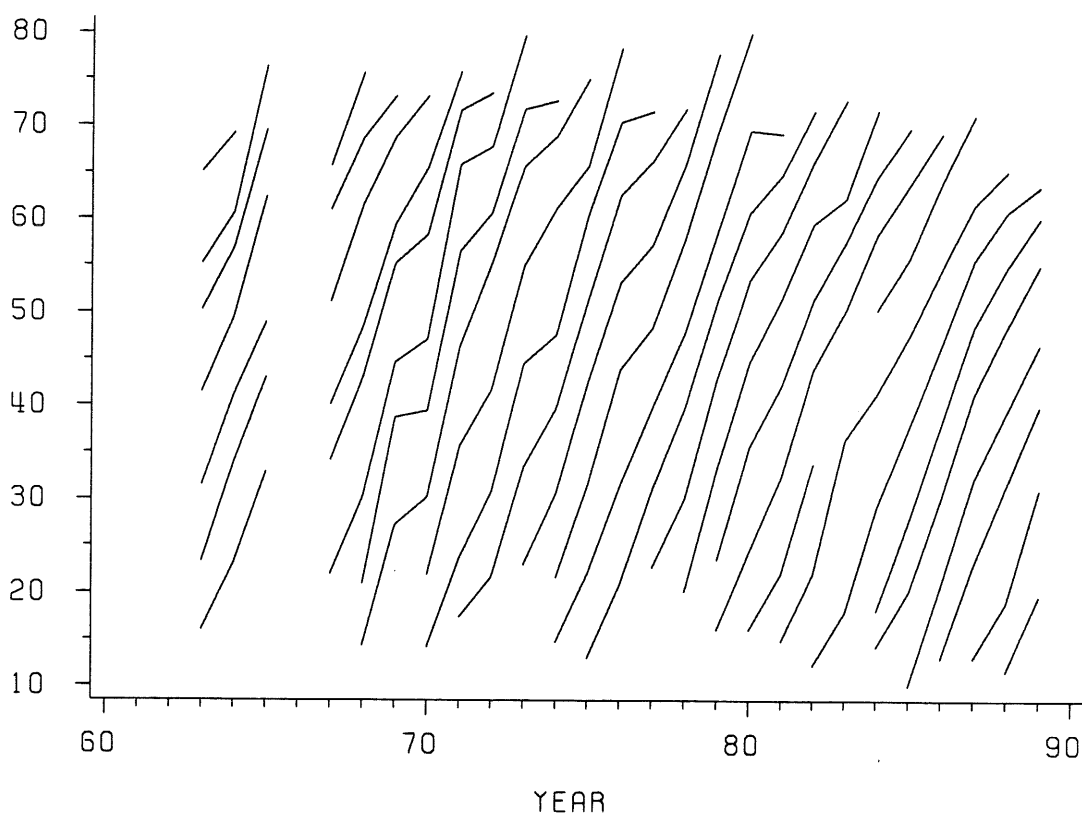


Figure 5.1.4.6. Cohort growth in terms of length at year in Div. 3L.

Newfoundland Div 2J

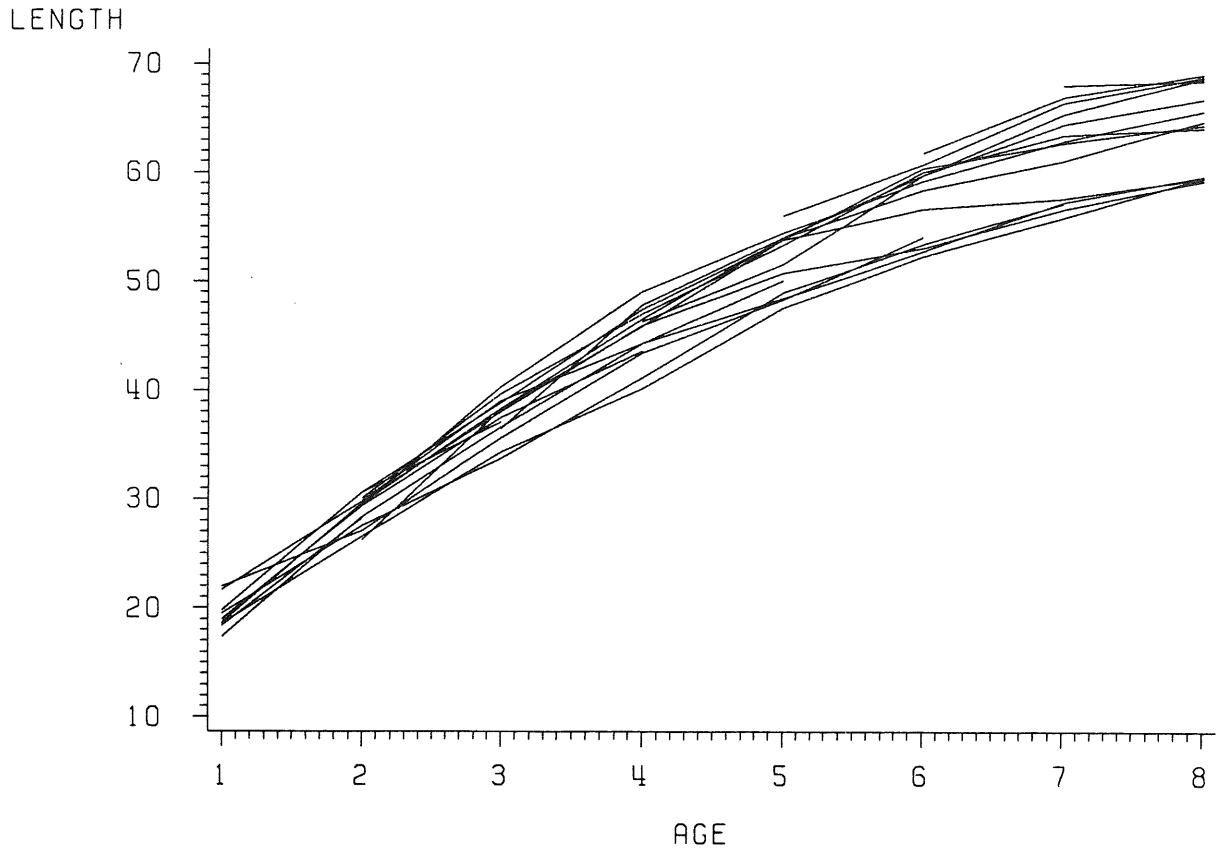


Figure 5.1.4.7. Cohort growth in terms of length at age in Div. 2J.

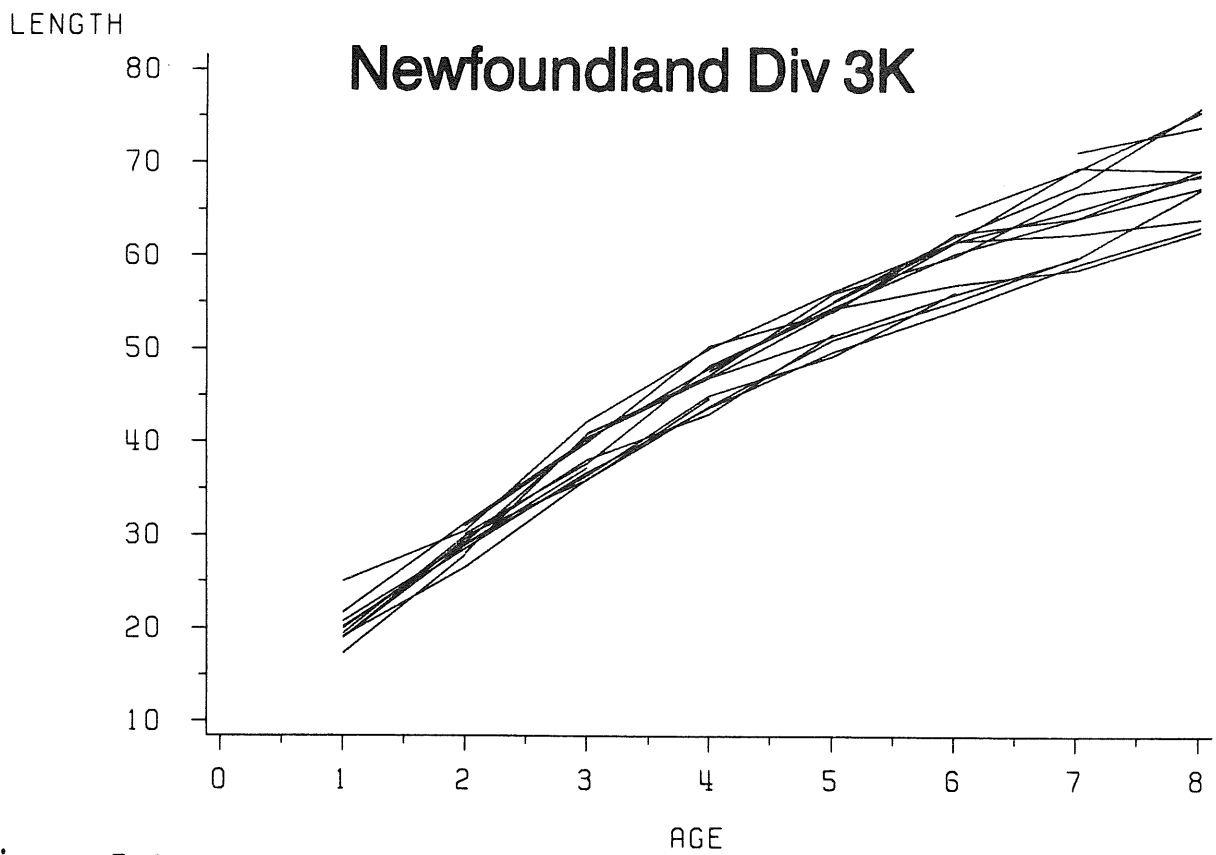


Figure 5.1.4.8. Cohort growth in terms of length at age in Div. 3K.

Newfoundland Div 3L

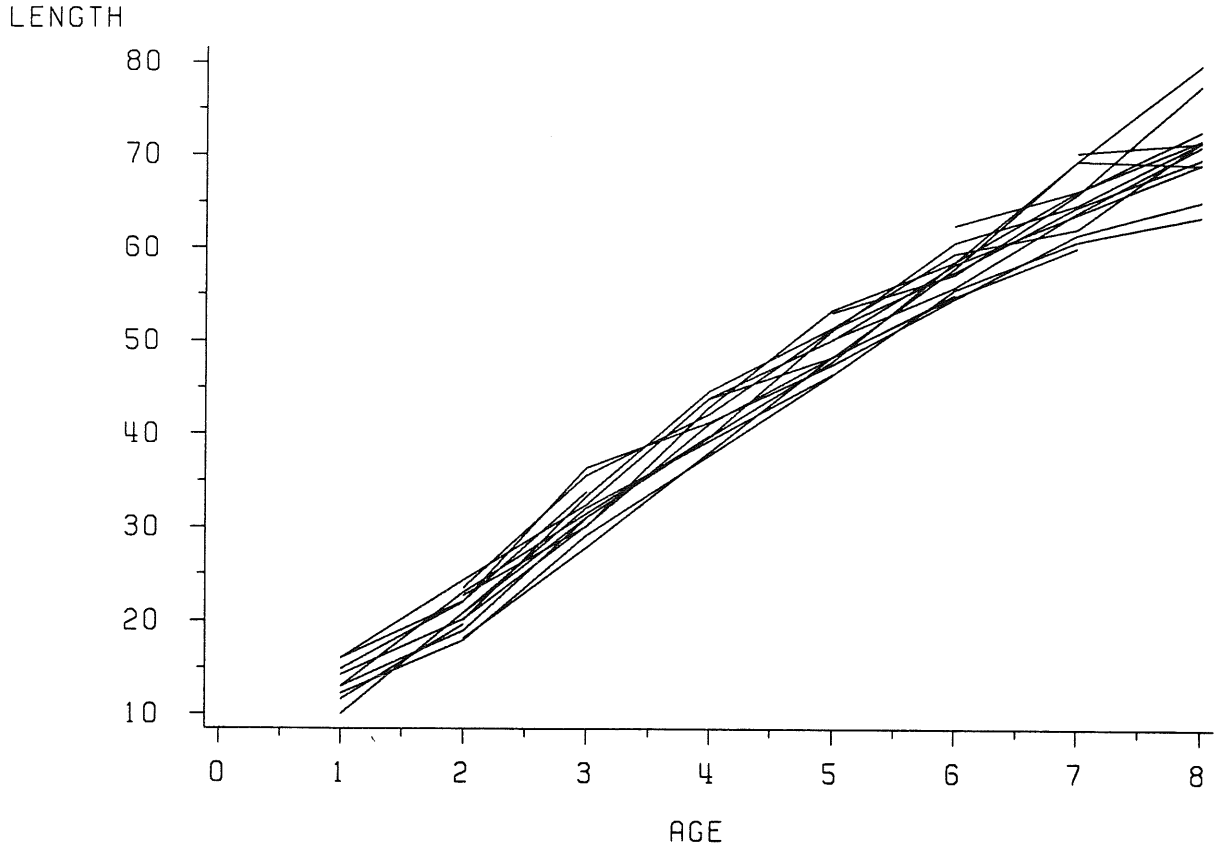


Figure 5.1.4.9. Cohort growth in terms of length at age in Div. 3L.

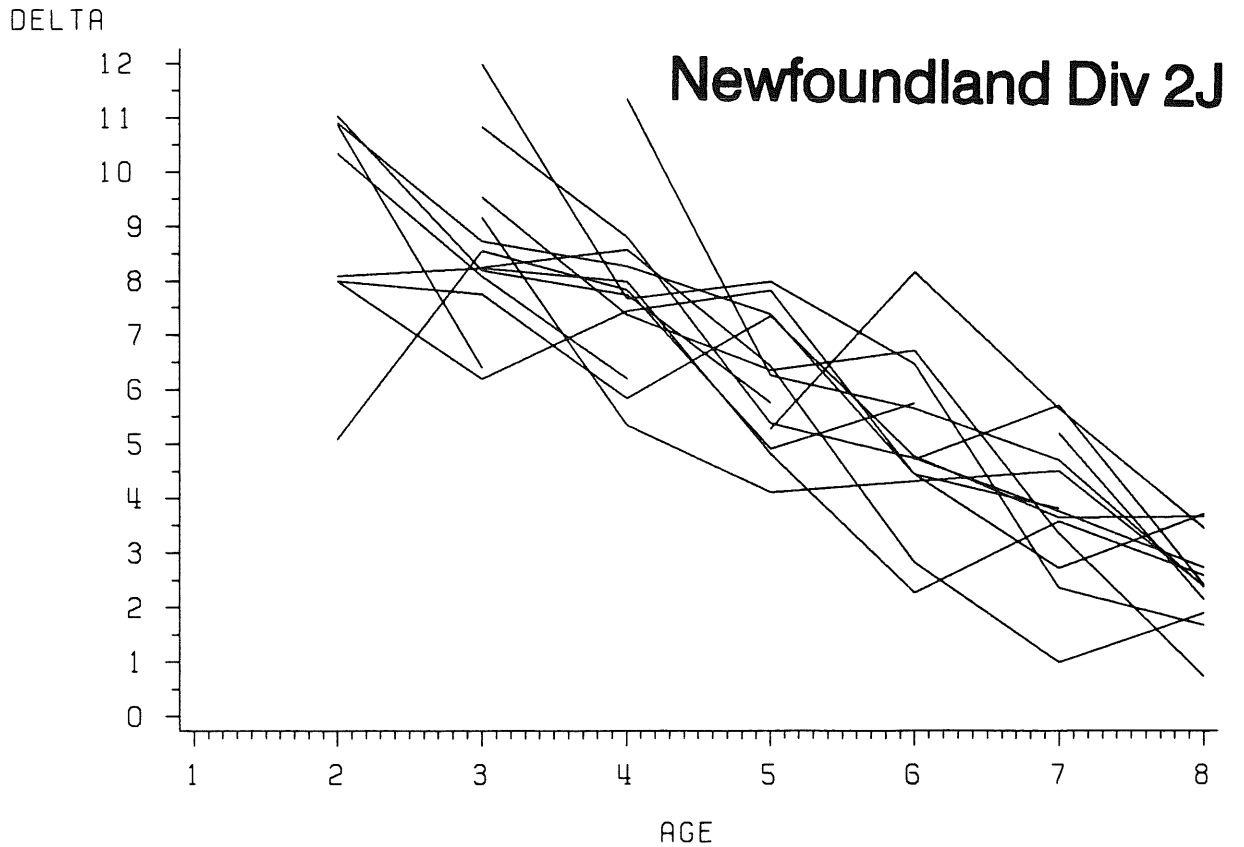


Figure 5.1.4.10. Length increment (delta) by cohort at each age in Div. 2J.

Newfoundland Div 3K

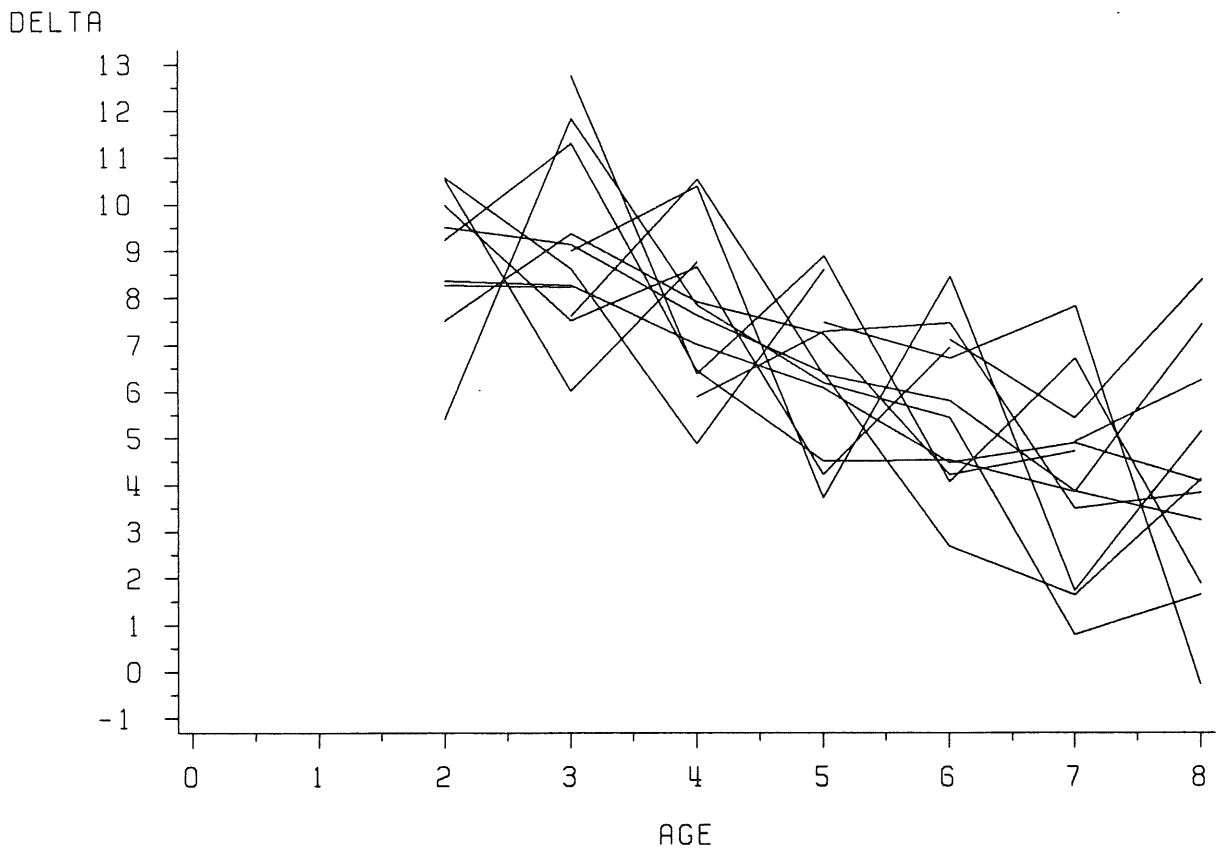


Figure 5.1.4.11. Length increment (delta) by cohort at each age in Div. 3K.

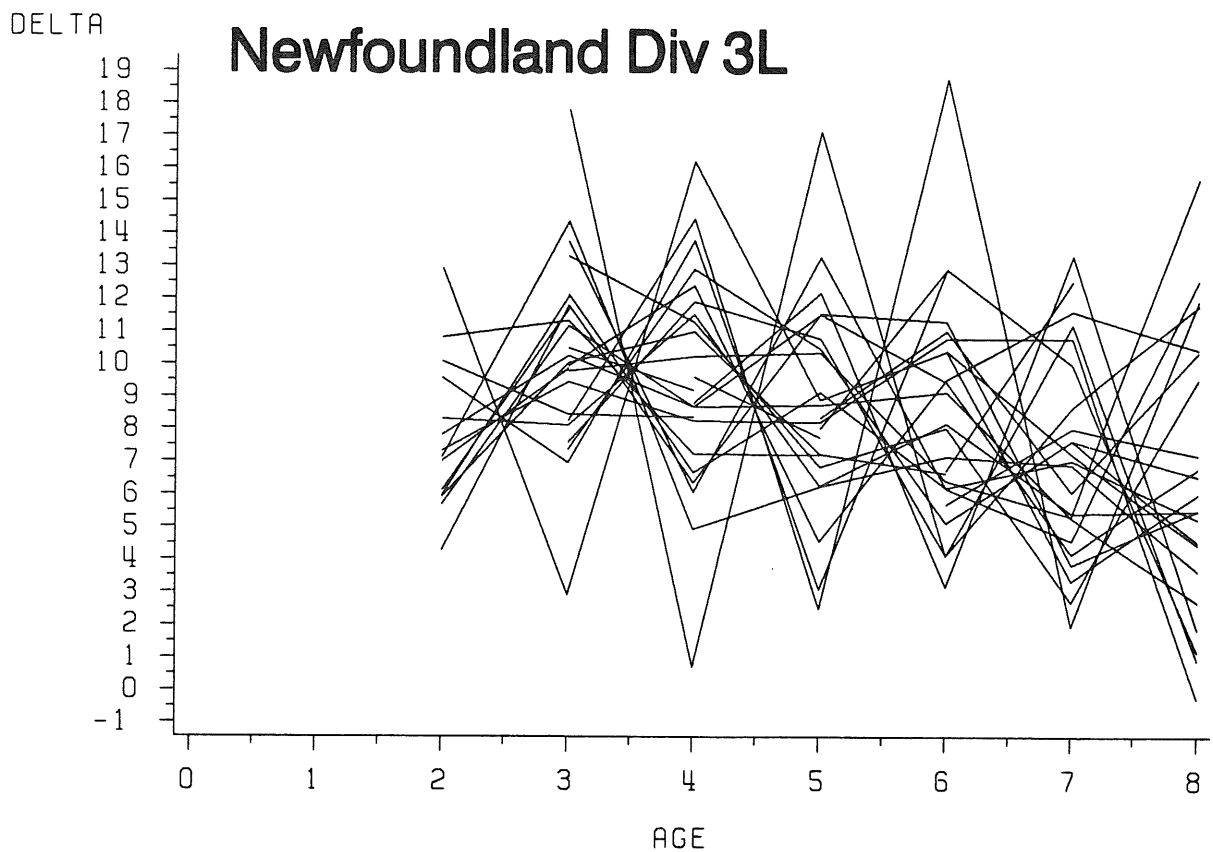


Figure 5.1.4.12. Length increment (delta) by cohort at each age in Div. 3L.

Newfoundland Div 2J

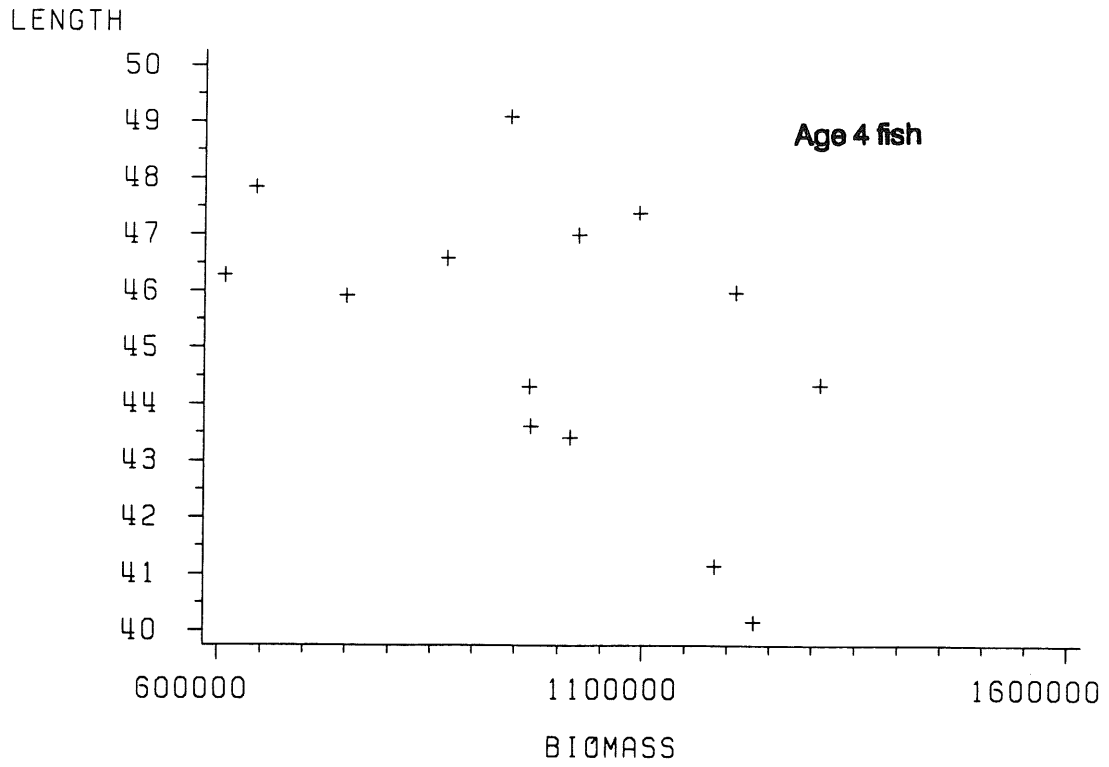


Figure 5.1.4.13. Length at age 4 in Div. 2J against biomass.

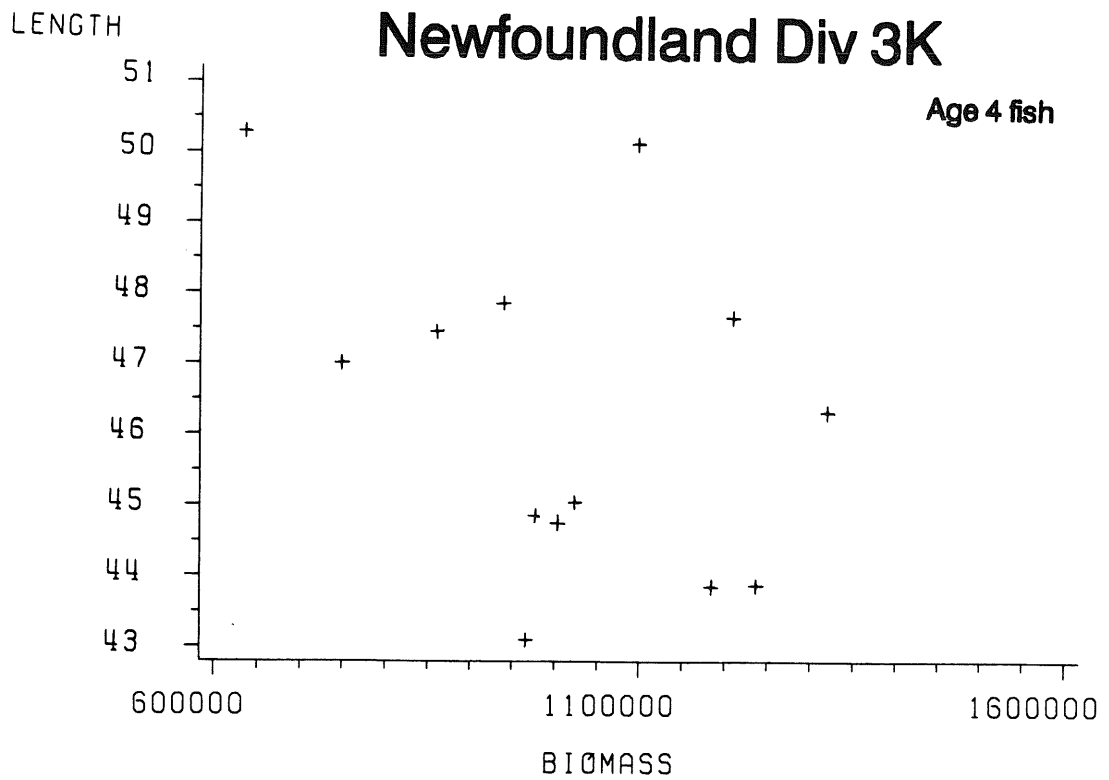


Figure 5.1.4.14. Length at age 4 in Div. 3K against biomass.

Newfoundland Div 3L

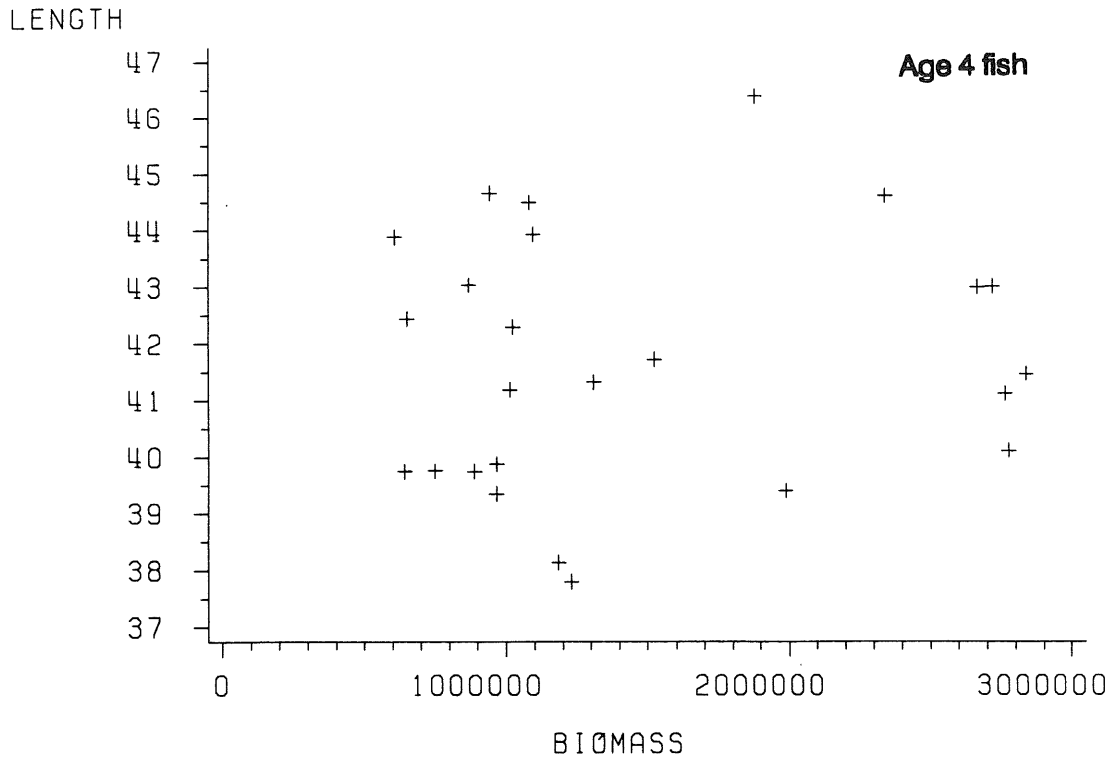


Figure 5.1.4.15. Length at age 4 in Div. 3L against biomass.

Newfoundland Div 2J

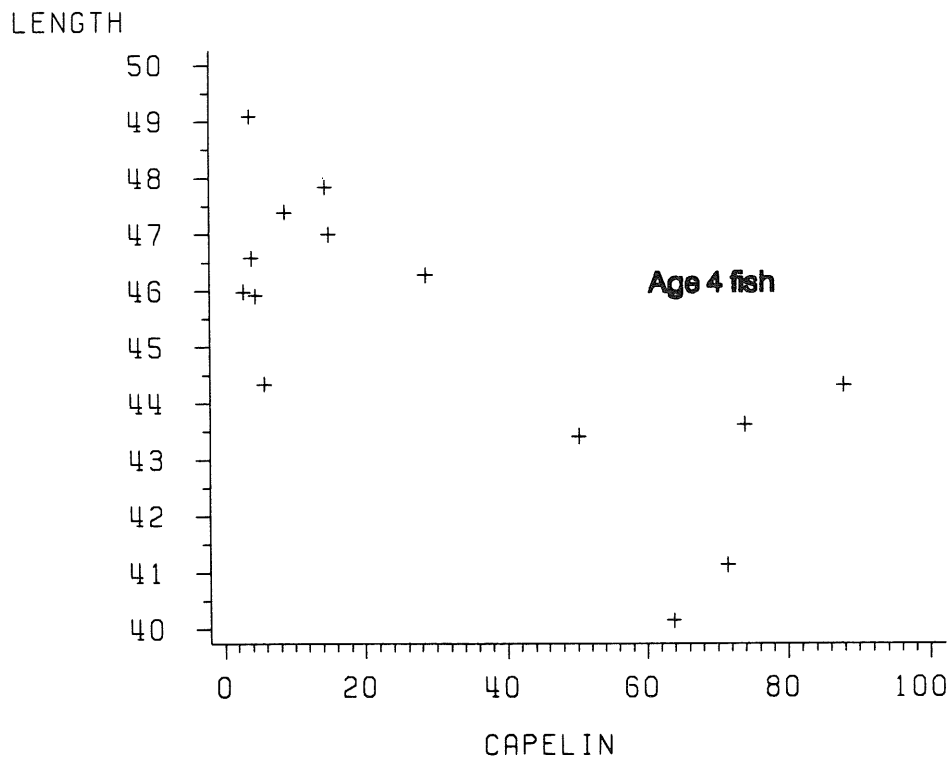


Figure 5.1.4.16. Length at age 4 in Div. 2J against capelin abundance.

Newfoundland Div 3K

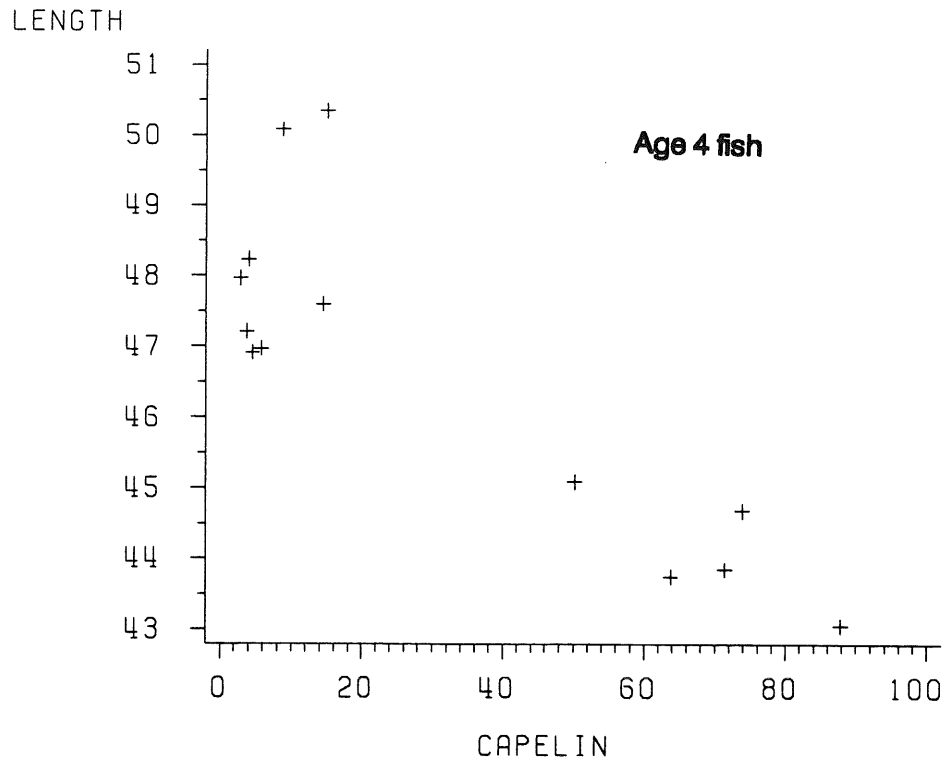


Figure 5.1.4.17. Length at age 4 in Div. 3K against capelin abundance.

Newfoundland Div 3L

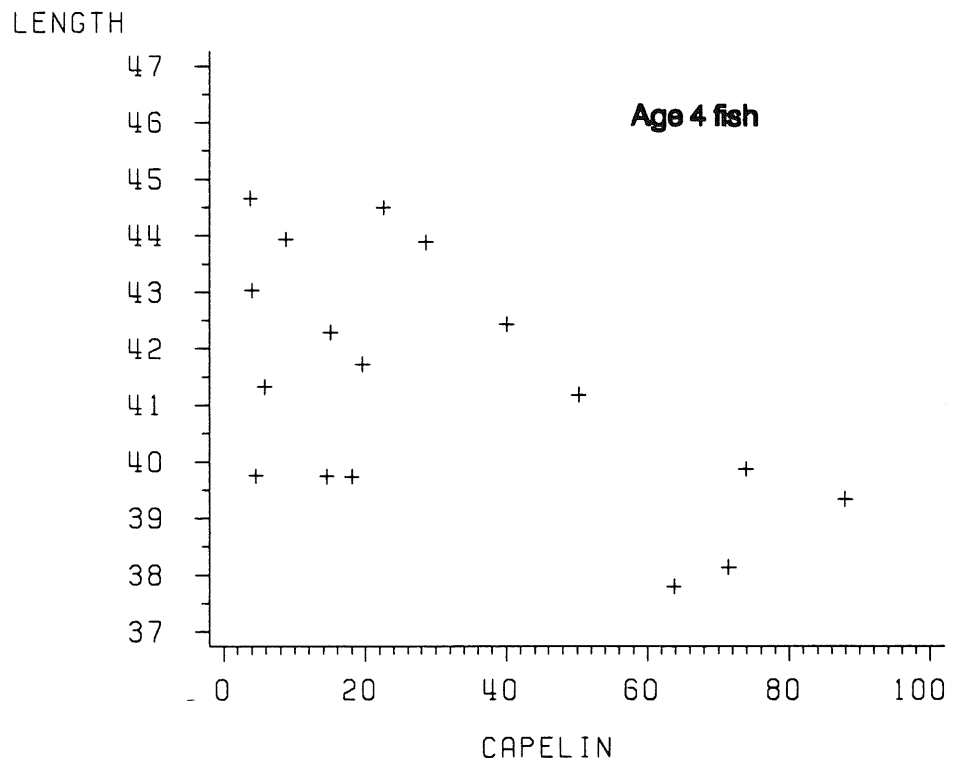


Figure 5.1.4.18. Length at age 4 in Div. 3L against capelin abundance.

Newfoundland Div 2J

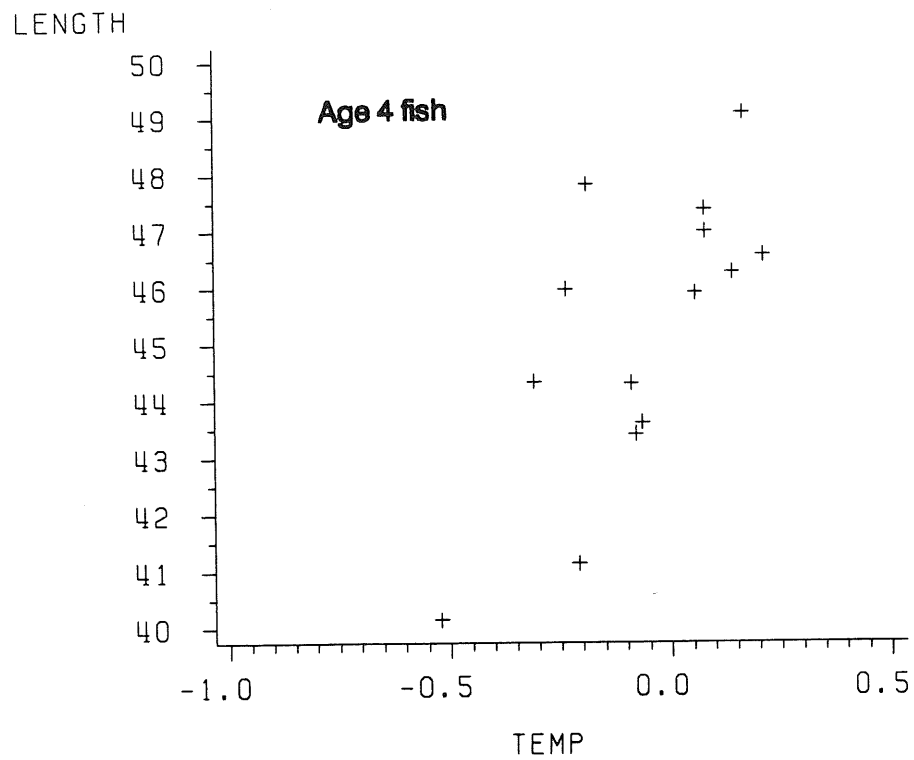


Figure 5.1.4.19. Length at age 4 in Div. 2J against temperature anomaly.

Newfoundland Div 3K

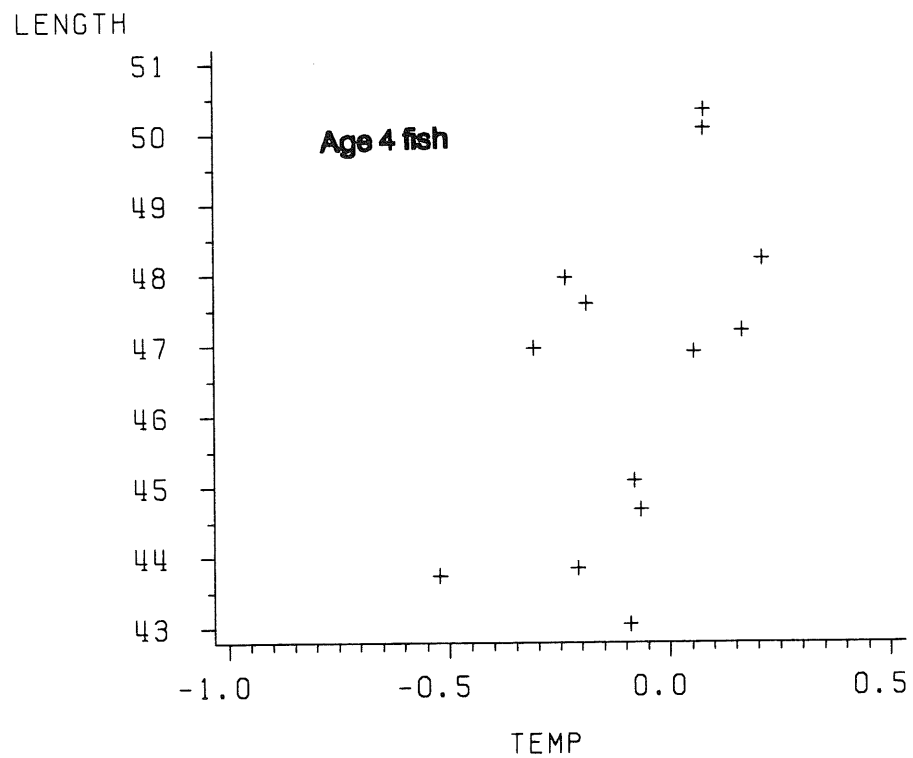


Figure 5.1.4.20. Length at age 4 in Div. 3K against temperature anomaly.

Newfoundland Div 3L

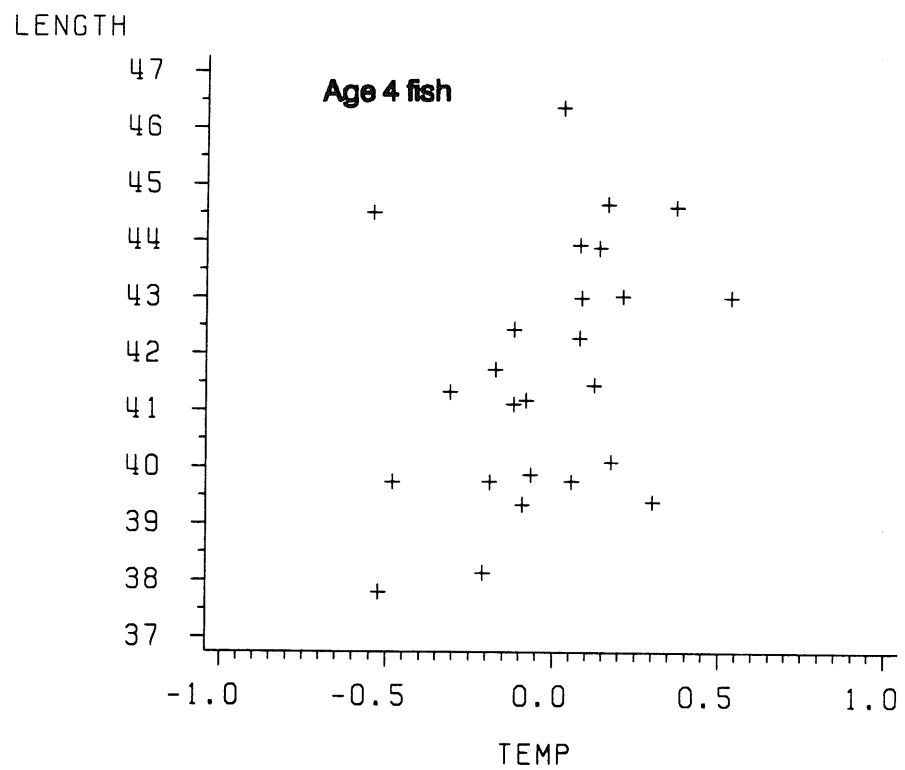


Figure 5.1.4.21. Length at age 4 in Div. 3L against temperature anomaly.

NEWFOUNDLAND 3K FALL

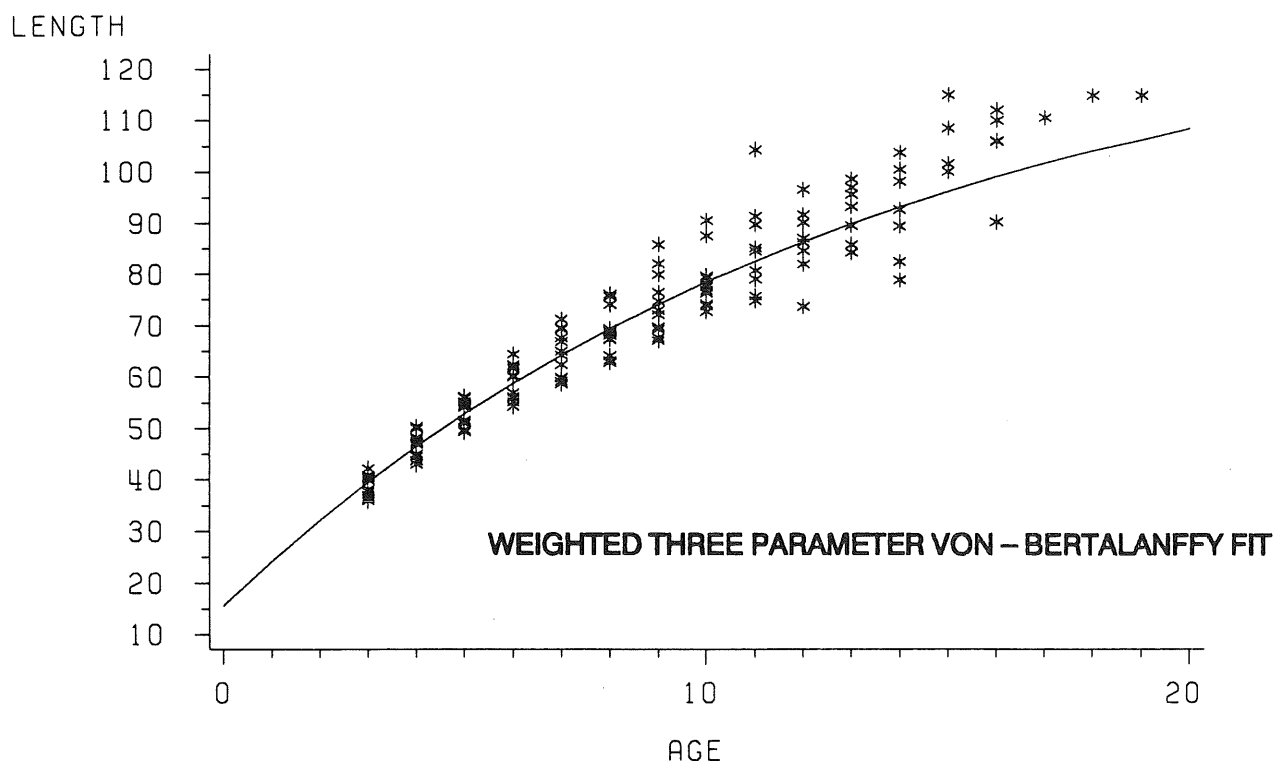


Figure 5.3.2.1.1. Length at age data and three parameter von-Bertalanffy least squares fit to Newfoundland Div. 3K.

NEWFOUNDLAND 3K FALL

COHORT=70

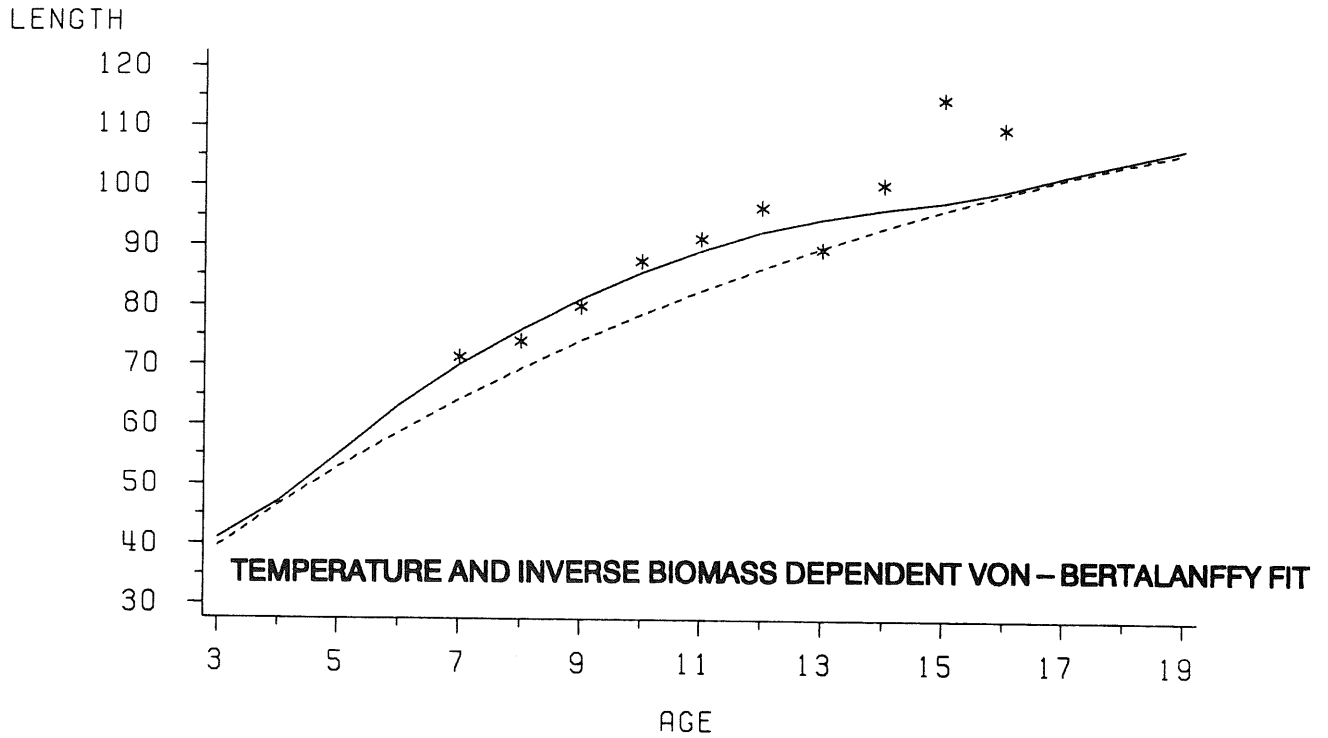
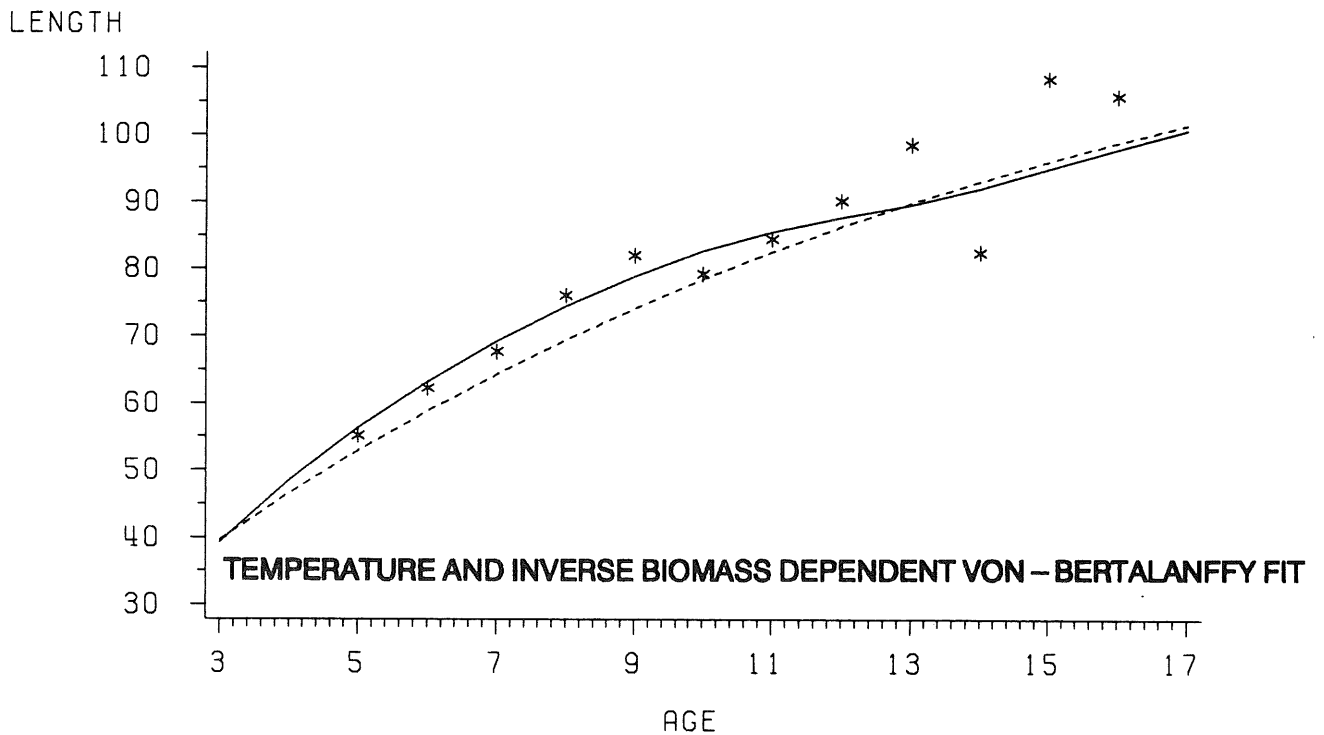


Figure 5.3.2.1.2. Length at age data and three parameter von-Bertalanffy fit (dashed line) and environmental fit using independent variables 1/cod biomass and temperature (solid line) for cohort 1970 in Newfoundland Div. 3K.

COHORT=72

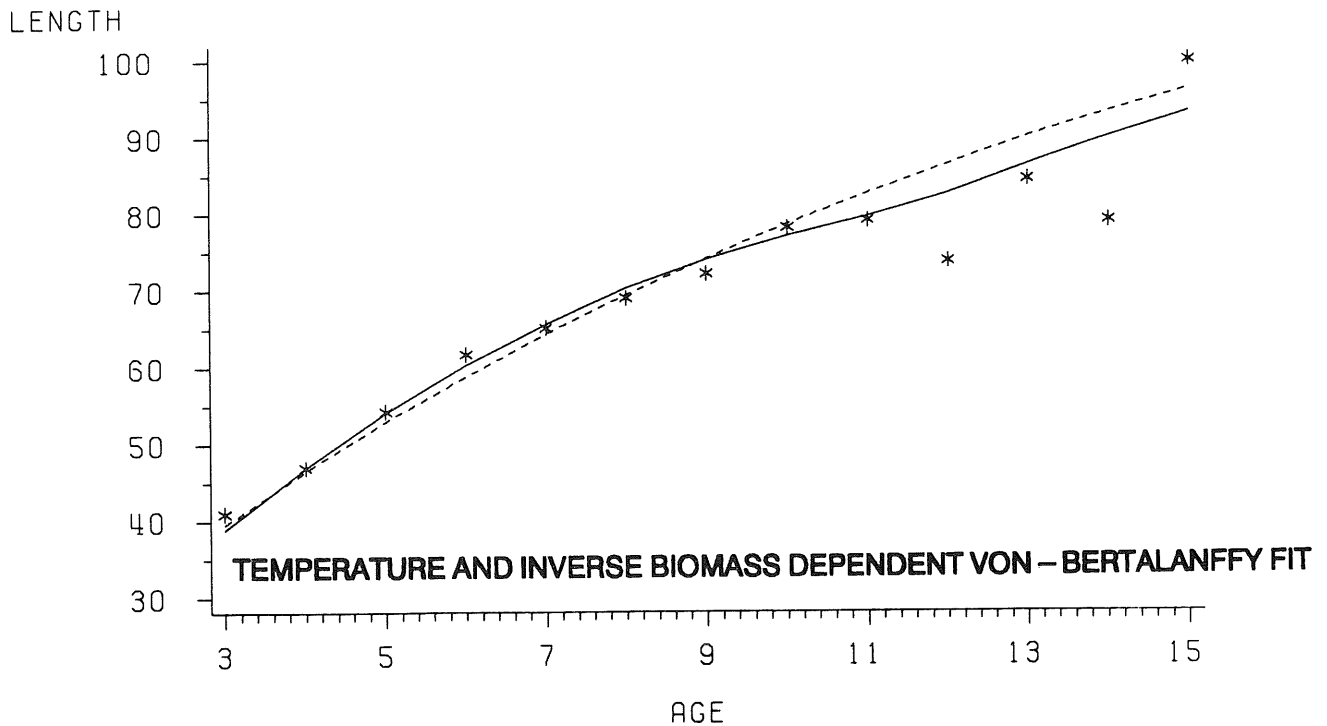


Figures 5.3.2.1.3. Length at age data and three parameter von-Bertalanffy fit (dashed line) and environmental fit using independent variables 1/cod biomass and temperature (solid line) for cohort 1972 in Newfoundland Div. 3K.

NEWFOUNDLAND 3K FALL

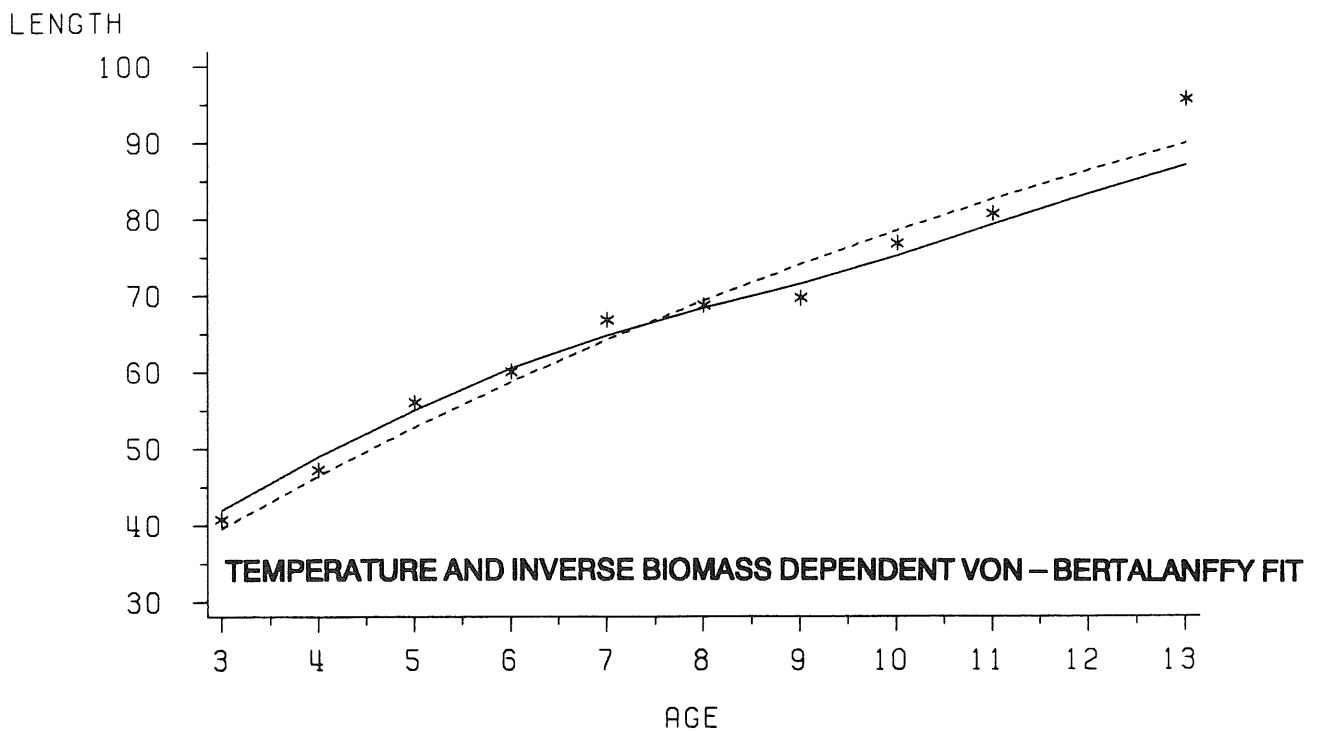
215

COHORT=74



Figures 5.3.2.1.4. Length at age data and three parameter von-Bertalanffy fit (dashed line) and environmental fit using independent variables 1/cod biomass and temperature (solid line) for cohort 1974 in Newfoundland Div. 3K.

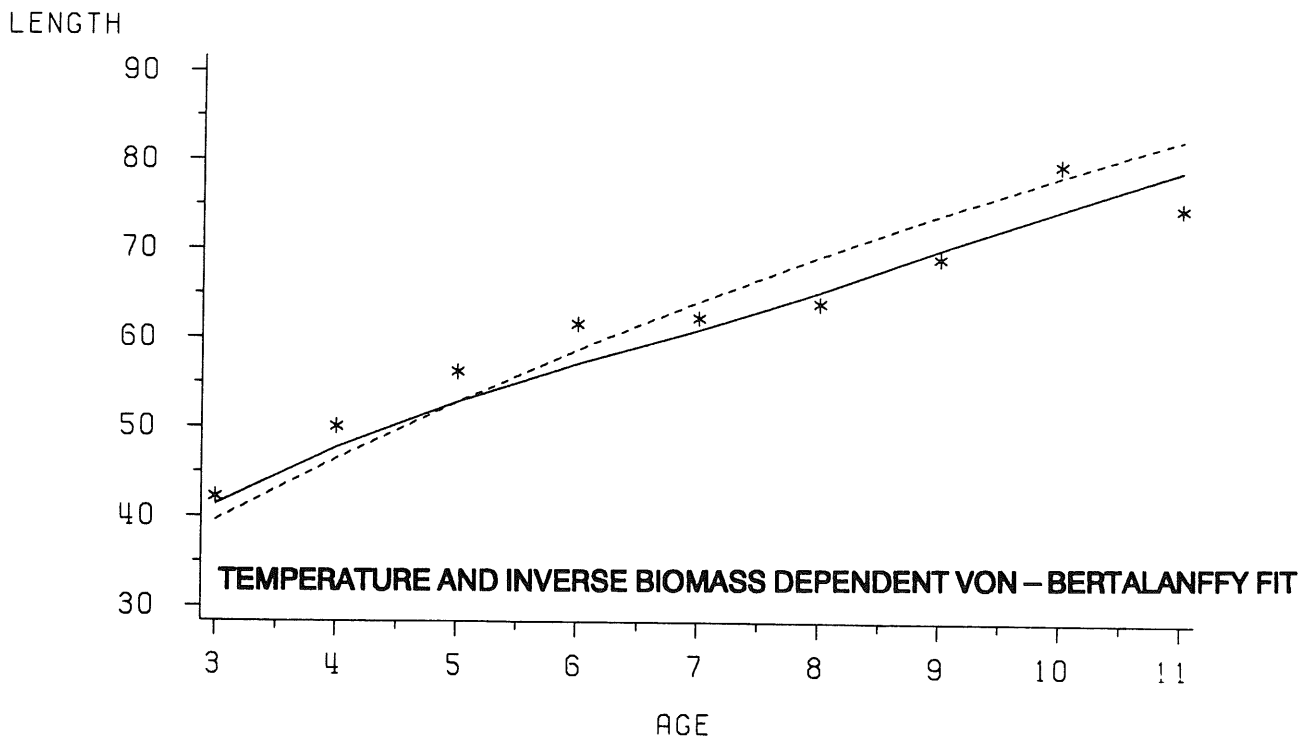
COHORT=76



Figures 5.3.2.1.5. Length at age data and three parameter von-Bertalanffy fit (dashed line) and environmental fit using independent variables 1/cod biomass and temperature (solid line) for cohort 1976 in Newfoundland Div. 3K.

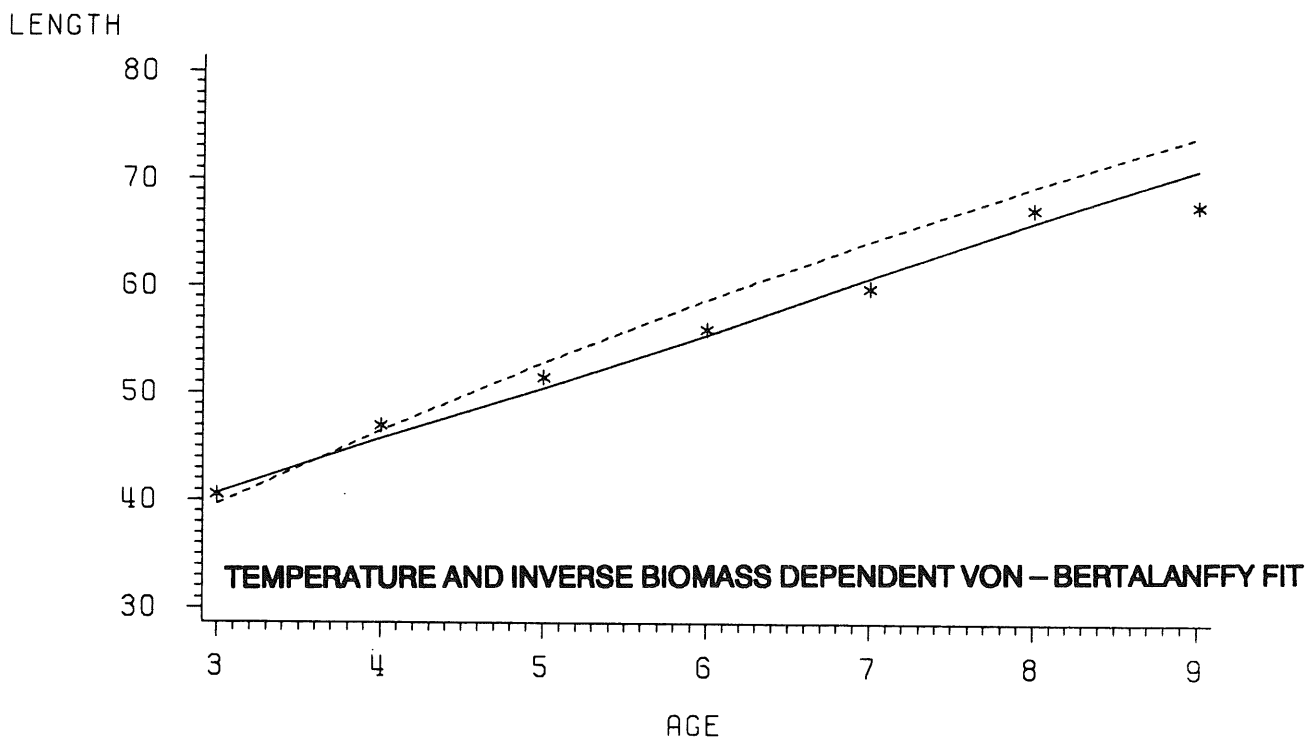
NEWFOUNDLAND 3K FALL

COHORT=78



Figures 5.3.2.1.6. Length at age data and three parameter von-Bertalanffy fit (dashed line) and environmental fit using independent variables 1/cod biomass and temperature (solid line) for cohort 1978 in Newfoundland Div. 3K.

COHORT=80



Figures 5.3.2.1.7. Length at age data and three parameter von-Bertalanffy fit (dashed line) and environmental fit using independent variables 1/cod biomass and temperature (solid line) for cohort 1980 in Newfoundland Div. 3K.

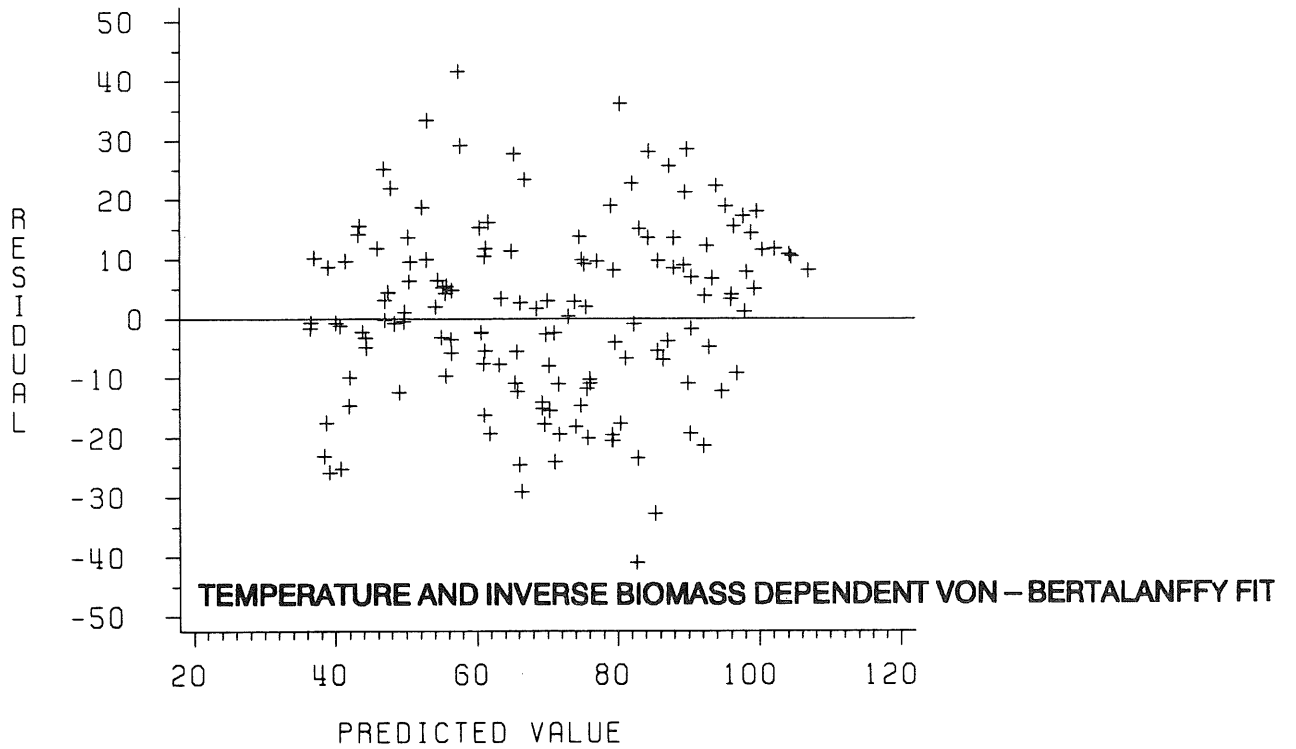


Figure 5.3.2.1.8. Residual plots for the environmental fit to Newfoundland Div. 3K, length at age data.

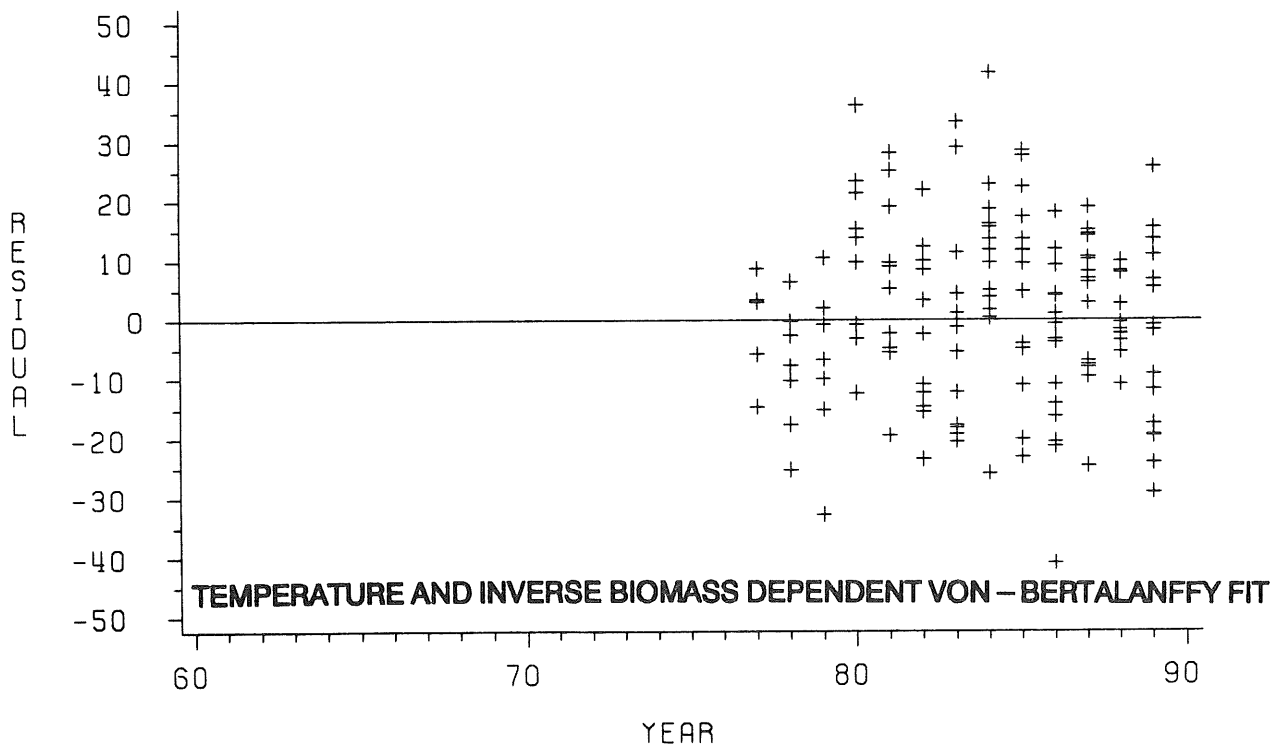


Figure 5.3.2.1.9. Residual plots for the environmental fit to Newfoundland Div. 3K, length at age data.

NEWFOUNDLAND 3K FALL

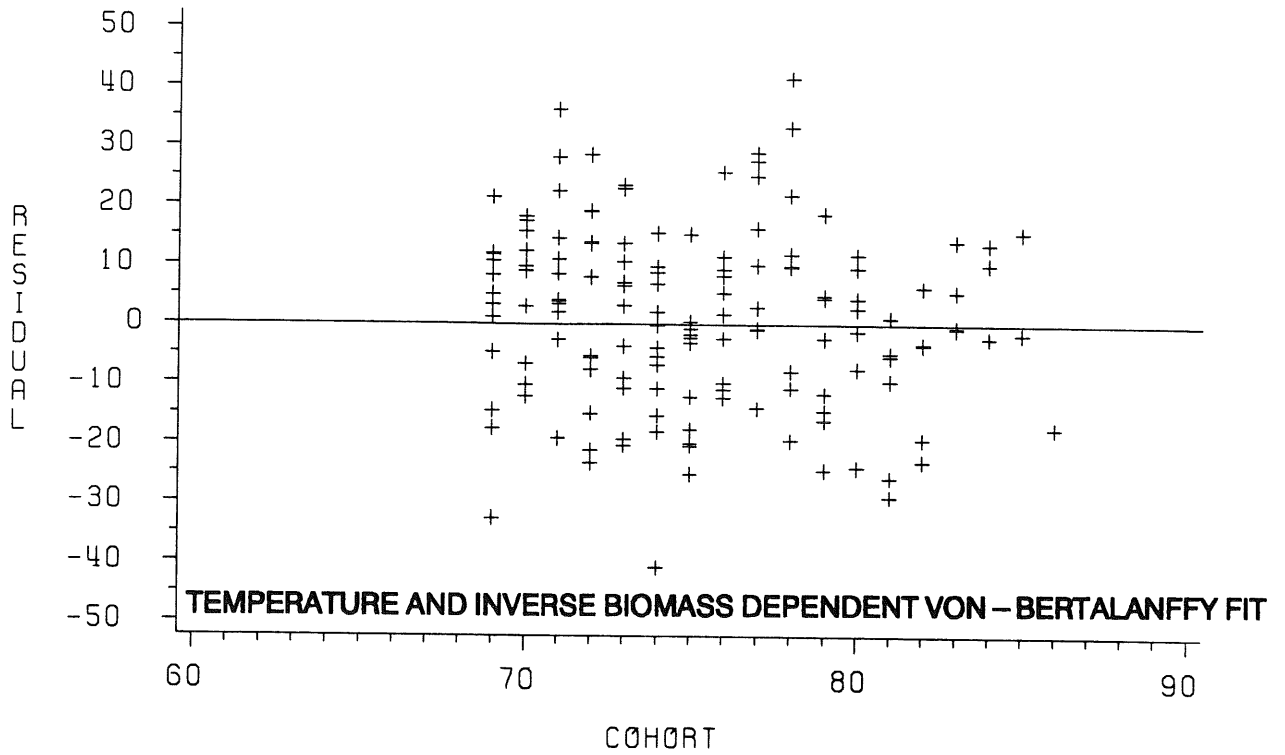


Figure 5.3.2.1.10. Residual plots for the environmental fit to Newfoundland Div. 3K, length at age data.

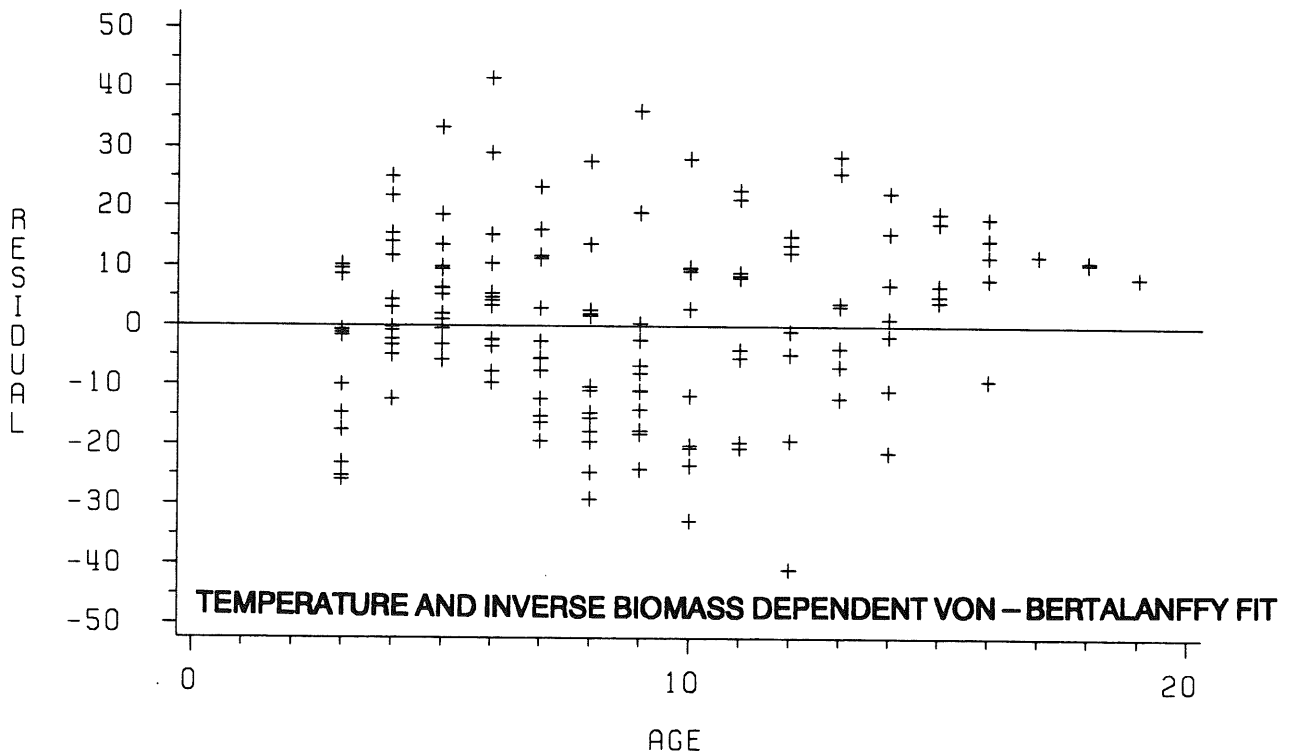


Figure 5.3.2.1.11. Residual plots for the environmental fit to Newfoundland Div. 3K, length at age data.

NEWFOUNDLAND 3K FALL

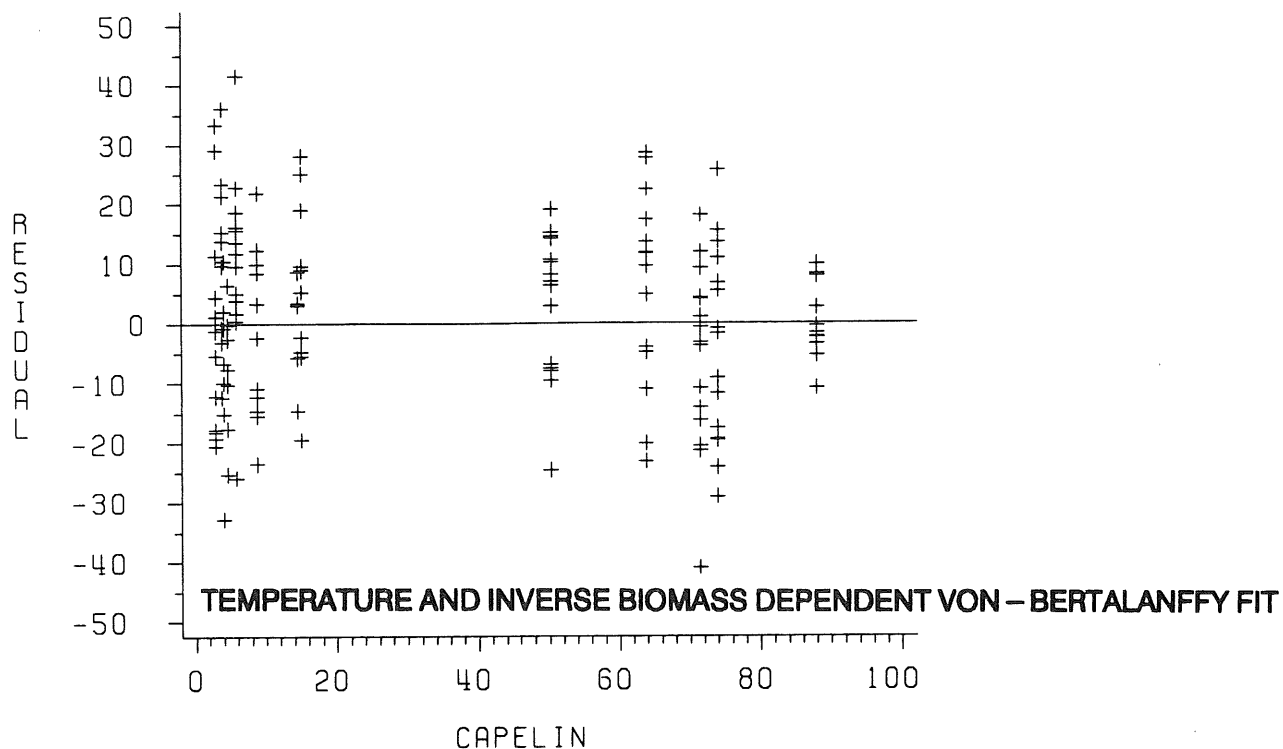


Figure 5.3.2.1.12. Residual plots for the environmental fit to Newfoundland Div. 3K, length at age data.

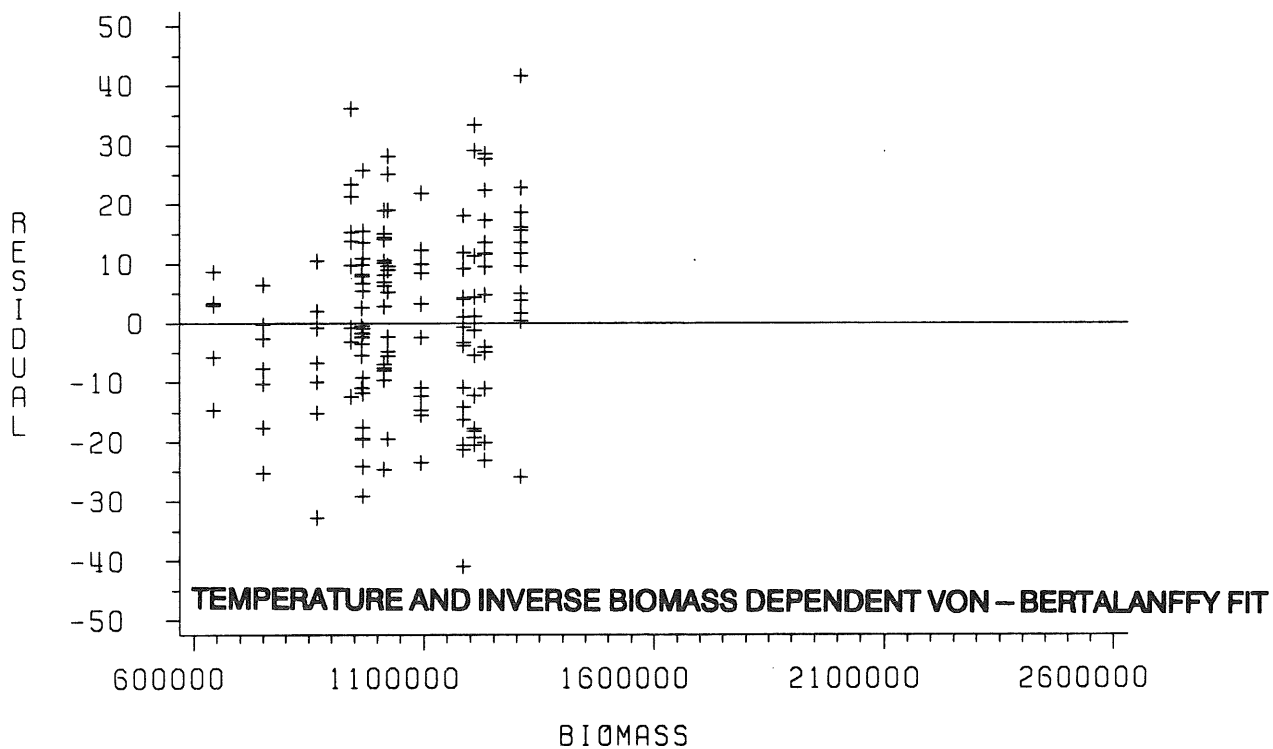


Figure 5.3.2.1.13. Residual plots for the environmental fit to Newfoundland Div. 3K, length at age data.

NEWFOUNDLAND 3K FALL

TEMPERATURE AND INVERSE BIOMASS DEPENDENT VON – BERTALANFFY FIT

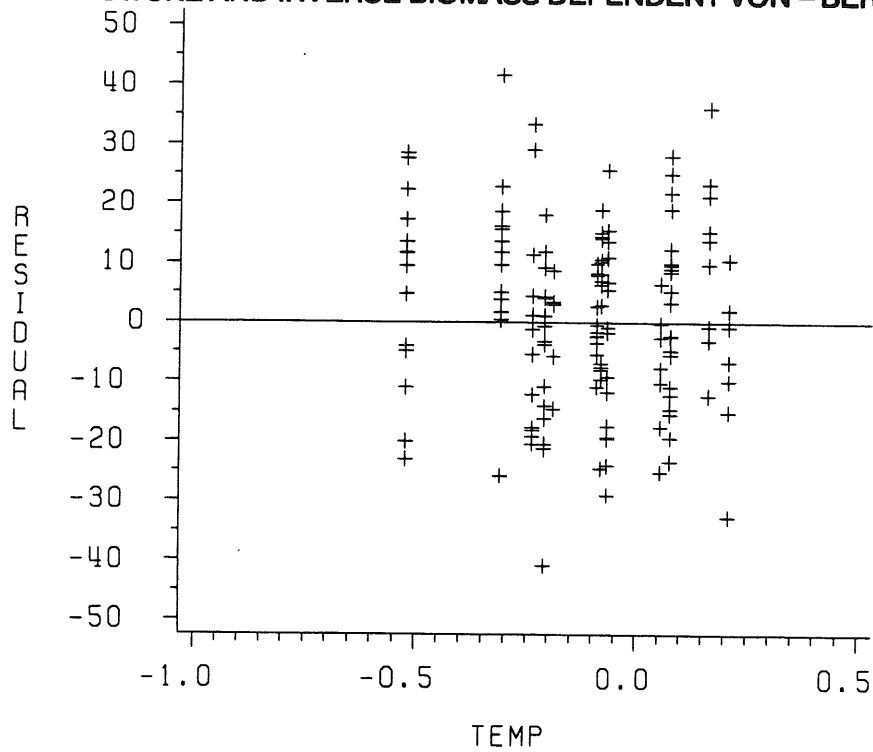


Figure 5.3.2.1.14. Residual plots for the environmental fit to Newfoundland Div. 3K, length at age data.

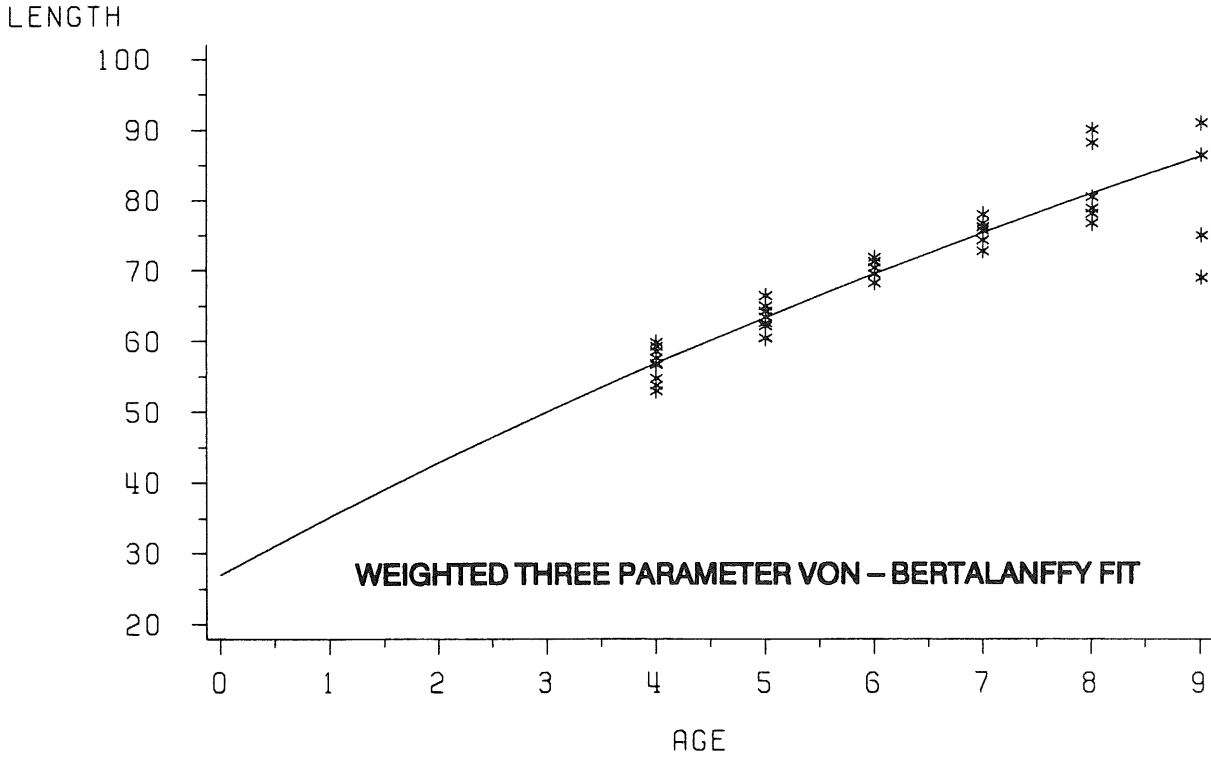


Figure 5.3.2.1.15. Length at age data and three parameter von-Bertalanffy least squares fit to Iceland, North East.

COHORT=76

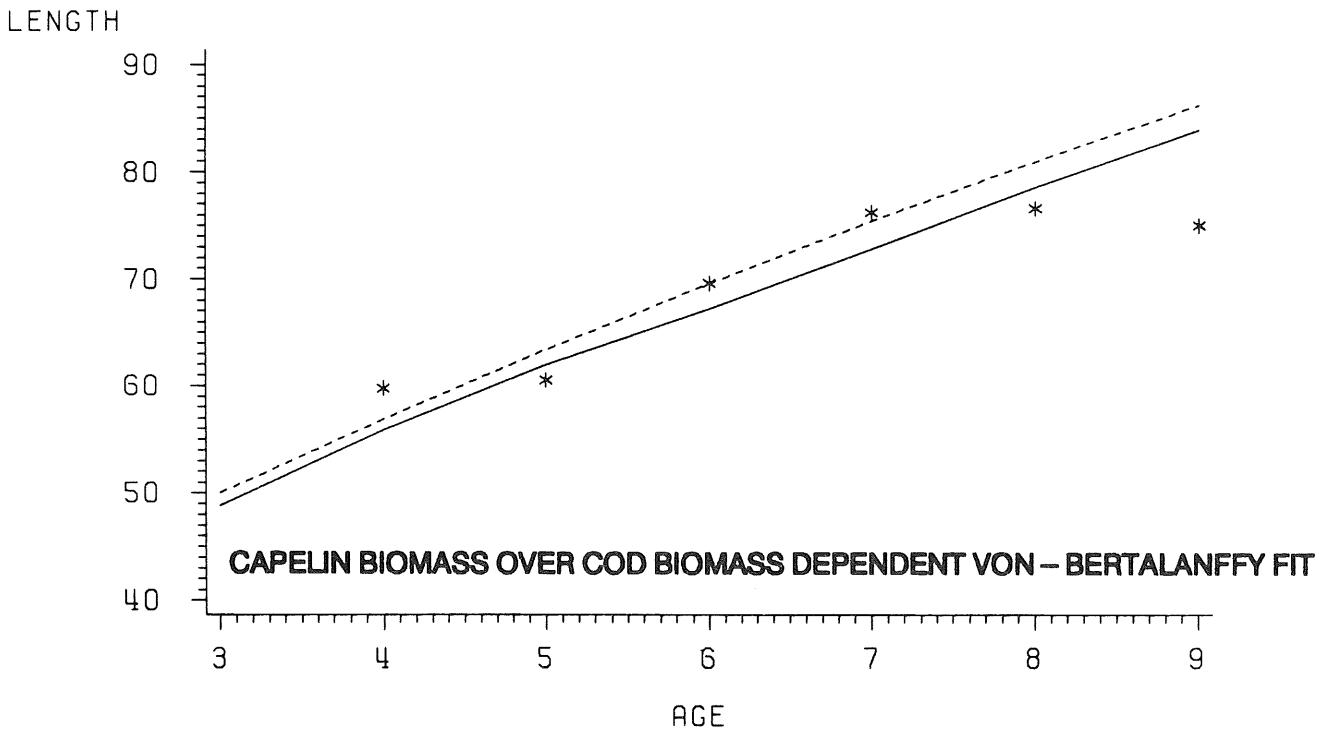


Figure 5.3.2.1.16. Length at age data and three parameter von-Bertalanffy fit (dashed line) and environmental fit using independent variable capelin biomass/cod biomass (solid line) for cohort 76 in Iceland, North East.

ICELAND

COHORT=77

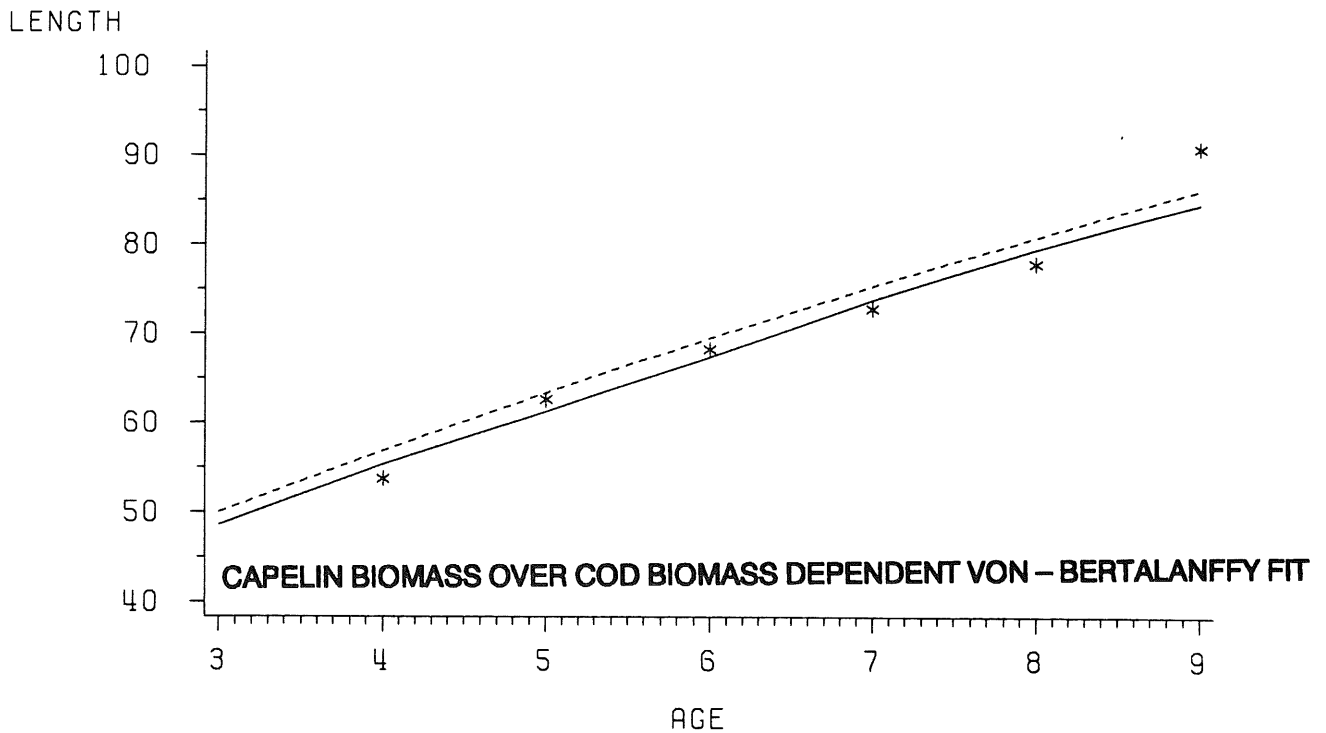


Figure 5.3.2.1.17. Length at age data and three parameter von-Bertalanffy fit (dashed line) and environmental fit using independent variable capelin biomass/cod biomass (solid line) for cohort 77 in Iceland, North East.

COHORT=78

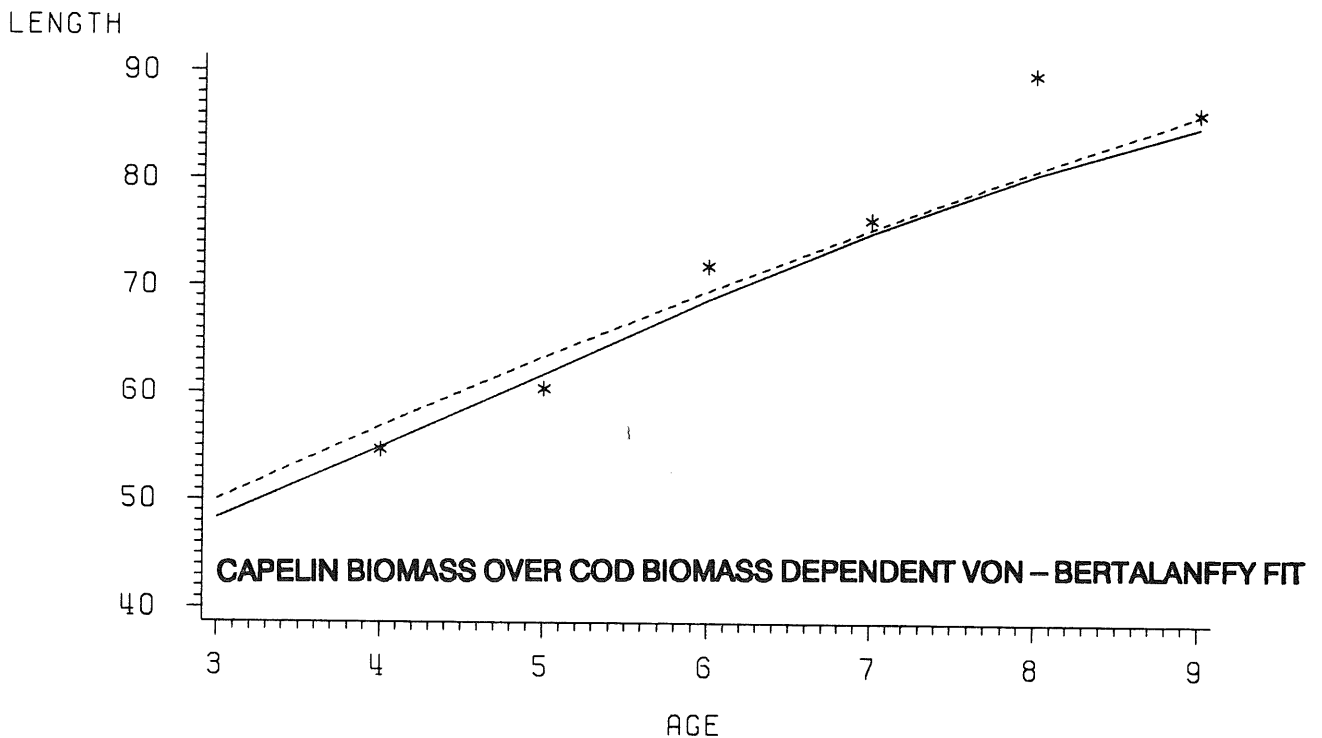


Figure 5.3.2.1.18. Length at age data and three parameter von-Bertalanffy fit (dashed line) and environmental fit using independent variable capelin biomass/cod biomass (solid line) for cohort 78 in Iceland, North East.

ICELAND

223

COHORT=79

LENGTH

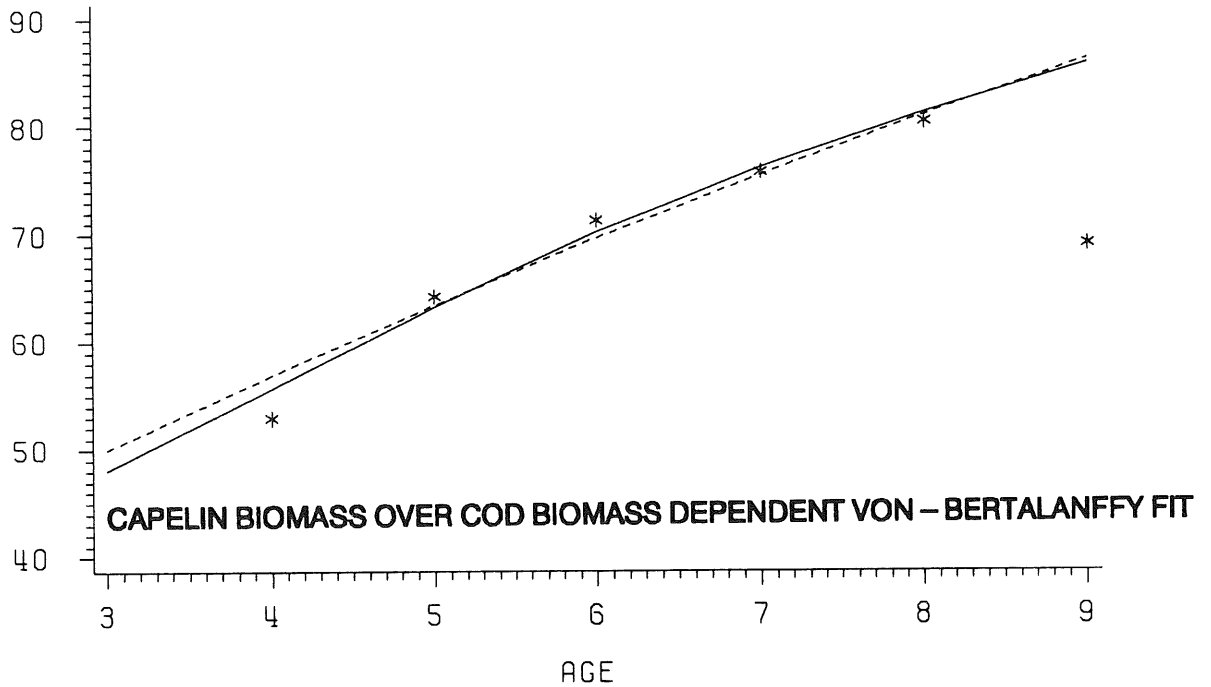


Figure 5.3.2.1.19. Length at age data and three parameter von-Bertalanffy fit (dashed line) and environmental fit using independent variable capelin biomass/cod biomass (solid line) for cohort 79 in Iceland, North East.

COHORT=80

LENGTH

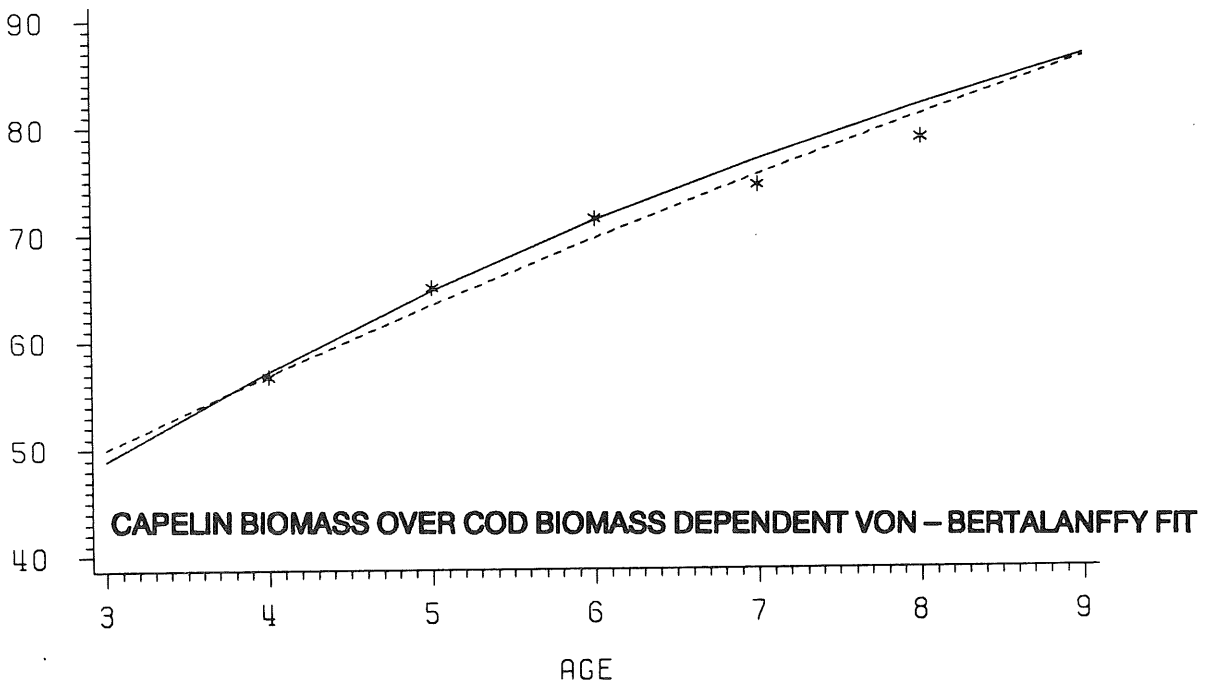


Figure 5.3.2.1.20. Length at age data and three parameter von-Bertalanffy fit (dashed line) and environmental fit using independent variable capelin biomass/cod biomass (solid line) for cohort 80 in Iceland, North East.

ICELAND

COHORT=81

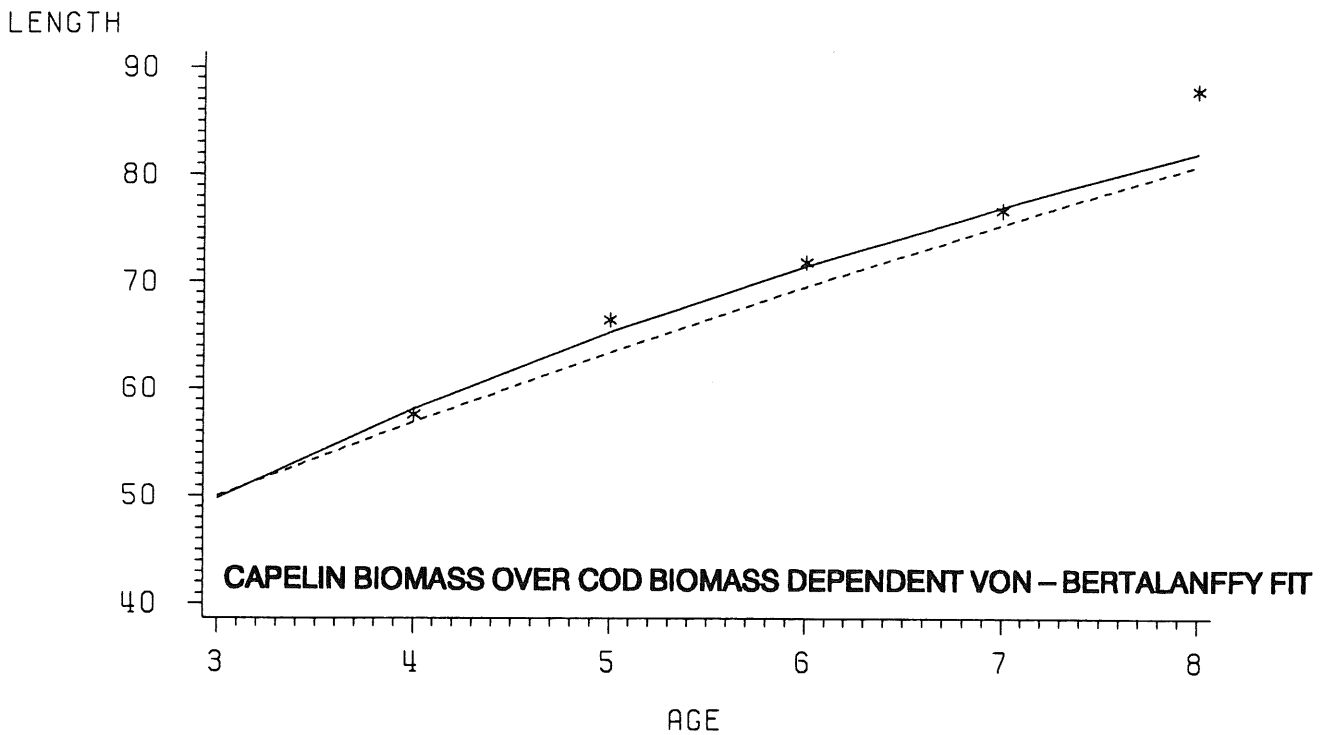


Figure 5.3.2.1.21. Length at age data and three parameter von-Bertalanffy fit (dashed line) and environmental fit using independent variable capelin biomass/cod biomass (solid line) for cohort 81 in Iceland, North East.

COHORT=82

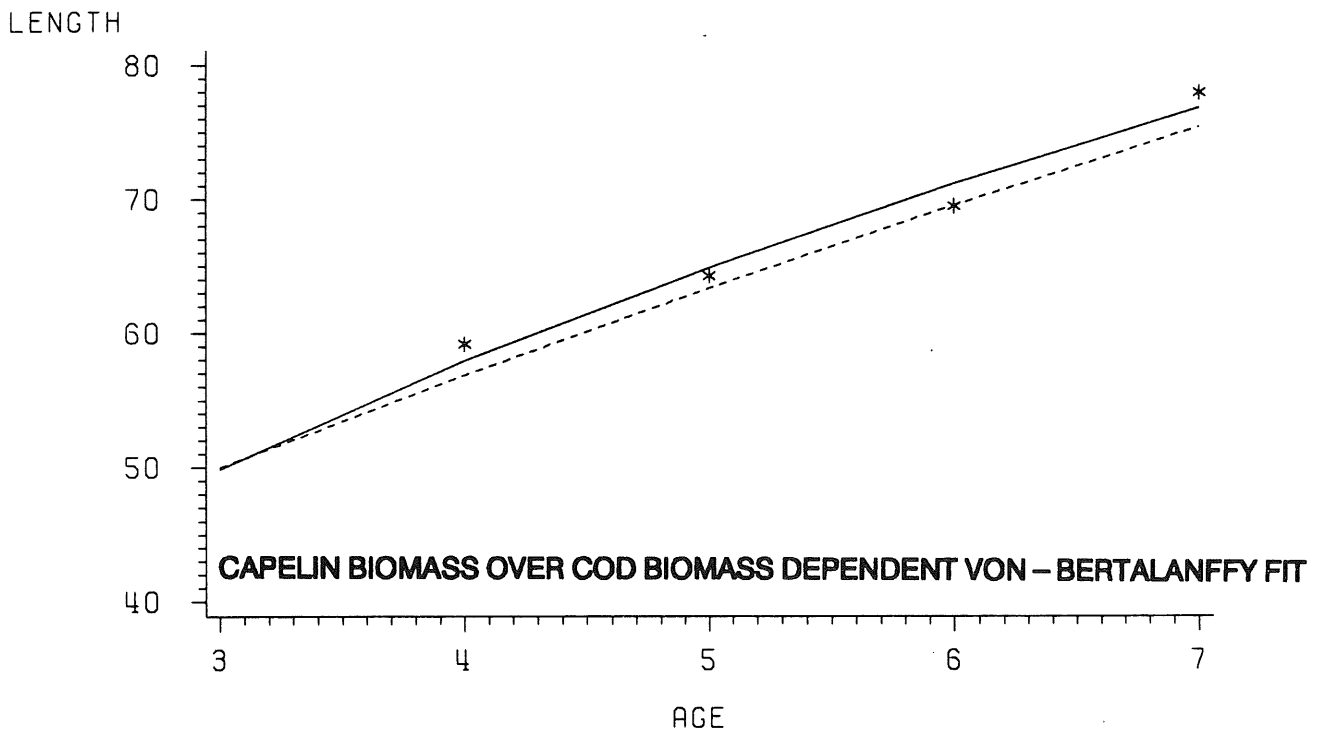


Figure 5.3.2.1.22. Length at age data and three parameter von-Bertalanffy fit (dashed line) and environmental fit using independent variable capelin biomass/cod biomass (solid line) for cohort 82 in Iceland, North East.

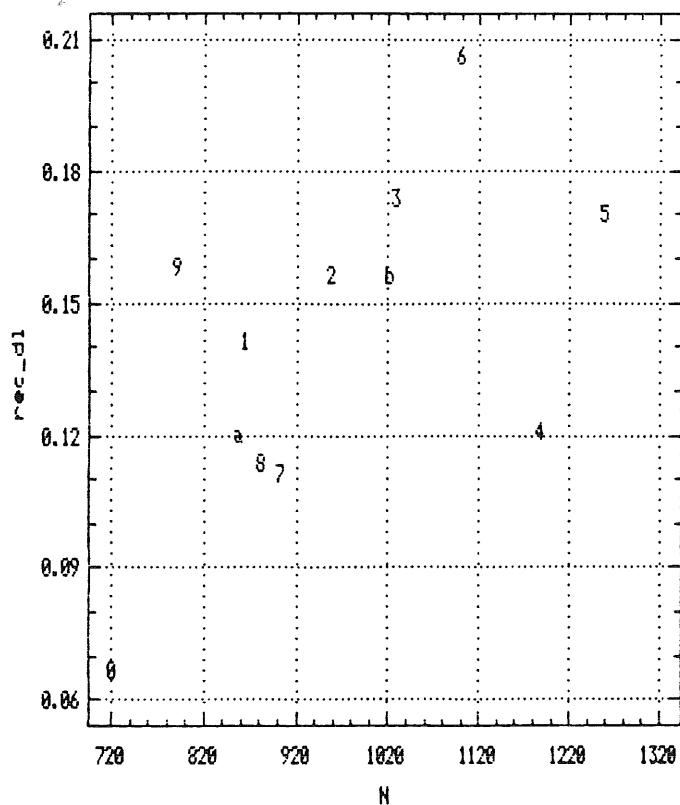


Figure 5.3.2.3.1. Plot of red_dl ($=1/(l_{t+1} - \exp(-K) l_t)$) vs. stock numbers for Newfoundland cod from Division 3K for years 1978-1989 (a=1988, b=1989).

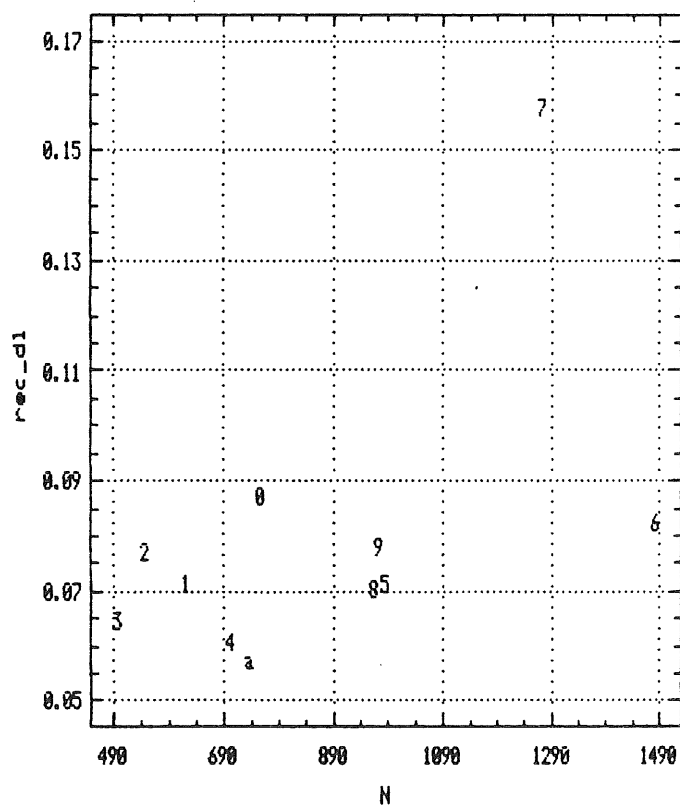


Figure 5.3.2.3.2. Plot of red_dl ($=1/(l_{t+1} - \exp(-K) l_t)$) vs. stock numbers for Barents Sea cod for years 1979-1989 (a=1989).

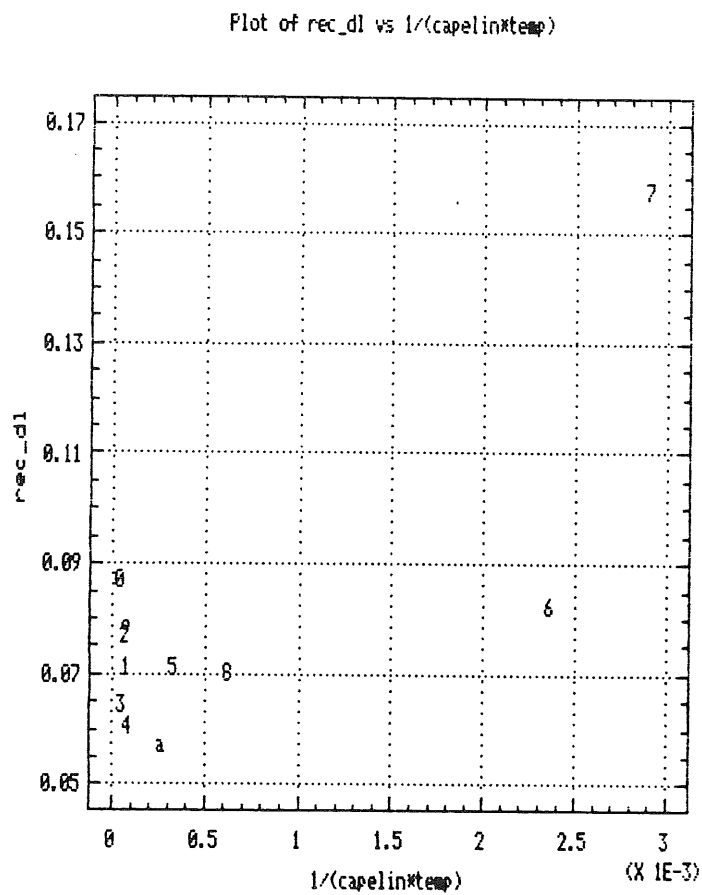


Figure 5.3.2.3.3. Plot of red_dl ($=1/(l_{t+1} - \exp(-K) l_t)$) vs. $1/(\text{capelin stock size} * \text{temperature})$ for Barents Sea cod for years 1979-1989 (a=1989).

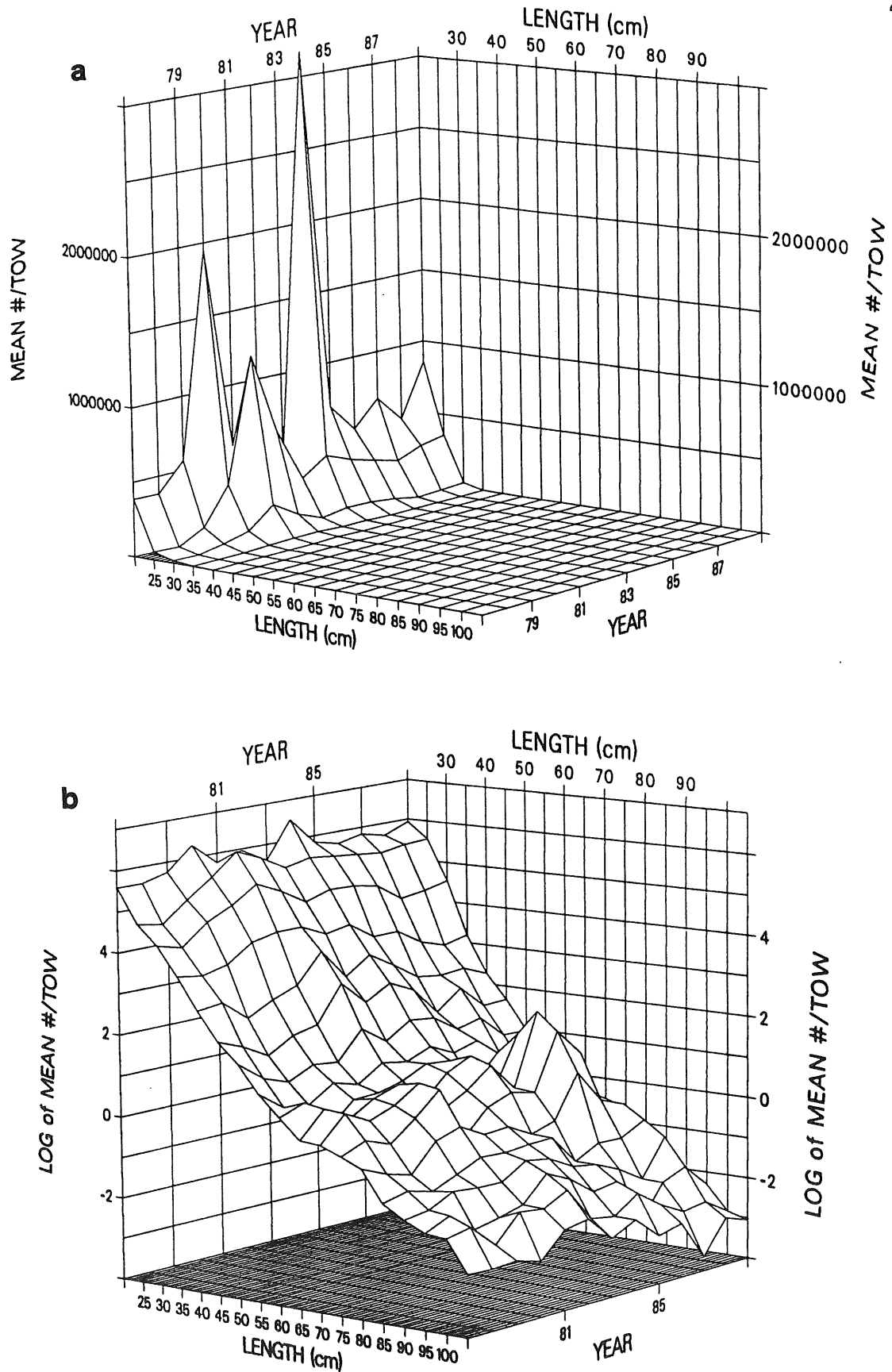


Figure 7.1.1. Multispecies length composition (numbers per hour trawling, in 5 cm length groups) for the English groundfish survey of the North Sea, 1977-1989. Data are expressed as numbers per tow (a, above) and \log_{10} numbers per tow (b, below).

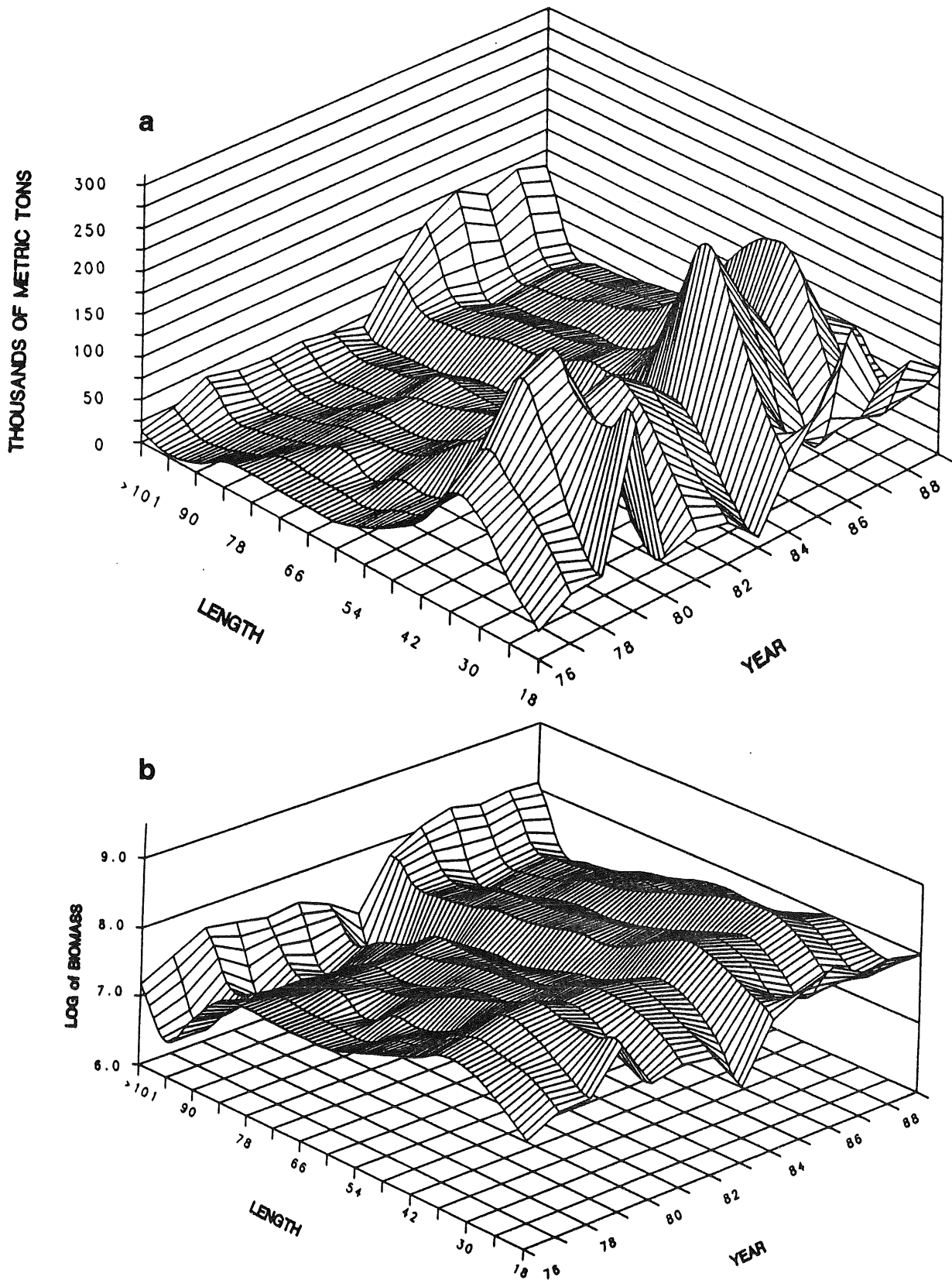


Figure 7.1.2. Multispecies length composition (areal-expansion estimate of total fish biomass, in 6 cm length groups) for Canadian bottom trawl surveys of NAFO Division 3LNO (Newfoundland), 1976-1989. Species include cod, thorny skate, haddock, golden redfish, Atlantic halibut, plaice, witch, yellowtail, turbot, and deepwater redfish. Data are expressed as biomass at length (a, above) and log biomass at length (b, below).

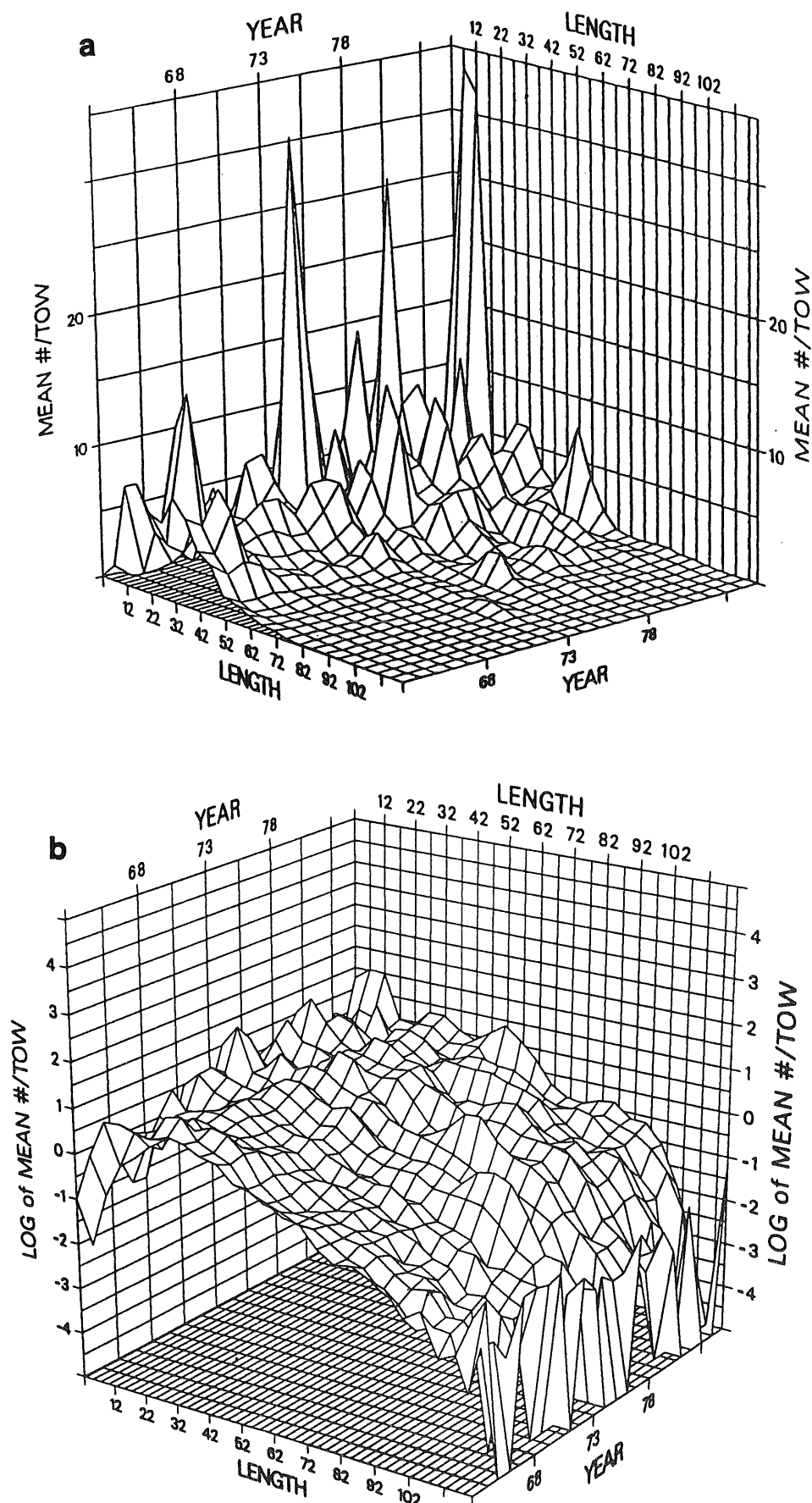


Figure 7.1.3. Multispecies length composition (numbers per standardized survey tow, in 5 cm length groups) for the Northeast Fisheries Center autumn bottom trawl survey of Georges Bank, 1963-1985. Data are expressed as number per tow (a, above) and \log_{10} number per tow (b, below).

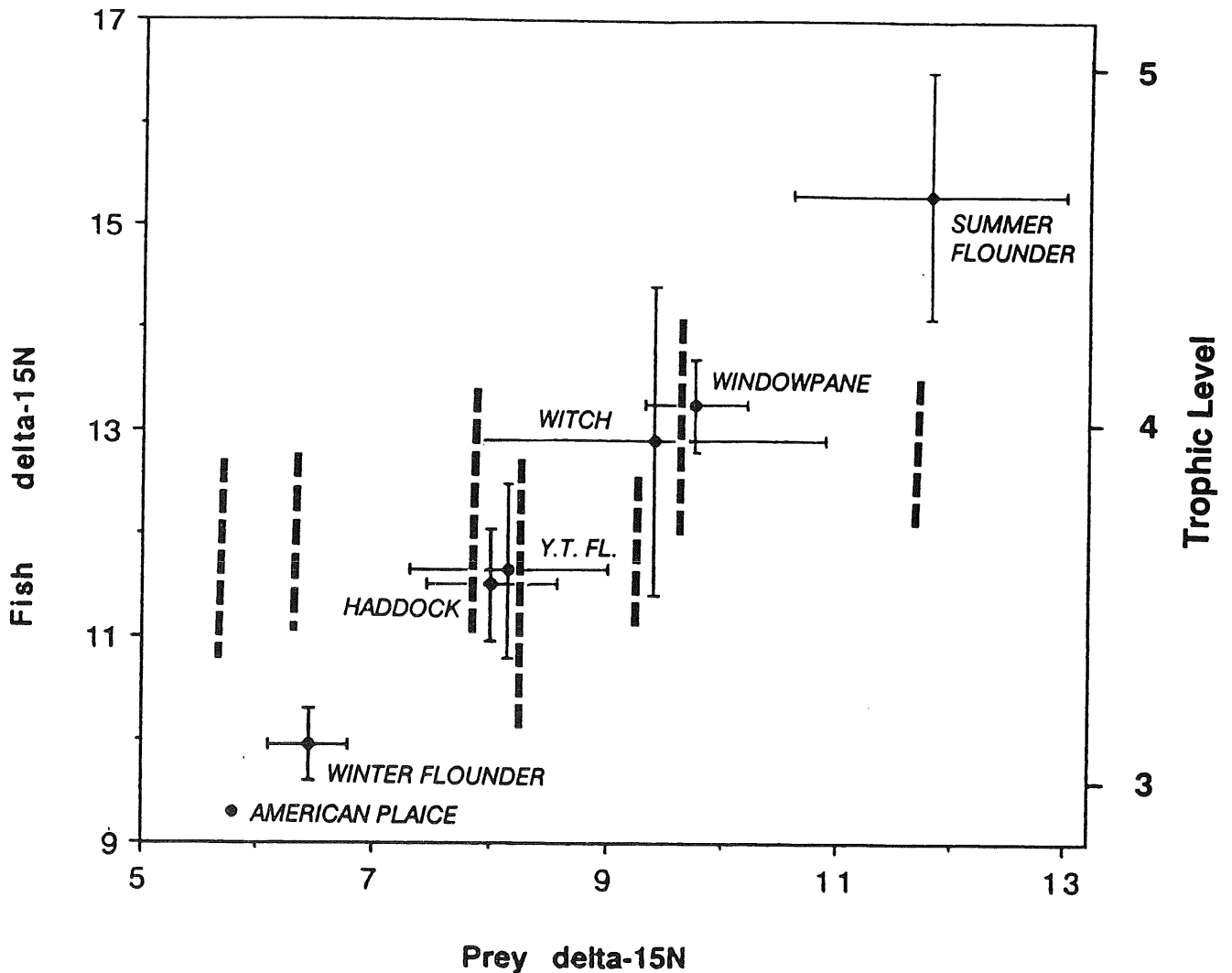


Figure 8.3.1. Predicted $\delta^{15}\text{N}$ values for seven demersal fish species from Georges Bank. Horizontal error bars are ranges of prey $\delta^{15}\text{N}$ values from published gut content data and measured $\delta^{15}\text{N}$ of prey items. Vertical error bars are predicted ranges of fish $\delta^{15}\text{N}$ values, calculated by adding the factor 3.5% (one trophic level) to the ranges of prey isotope values. Bold, dotted vertical lines are ranges of actual measures stable isotope values for fish (including variation due to size of fish and year collected). The right-hand scale is based on the relationship: trophic level = $\delta^{15}\text{N}/3.50/00\delta^{15}\text{N}$.

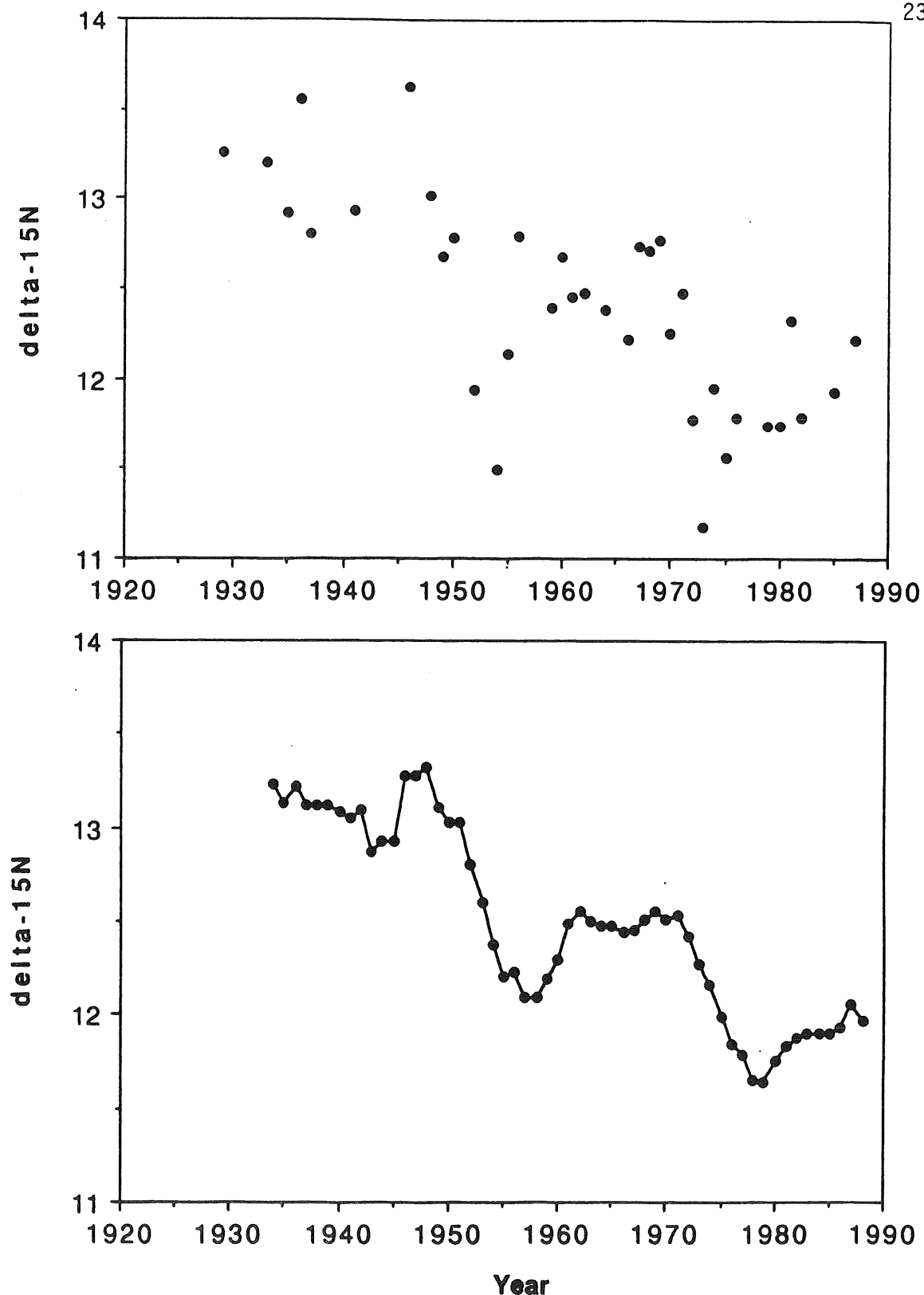


Figure 8.3.2. Values of $\delta^{15}\text{N}$ determined from Georges Bank haddock, 1930-1986. The top Figure plots values for composite samples of scales from 4-7 individual fish collected from Georges Bank in autumn. All individuals were 40 ± 2 cm. Analyses were conducted with a Finnigan stable isotope ratio mass spectrometer. The bottom figure is a 6-year running average of raw data.

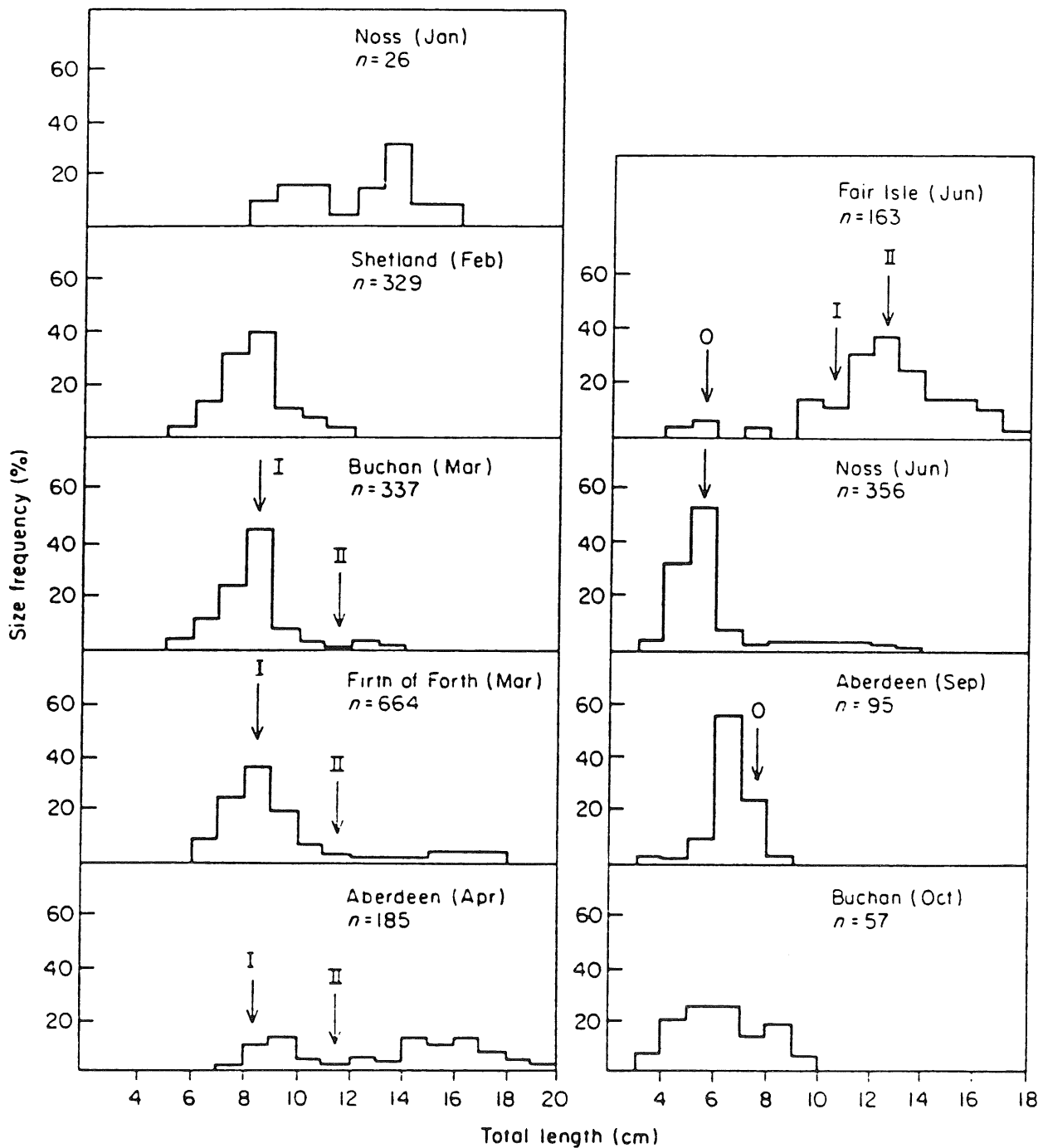
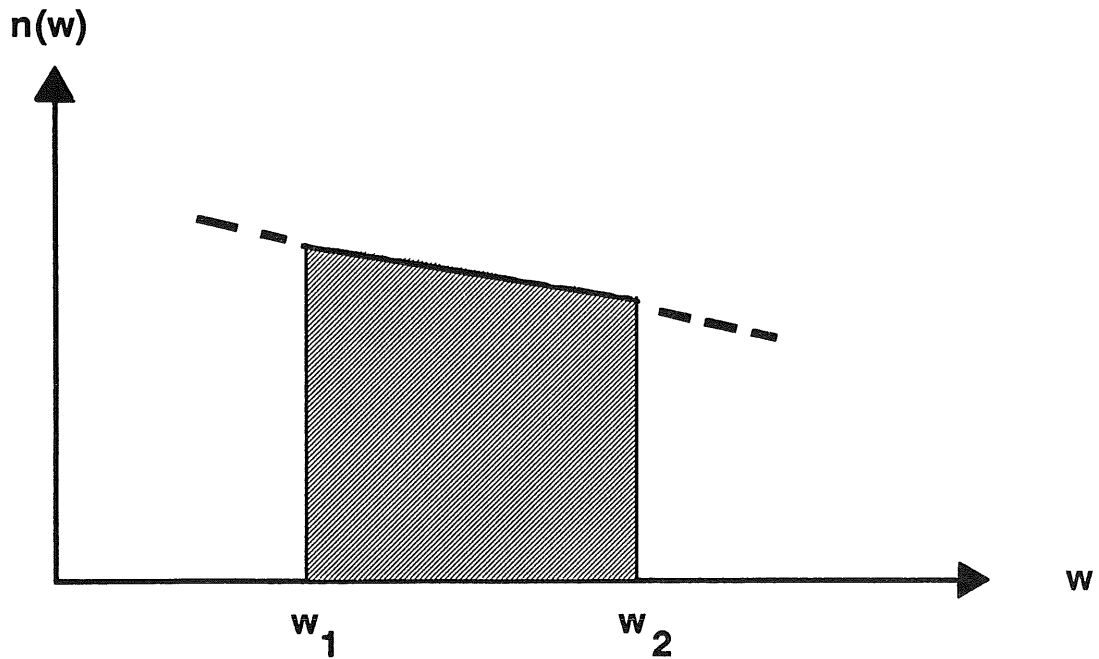


Figure 8.4.1. Sandeel lengths calculated from otoliths in guillemot stomachs. Arrows indicate the mean length of age classes derived from the closest available fisheries date: March, commercial sample, Shetland, April 1981; April as March; June, commercial sample, Fair Isle, June 1981; September, commercial sample, Shetland, September 1981 (from Blake et al. 1984).



$$N(w_1, w_2) = \int_{w_1}^{w_2} n(w) dw$$

$$\frac{dC(w_1, w_2)}{dt} = \int_{w_1}^{w_2} F(w)n(w) dw$$

$$B(w_1, w_2) = \int_{w_1}^{w_2} b(w) dw$$

$$\frac{dY(w_1, w_2)}{dt} = \int_{w_1}^{w_2} F(w)b(w) dw$$

Figure 8.5.1.1. The steady state spectrum is specified by $n(w)$, the number density or $b(w) = wn(w)$, the biomass density. Total numbers, biomass, catch and yield rates from a window in the spectrum are simply obtained by integration. $F(w)$ denotes the (size dependent) rate of fishing mortality.

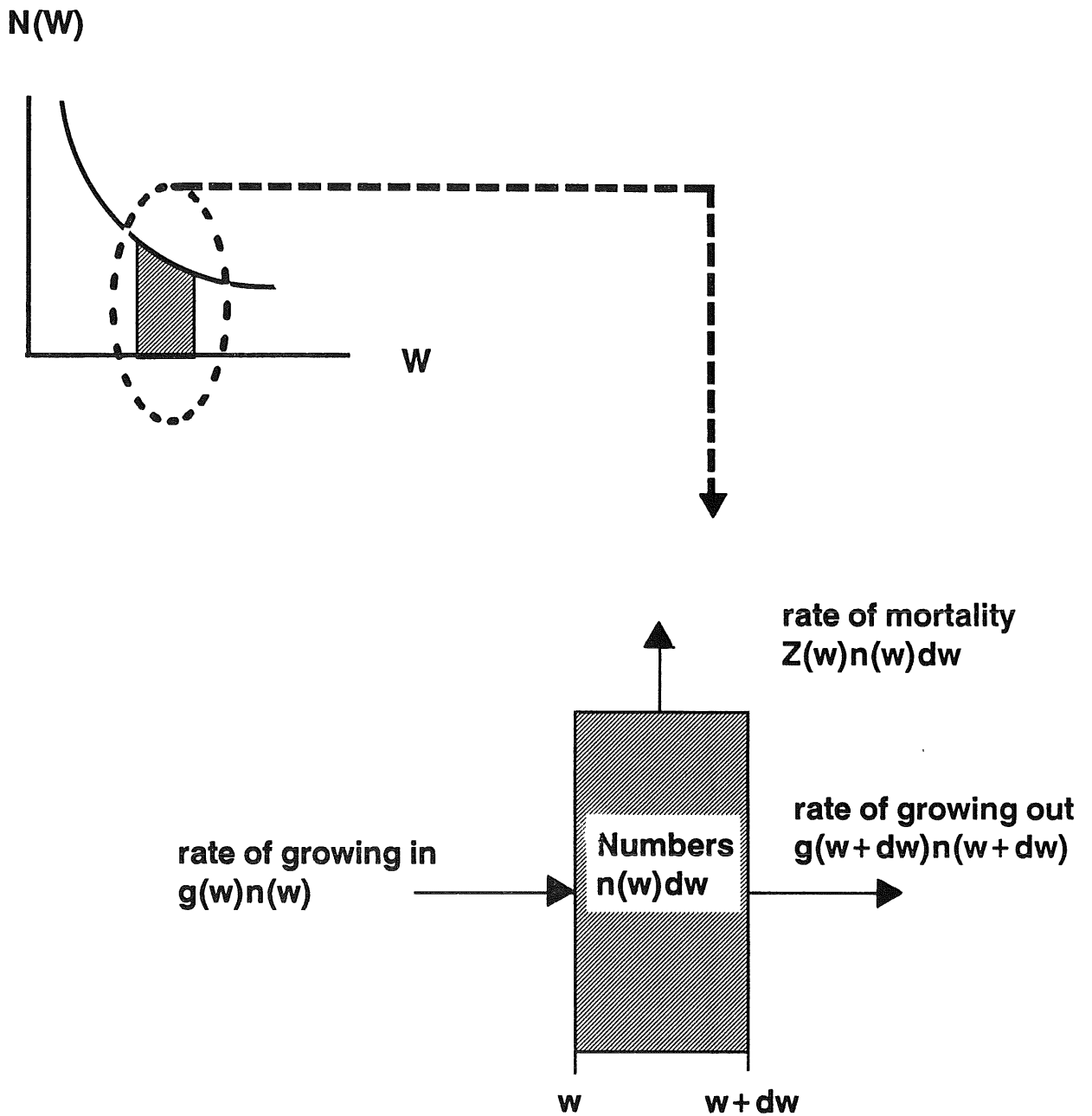


Figure 8.5.1.2. Steady state condition for any window in the spectrum: The rate of fish growing into the weight interval must equal the rate of fish disappearing from the interval (i.e. dying or growing out).

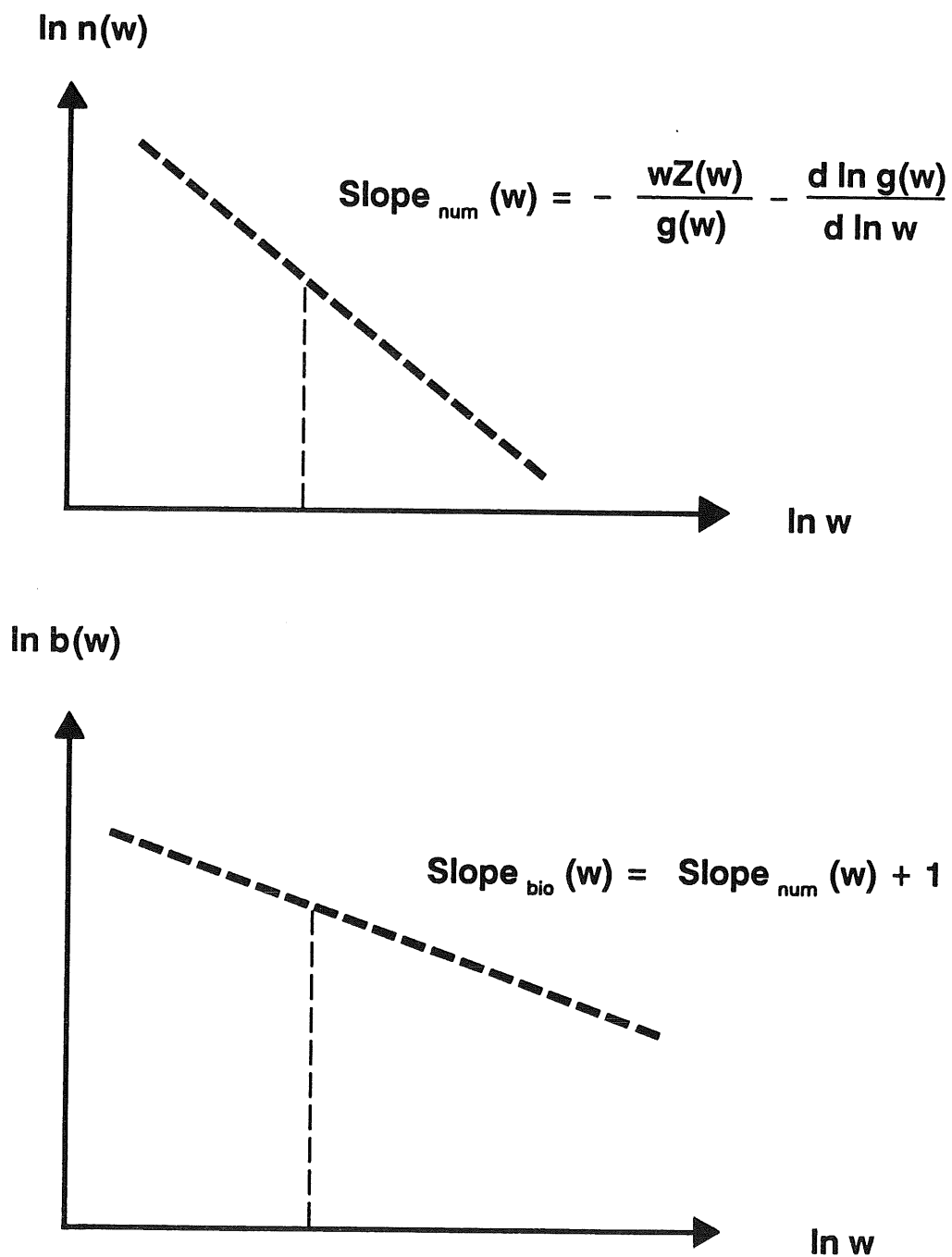


Figure 8.5.1.3. Determination of slopes at size of the spectra in steady state as a function of growth, $g(w)$, and mortality, $Z(w)$. The actual slope of the spectrum depends on the way the growth and mortality rates are quantified.

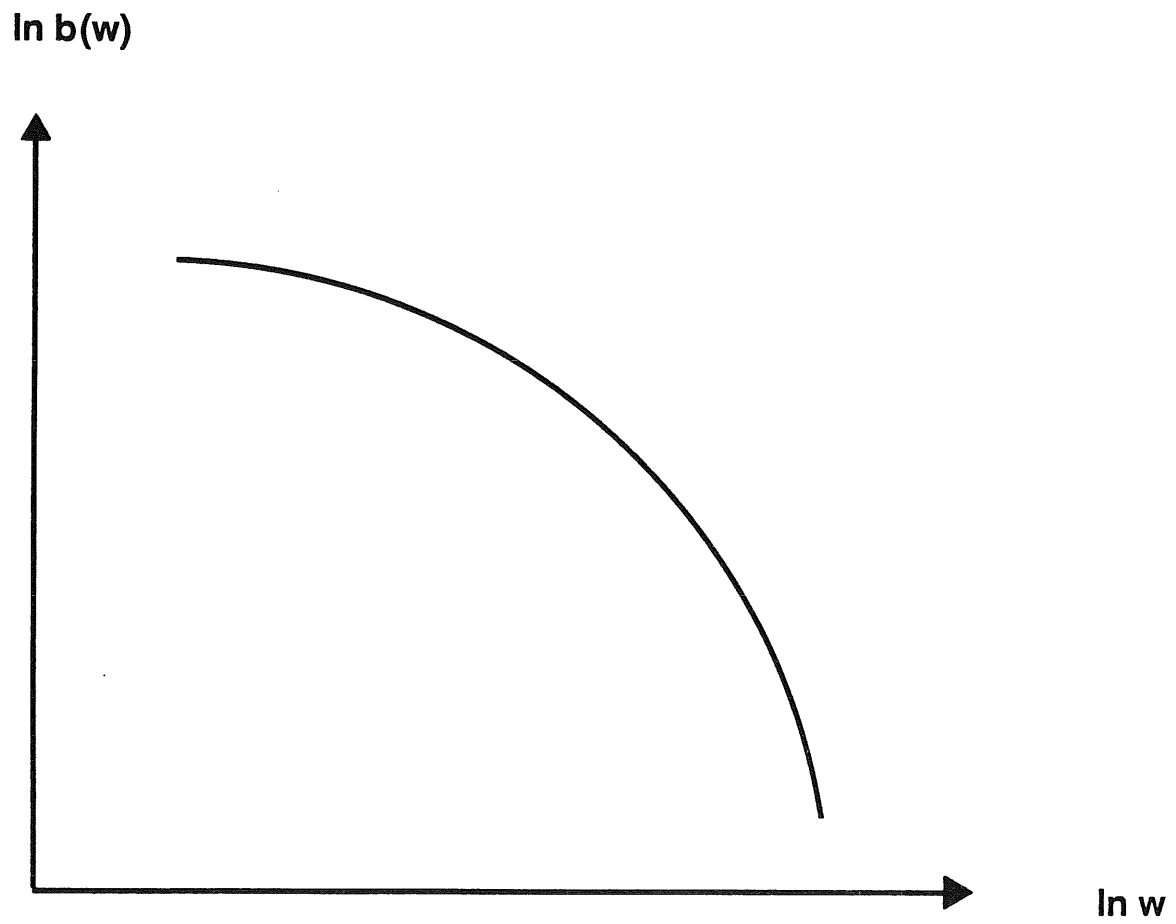


Figure 8.5.2.1. Convex slope of the biomass spectrum in case of allometric growth and constant (size-independent) mortality ($Z=F+M$).

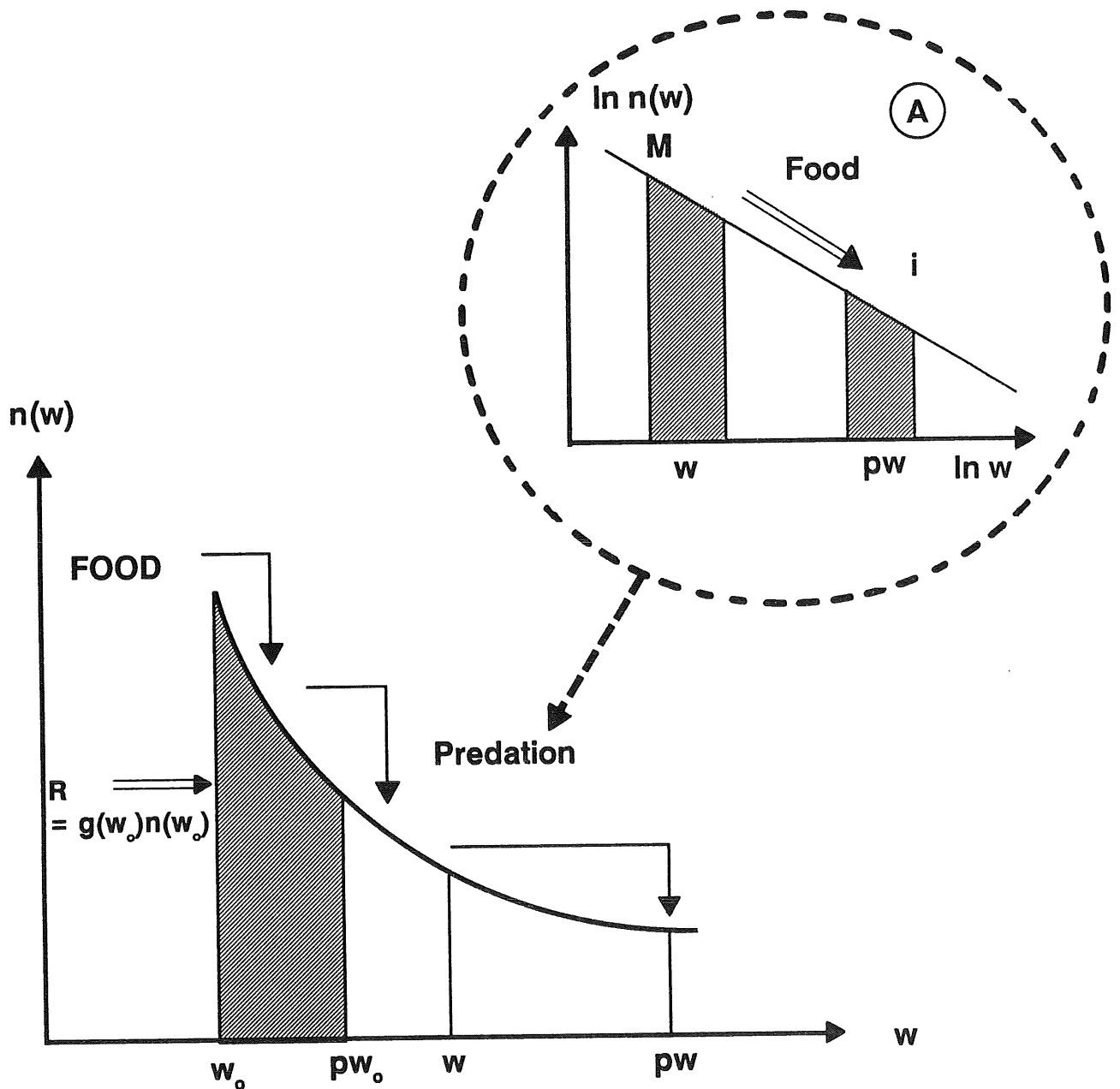


Figure 8.5.2.2. The size spectrum with predation and recruitment included. Food for the lower part of the spectrum is provided by smaller animals not accounted for in a presentation based on the part of the spectrum containing fish, and serves as exogenous input. A : Mass balance in the predation process expresses that the rate of prey biomass removed by predation equals the rate of food consumption by the predators at any size. Using allometric models the predation mortality $M(w)$ becomes proportional to $I(w)$, the specific rate of food consumption.

Biomass spectrum North Sea 74-89

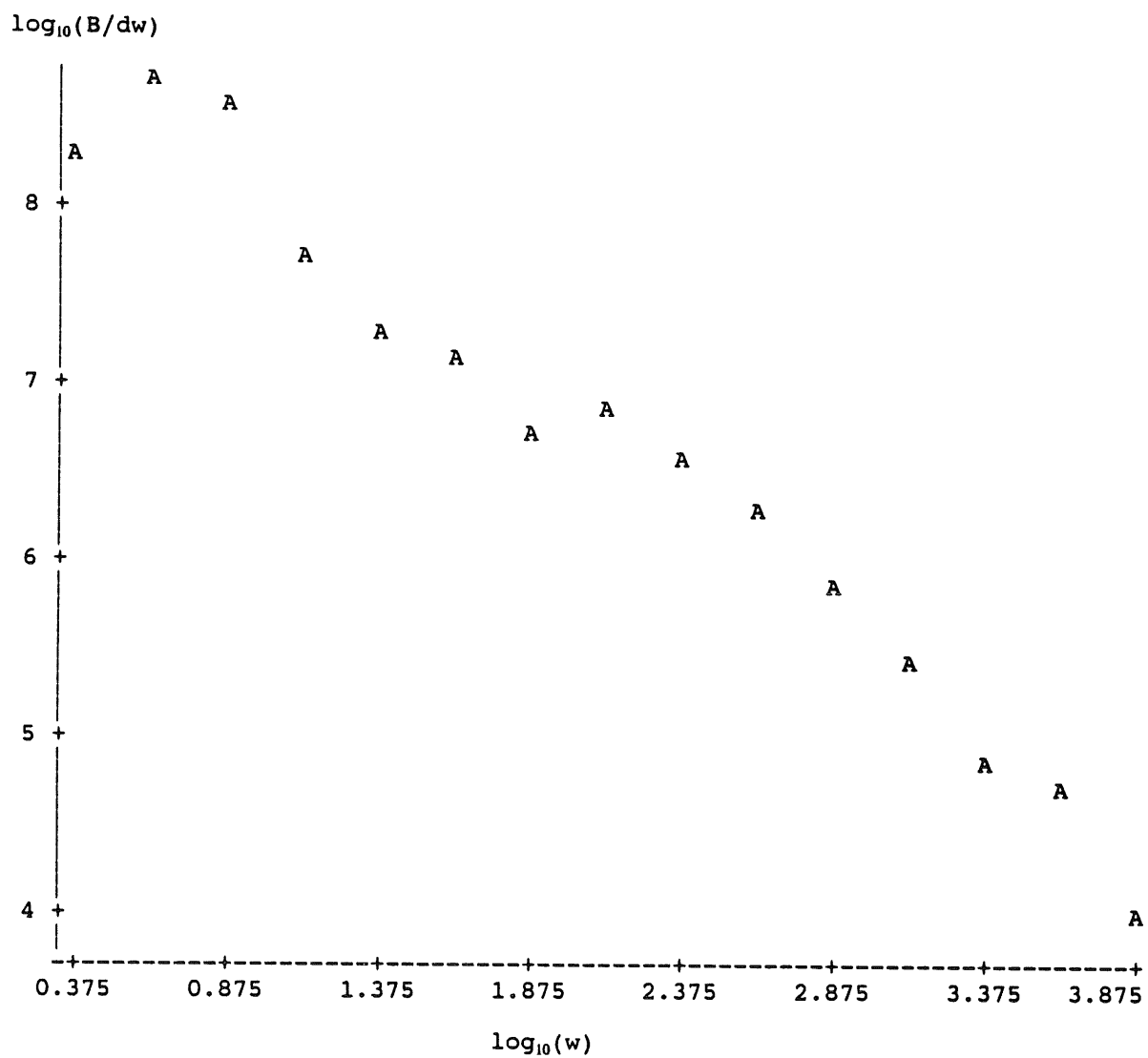


Figure 8.5.4.1. The biomass spectrum of the North Sea 74-89.

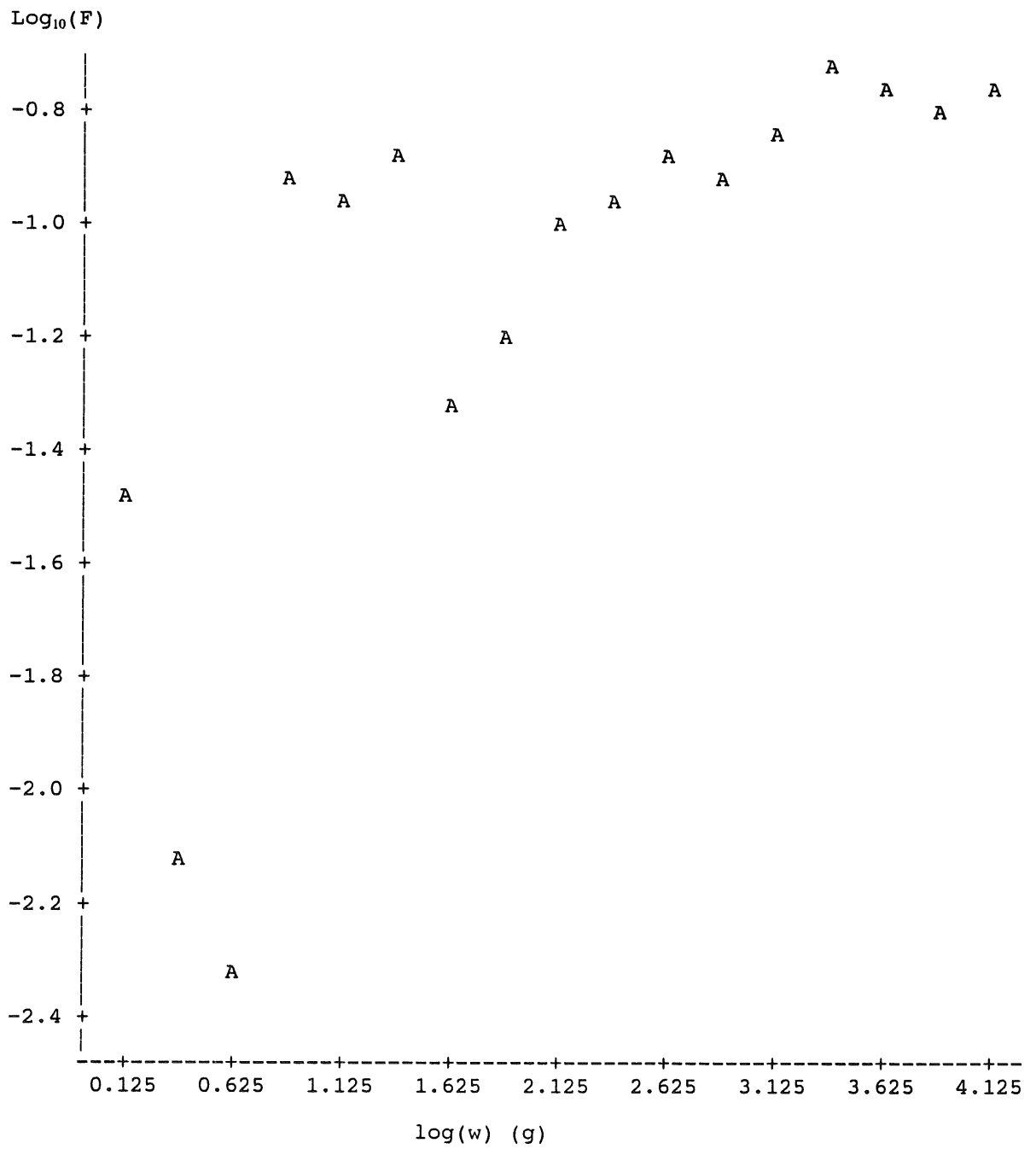


Figure 8.5.4.2. Mean fishing mortality as function of size, North Sea 1974-89.

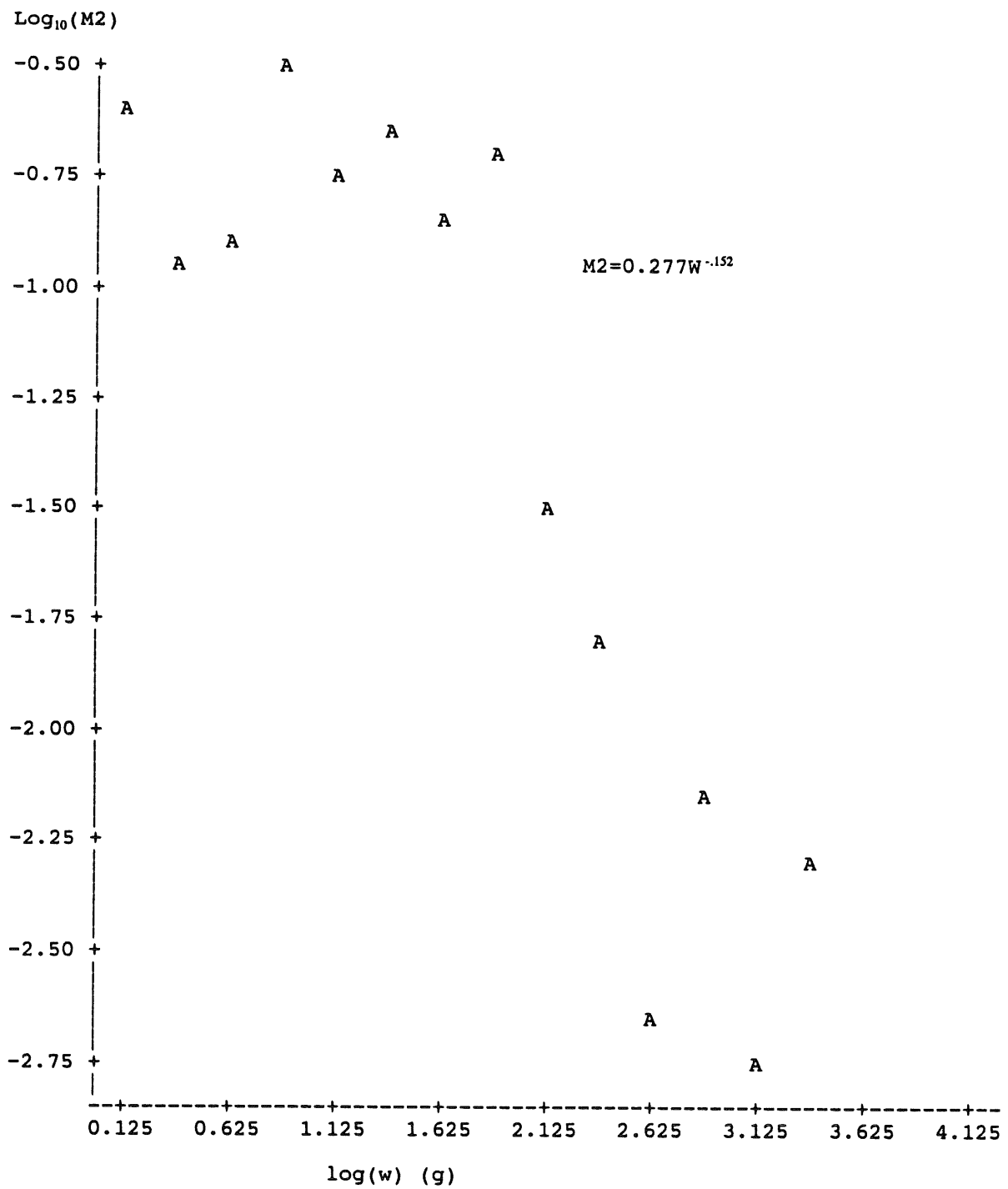


Figure 8.5.4.3. Mean predation mortality as function of size. North Sea 1974-89.

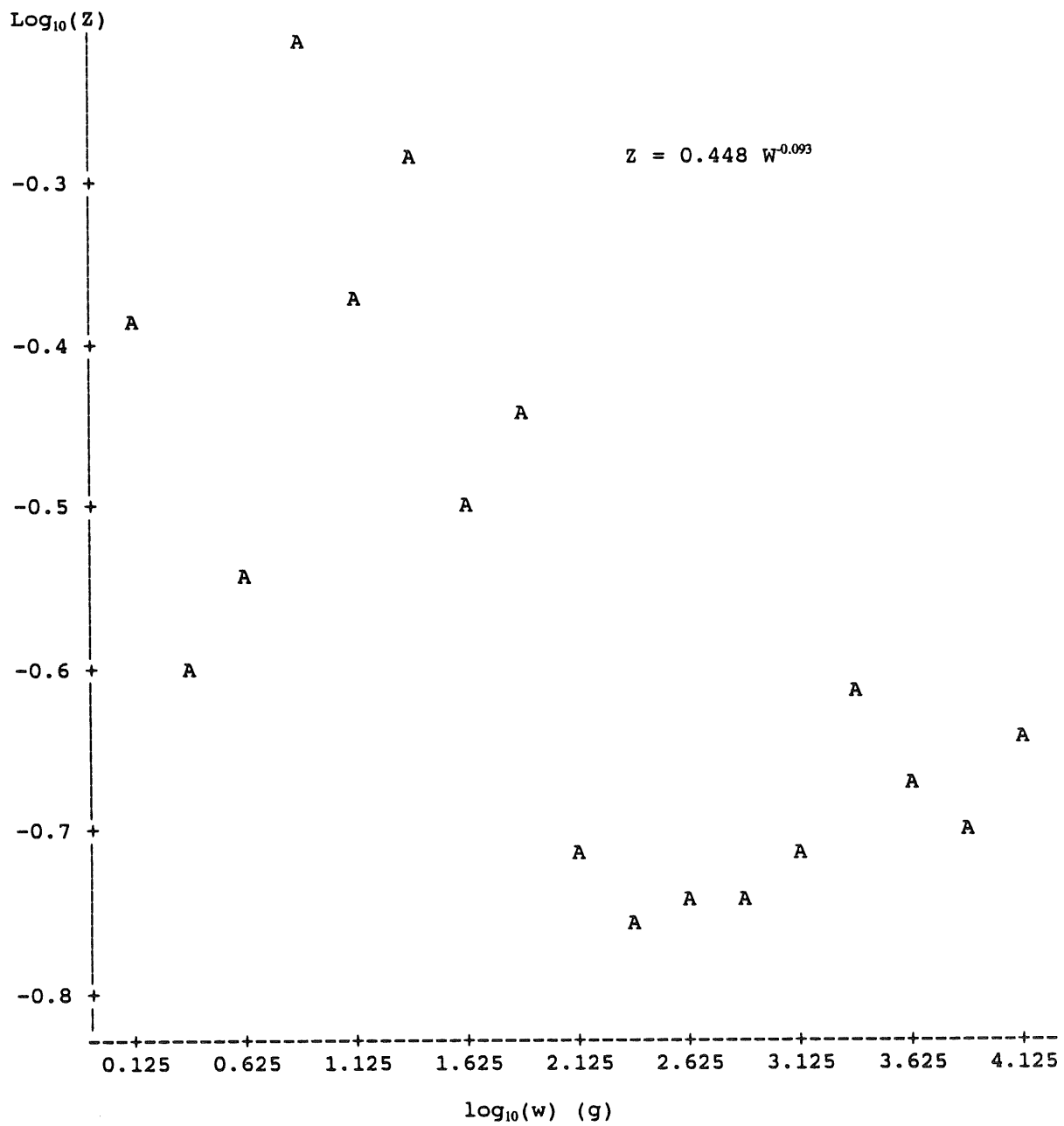


Figure 8.5.4.4. Mean total mortality as function of size. North Sea 1974-89.

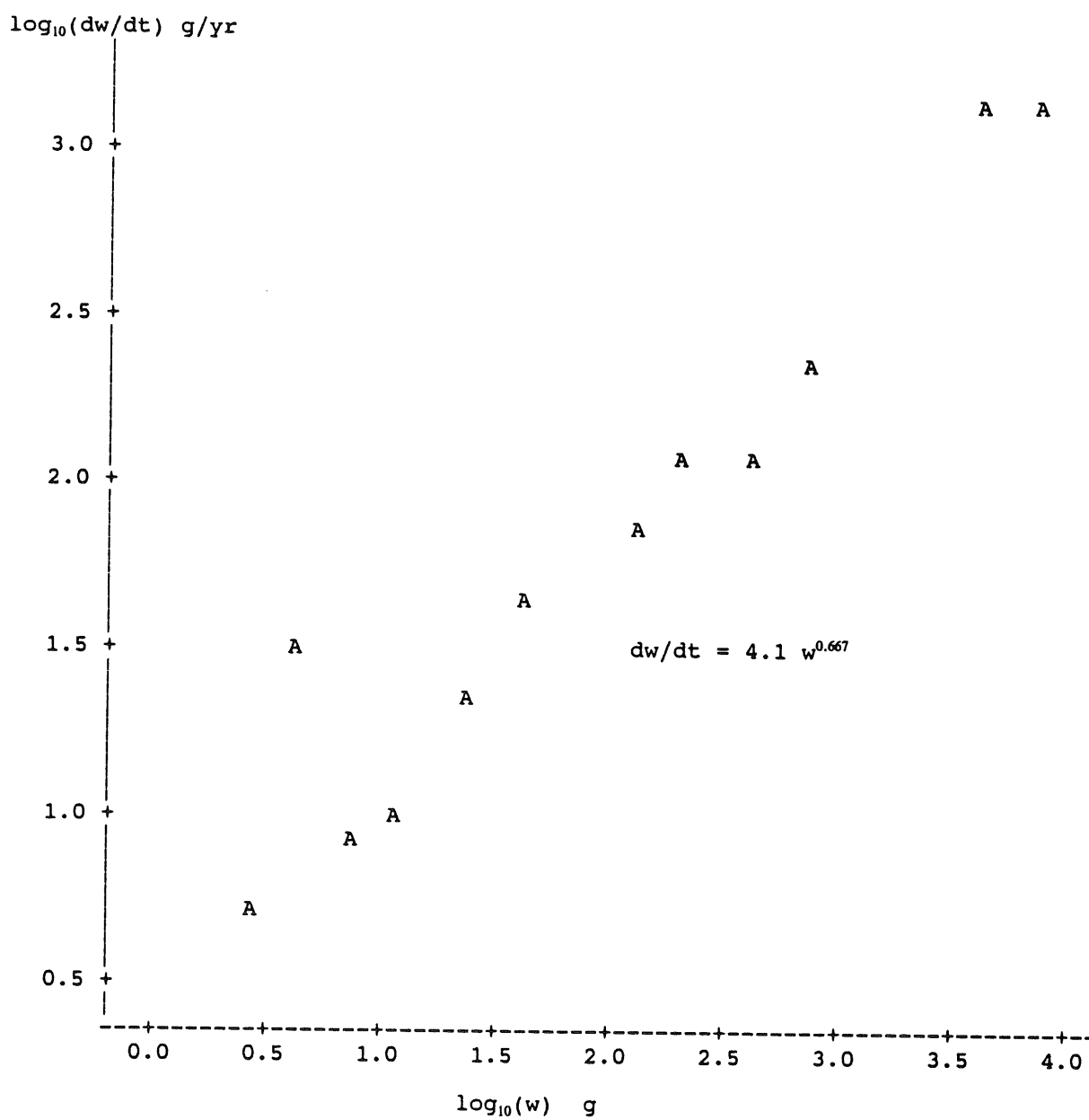


Figure 8.5.4.5. Growth rate as a function of weight. North Sea 1974-89

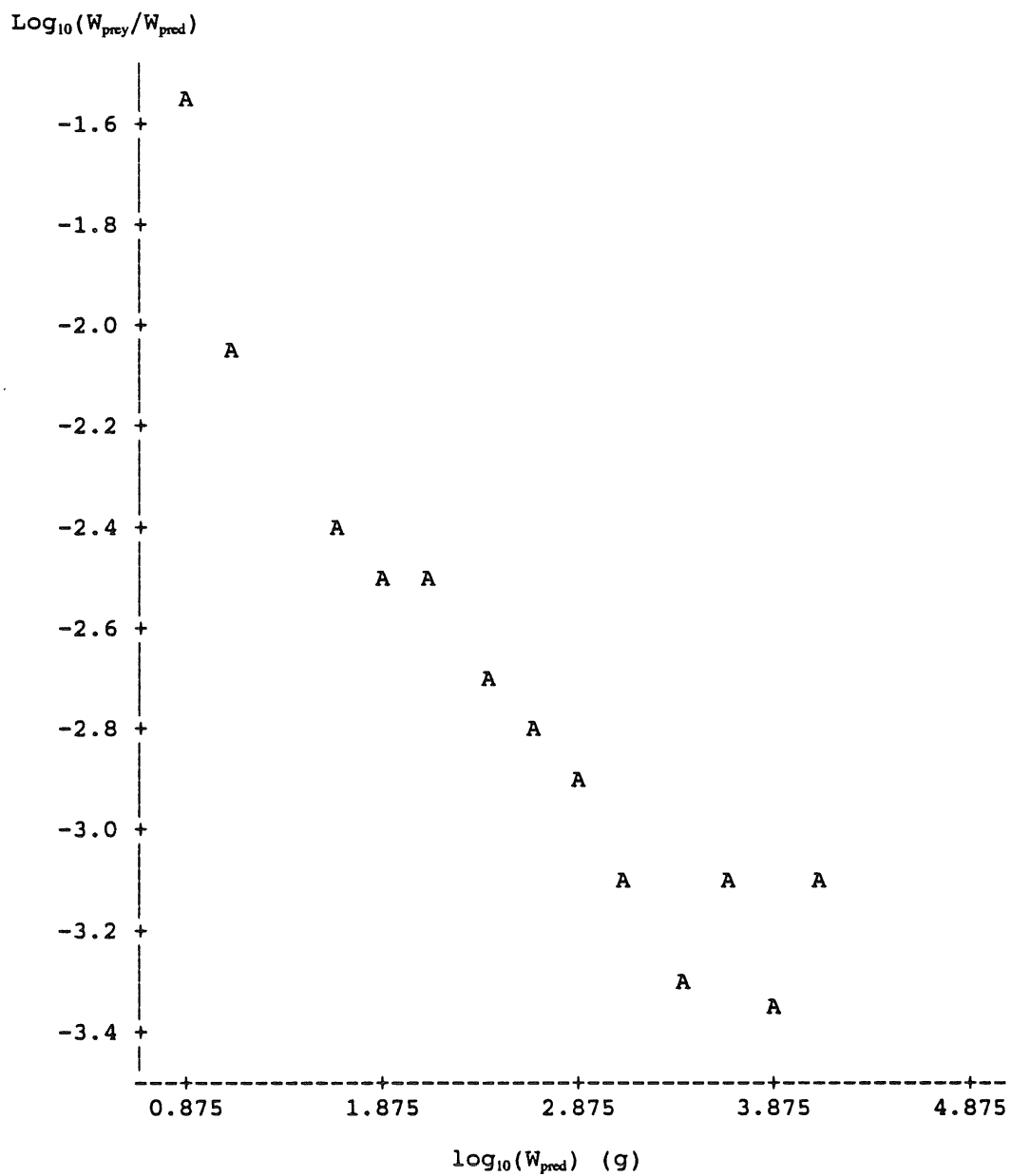


Figure 8.5.4.6. Prey selection ratio as function of predator size. North Sea 1974-1989.

Average Stomach Content Whiting

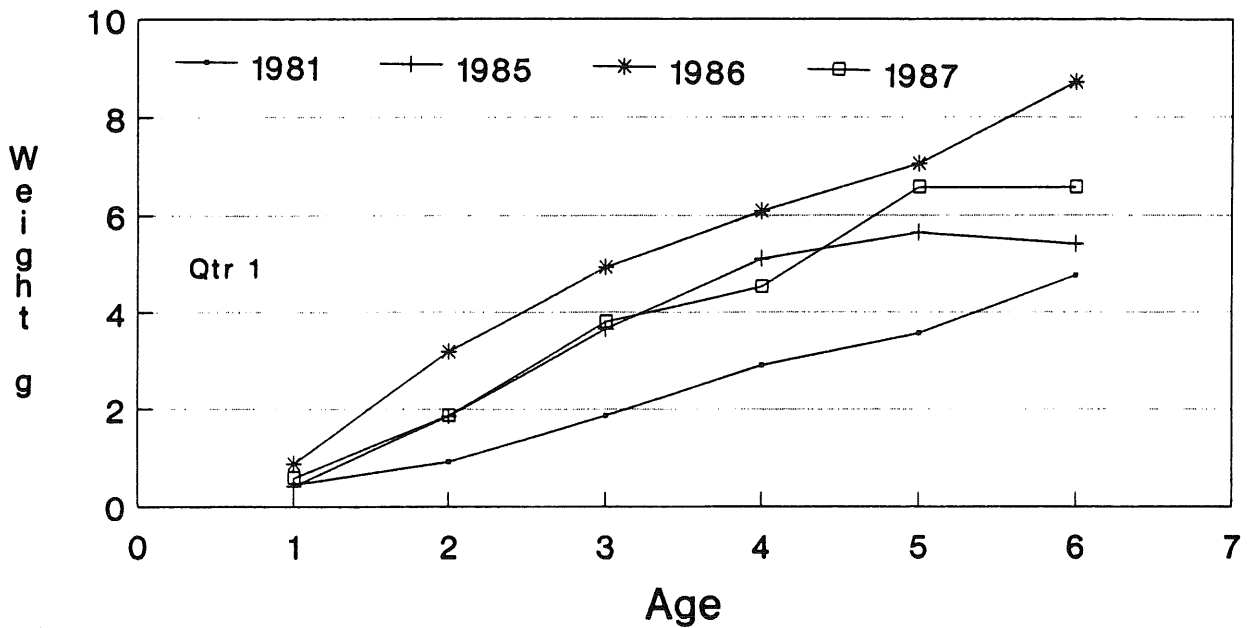


Figure 8.6.1. Average stomach content (weight, g) at age of whiting sampled in quarter 1 during 1981, 1985, 1986, and 1987.

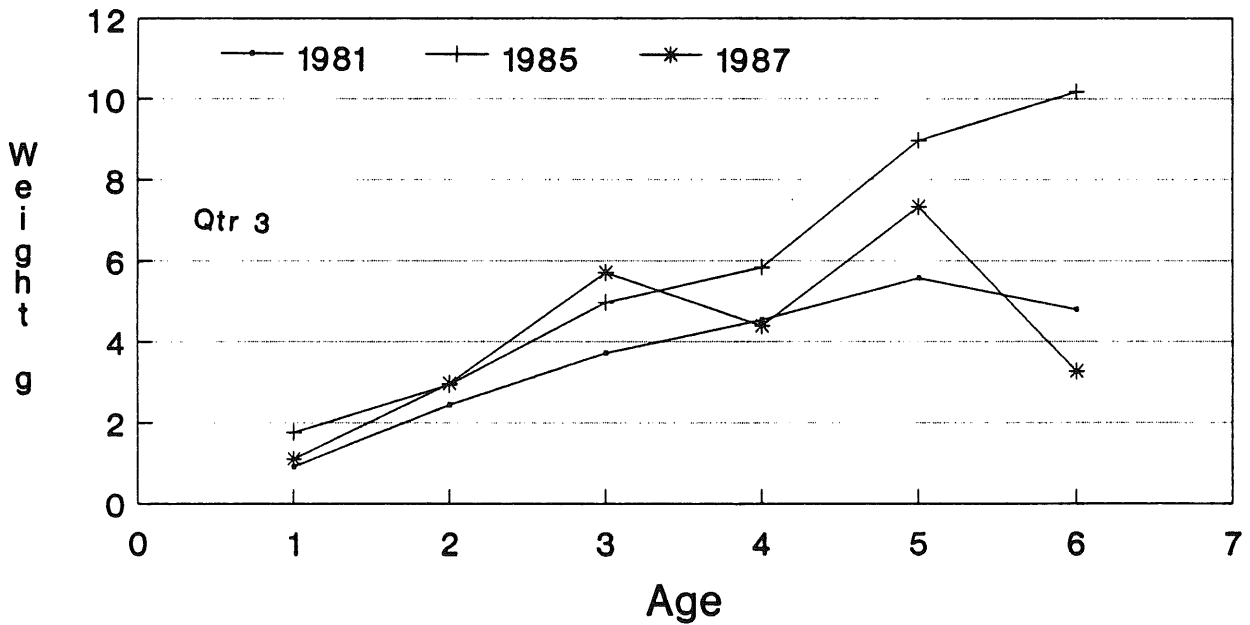


Figure 8.6.2. Average stomach content (weight, g) at age of whiting sampled in quarter 3 during 1981, 1985, and 1987.

Cod

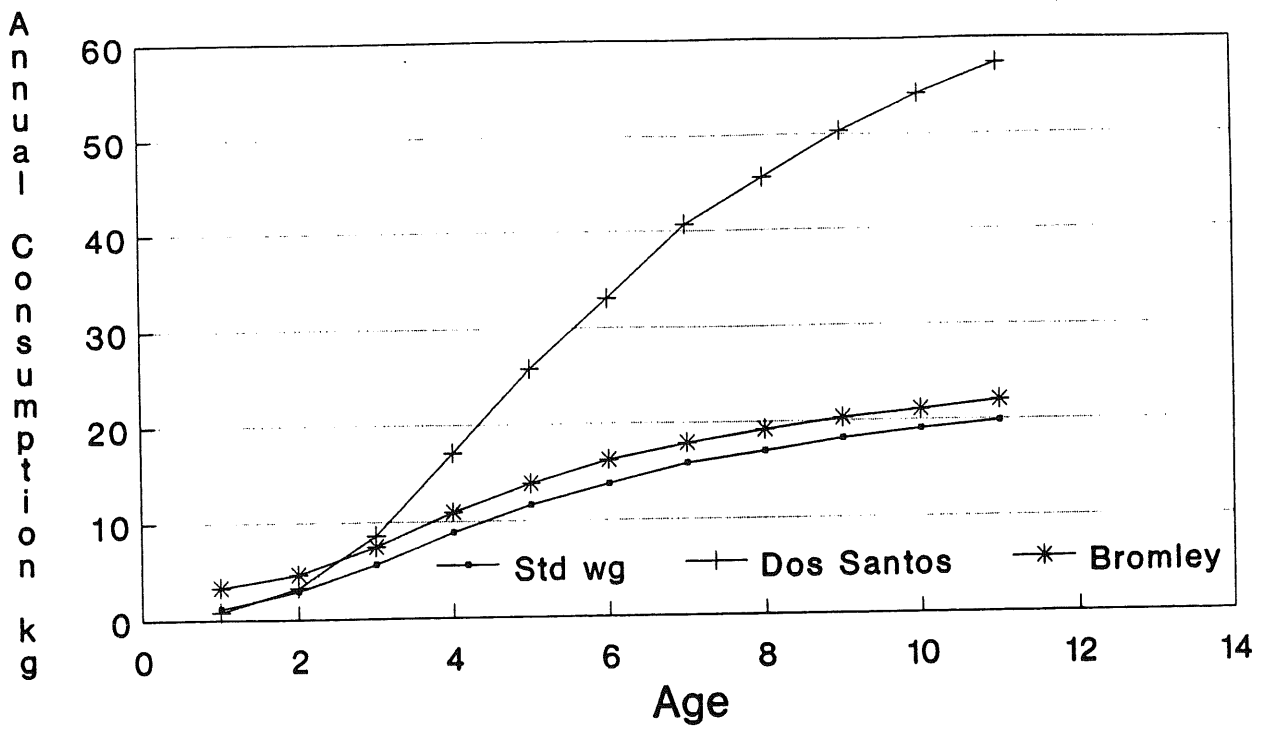


Figure 8.6.3. Predicted annual consumption (weight, kg) at age by North Sea cod, based on standard Working Group calculations, as well as consumption models of dos Santos and Bromley (see text).

Whiting

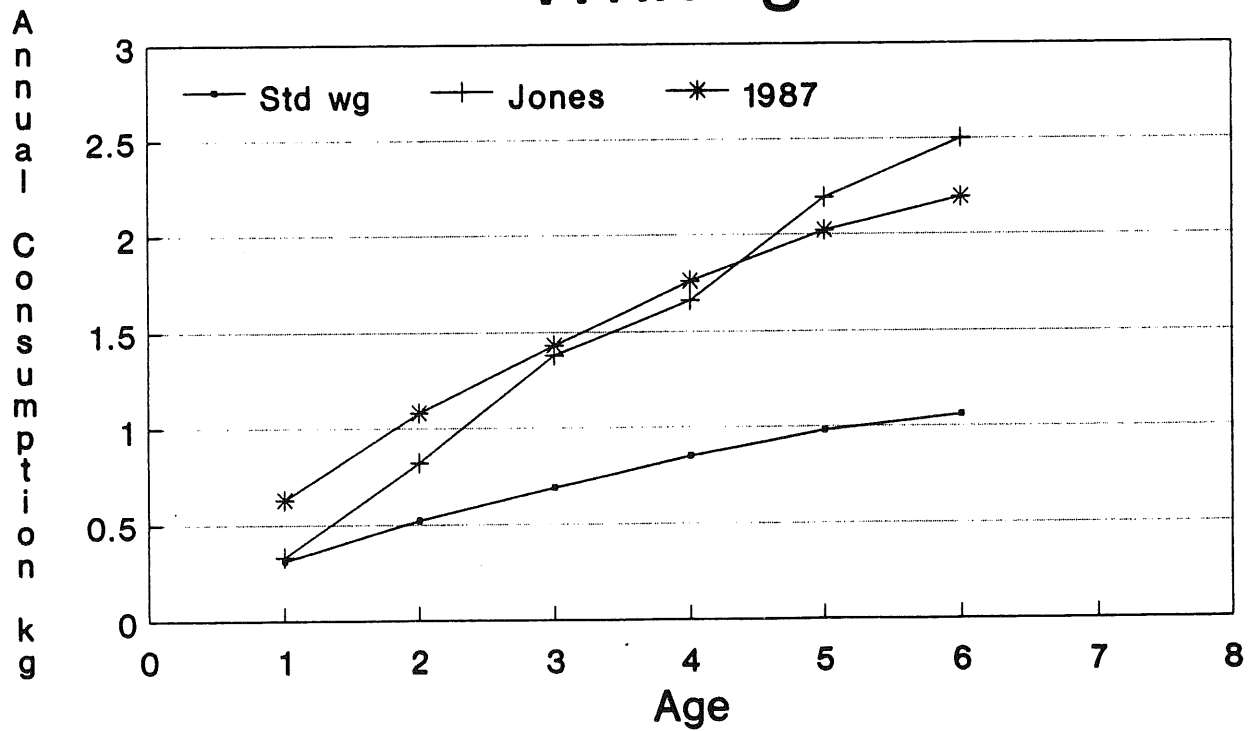


Figure 8.6.4. Predicted annual consumption (weight, kg) at age by North Sea whiting, based on standard Working Group calculations, as well as the consumption model of Jones and assuming 1987 average stomach contents weight (see text).

APPENDIX A

Numbers of Stomachs to be Collected per Size Class per Haul

Size class, cm	Species								
	Cod	Whiting	Saithe	Mackerel	Haddock	Scad	Gurnards	Rays	Other*
5-5.9	5	5	5	5	5	5			
6-6.9	5	5	5	5	5	5			
7-7.9	5	5	5	5	5	5			
8-9.9	5	5	5	5	5	5			
10-11.9	5	5	5	5	5	5			
12-14.9	5	5	5	5	5	5			
15-19.9	10	10	25	25	5	10	10	10	
20-24.9	10	10	25	25	5	10	10	10	
25-29.9	10	10	25	25	5	10	10	10	
30-34.9	10	10	25	25	5	10	10	10	
35-39.9	10	10	25	25	5	10	10	10	
40-49.9	10	10	25	25	5	10	10	10	
50-59.9	10	10	25		5			10	
60-69.9	25	10	25		5			10	
70-79.9	25		25		5			10	
80-99.9	25		25					10	
100-119.9	25		25					10	
>120	25		25					10	

*Pelagic 0-group gadoids, Herring, Sandeels: Ca-50 individuals per haul

Species which could be sampled opportunistically include: Ling, Angler (Lophius piscatorius) Long rough dab (Hippoglossoides platessoides).

APPENDIX B

Provisional Commitments to 1991 Stomach Sampling Project

Country	Sampling period			
	Jan-Mar	Apr-Jun	Jul-Sep	Oct-Dec
Belgium	?	?	?	?
Denmark	x	x		x
France	?	?	?	?
Germany	(x)	x		
Netherlands	x	x	x	x
Norway	x	x	(x)	x
Sweden	?	?	?	?
UK England		x	x	x
UK Scotland	x	x	x	